NASA TECHNICAL NOTE

NASA TN D-8135

NASA TN D-8135

ATS-6 SPACECRAFT: IN-FLIGHT ANTENNA PATTERN MEASUREMENT

L. W. Nicholson, H. Hanft,
B. G. Bemis, and R. L. Baldridge
Goddard Space Flight Center
Greenbelt, Md. 20771

NATIONAL AERONAUTICS AND SPACE ADMINISTRATION • WASHINGTON, D. C. • JANUARY 1976

1. Report No.	2. Government Accession No.	3. Recipient's Catalog No.
NASA TN D-8135		
4. Title and Subtitle ATS-6 Spacecraft: In-Flight Antenna Pattern Measurement		5. Report Date January 1976
		6. Performing Organization Code 724
7. Author(s) L. W. Nicholson, H. Hanft, B. G. Bemis, R. L. Baldridge		8. Performing Organization Report No. G-7614
9. Performing Organization Name and Address Goddard Space Flight Center Greenbelt, Maryland 20771		10. Work Unit No.
		11. Contract or Grant No.
12. Sponsoring Agency Name and Address National Aeronautics and Space Administration Washington, D.C. 20546		13. Type of Report and Period Covered Technical Note
		14. Sponsoring Agency Code

15. Supplementary Notes

16. Abstract

Antenna patterns, principally associated with the 9.1 meter parabolic antenna of the ATS-6 spacecraft, were measured while in orbit at quasi-stationary synchronous altitude. Controlling the spacecraft attitude permitted a scanning of the spacecraft antenna pattern over the Rosman ground station, thus achieving the measurement of the antenna pattern contour. Patterns were determined in terms of relative gain referenced in position to the spacecraft body coordinates by means of signal power measurements made using a linear detector. These data were subsequently correlated with the attitude data to define the antenna patterns.

Antenna patterns measured are presented and compared with available preflight patterns.

17. Key Words (Selected by Author(s))	18. Distribution Statement
Dish, Parabolic, Space, Performance, Measurement, ATS-6, Pattern, Antenna, and Synchronous	Unclassified—Unlimited Cat 32

19. Security Classif. (of this report)	20. Security Classif. (of this page)	21. No. of Pages	22. Price*
Unclassified	Unclassified	144	$5.75

*For sale by the National Technical Information Service, Springfield, Virginia 22161

CONTENTS

ILLUSTRATIONS

ILLUSTRATIONS – (continued)

ILLUSTRATIONS – (continued)

ATS-6 SPACECRAFT: IN-FLIGHT ANTENNA PATTERN MEASUREMENT

L. W. Nicholson
ATS Project Office

H. Hanft
B. G. Bemis
R. L. Baldridge
Westinghouse Defense & Electronic Systems Center

INTRODUCTION

The ATS-6 satellite employs a 9.1-meter-diameter parabolic antenna as a major component of its many configurations of communication links. Figure 1, ATS-6 configuration in-orbit and prime focus feed diagram, provides a visual description of the antenna and prime focus feed. A number of additional antennas are carried aboard ATS-6 to provide operational communications and data links for the technically diverse experimental missions.

A method of measuring in-flight antenna patterns was developed by employing the equipment used in the RFI experiment for the investigation of C-band terrestrial noise sources. Specific antenna pattern measurement was accomplished by predetermined spacecraft maneuvers that were executed from the ATS Operations Control Center (ATSOCC). The actual resultant attitudes during the maneuvers were measured, specifically, referring to the line of sight to the Rosman ground station, in spacecraft body coordinates. The attitudes were computed and correlated to GMT at the ATSOCC in 3-second intervals and relayed to Rosman for input to the RFI Receiver/Analyzer system (employing a PDP-11 computer). Relative signal power measurements were determined by using the linear detector in the RFI Receiver/Analyzer and correlated to GMT. The signal level measurement data and attitude measurement data were recorded together on digital magnetic tape and subsequently correlated by means of the GMT data. The results provided relative signal level power measurements, corresponding to attitude data suitable for antenna pattern plots. The patterns obtained from this method were those of radio frequency beams transmitted from the spacecraft. A similar method was employed to achieve received antenna patterns while recording the signal level received by the spacecraft.

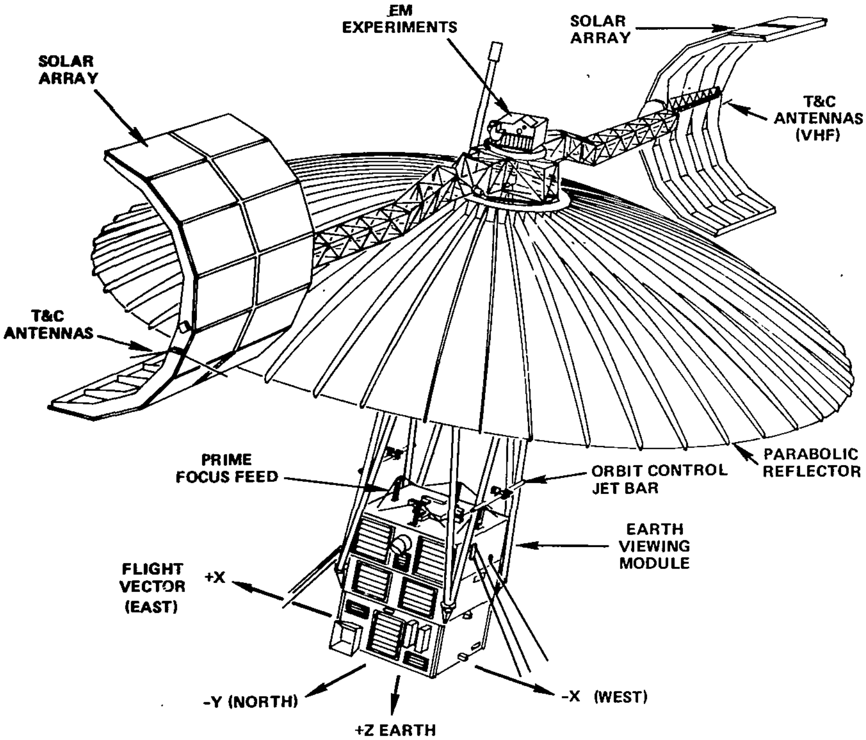

ATS-6 CONFIGURATION IN ORBIT

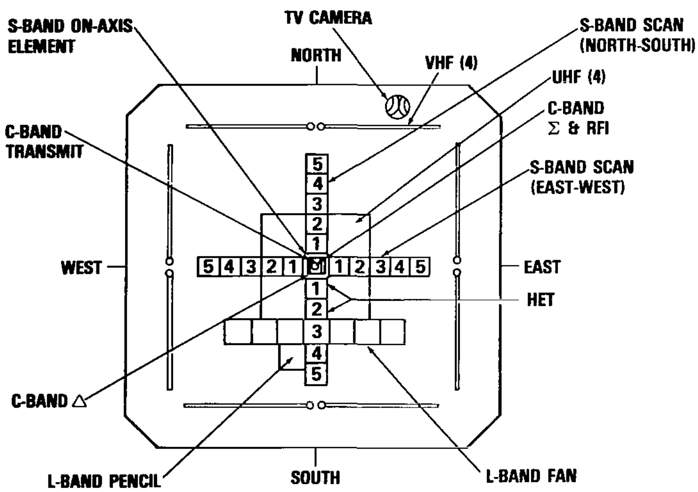

DIAGRAM OF PRIME FOCUS FEED

Figure 1. ATS-6 configuration in-orbit and prime focus feed diagram.

PREFLIGHT ANTENNA PATTERN MEASUREMENT

Preflight antenna patterns were made by conventional means with the normal coordinates in rectangular form, providing plots of relative power versus angle. The patterns were annotated with the directional measurements of N, S, E, and W. These directions are defined according to Figure 2, spacecraft-earth geometry, which also defines the axes of the ATS spacecraft.

For most of the preflight patterns measured, the center of the main lobe was considered to be zero, or on boresight. The types of antenna pattern measurements made include the following:

Hard Dish Patterns

Hard dish measurements used a full-size approximation of ATS-6 having a 9.1-meter-diameter metallic parabolic dish. The model included the earth viewing module (EVM) supporting structure and members representing components like the orbit control jets and associated bar support. Figure 3 is a photograph of the 9.1-meter hard dish and model.

Soft Dish Patterns

Soft dish measurements were made using a 9.1-meter final type antenna reflector (protoflight model) with its flexible ribs supported to provide the desired contour.

Best Contour Patterns (Soft Dish)

The 9.1-meter soft dish was held to a good parabolic shape.

Worst Contour Patterns (Soft Dish)

The 9.1-meter soft dish was distorted to provide a "worst contour" based upon calculated distortion due to the extreme temperature change the spacecraft would experience in orbit.

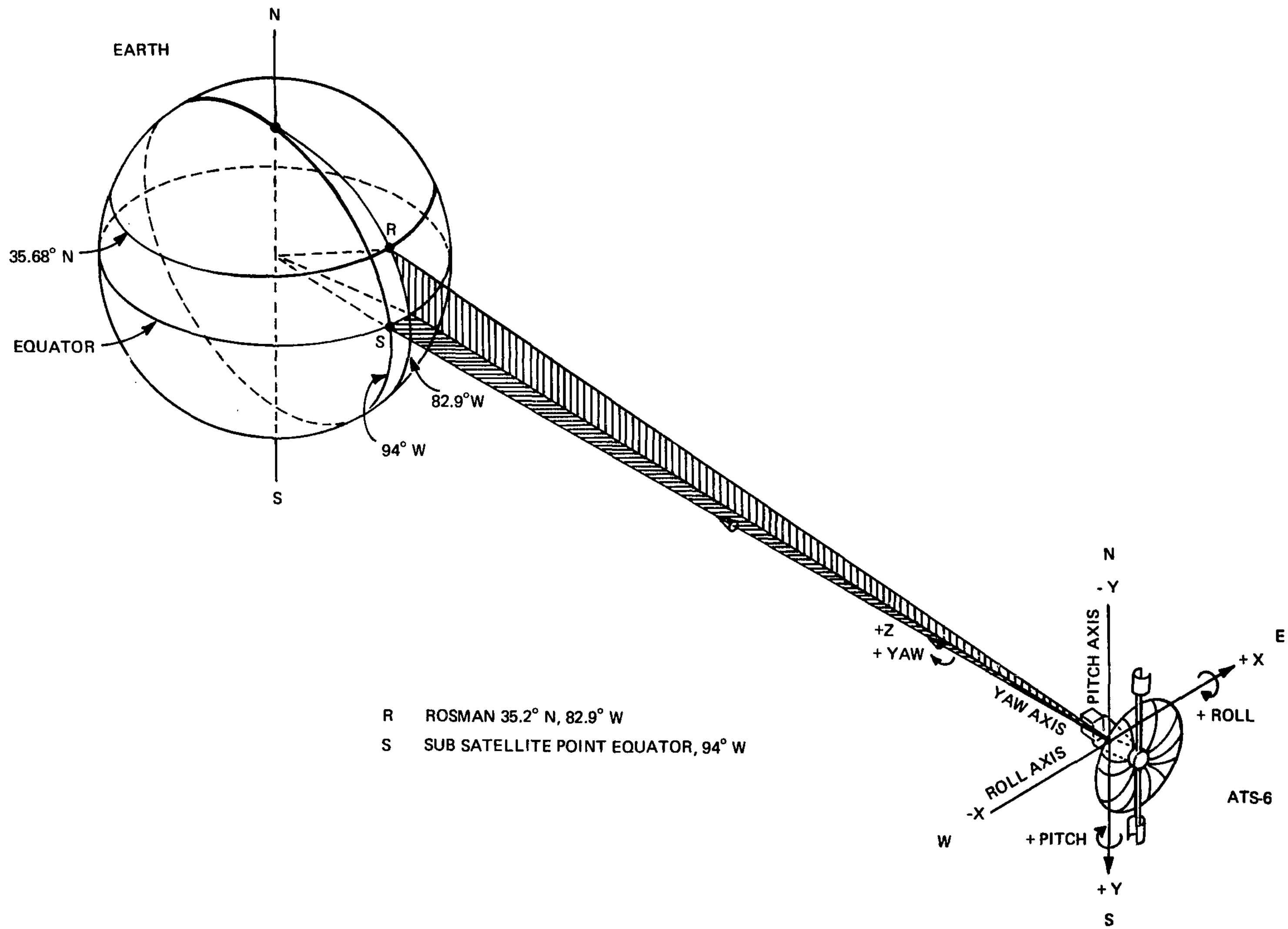

Figure 2. Spacecraft-earth geometry.

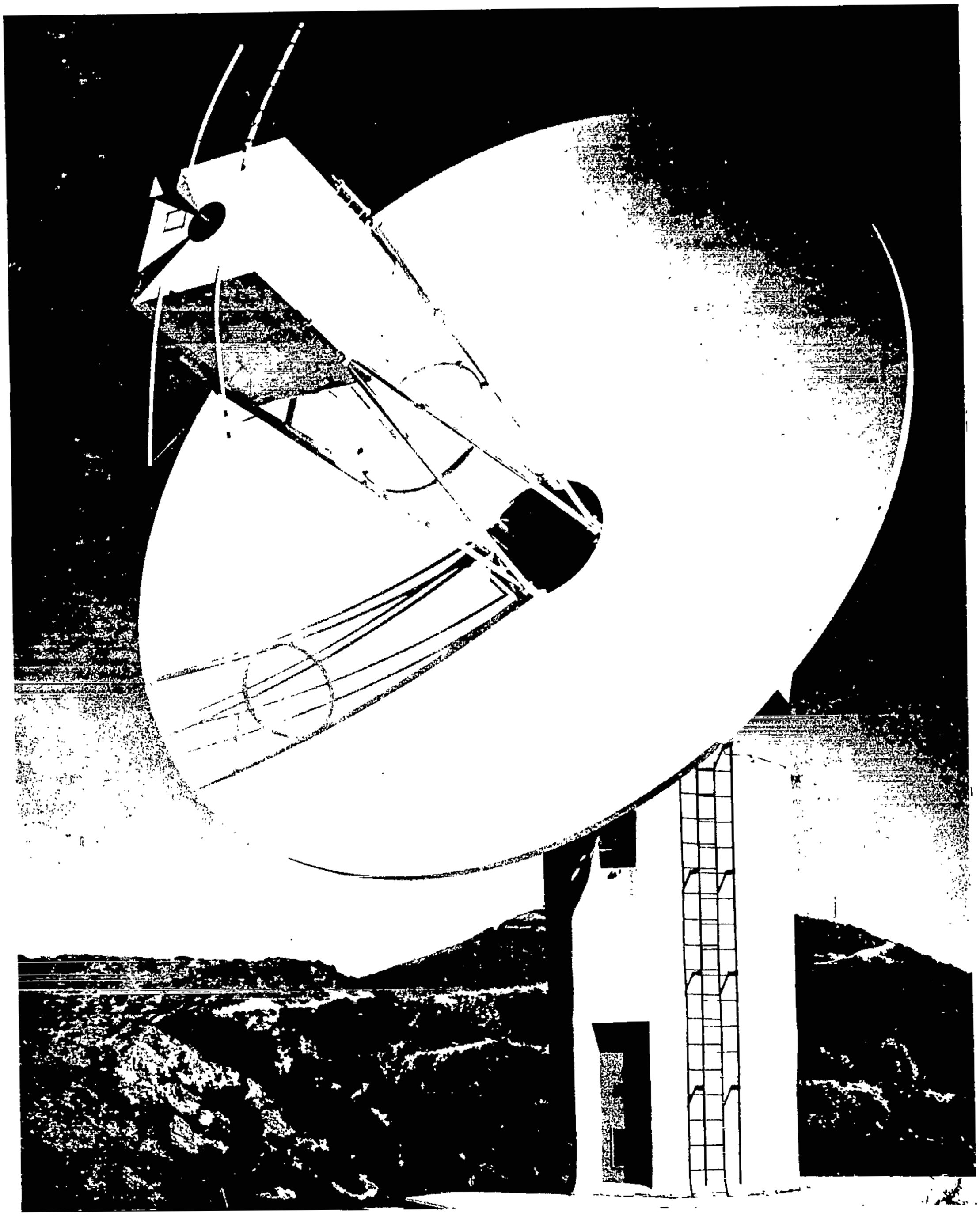

Figure 3. 9.1-meter hard dish model.

MEASUREMENT AND SIGNAL PROCESSING

The complex processing techniques and methods of determining "in-orbit" antenna patterns will be limited only to a very general discussion in this document.

The antenna patterns are derived by measurement of signal power received at the ground station and at the spacecraft. These signals are collected at the ground station by employing the Radio Frequency Interference (RFI) Experiment equipment that includes a special receiver/analyzer. The method determines the patterns in terms of relative gain, and positions the patterns in spacecraft body coordinates. The results of the measurement are recorded at the ground station on digital tapes and ATSOCC line printers for computer and manual reduction, respectively.

The general procedure for antenna pattern measurement is to control the spacecraft attitude so it scans the antenna pattern to be measured (by slewing the spacecraft) over the Rosman ground station. The maneuver is executed from the ATSOCC using the digital operational controller (DOC) in interated angle slew and offset point modes to achieve the desired pattern contours or corresponding "cuts". The actual resultant attitude, defining the line of sight to Rosman as the reference point in terms of spacecraft body coordinates, shown in Figures 4 and 5, is computed and relayed to Rosman in 3-second intervals for input to the RFI receiver/analyzer system (PDP-11). Figure 6, equipment required for antenna pattern measurement, is a functional diagram. Signal level power measurements are made by use of the linear detector in the RFI receiver/analyzer and are subsequently correlated with the attitude data to define the antenna patterns. The measurement results are output from the RFI receiver/analyzer in these forms:

1. Raw Data
   This data is the raw digital data tape used for off-line computer determination and analysis of antenna patterns. The data contains the attitude, time of year, and selected telemetry parameters, all on a 3-second sample period and the identified power measurements on a 100-ms sample period.

2. Reduced Data
   This data output is a line printer output of derived antenna pattern data which is used for off-line manual determination and analysis of the antenna patterns. This data includes relative antenna gain, attitude, time of year, and selected telemetry parameters. All data is on a 3-second sample period.

IN-ORBIT ANTENNA PATTERN MEASUREMENT

In-orbit antenna patterns were made by slewing the spacecraft. The attitude of the spacecraft during the slews, in particular the direction of the line of sight to the Rosman ground station, are described in a spacecraft body centered coordinate system. Figure 4 shows the defining geometry of the body centered Zaz, Zcoel (Zazimuth, Zcoelevation) coordinate system in which the line of sight to the ground station is described during an

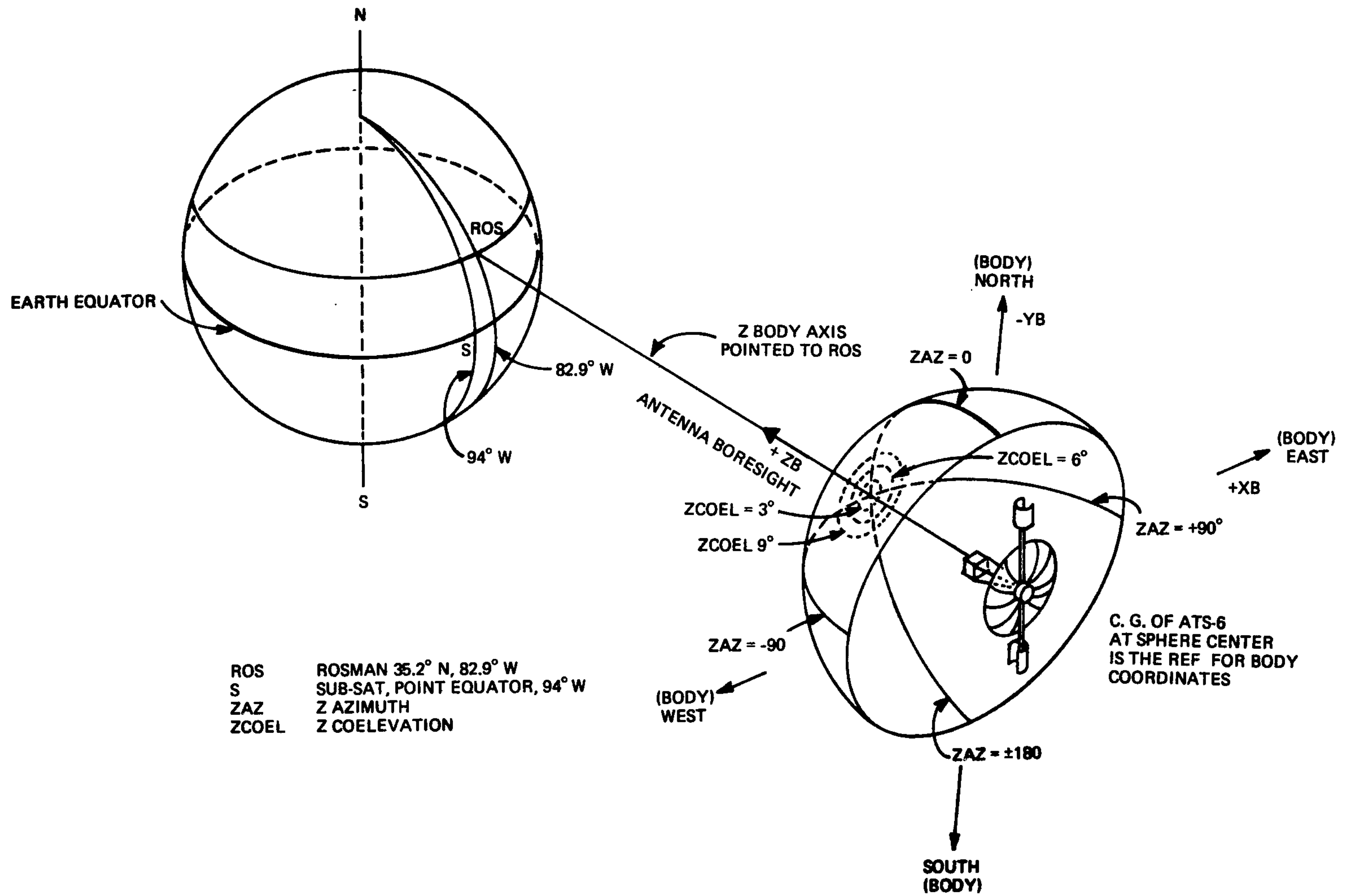

Figure 4. ATS-6 body coordinates.

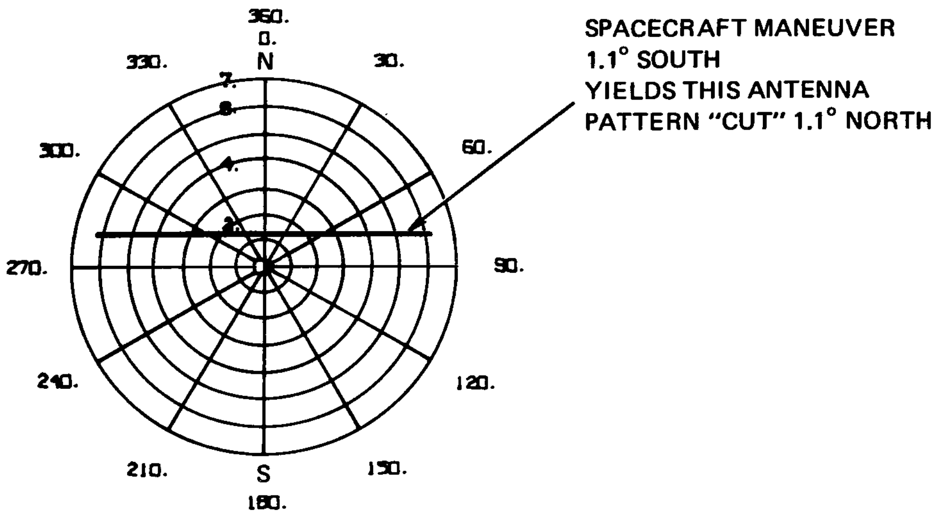

RADIAL LINES REPRESENT ZAZ (Z AZIMUTH) 0° TO 360°
CONCENTRIC CIRCLES REPRESENT ZCOEL (Z COELEVATION)
0° TO 180° (0° TO 7° ON DIAGRAM)

Figure 5. ATS-6 body coordinates for antenna patterns.

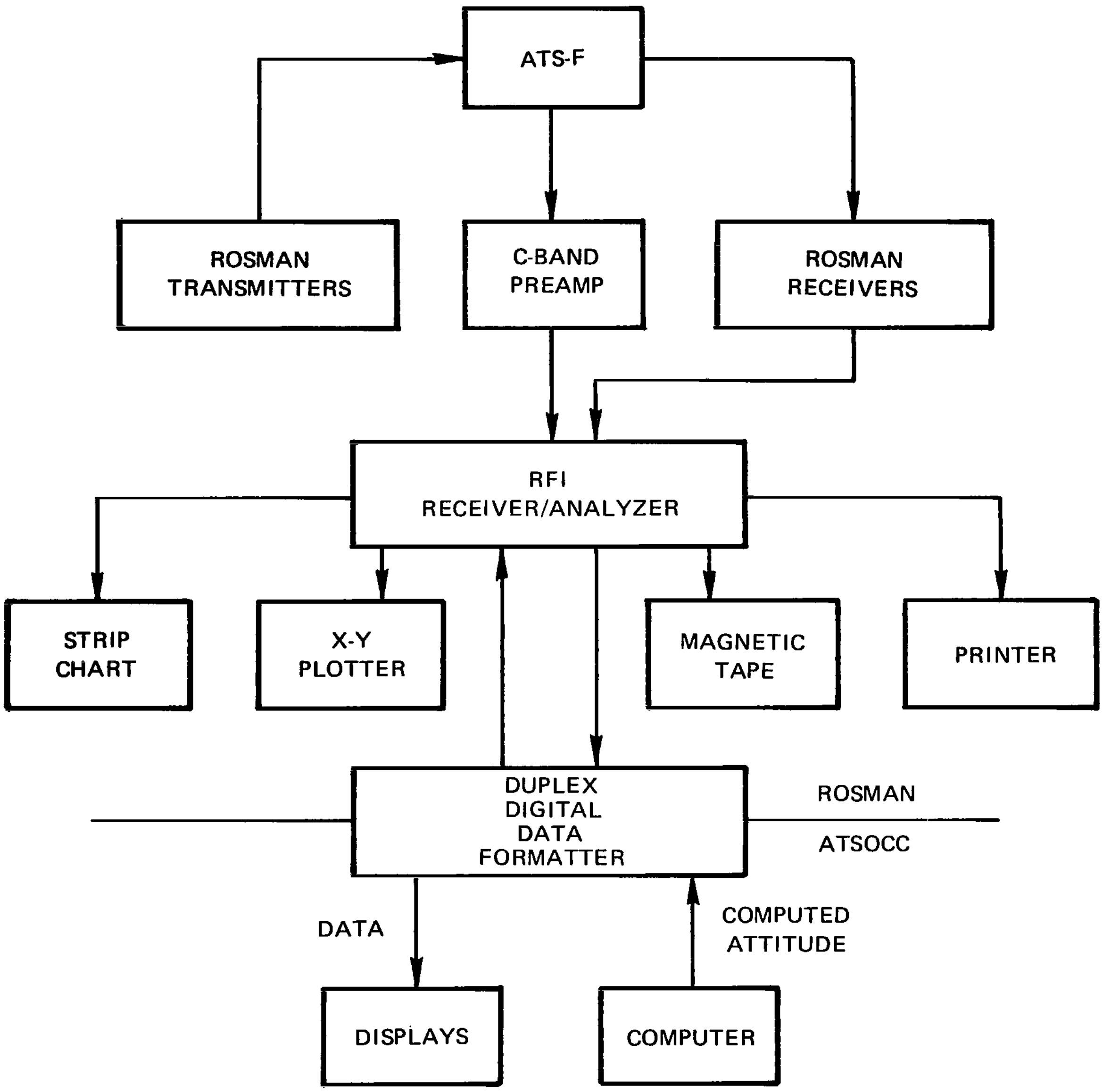

Figure 6. Equipment required for antenna pattern measurement.

antenna pattern measurement slew. For the patterns presented in this document, the range of Zaz (azimuth) has been changed to all positive angles in the range 0° to 360° (with no change in the 0° to $+180^\circ$ region). These plots accompany the antenna patterns and indicate the relative motion between the ground station and spacecraft (ATS-6). Some of the patterns also include a diagram identifying the antenna feed elements on the prime focus feed (PFF). The coordinates defined in Figure 5 are the ATS-6 body coordinates for antenna patterns, used in the Zaz, Zcoel diagrams that accompany the patterns. Figure 5 dipicts an east-west antenna pattern cut 1.1° north of the body Z-axis. The spacecraft maneuver to achieve this cut is a west-to-east maneuver 1.1° north of the roll axis.

The next section, VHF patterns, describes the necessary spacecraft maneuvers for the antenna patterns measured. The earth disk display of spacecraft maneuvers for the VHF pattern measurement, Figure 7 and Figure 8, antenna pattern cuts for VHF measurement, is an example of how the antenna pattern measurements are accomplished.

VHF PATTERNS

The VHF prime focus feed patterns were measured at 137.11 MHz. The antenna feed element locations are shown in Figure 1.

Figure 7, display of earth disk, shows ATS-6 maneuvers for VHF antenna pattern measurement. The display is one that depicts the motion of the spacecraft Z-axis on the earth surface during the maneuvers. Arrows have been added to indicate the directions of the slewing.

For the maneuvers (especially for wide angle antenna beams) care is taken not to point the spacecraft much beyond the earth's disk, in order to maintain control of the spacecraft. Therefore, the resulting patterns corresponding to these slews appear incomplete. However, by overlaying the separate patterns, the very good symmetry of the VHF pattern is revealed.

It should be noted that when the spacecraft is maneuvered in a northern direction (for a north-south slew) the southern portion of the antenna pattern is measured, or when the spacecraft is moving in a southern direction, the northern portion of the antenna pattern is measured. Figure 8 illustrates antenna pattern cuts corresponding to Figure 7. Figures 9 through 12 are VHF antenna patterns.

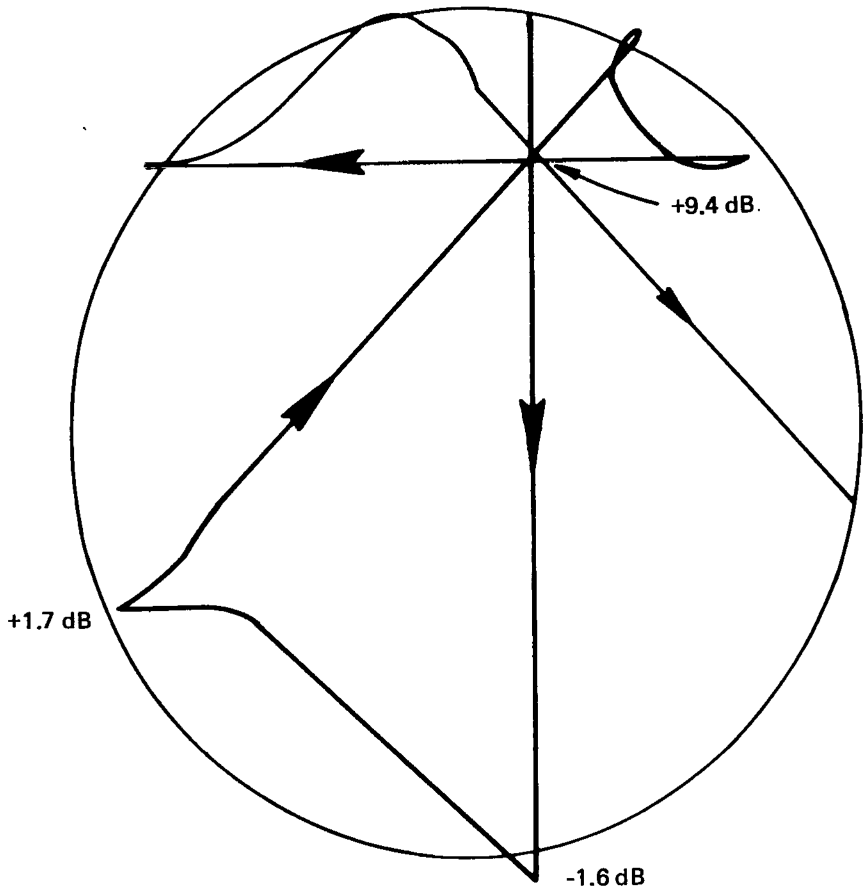

REFERENCE NOTATIONS AND VALUES HAVE BEEN MANUALLY ADDED.

Figure 7. Earth disk display of spacecraft maneuvers for VHF antenna pattern measurement.

ATS-6 ANTENNA PATTERN GAIN VS. ATTITUDE

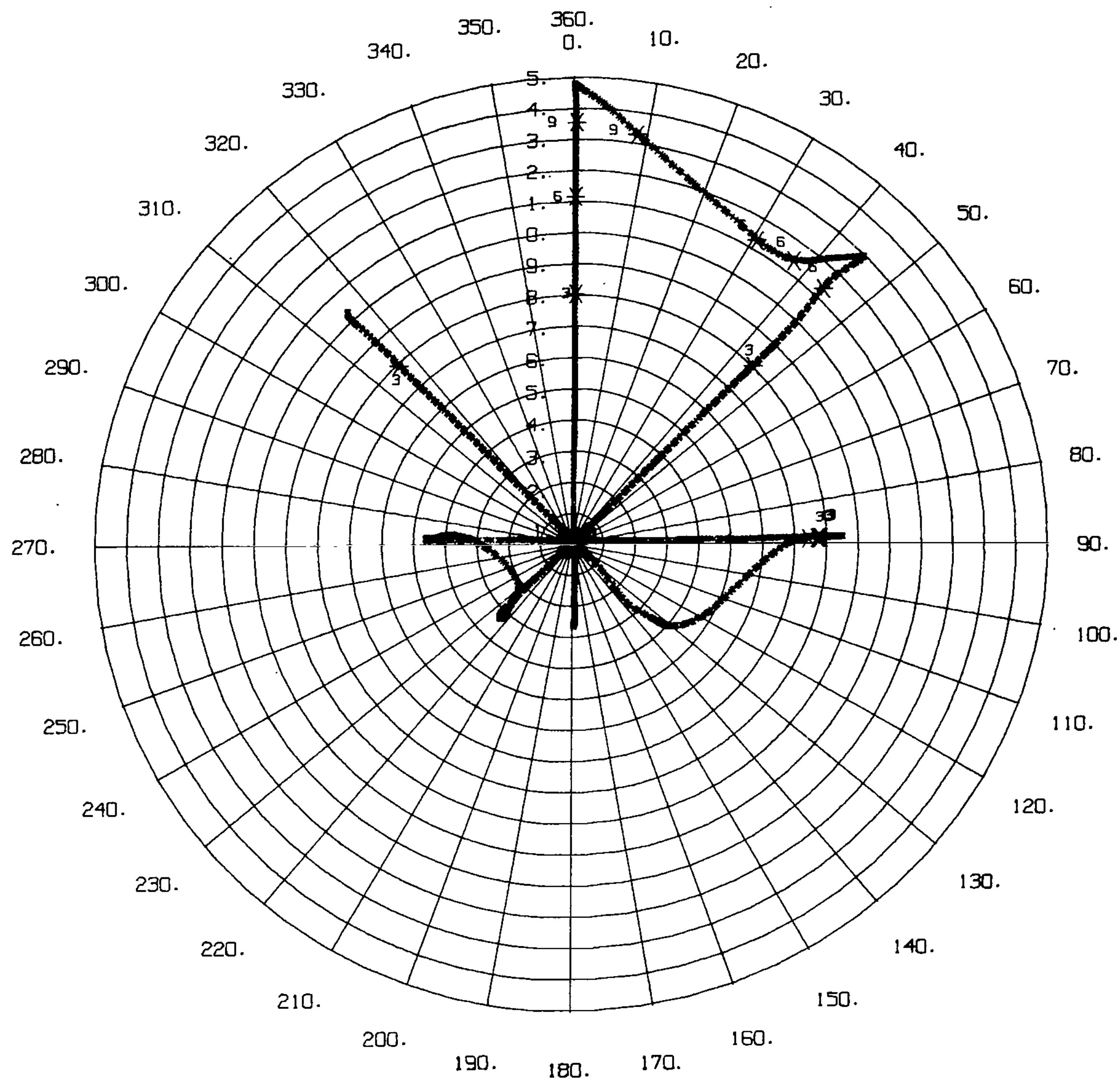

ATTITUDE EXPRESSED AS ZAZ AND ZCOEL IN DEGREES

Figure 8. Antenna pattern "cuts" for VHF measurement.

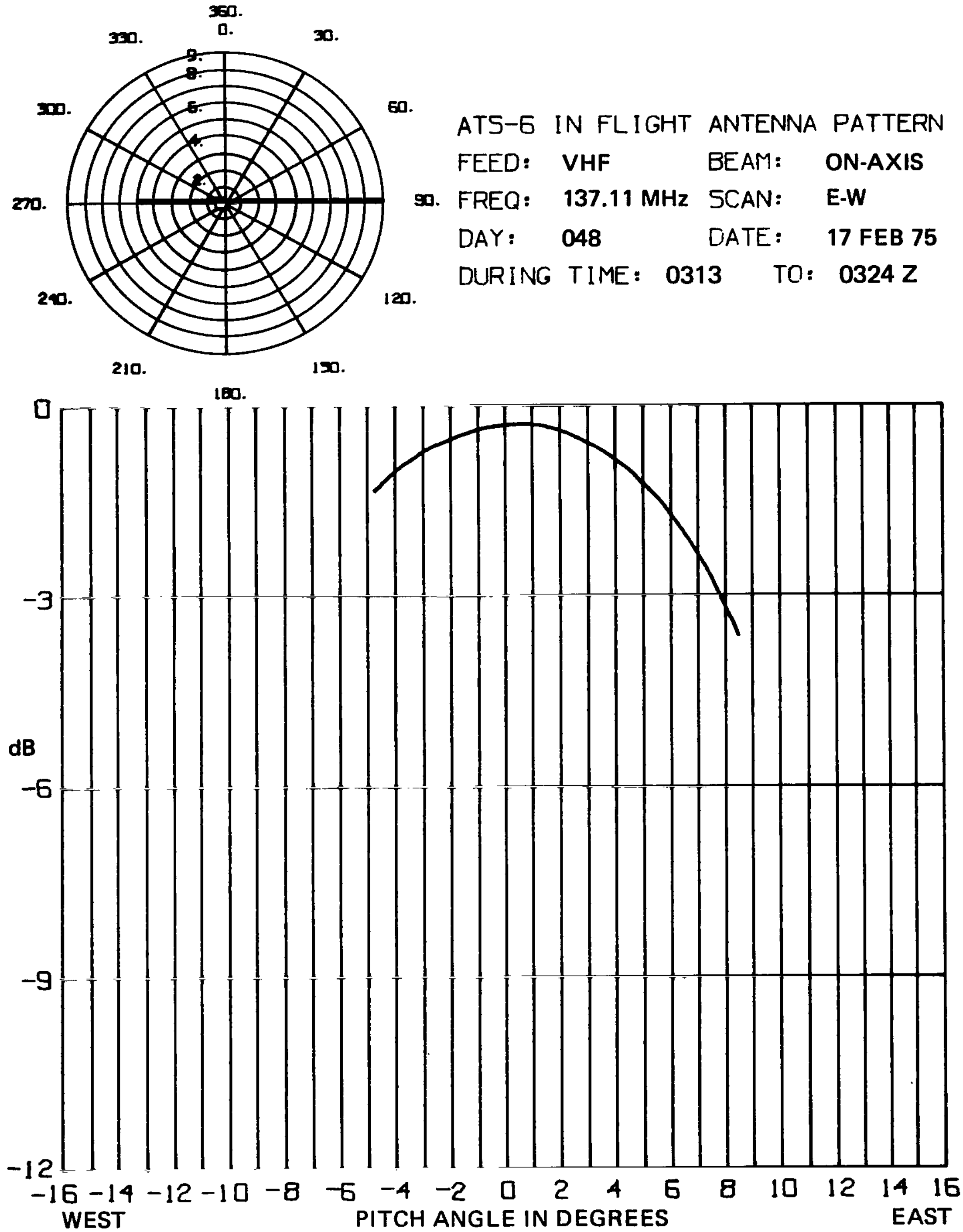

Figure 9. VHF antenna pattern E – W.

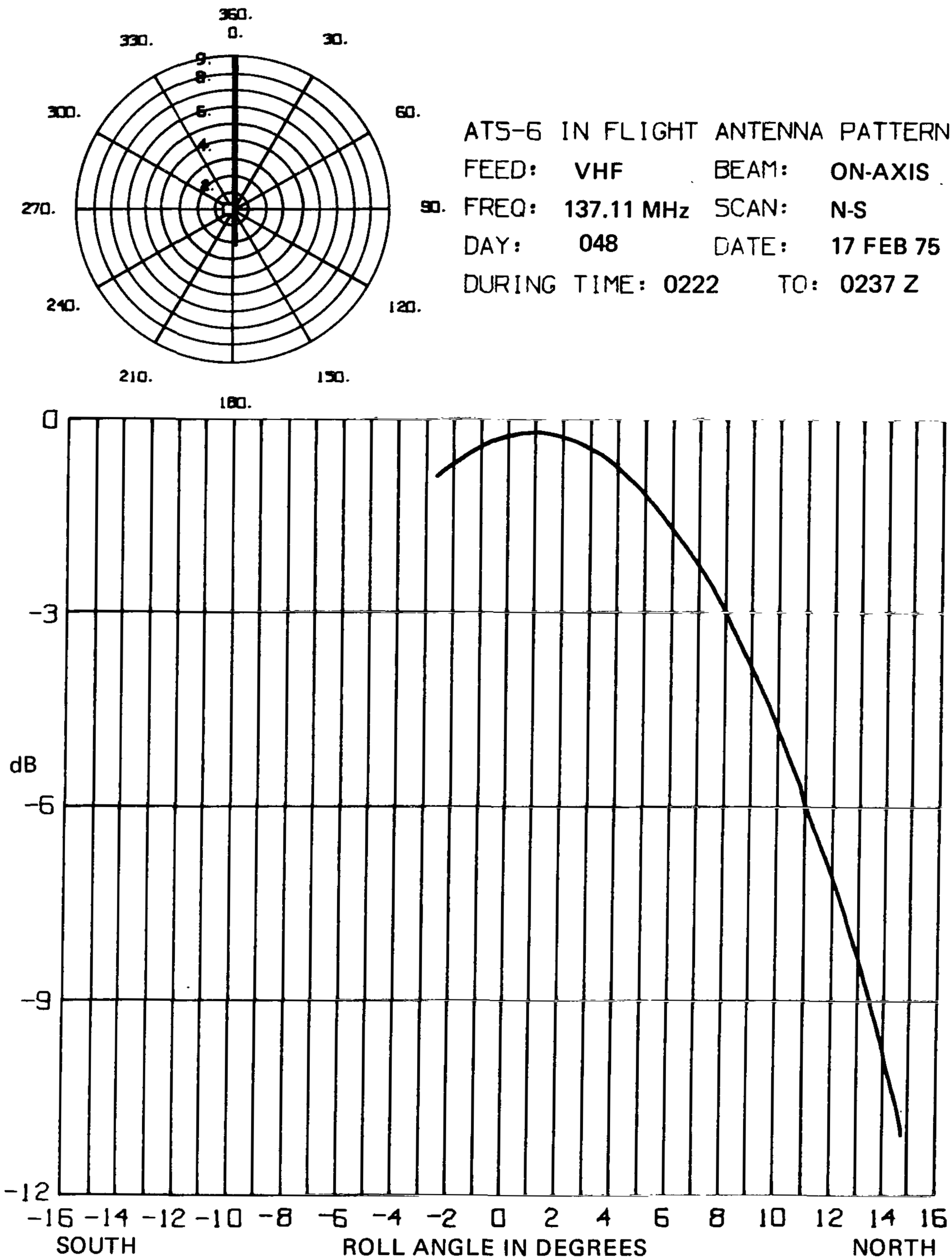

Figure 10. VHF antenna pattern N – S.

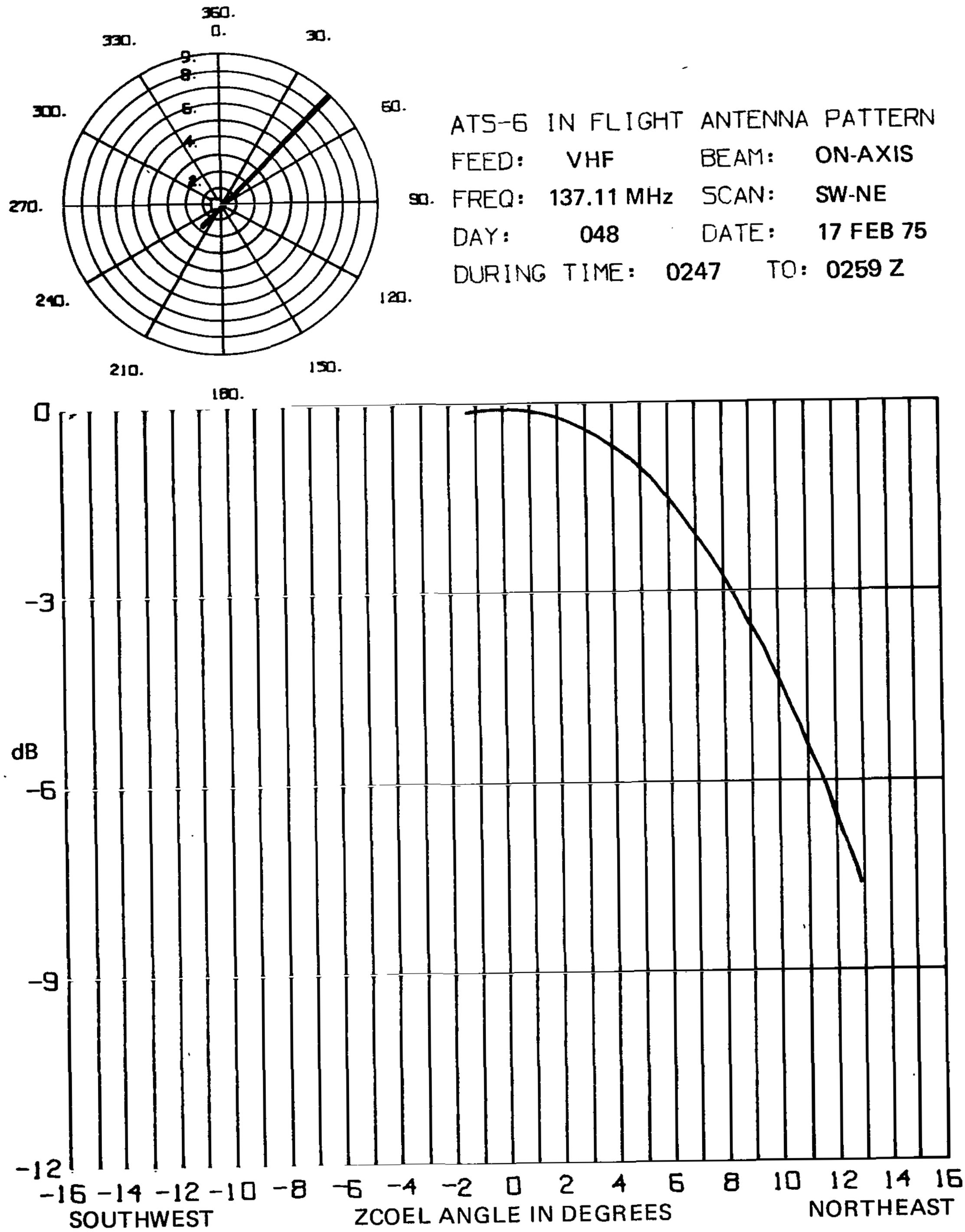

Figure 11. VHF antenna pattern SW – NE.

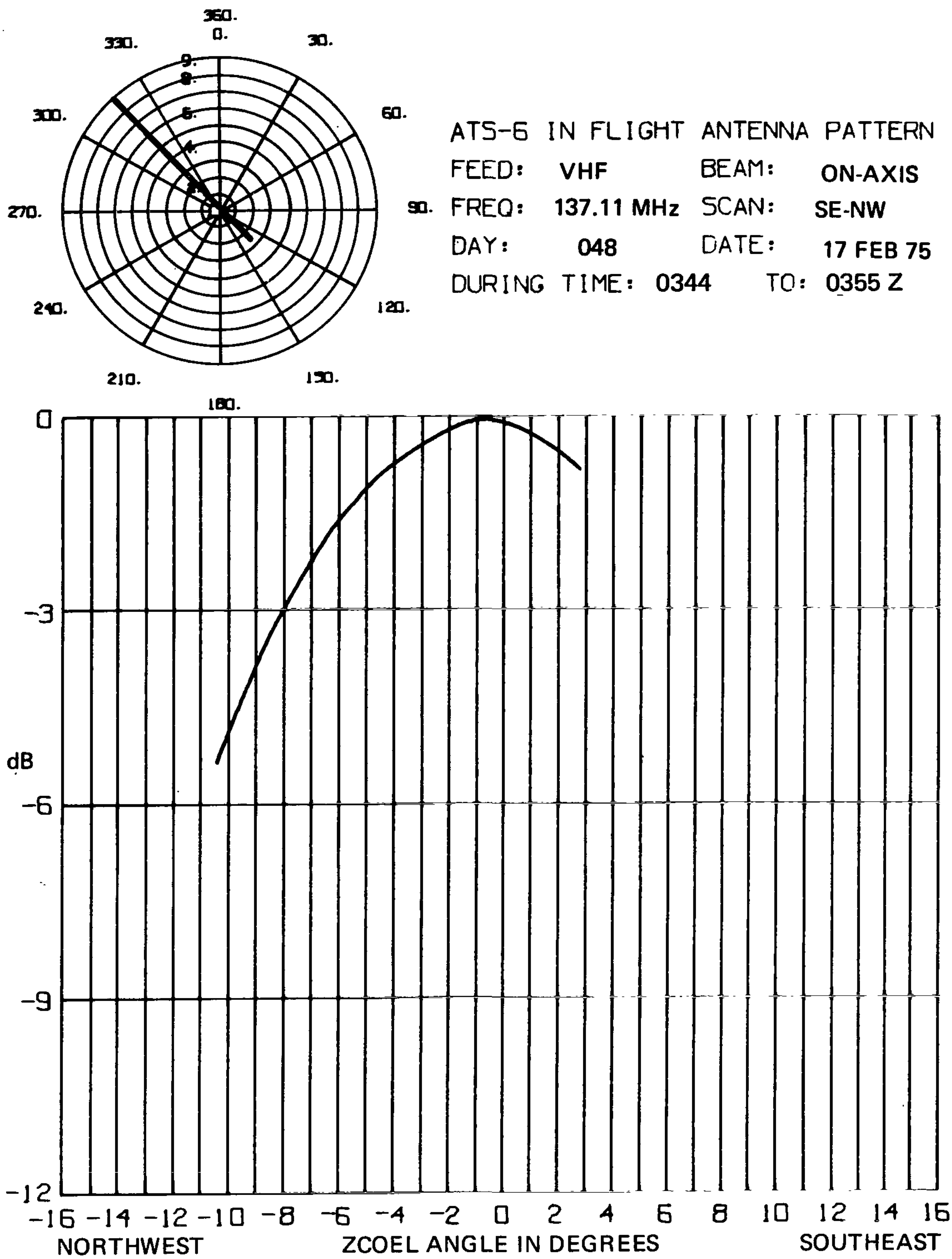

Figure 12. VHF antenna pattern NW – SE.

UHF ANTENNA PATTERNS

The UHF patterns were measured at 860 MHz. Antenna feed locations on the PFF are shown in Figure 1.

For the UHF patterns a comparison may be made between the preflight and in-orbit measurements since they are plotted together. From this comparison good agreement between preflight and in-orbit patterns is evident for the main lobe. The first sidelobes are about 2 dB higher in power level for the in-orbit pattern compared to the preflight pattern. This may be due to the differences between the hard dish model and the actual flight model. There is a difference between the hard dish model and the flight model in the area of the orbit control jet (OCJ) bar located on the east and west truss structure. Figures 13 through 16 are UHF antenna patterns.

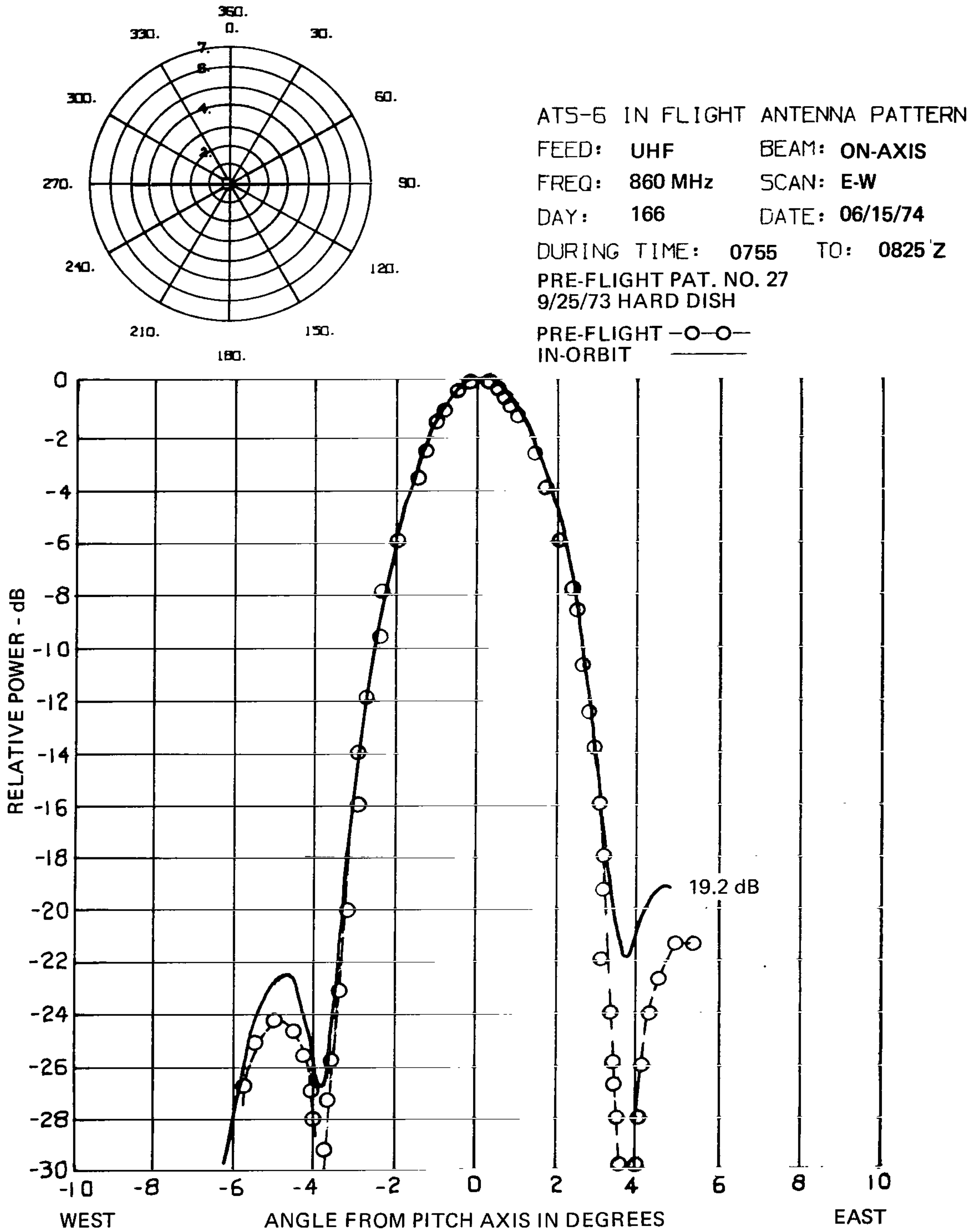

Figure 13. UHF antenna pattern E — W.

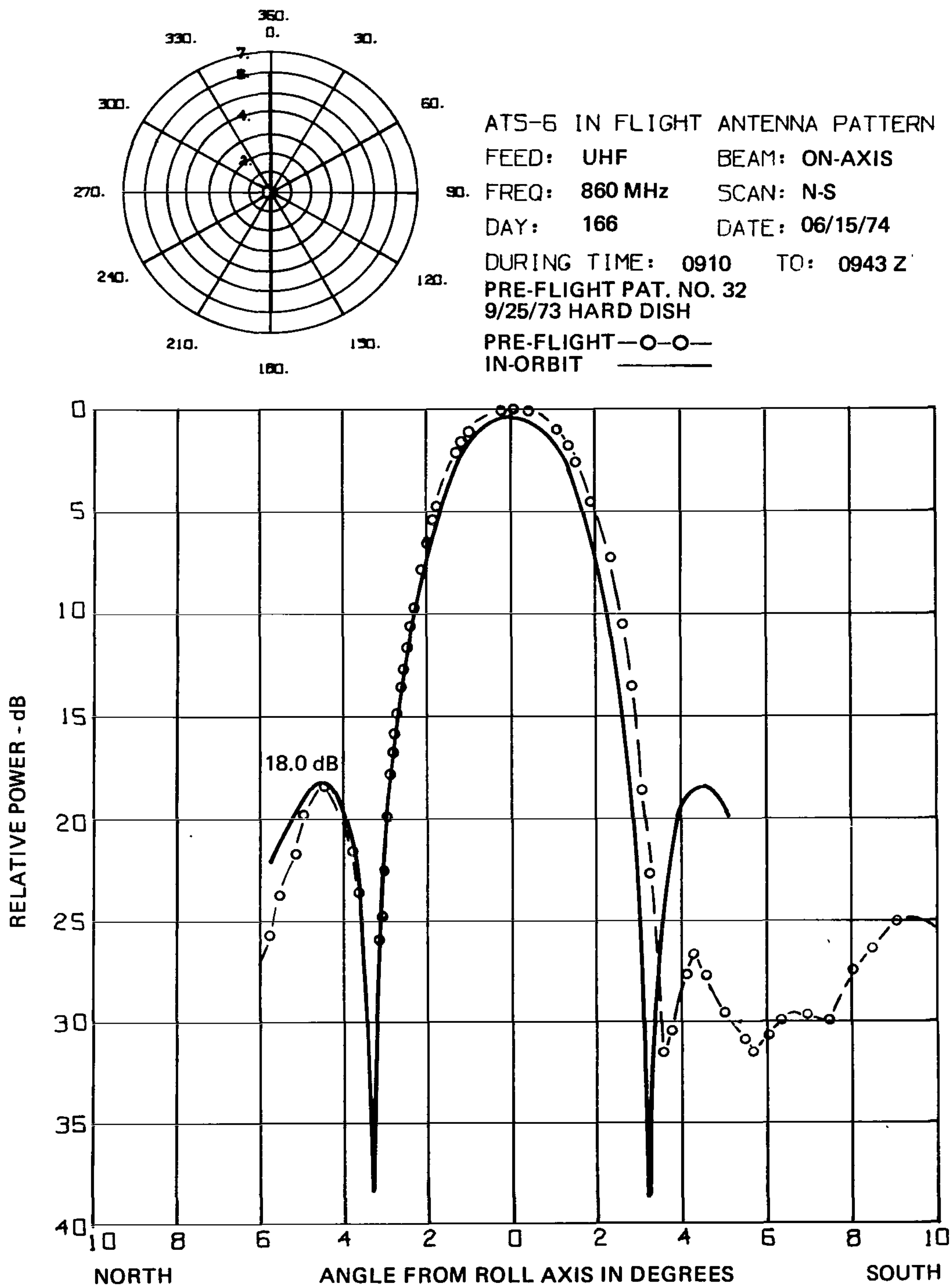

Figure 14. UHF antenna pattern N – S.

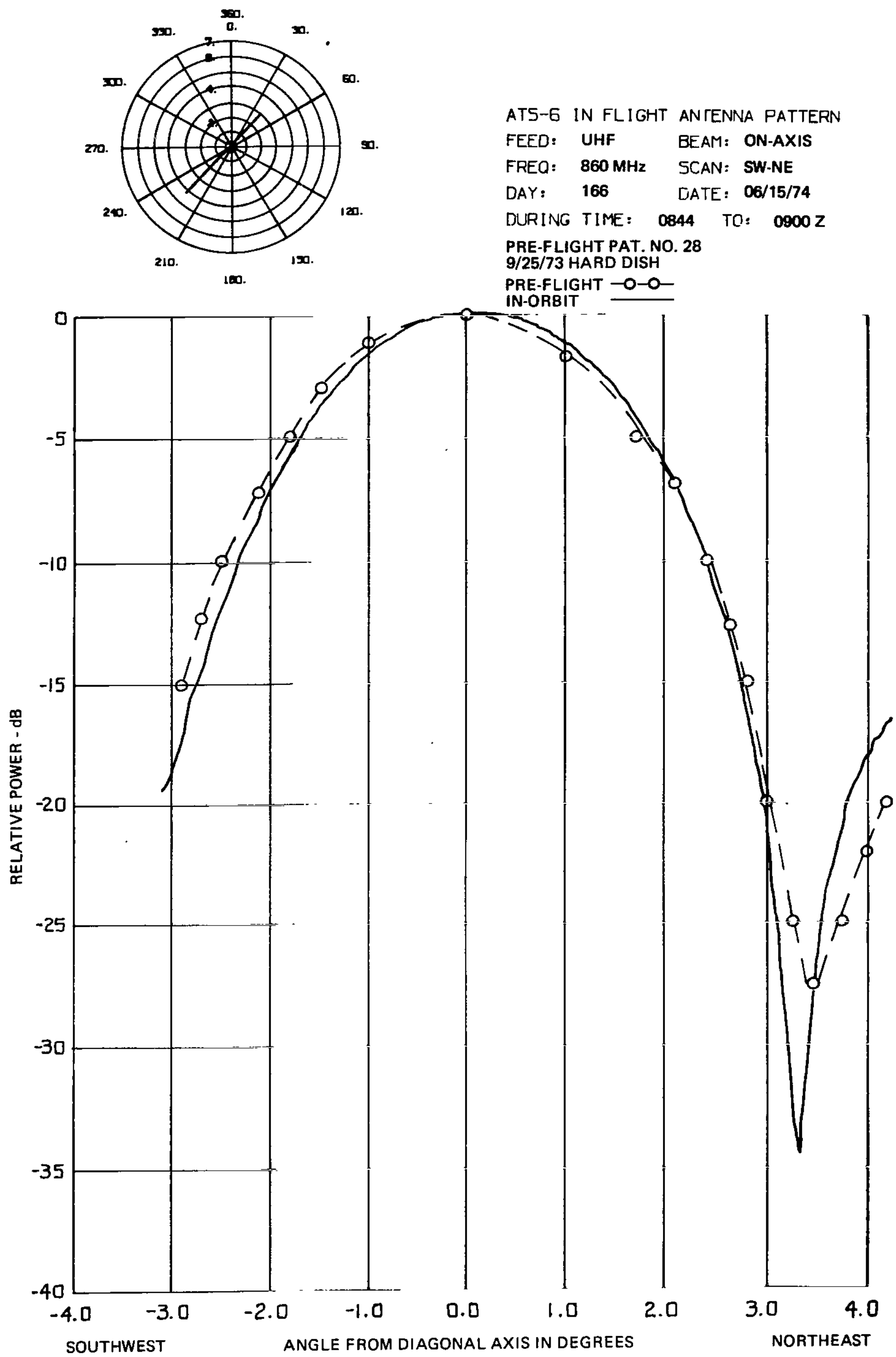

Figure 15. UHF antenna pattern SW – NE.

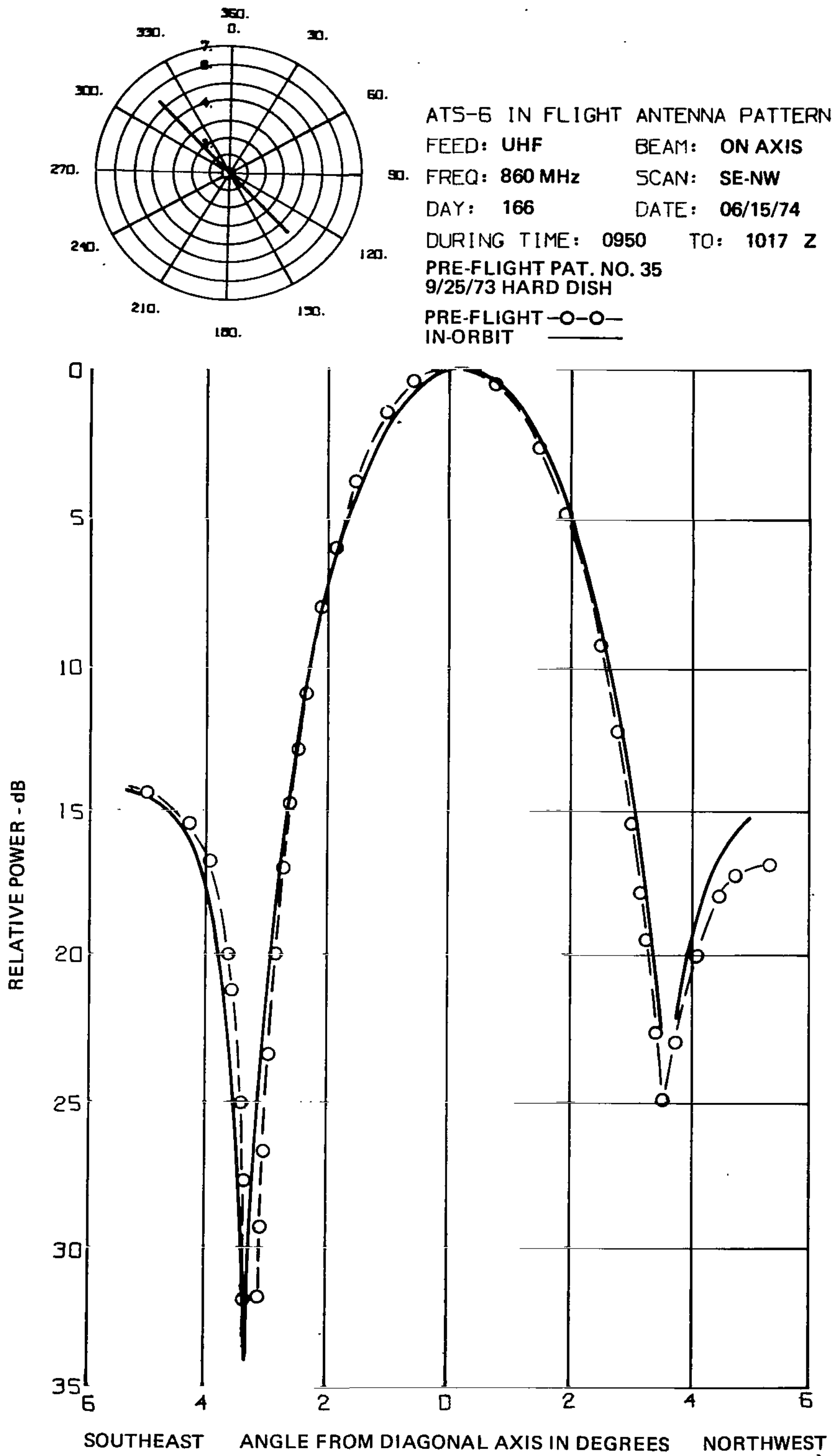

Figure 16. UHF antenna pattern SE – NW.

L-BAND PENCIL BEAM PATTERNS

The L-band pencil beam is of the "offset" type, specifically seen to be offset from the spacecraft Z-axis by 1° to the east and 3.9° to the north. (Figure 1 shows feed offset to the west which places beam offset to the east.)

In-flight patterns for various cuts were accomplished. The two W–E patterns at 4° N, Figure 17 and 3.84° N, Figure 18 were made to check the repeatability of the measurements, which showed it to be good. The SW–NE measurement was made because of the interest in the pencil beam's northeasterly direction. Figures 17 through 20 are L-band pencil beam antenna patterns.

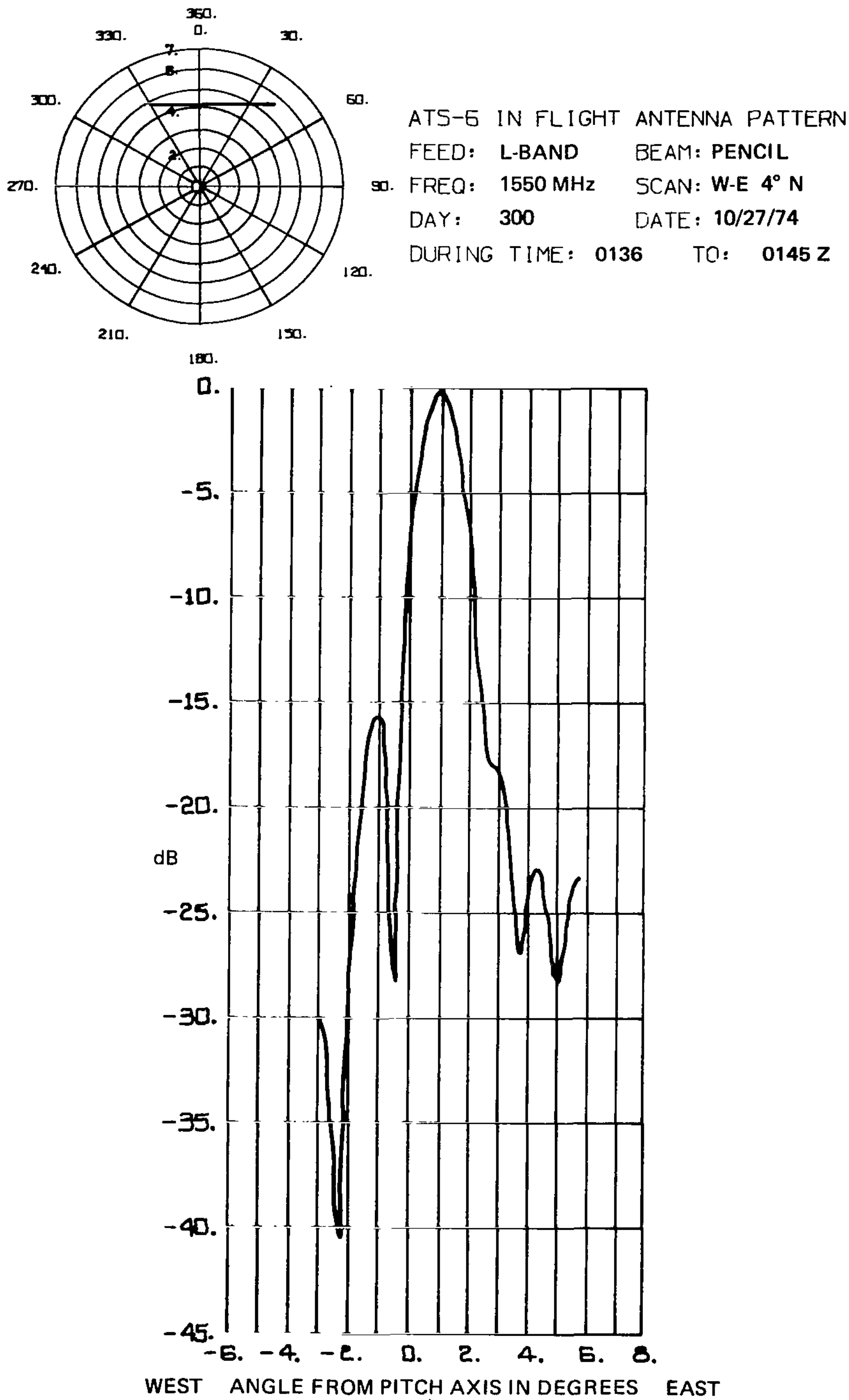

Figure 17. L-band pencil beam pattern E – W.

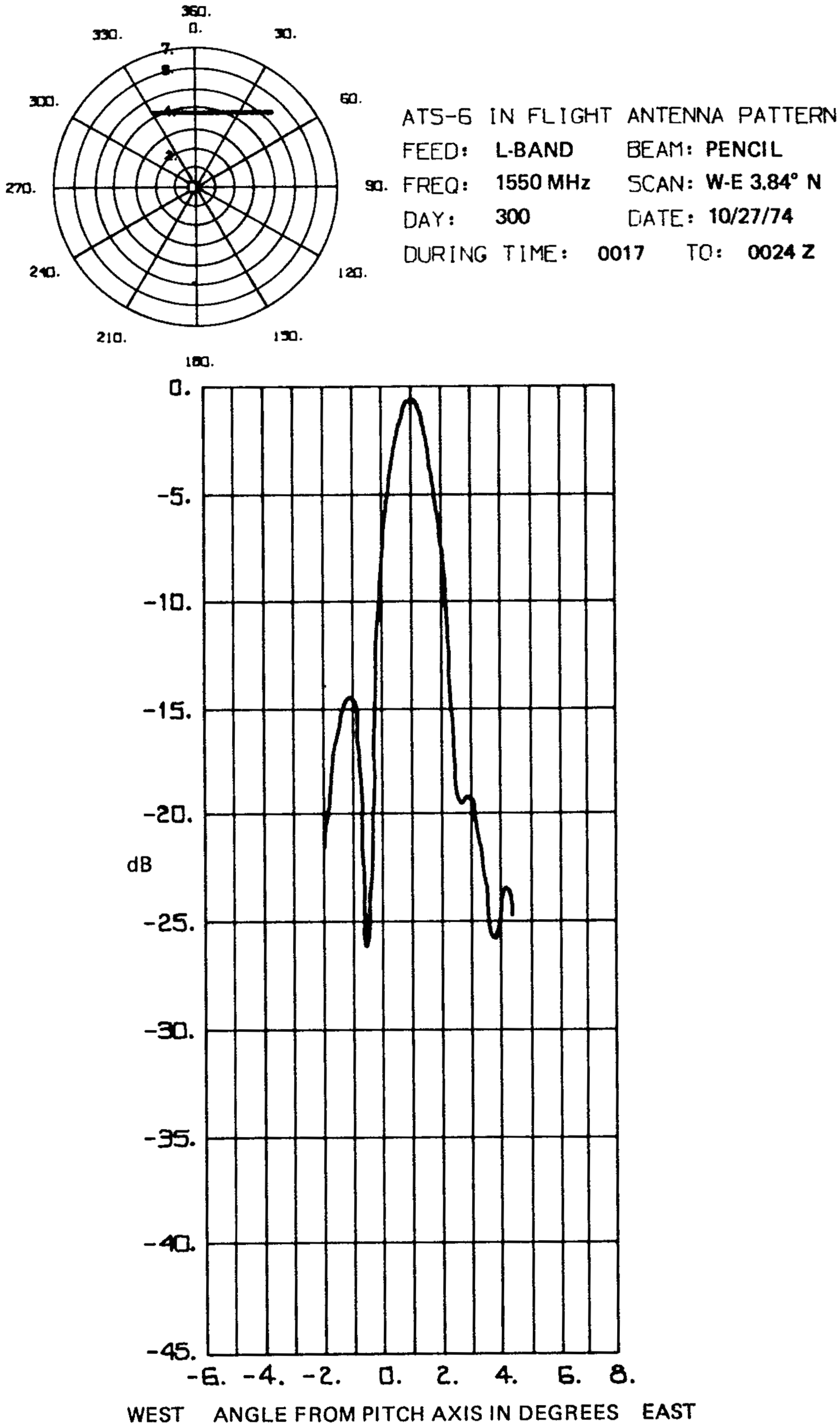

Figure 18. L-band pencil beam pattern E – W.

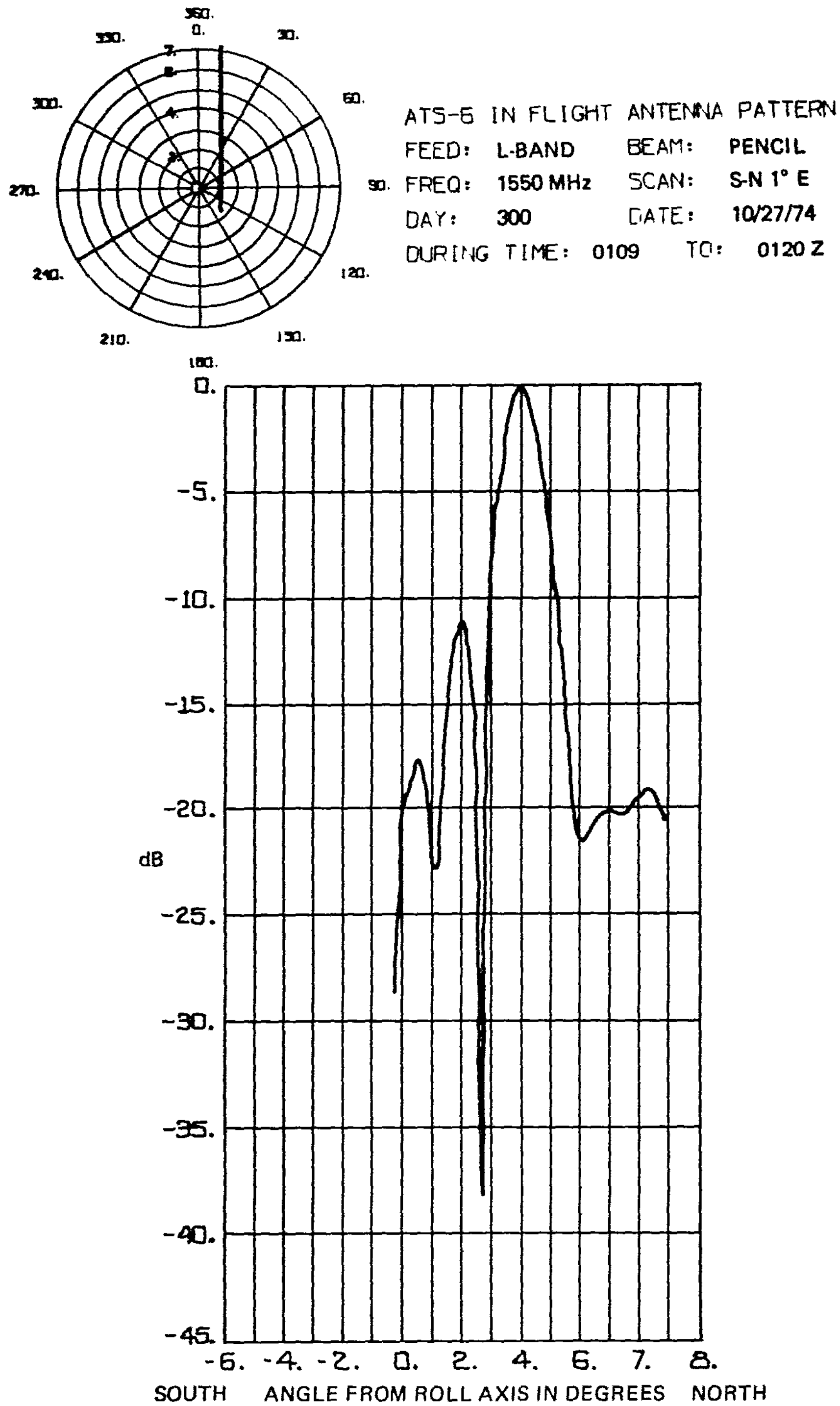

Figure 19. L-band pencil beam pattern N – S.

L-BAND FAN BEAM PATTERNS

The L-band fan beam is of the offset type in order to cover the North Atlantic area with the fan beam when ATS-6 is at 94° W longitude.

In attempting to compare the in-flight patterns with those preflight, the cuts chosen were 3.1° N for the E–W slew and 1° E for the N–S slew. These patterns were "overlayed" on the preflight pattern, and the results are shown in Figures 21 and 22. The correlation is quite good for the E–W results except for the "dip". This may be because the preflight pattern was not measured at the same angular distance (3.1° N) as the in-flight pattern. Similarly, and for the same reason, the results for the N–S patterns show some discrepancy. However, extensive in-flight antenna patterns for the L-band beam for a series of E–W cuts (Figure 21 and Figures 23 through 30; Figure 22 is not E–W), and N–S cuts (Figures 31 through 52) were made.

A contour pattern of the L-band fan beam showing contours of equal power levels, scaled to degrees in pitch and roll, is shown in Figure 53.

A three-dimensional model was constructed and is shown in Figure 54 pictorial form.

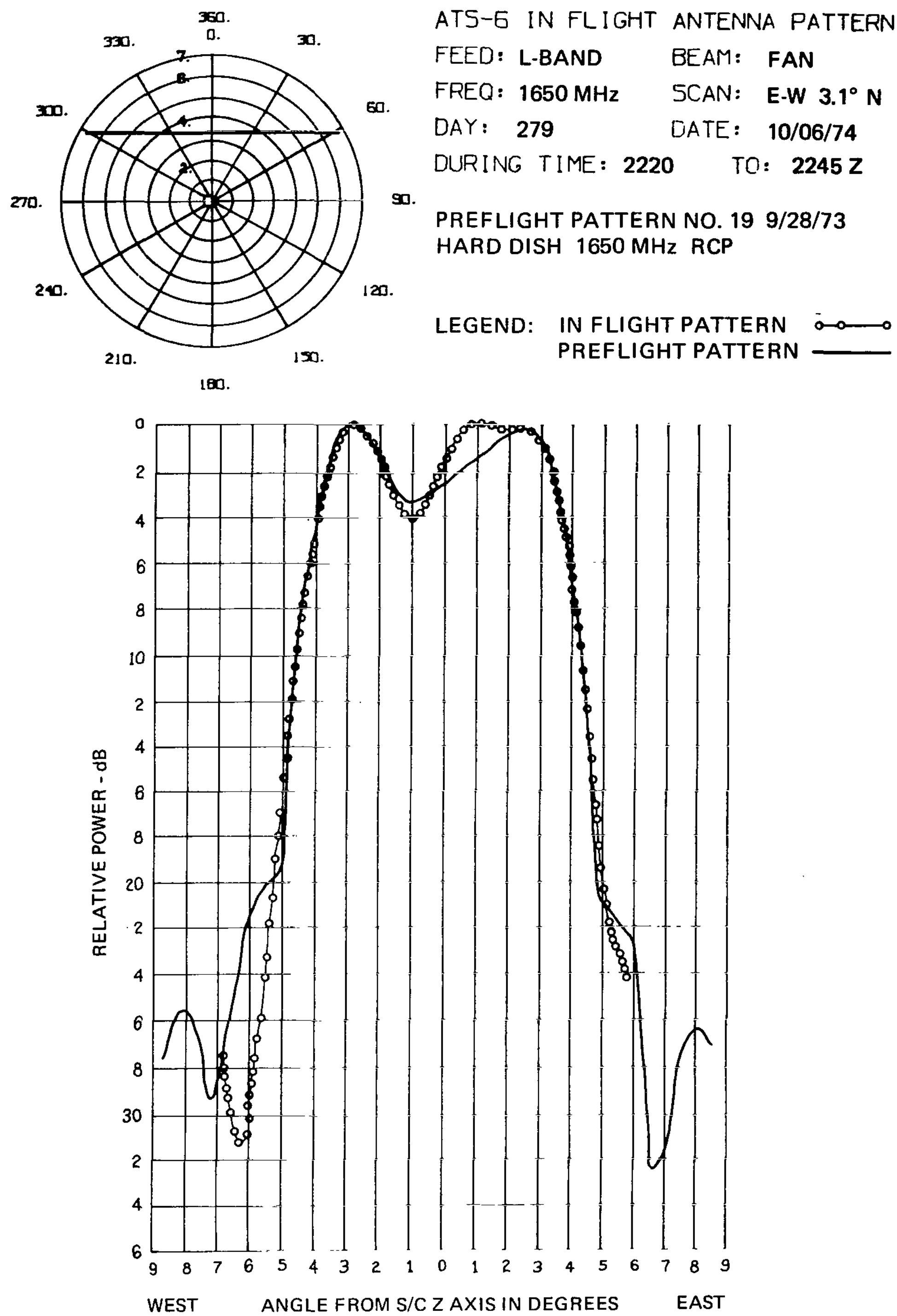

Figure 21. L-band fan beam pattern E – W 3.1° W.

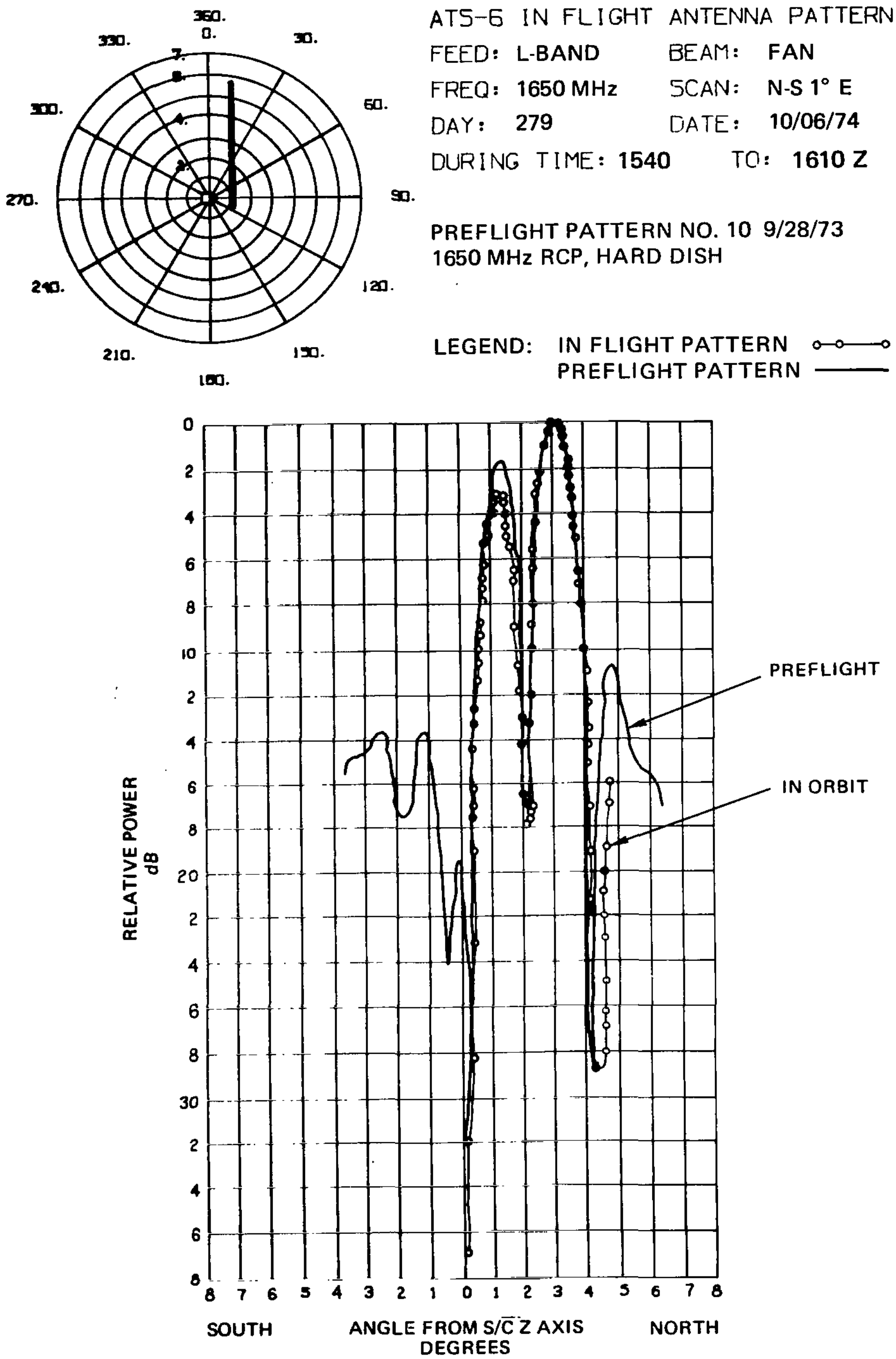

Figure 22. L-band fan beam pattern N – S 1° E.

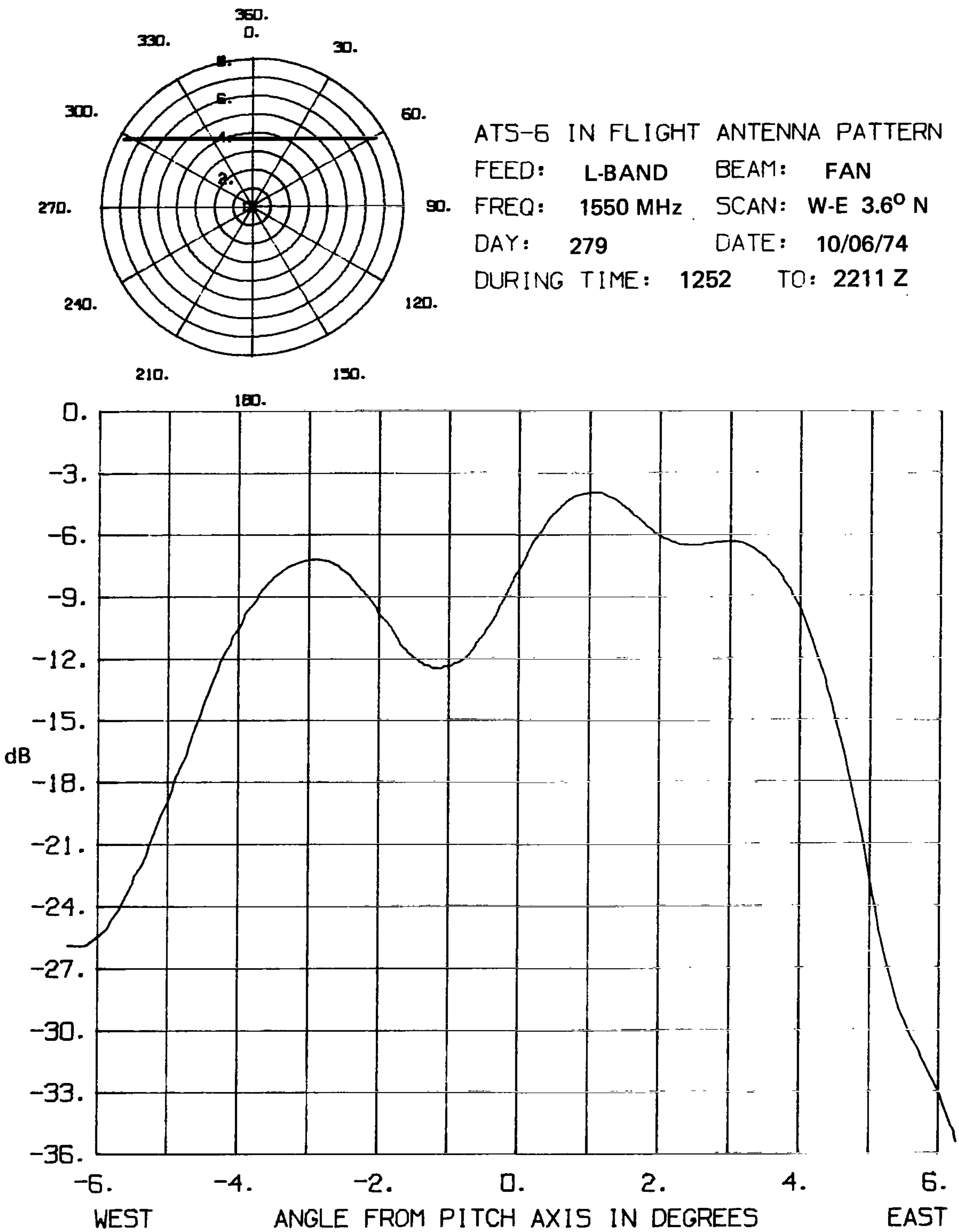

Figure 23. L-band fan beam pattern E – W 3.6° N.

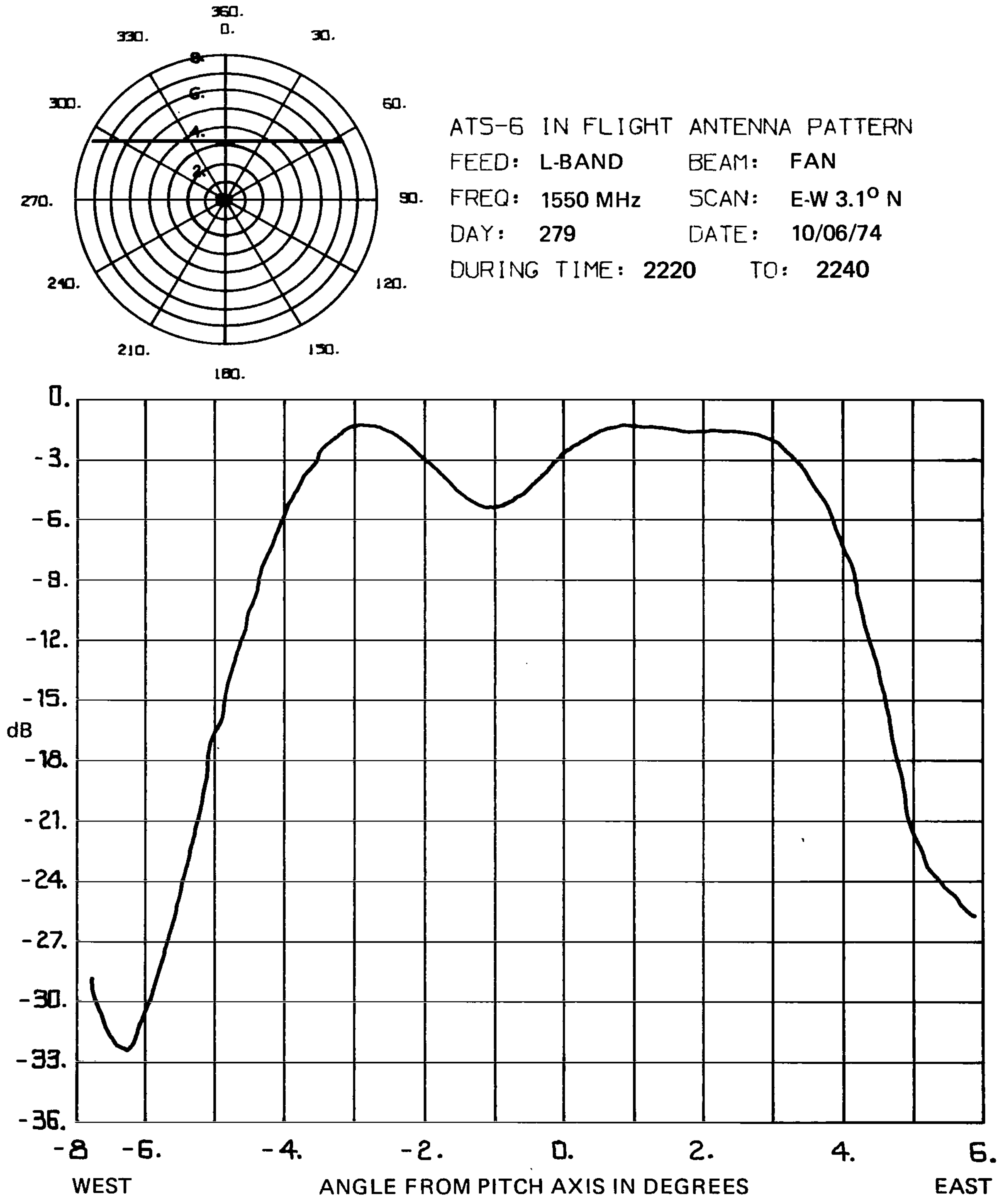

Figure 24. L-band fan beam pattern E – W 3.1° N.

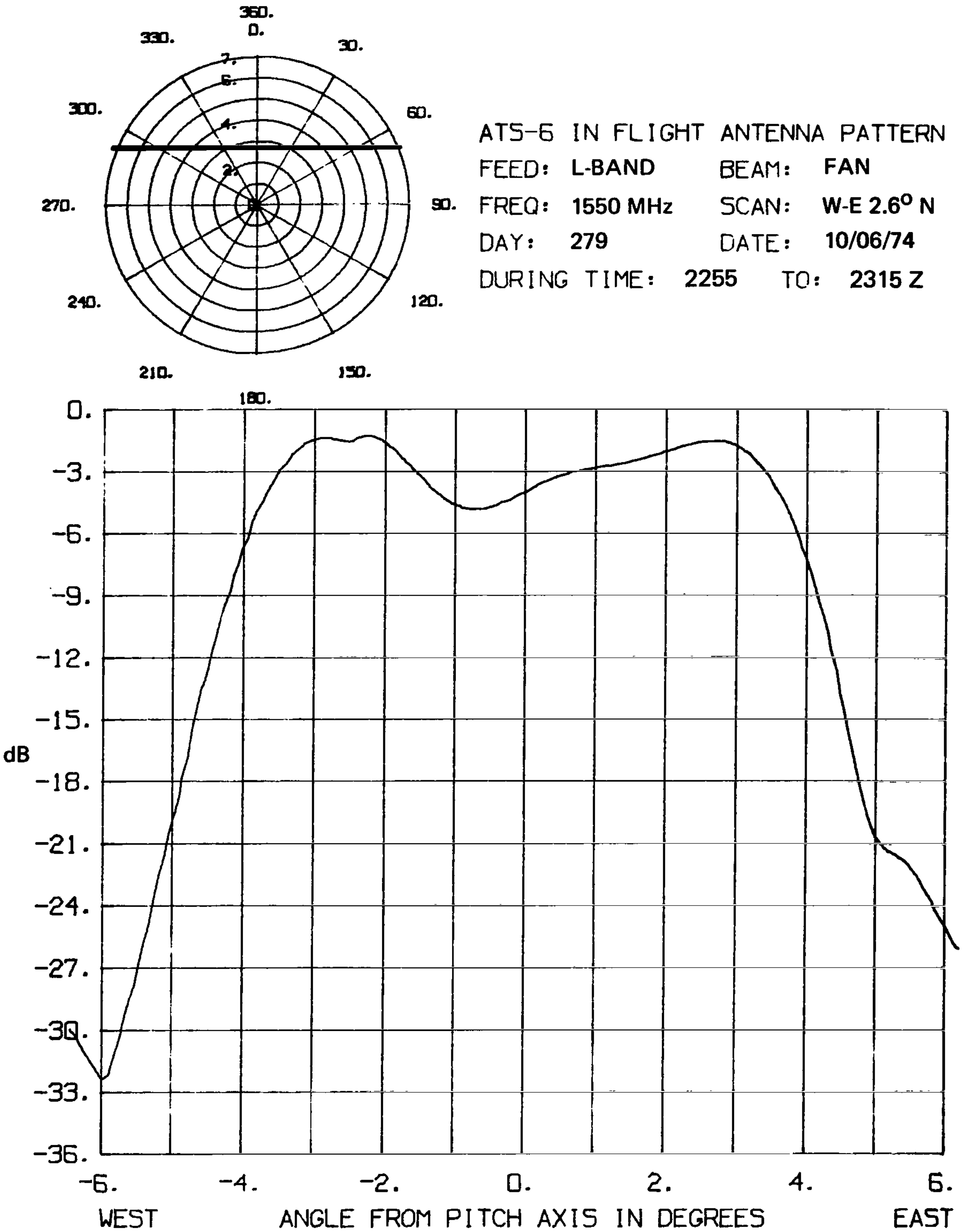

Figure 25. L-band fan beam pattern E – W 2.6° N.

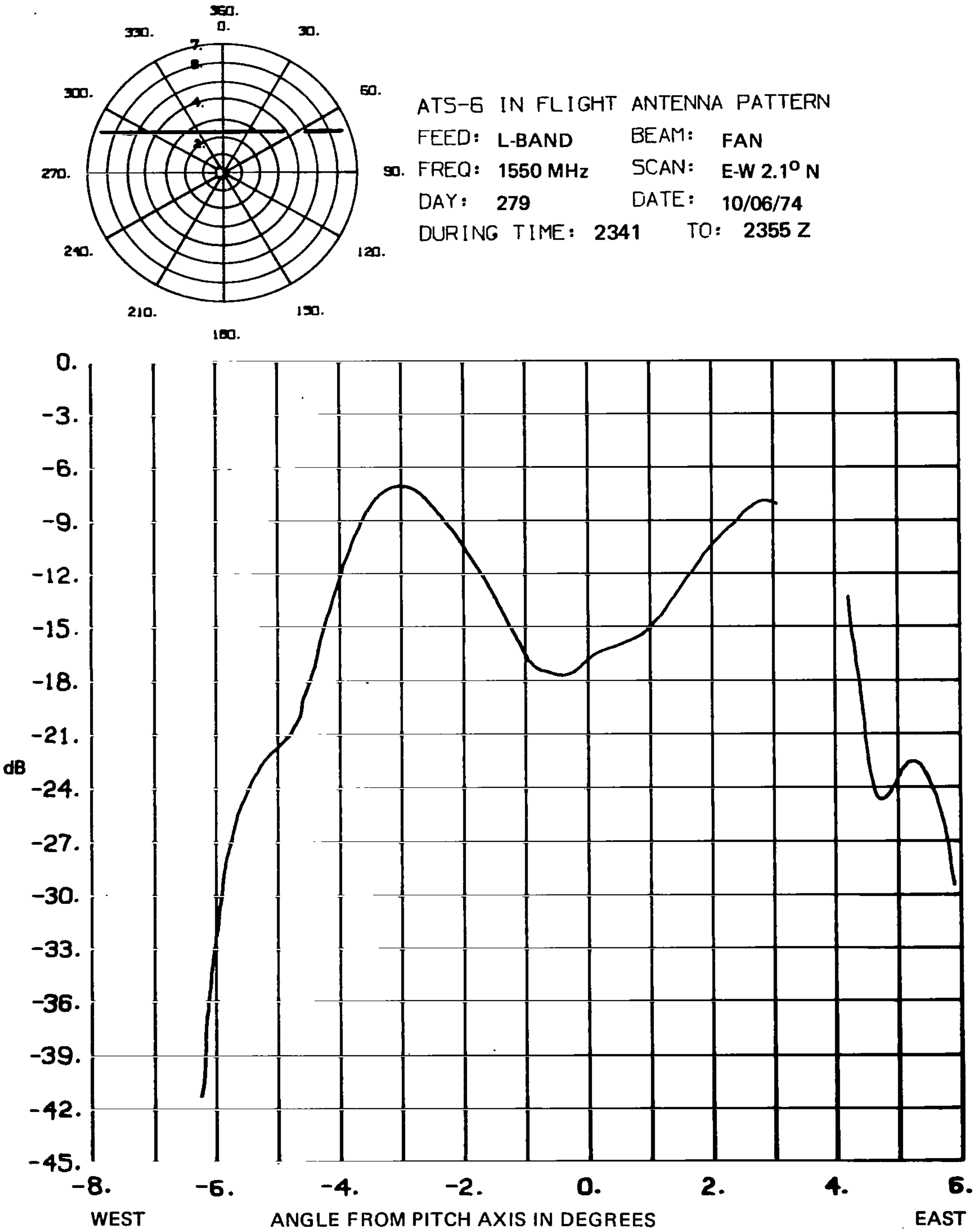

Figure 26. L-band fan beam pattern E – W 2.1° N.

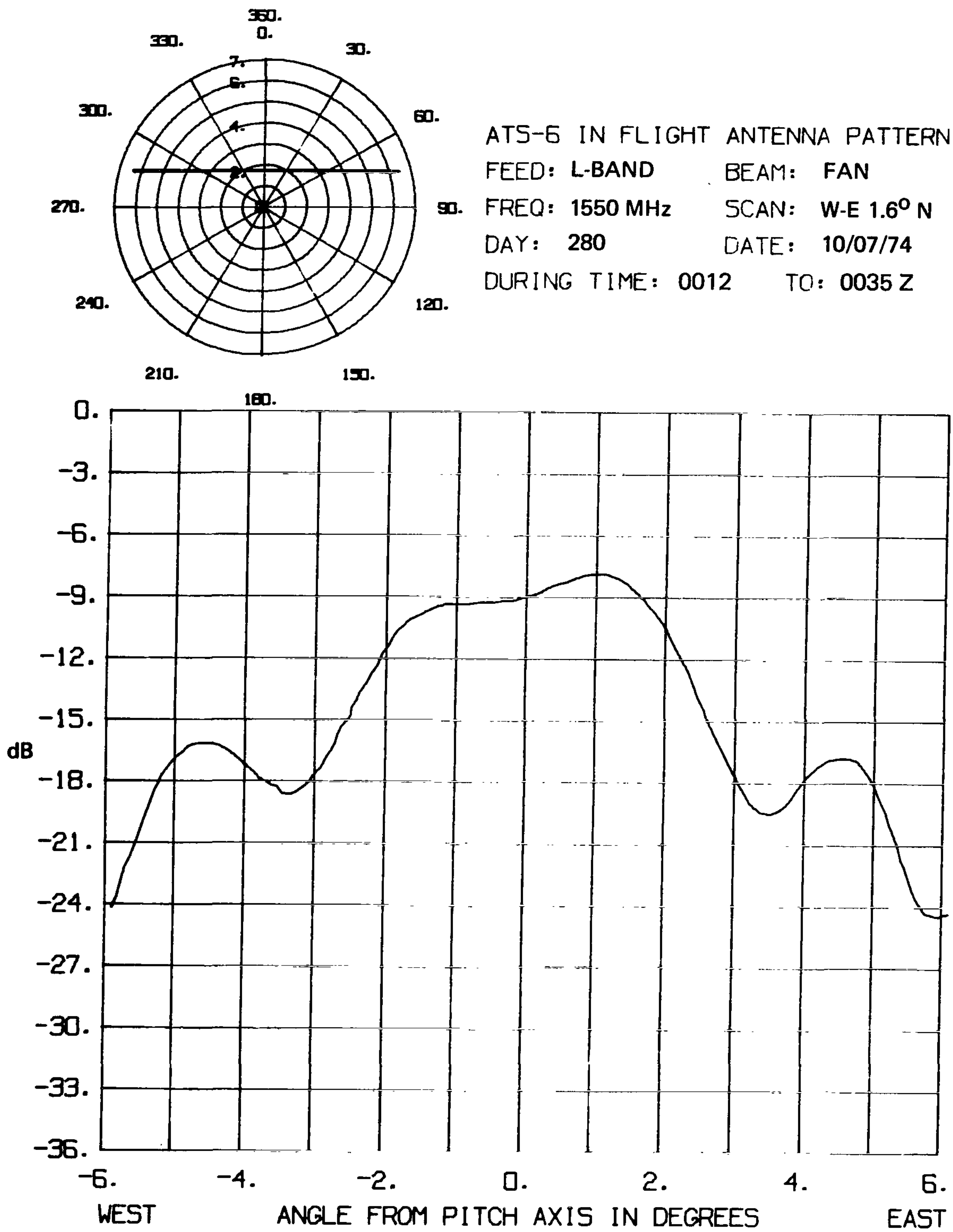

Figure 27. L-band fan beam pattern E – W 1.6° N.

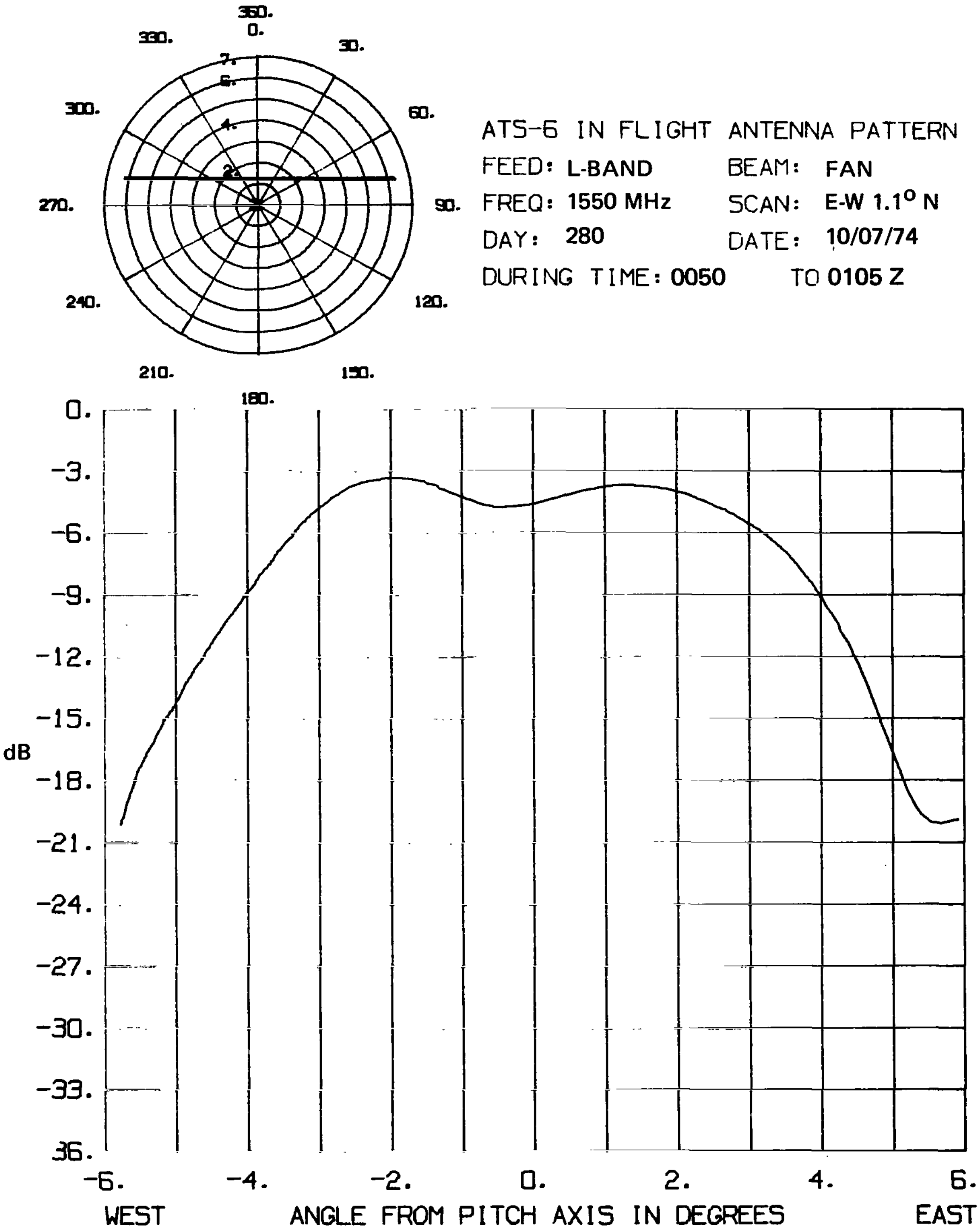

Figure 28. L-band fan beam pattern E – W 1.1° N.

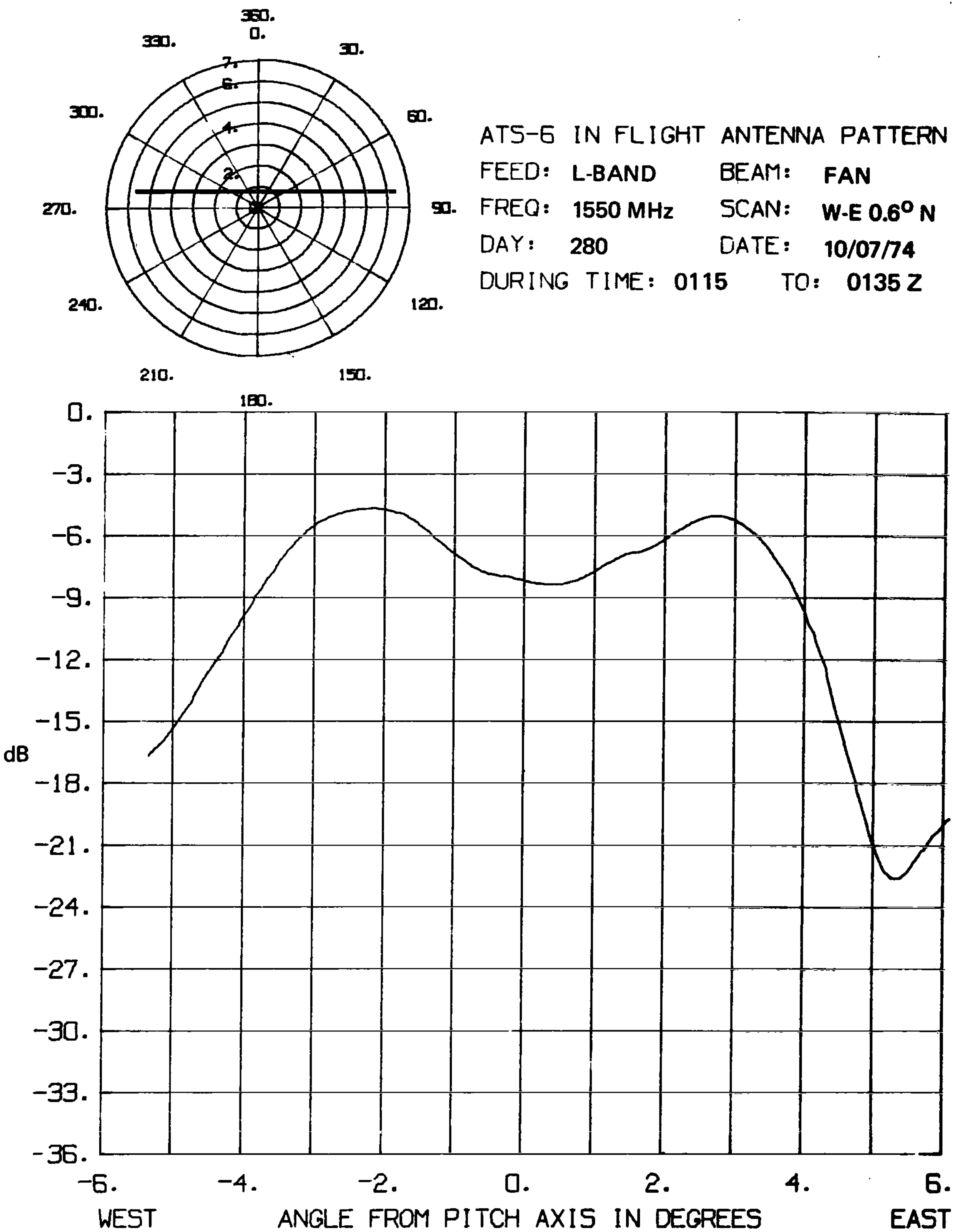

Figure 29. L-band fan beam pattern E – W 0.6° N.

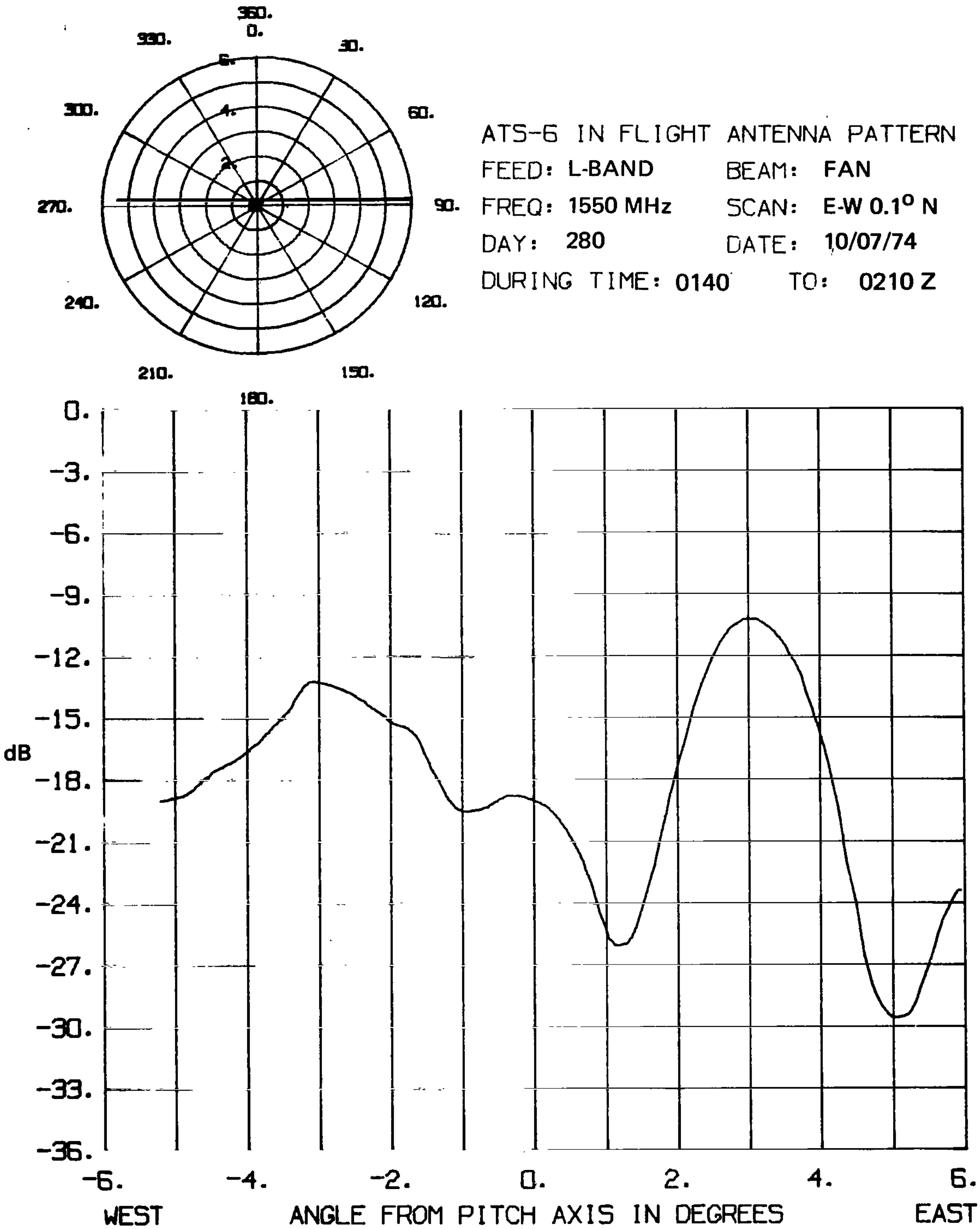

Figure 30. L-band fan beam pattern E – W 0.1° W.

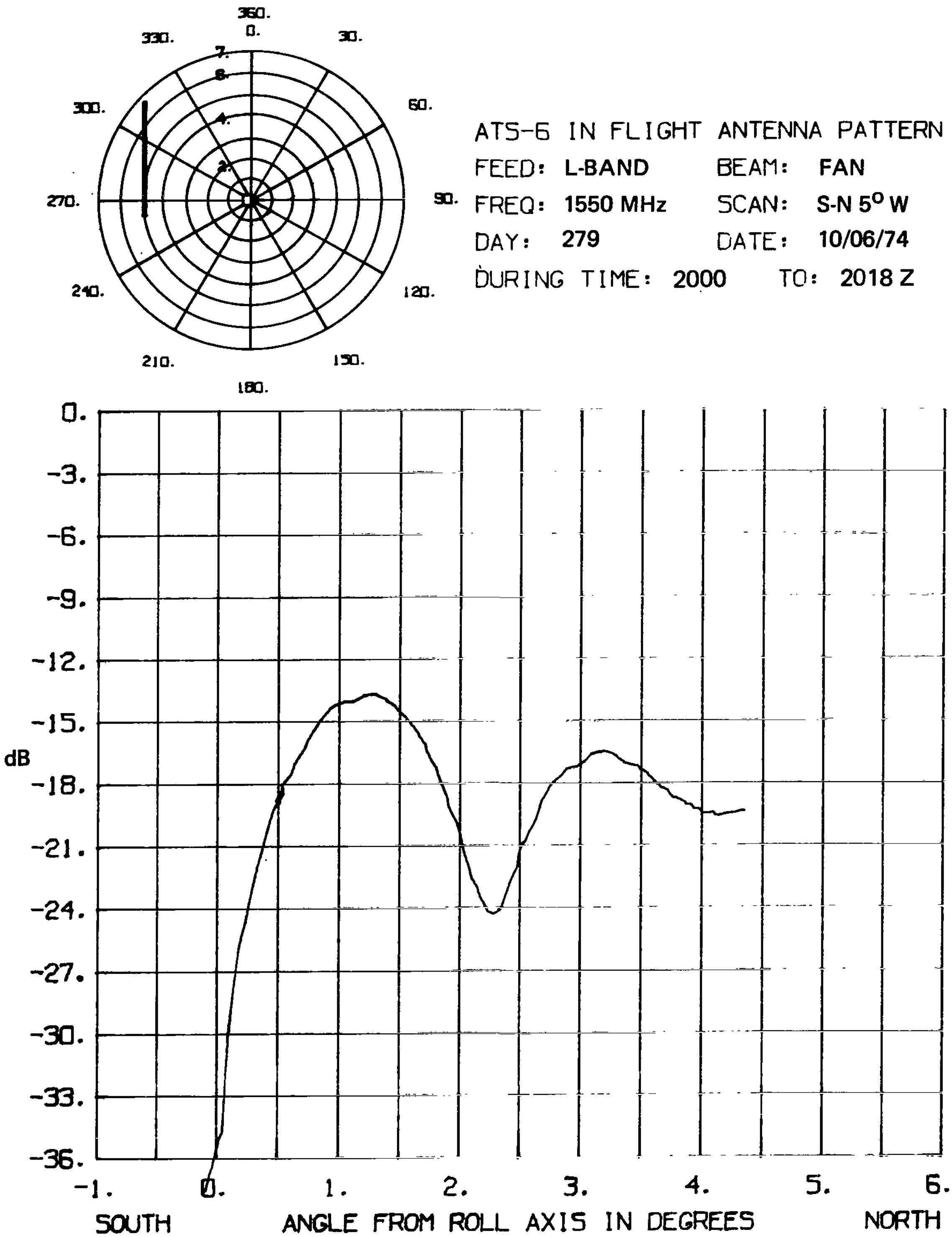

Figure 31. L-band fan beam pattern N – S 5° W.

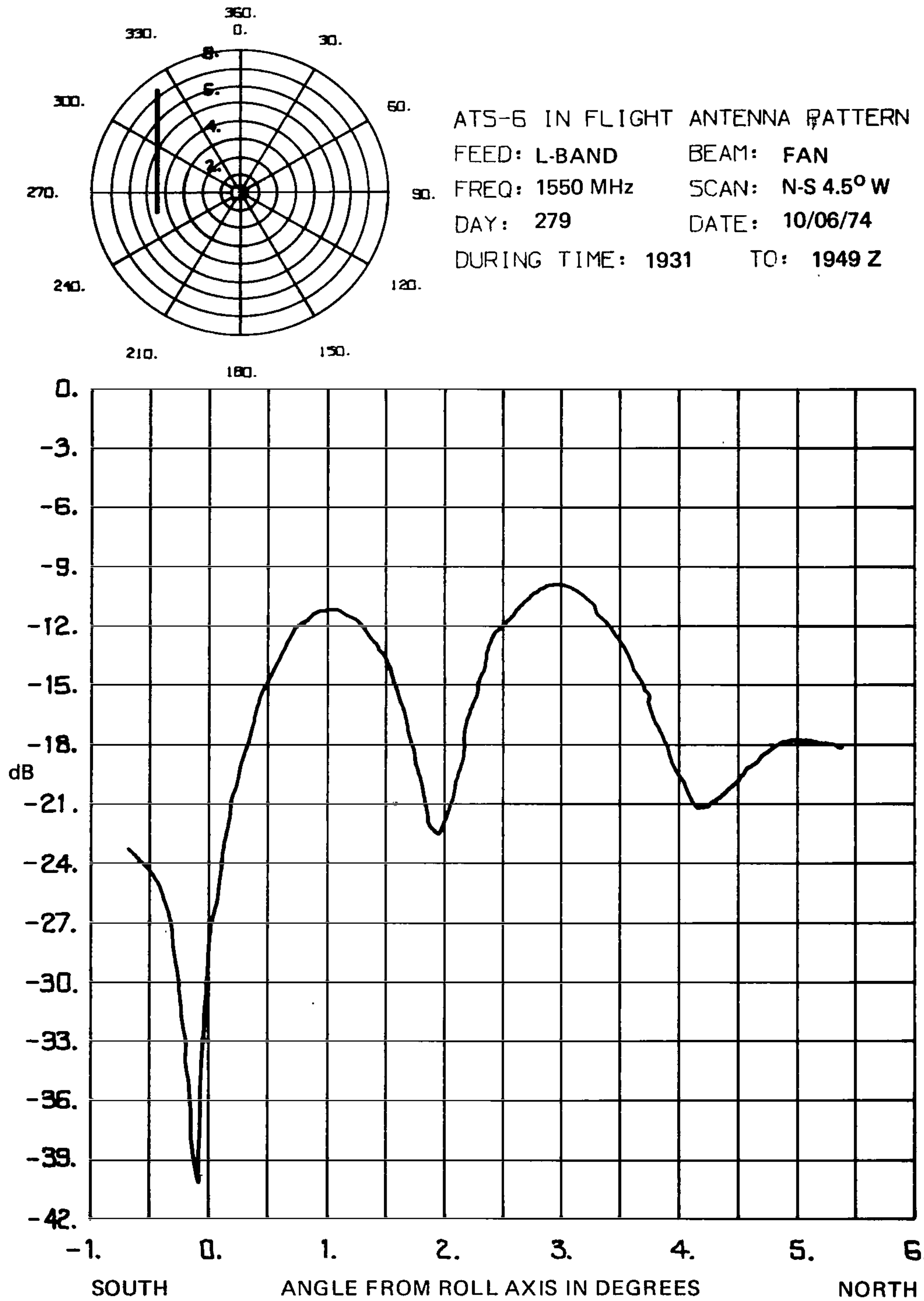

Figure 32. L-band fan beam pattern N – S 4.5° W.

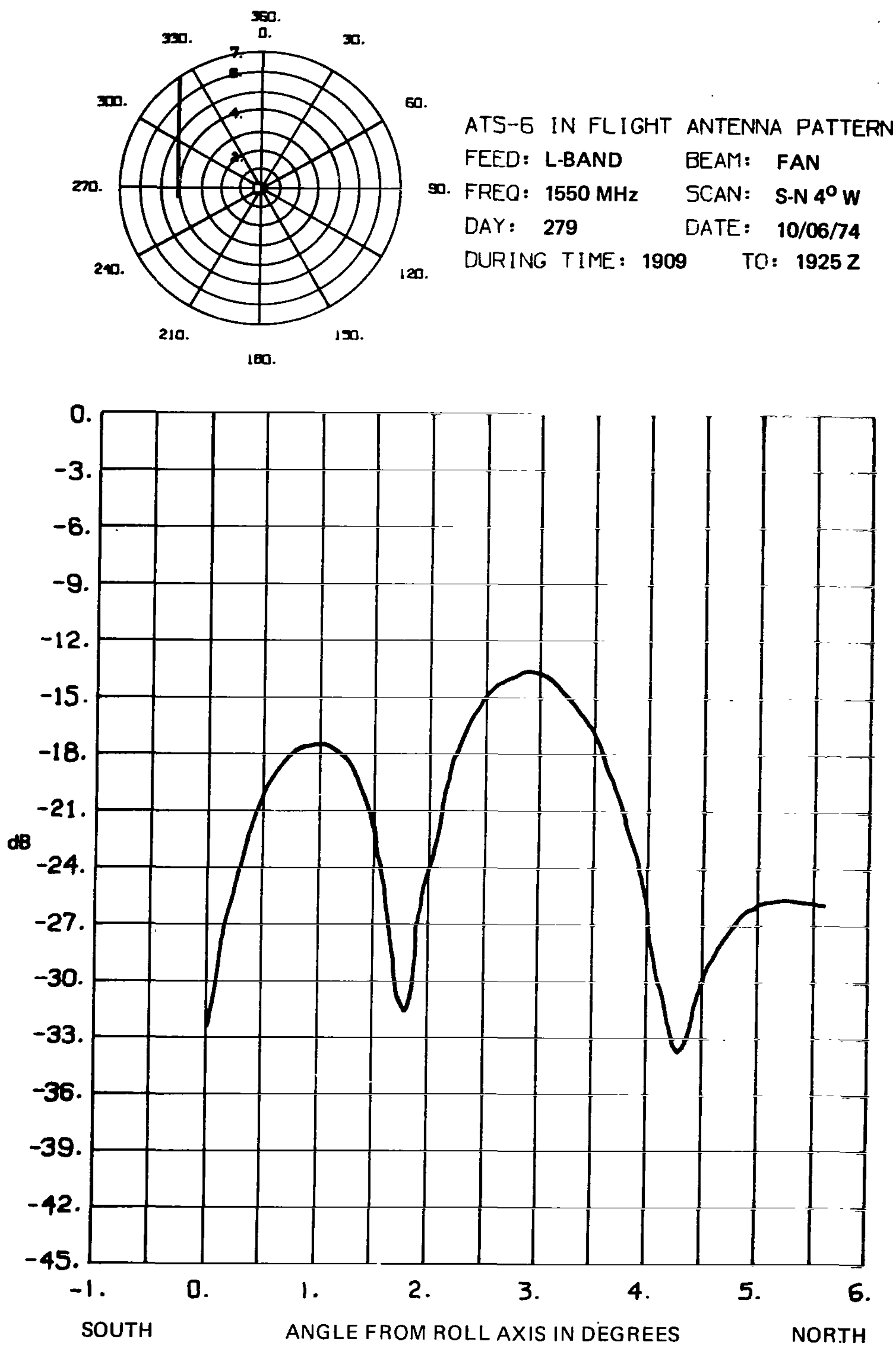

Figure 33. L-band fan beam pattern N – S 4.0° W.

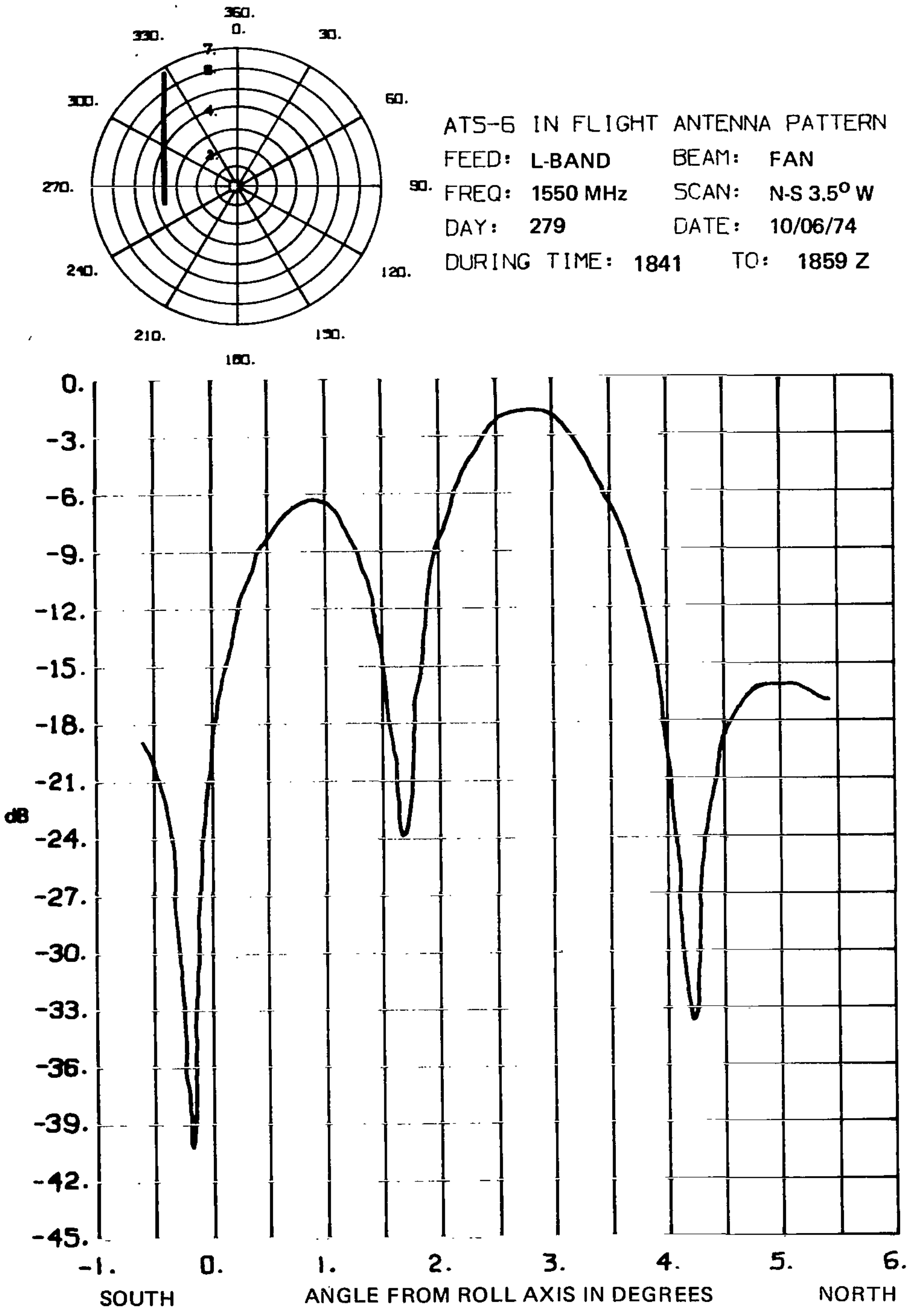

Figure 34. L-band fan beam pattern N – S 3.5° W.

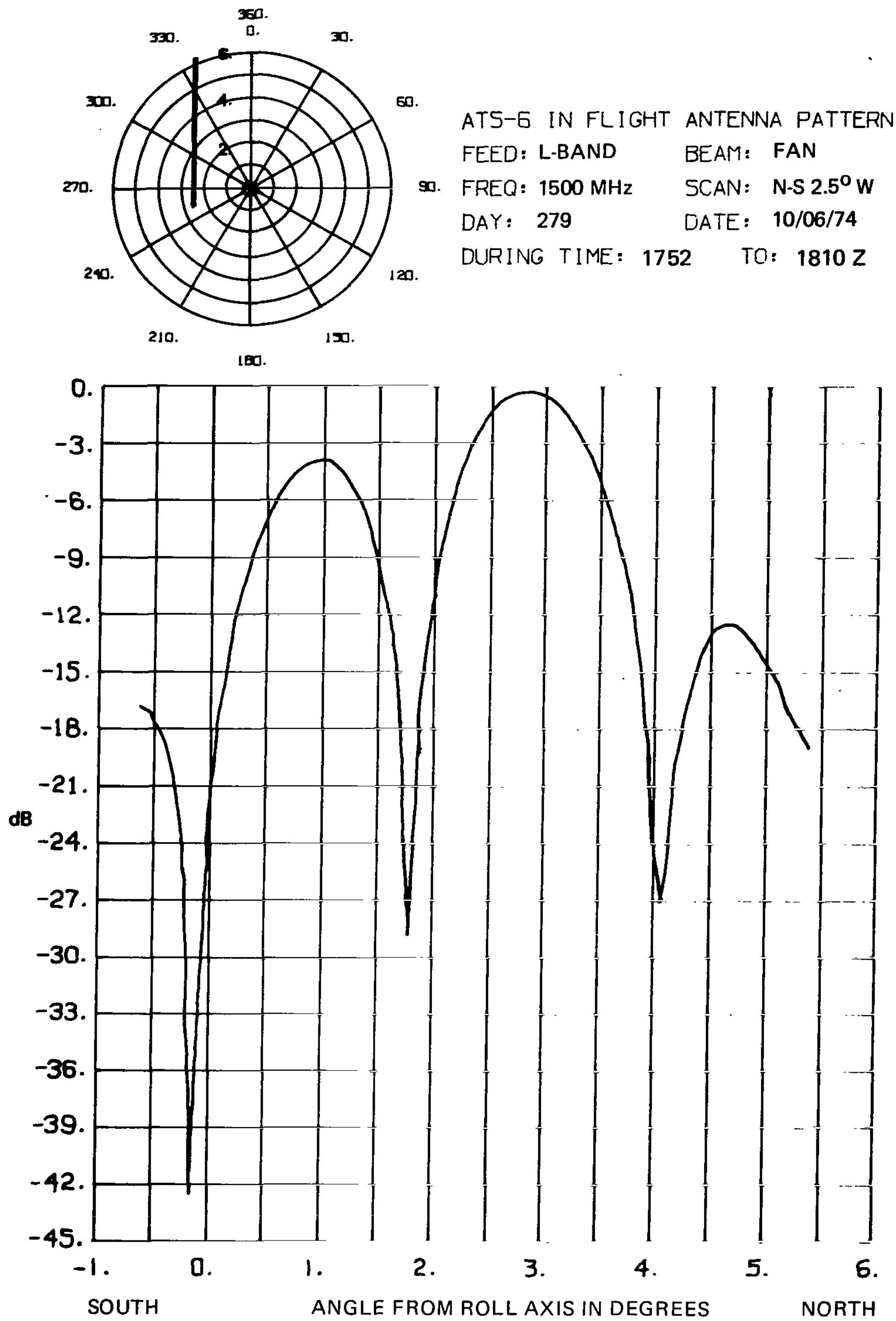

Figure 35. L-band fan beam pattern N – S 2.5° W.

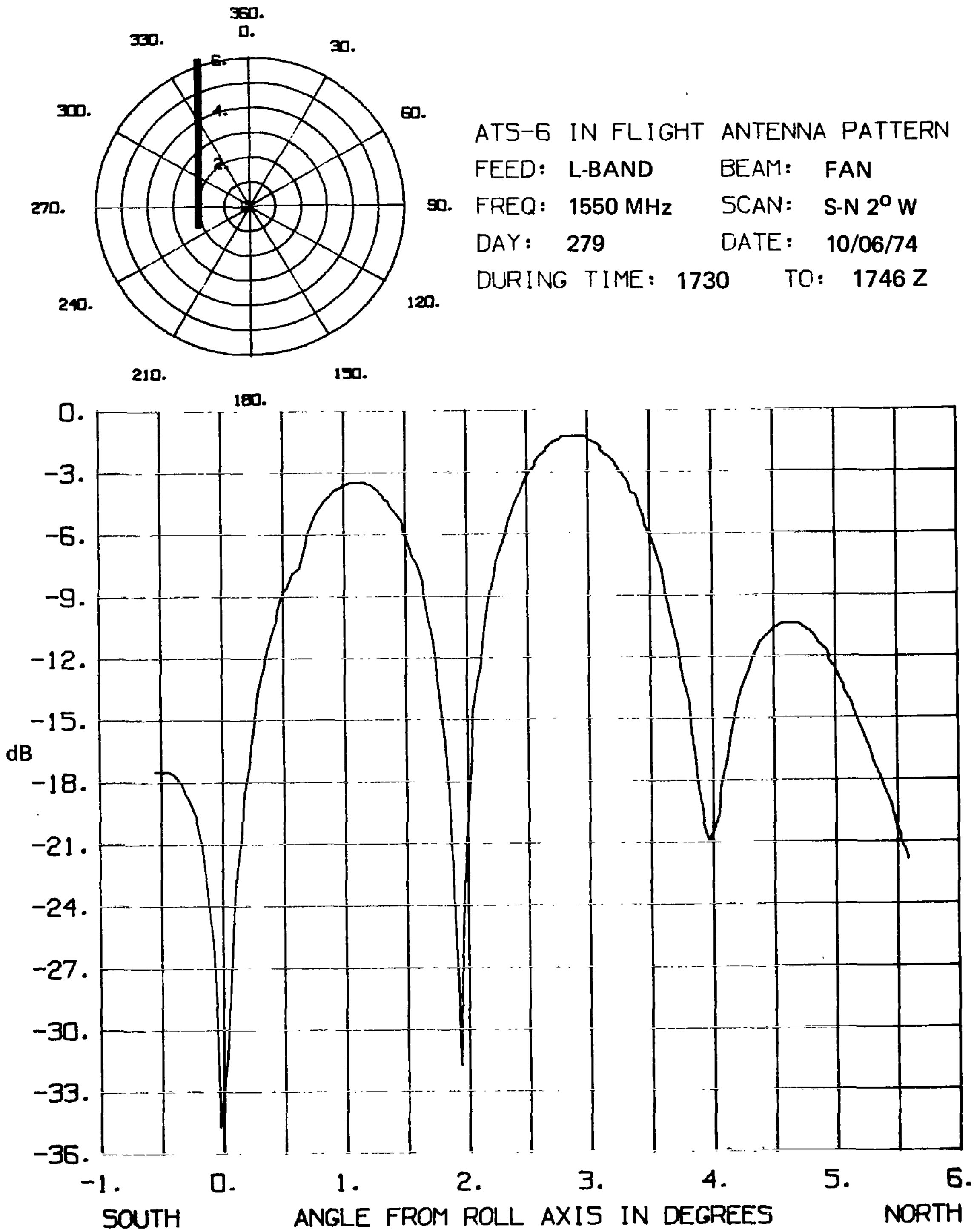

Figure 36. L-band fan beam pattern N – S 2° W.

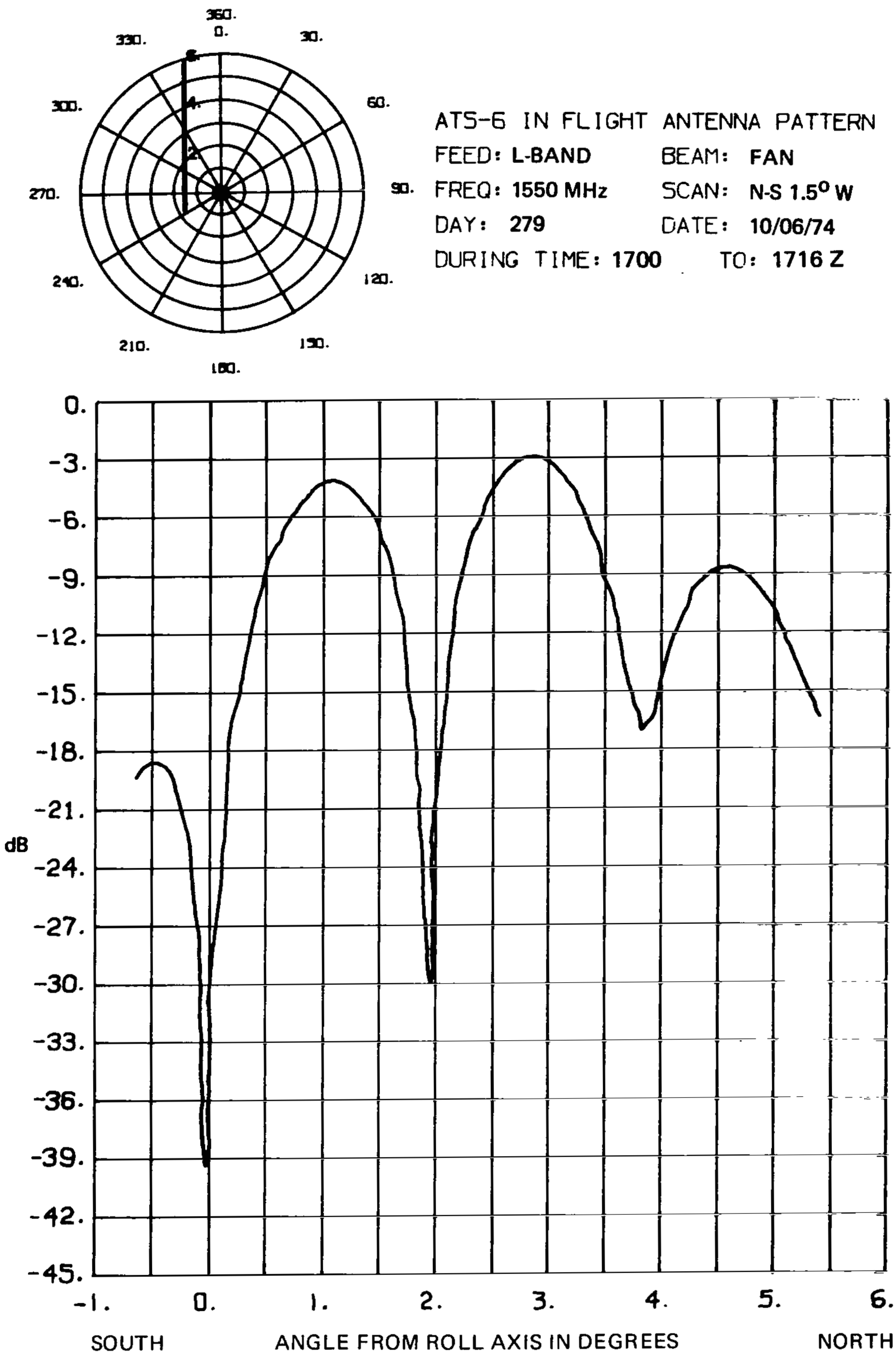

Figure 37. L-band fan beam pattern N – S 1.5° W.

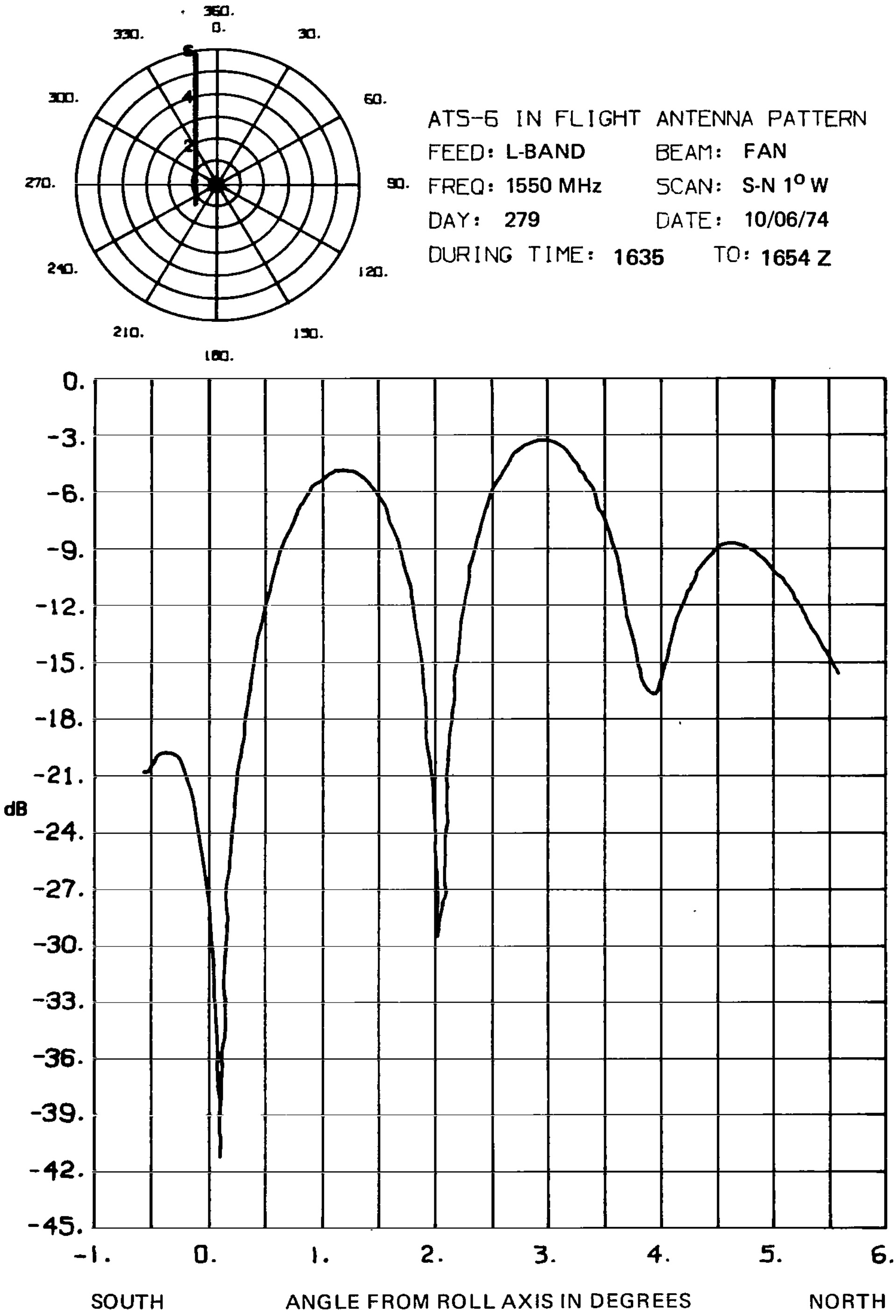

Figure 38. L-band fan beam pattern N – S 1° W.

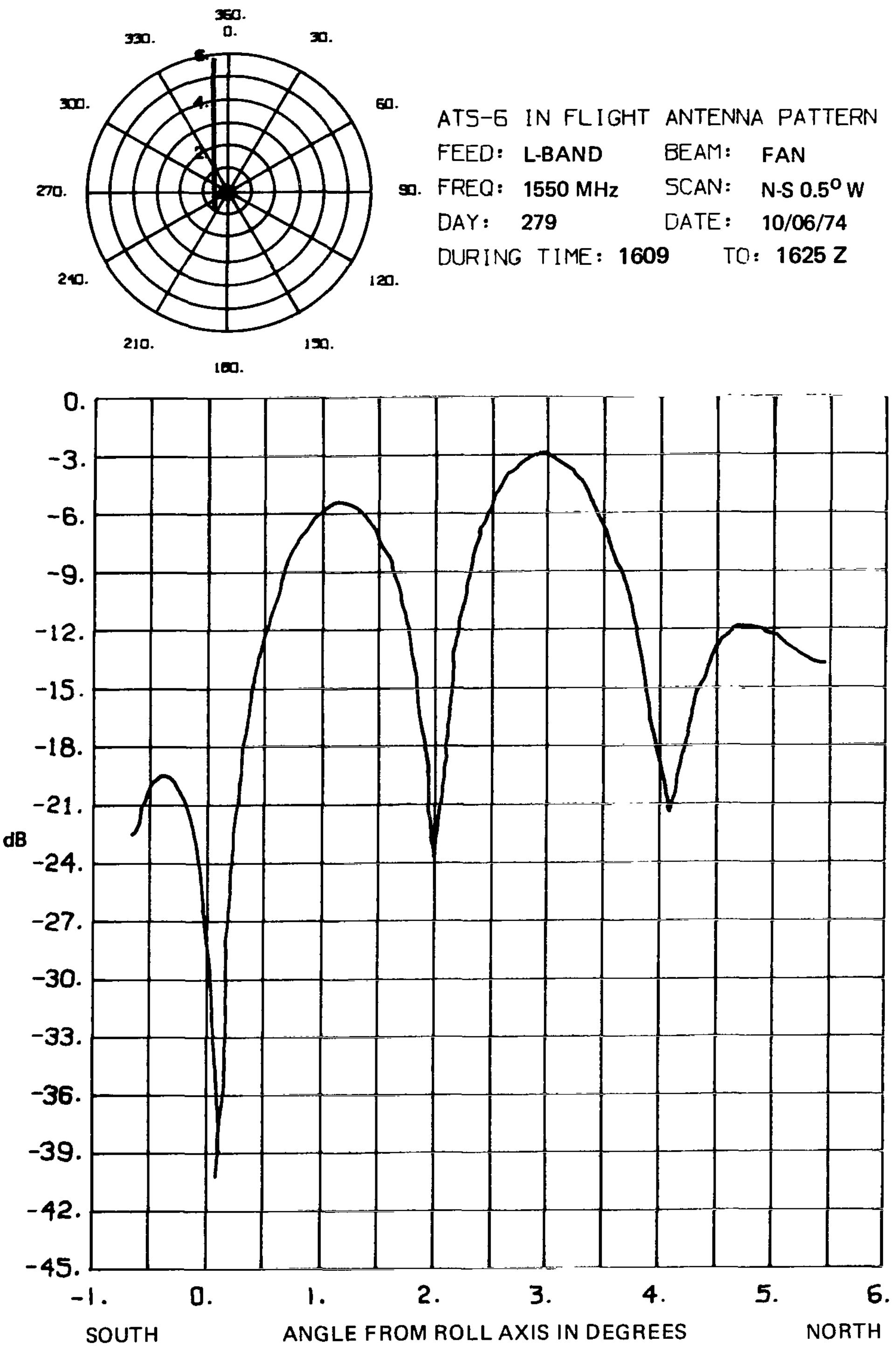

Figure 39. L-band fan beam pattern N – S 0.5° W.

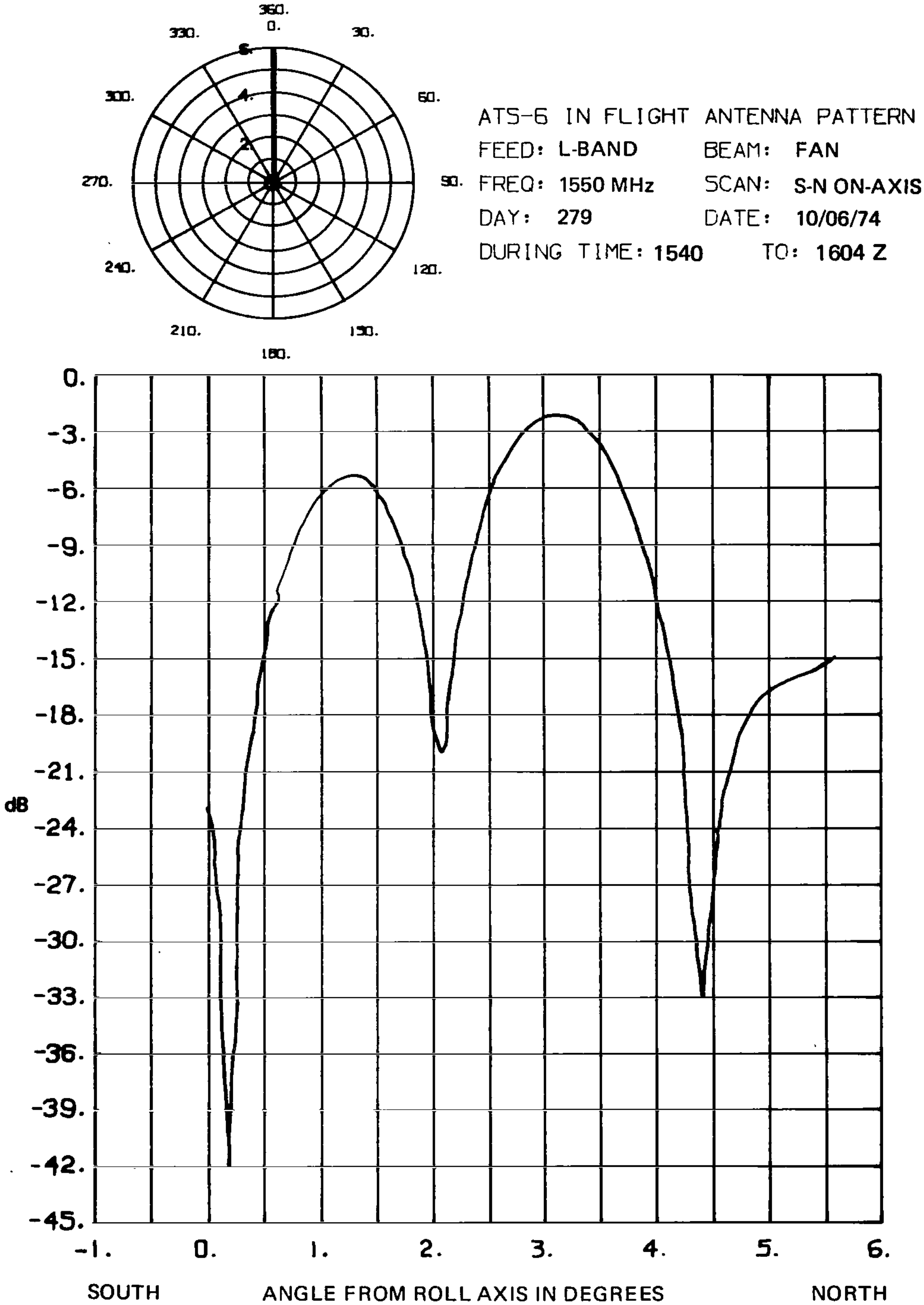

Figure 40. L-band fan beam pattern N – S on-axis.

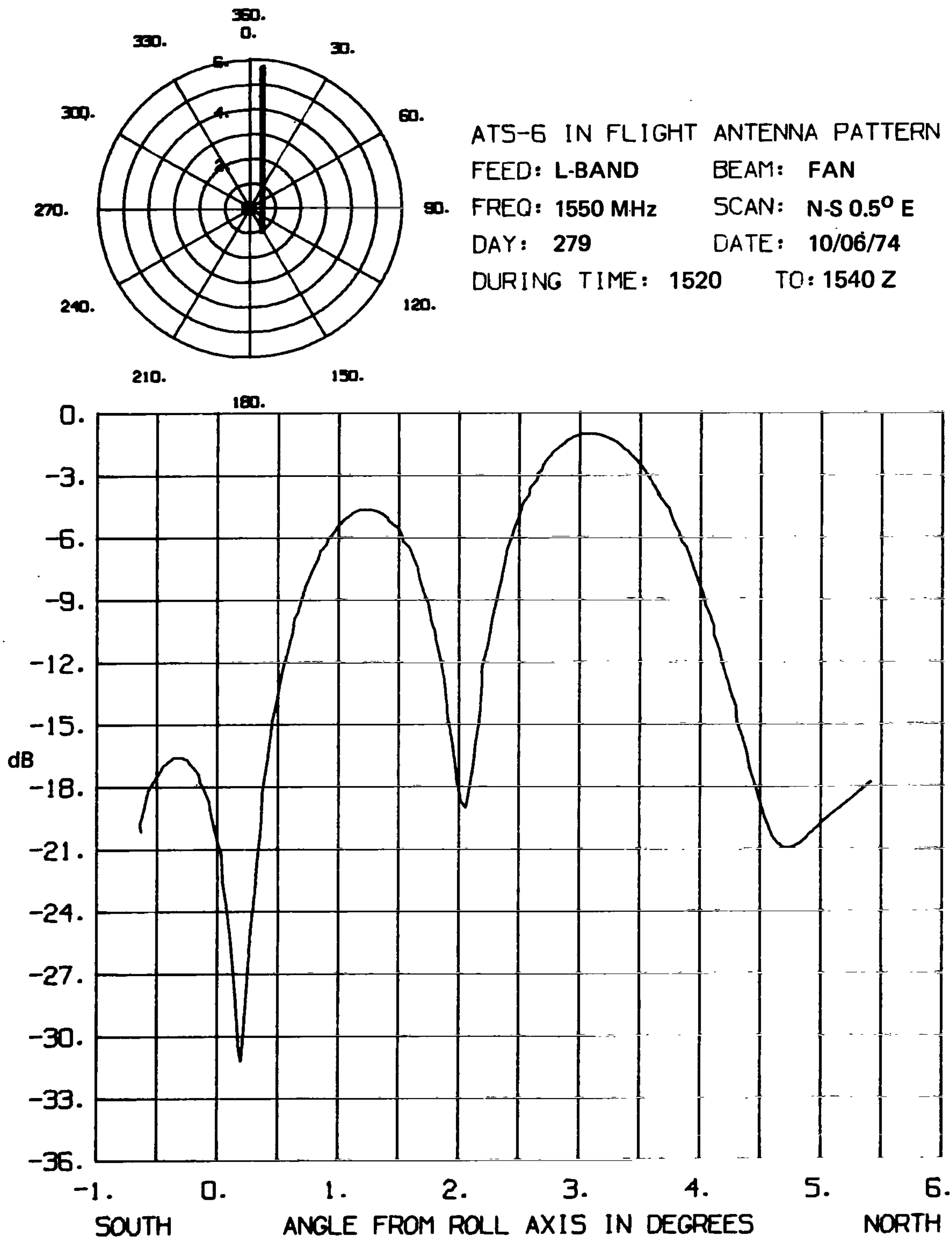

Figure 41. L-band fan beam pattern N – S 0.5° E.

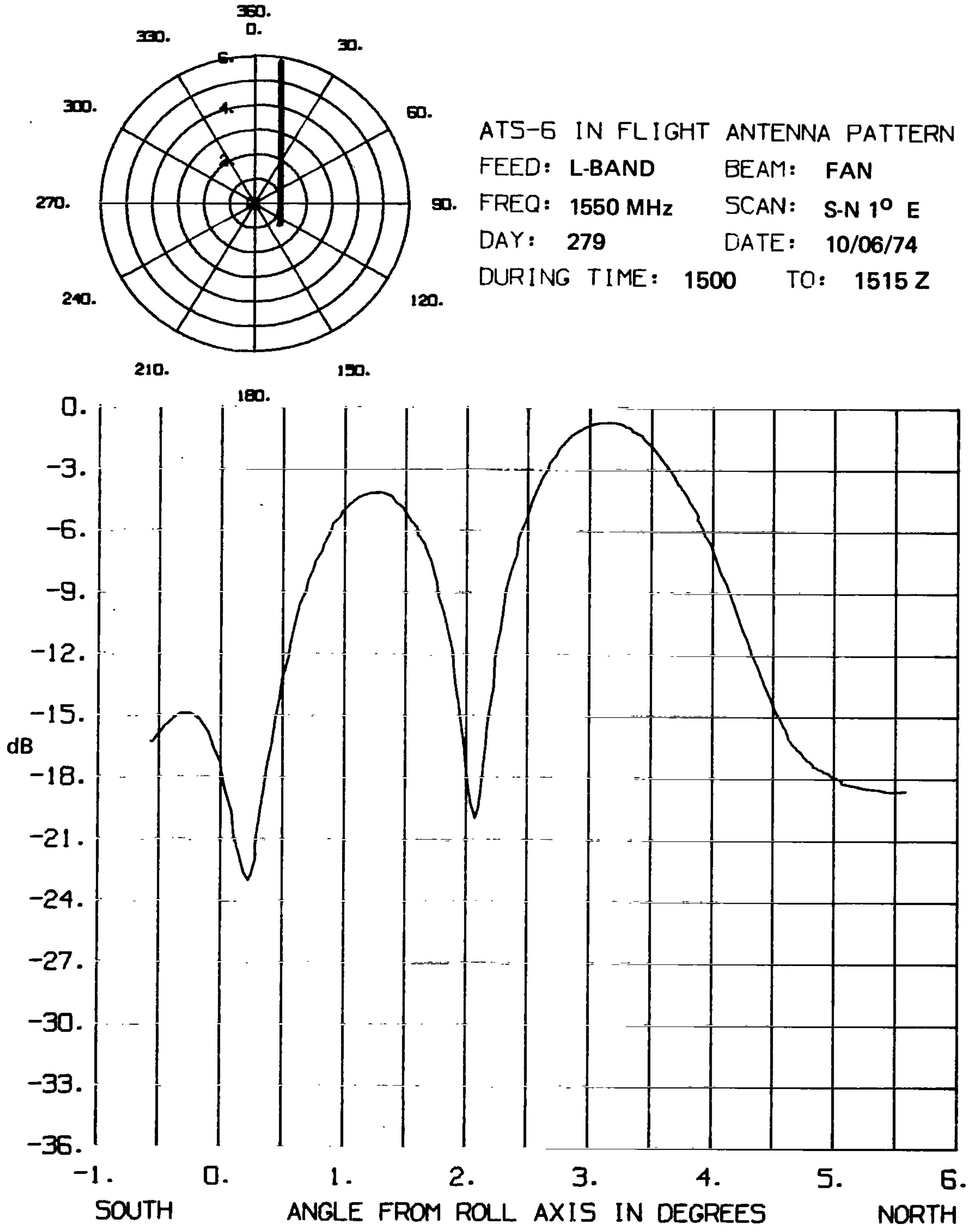

Figure 42. L-band fan beam pattern N – S 1° E.

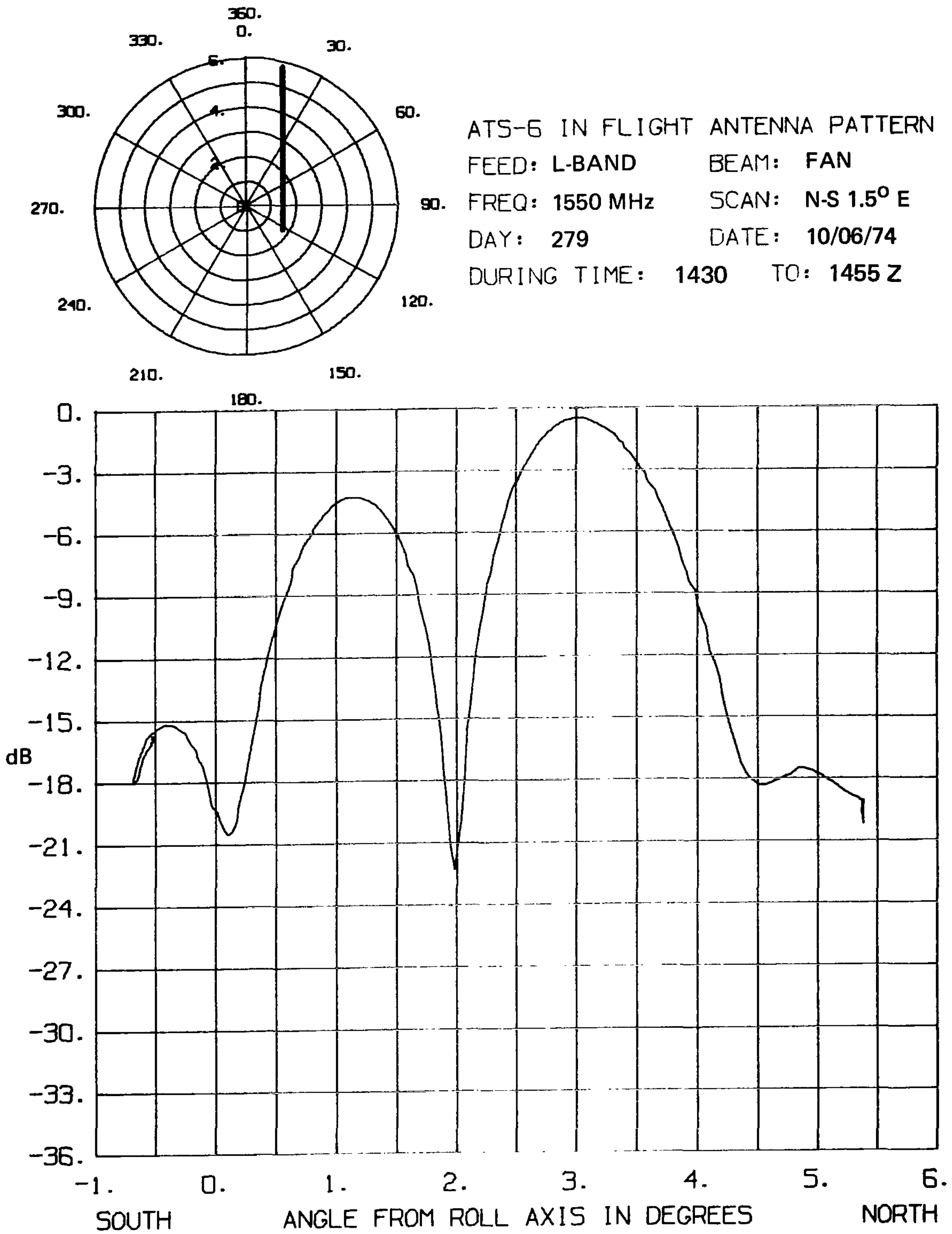

Figure 43. L-band fan beam pattern N – S 1.5° E.

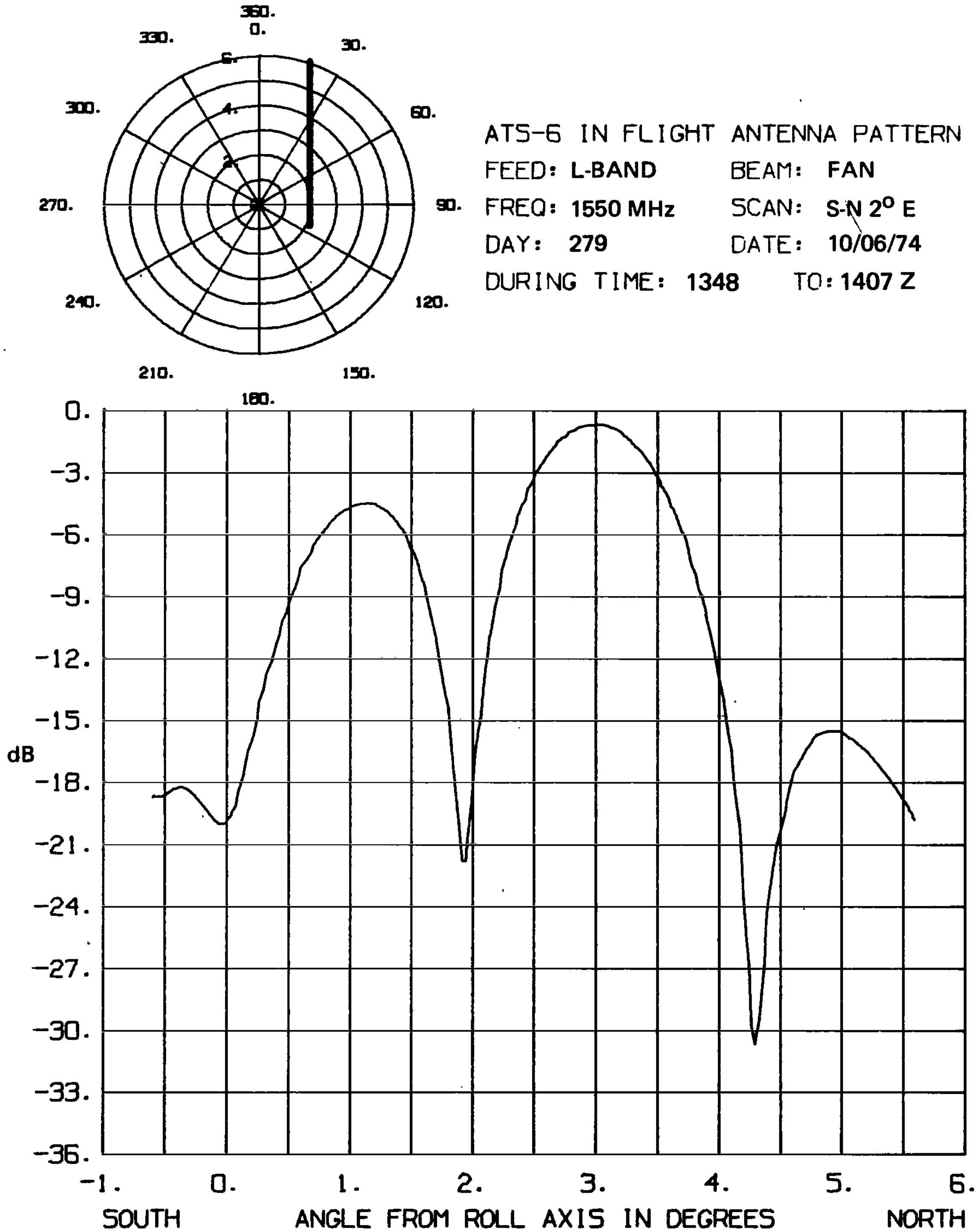

Figure 44. L-band fan beam pattern N – S 2° E.

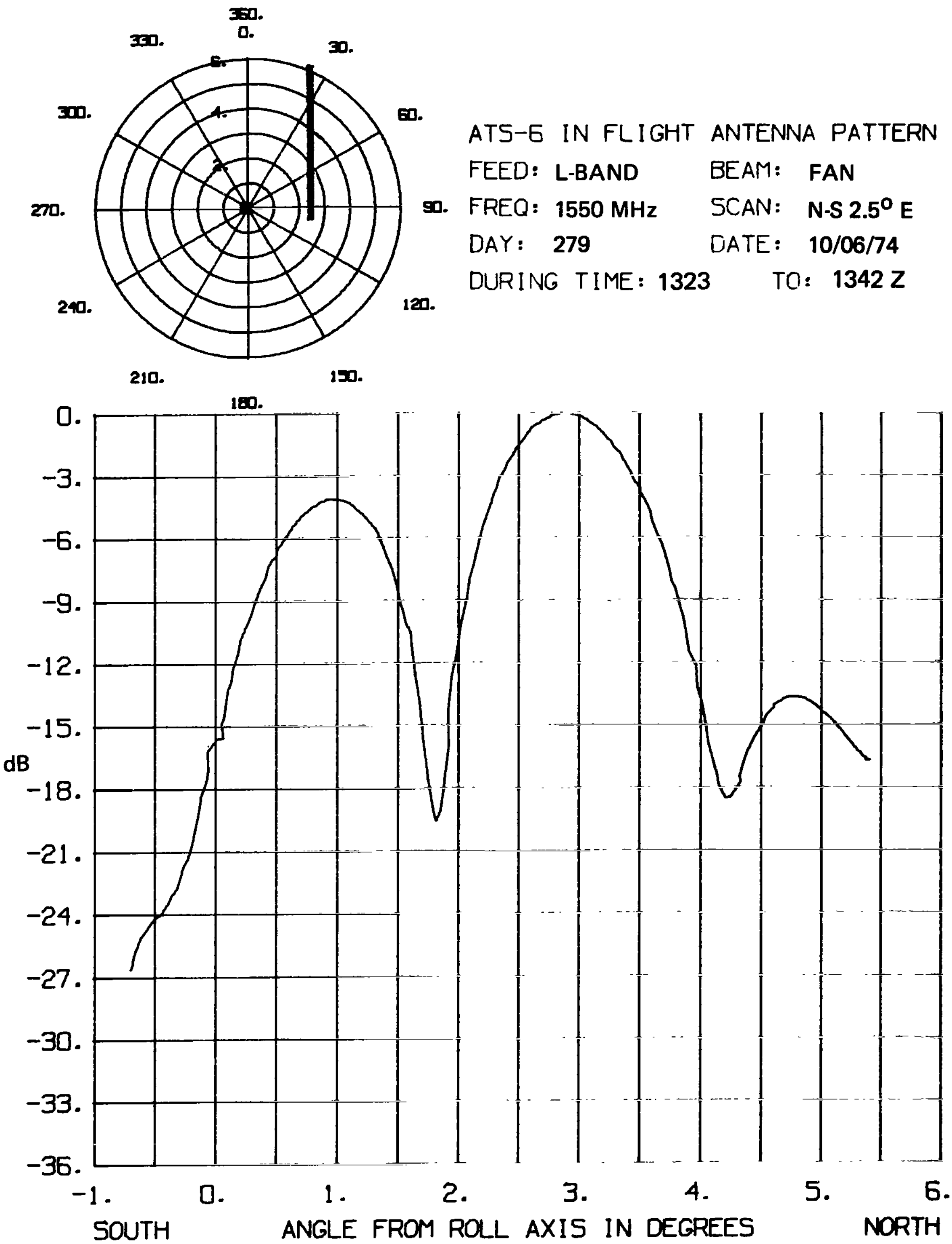

Figure 45. L-band fan beam pattern N – S 2.5° E.

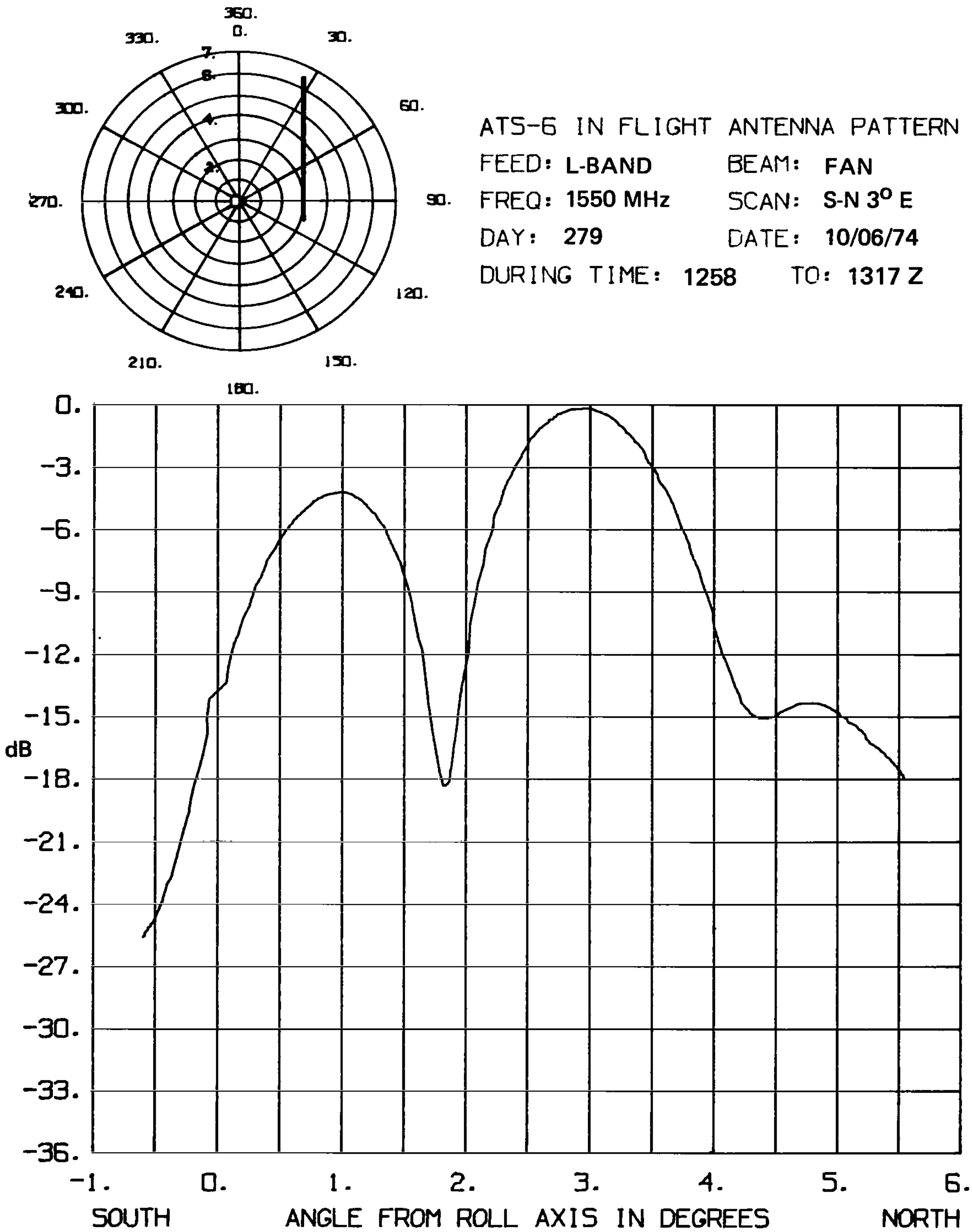

Figure 46. L-band fan beam pattern N – S 3^{o} E.

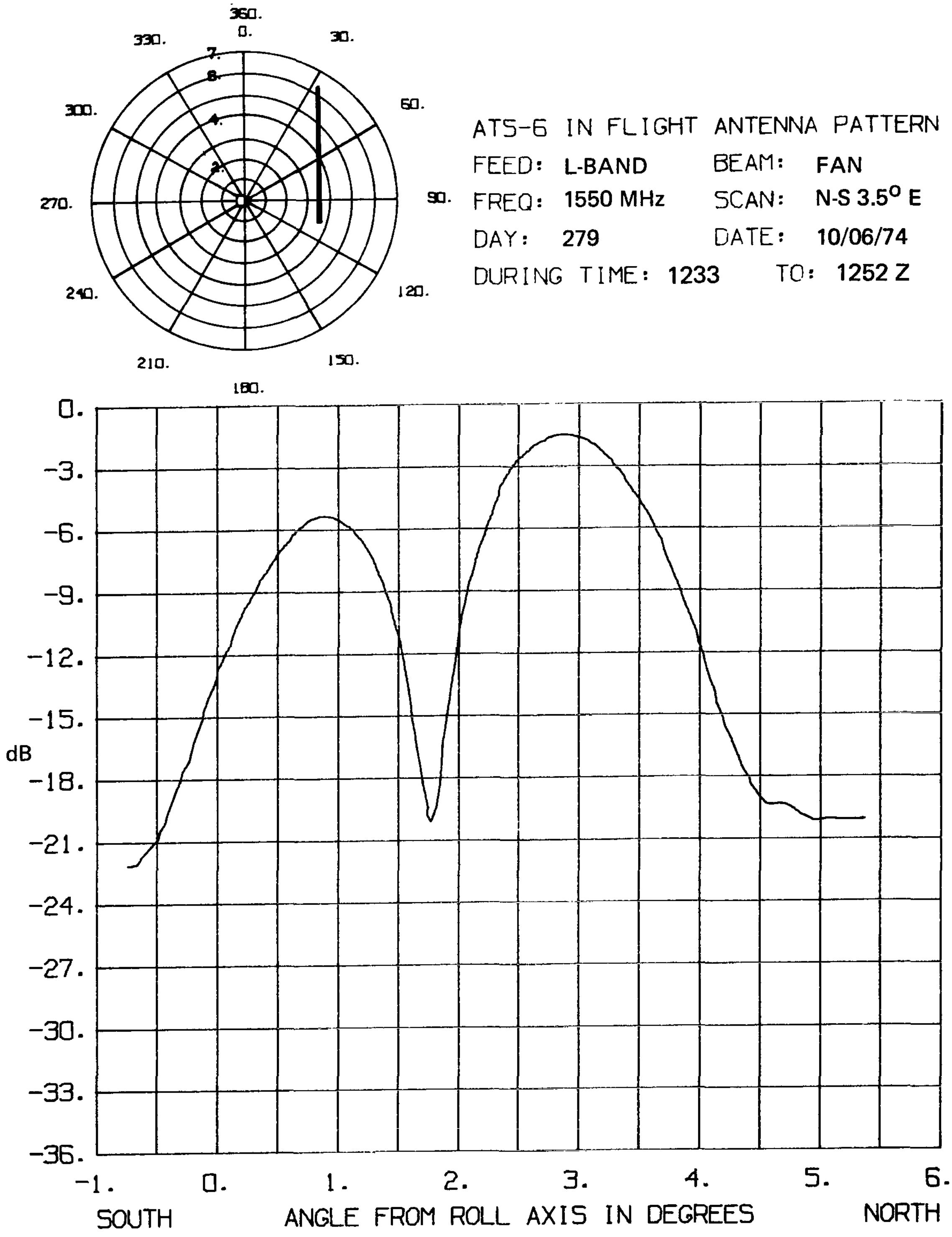

Figure 47. L-band fan beam pattern N – S 3.5° E.

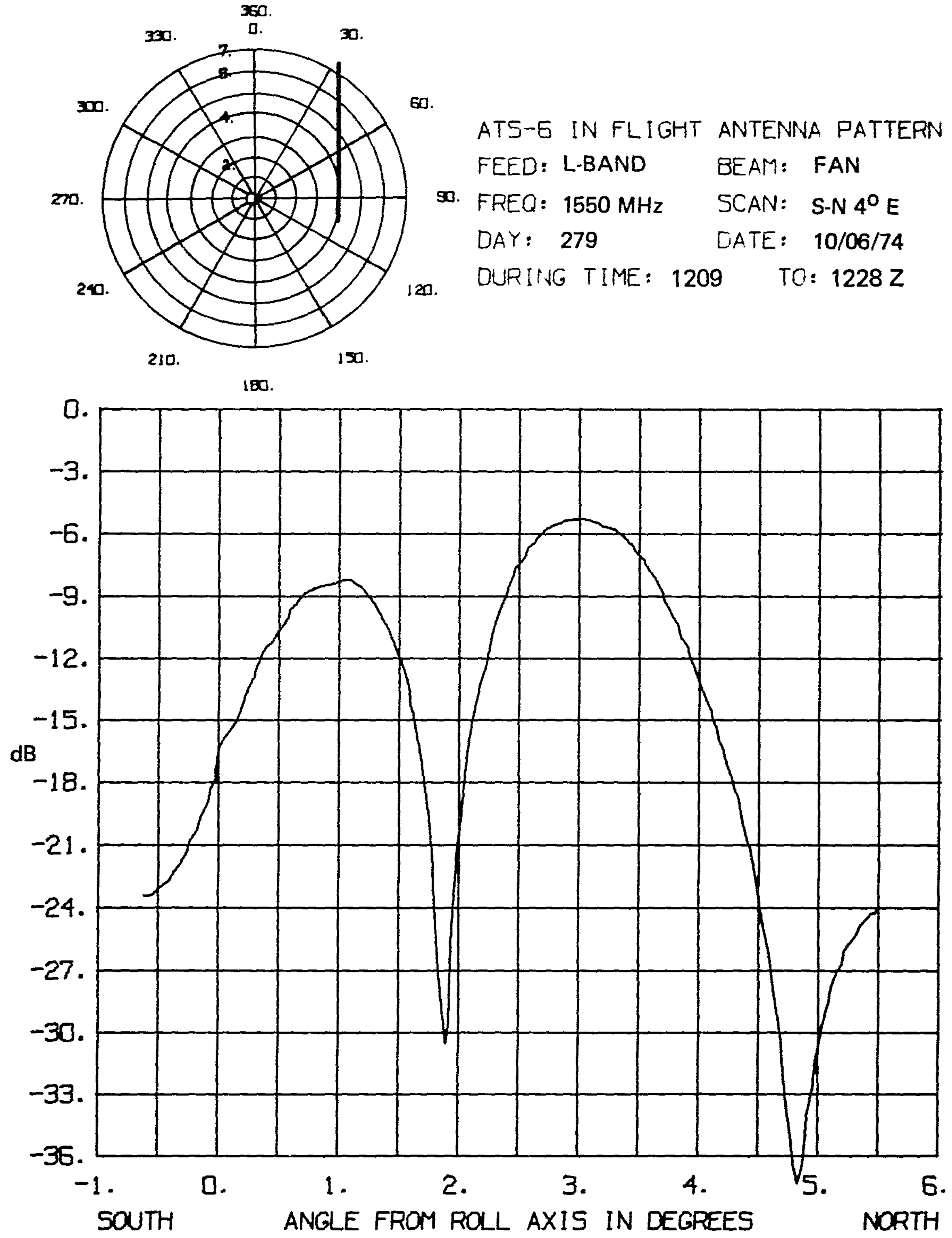

Figure 48. L-band fan beam pattern N – S 4° E.

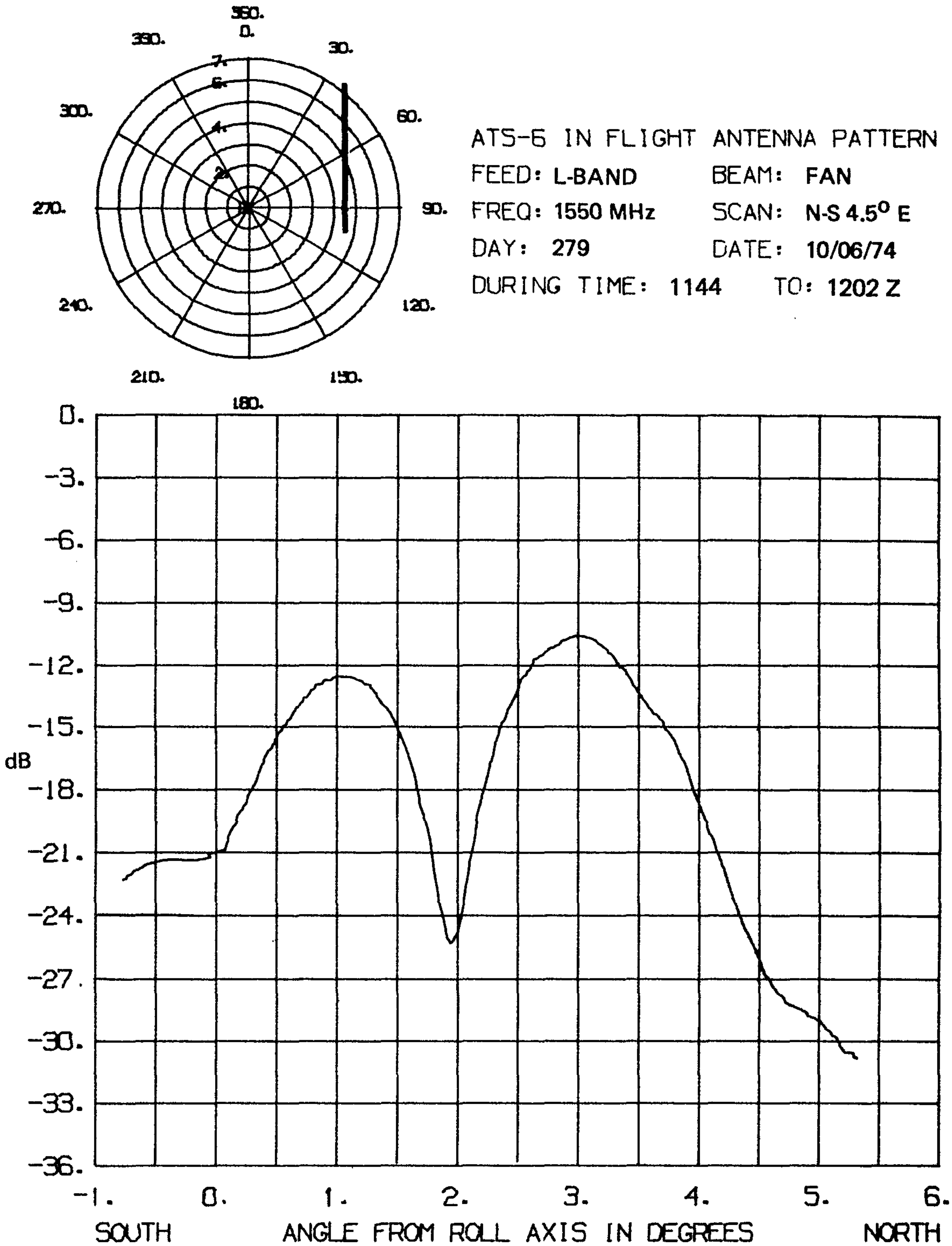

Figure 49. L-band fan beam pattern N – S 4.5° E.

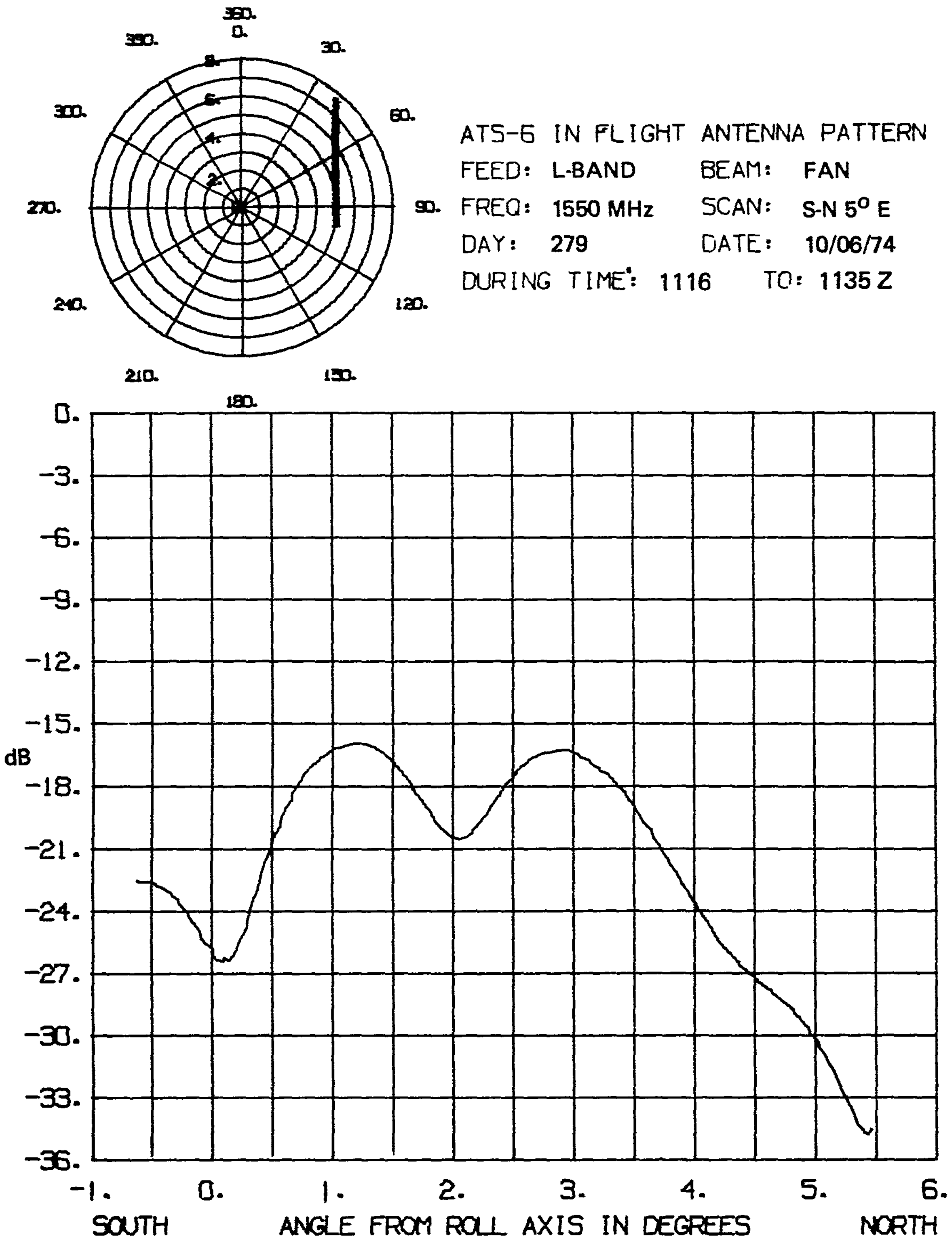

Figure 50. L-band fan beam pattern N – S 5° E.

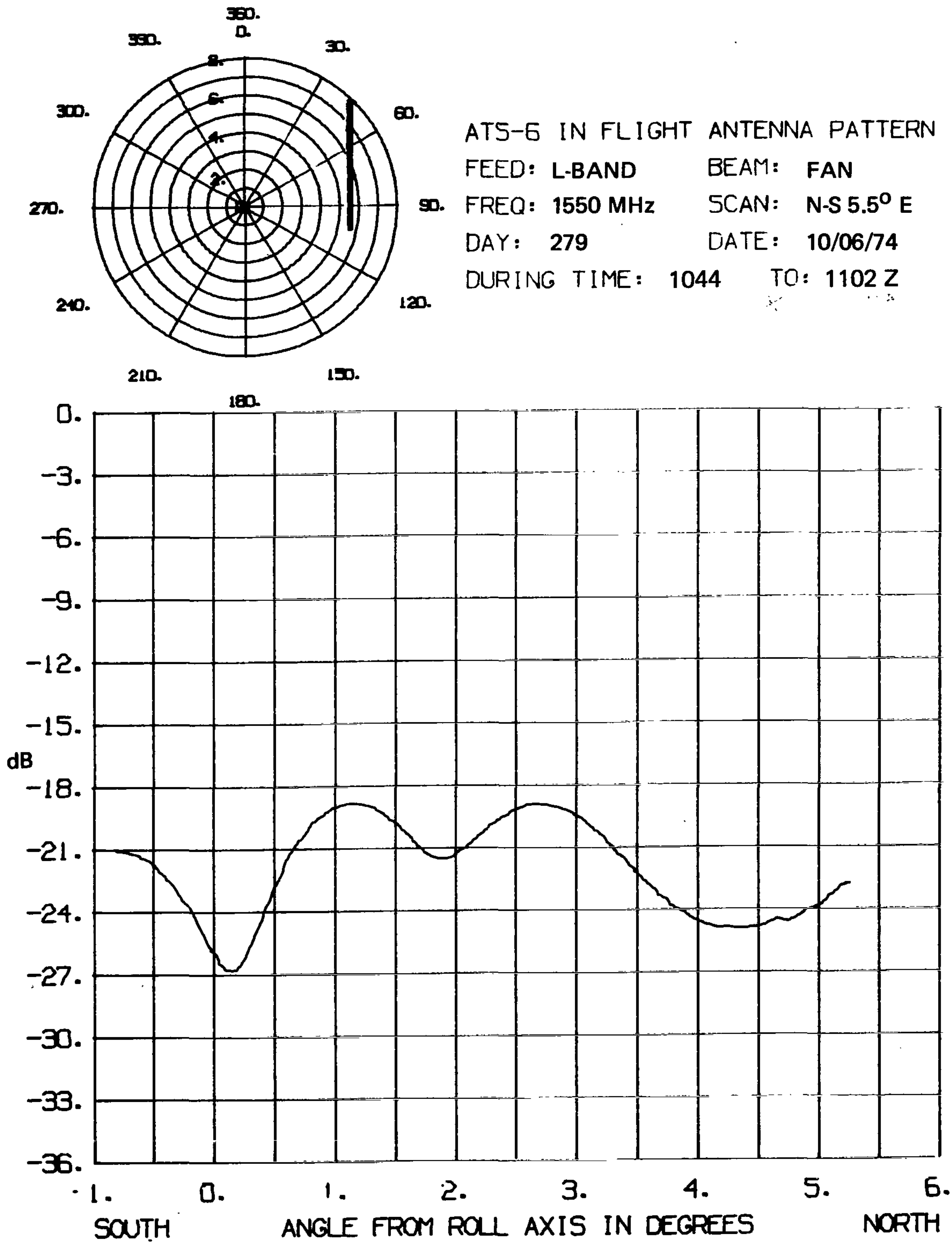

Figure 51. L-band fan beam pattern N – S 5.5° E.

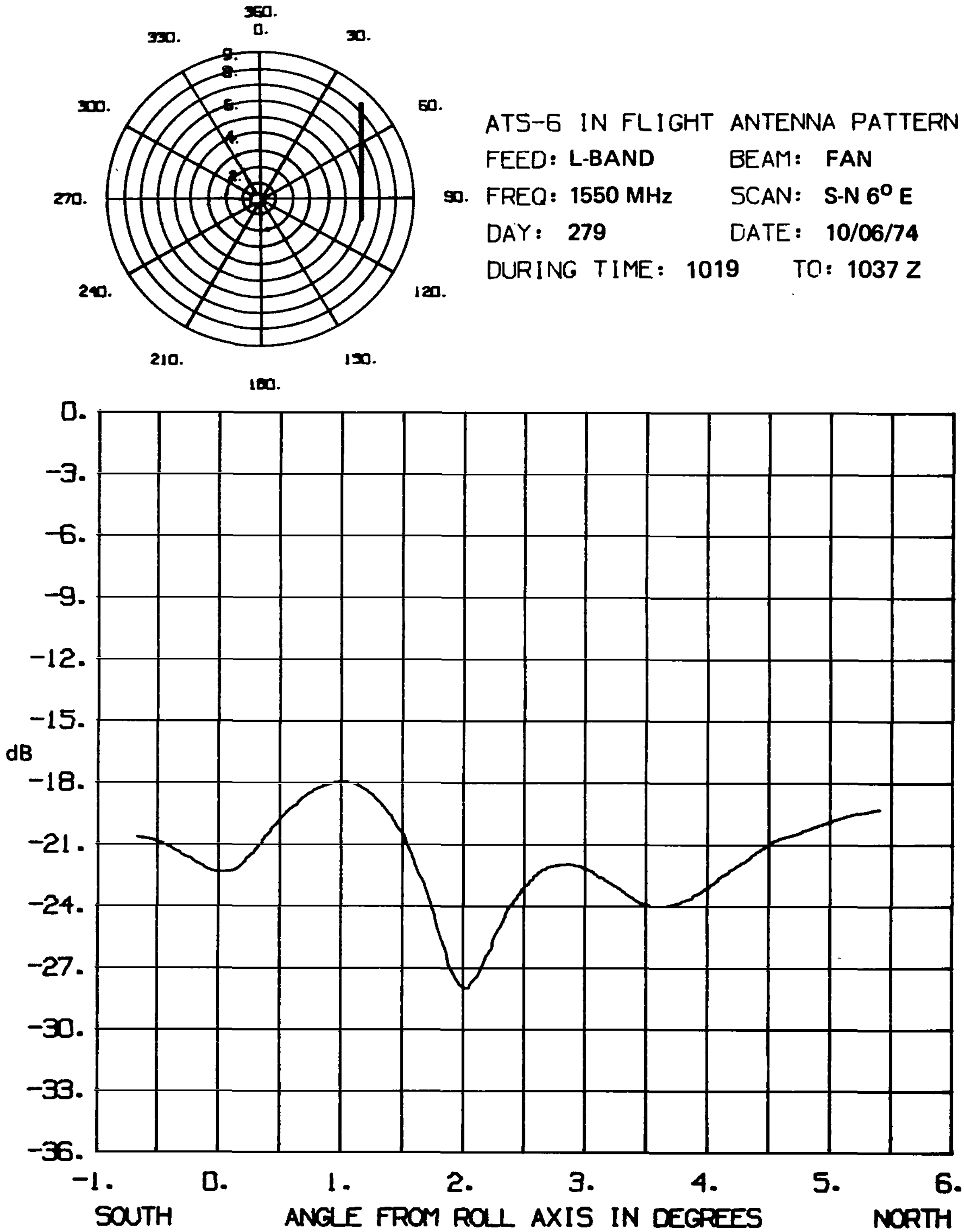

Figure 52. L-band fan beam pattern N – S 6° E.

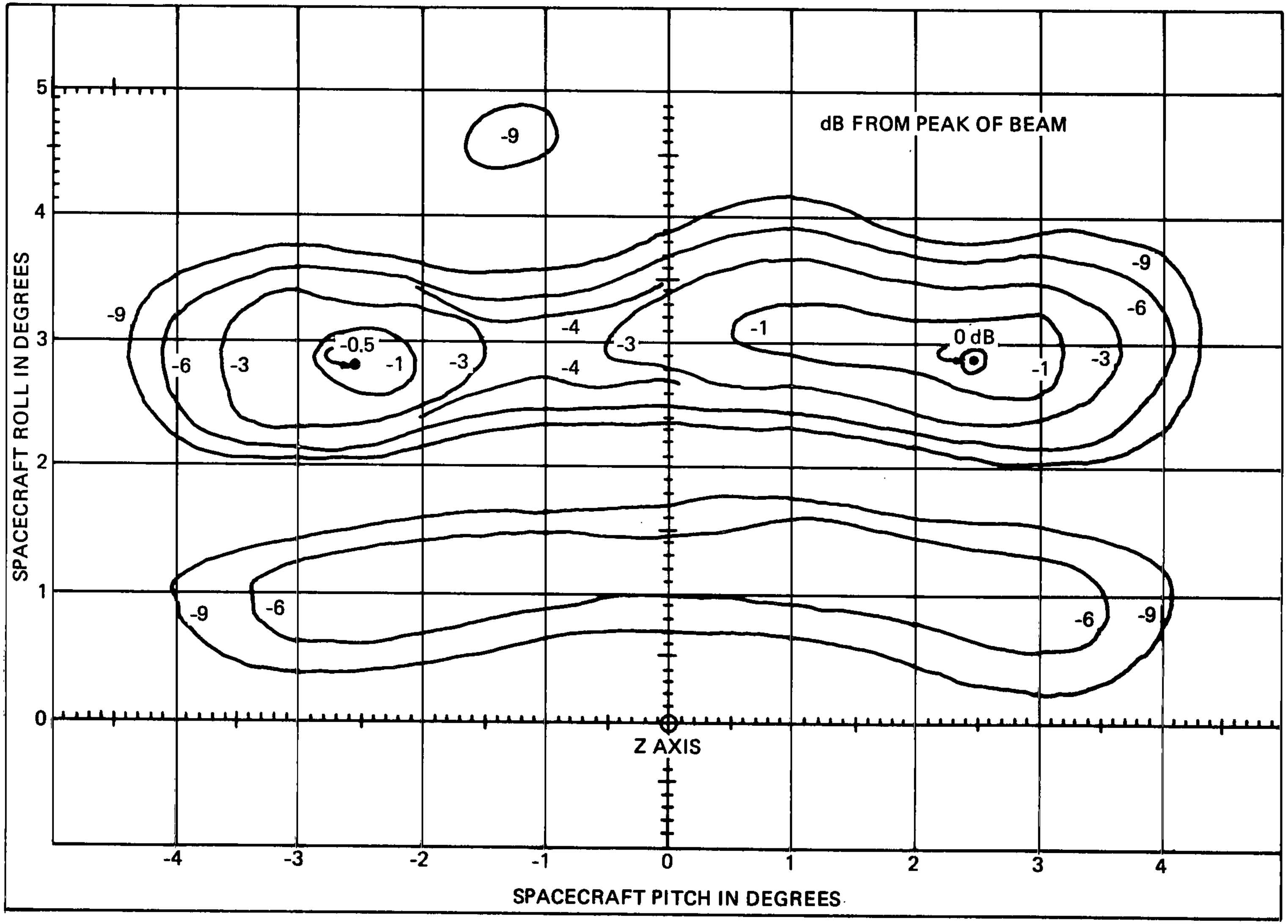

Figure 53. L-band fan beam contours of equal power levels.

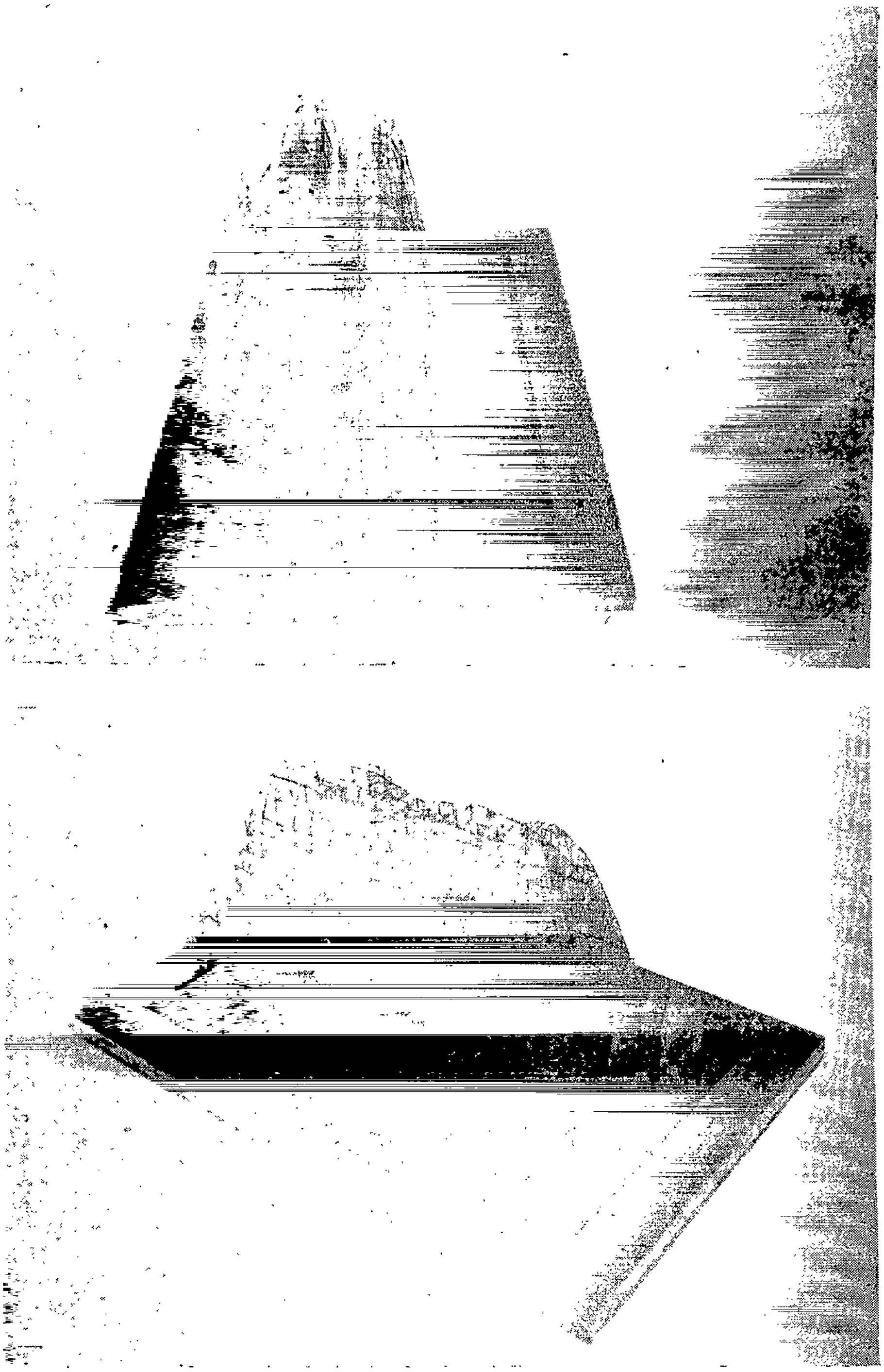

Figure 54. L-band fan beam model.

S-BAND ANTENNA PATTERNS

The Prime Focus Feed (PFF) diagram, Figure 1, shows that it contains more S-band antenna elements than any of the other frequency bands. The on-axis feed consists of the antenna elements (annulus) surrounding the C-band feed. The antenna patterns for the on-axis antenna are presented in Figures 55 through 58.

The S-band cross-axis antenna elements are presented in a composite fashion for the E – W and N – S axis; the diagram of the PFF is included. These antenna patterns essentially show only the main lobes and are compared with the preflight patterns. Good correlation is achieved for these patterns. These are shown in Figures 59 and 60 respectively.

Patterns for individual S-band feeds were measured with extra attention paid to the N1 and N2 beams for the HET experiment. Figures 61 through 64 present the patterns for beam N1 with Figures 61 and 62 showing the comparison to preflight patterns. Care was taken to make the antenna pattern cuts go as close as possible through the peak of the beam.

The HET beam, N1, was further measured by taking antenna patterns for a series of "cuts." These are shown in Figures 65 through 75. These measurements were made for spacecraft maneuvers in the N – S and E – W directions, for each direction the maneuvers were 0.1° apart. The results show the peak of the beam location to within 0.1°. Similar measurements were accomplished for the N2 beam (HET) and are presented in Figures 76 through 88.

Beam S1 is shown in Figures 89 and 90 while Beam W1 was measured and is given in Figures 91 through 94. These patterns indicate the position of the "Beam Peak" with respect to the spacecraft axis.

Beam W2 antenna patterns are shown in Figures 95 through 97.

Beam N4 is shown in Figures 98 and 99.

Beam N5 was measured and presented in Figures 100 and 101. This beam provided an example of an antenna pattern for a feed element at the extreme southern position in the PFF.

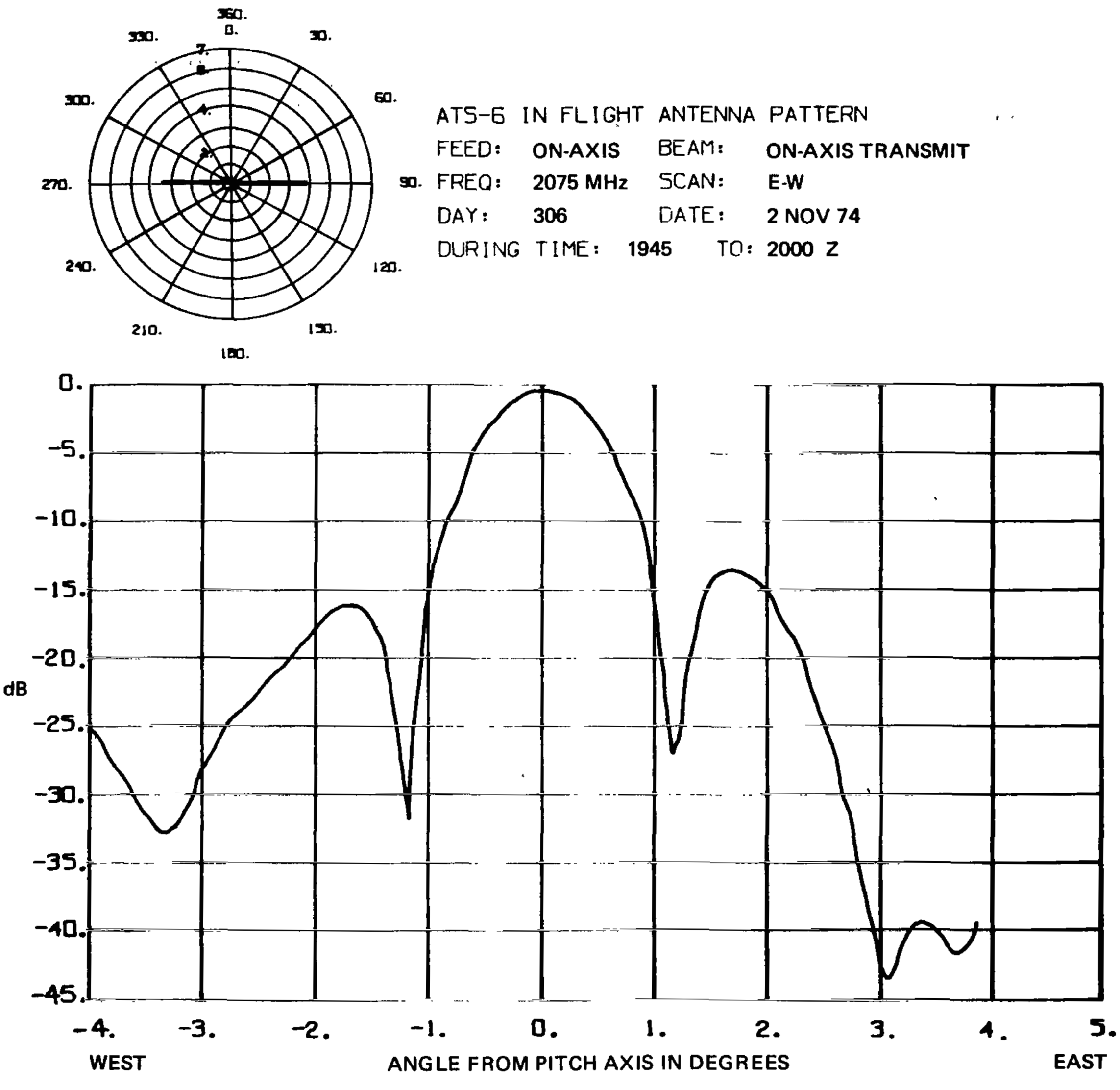

Figure 55. S-band on-axis beam E — W.

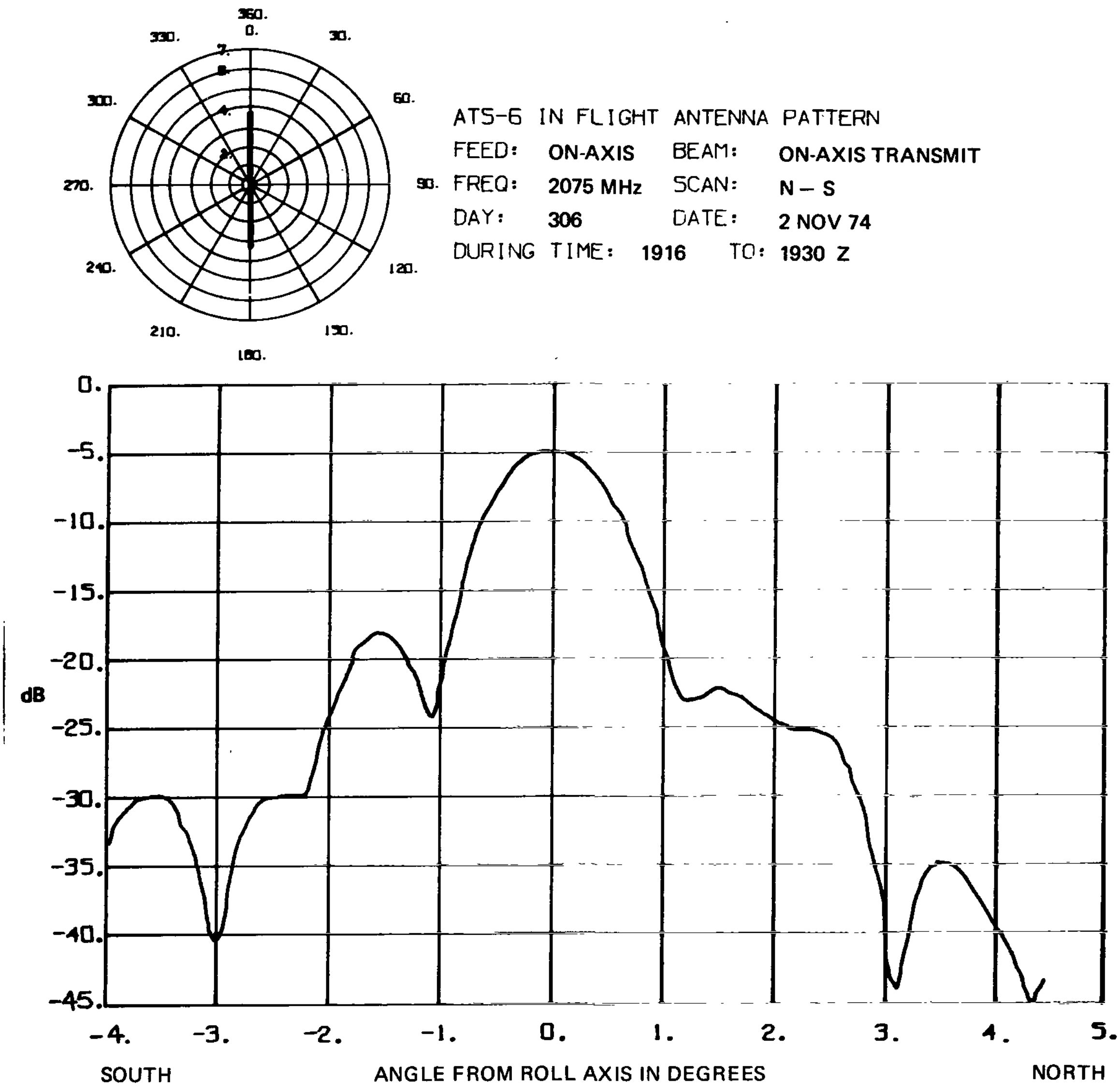

Figure 56. S-band on-axis beam N – S.

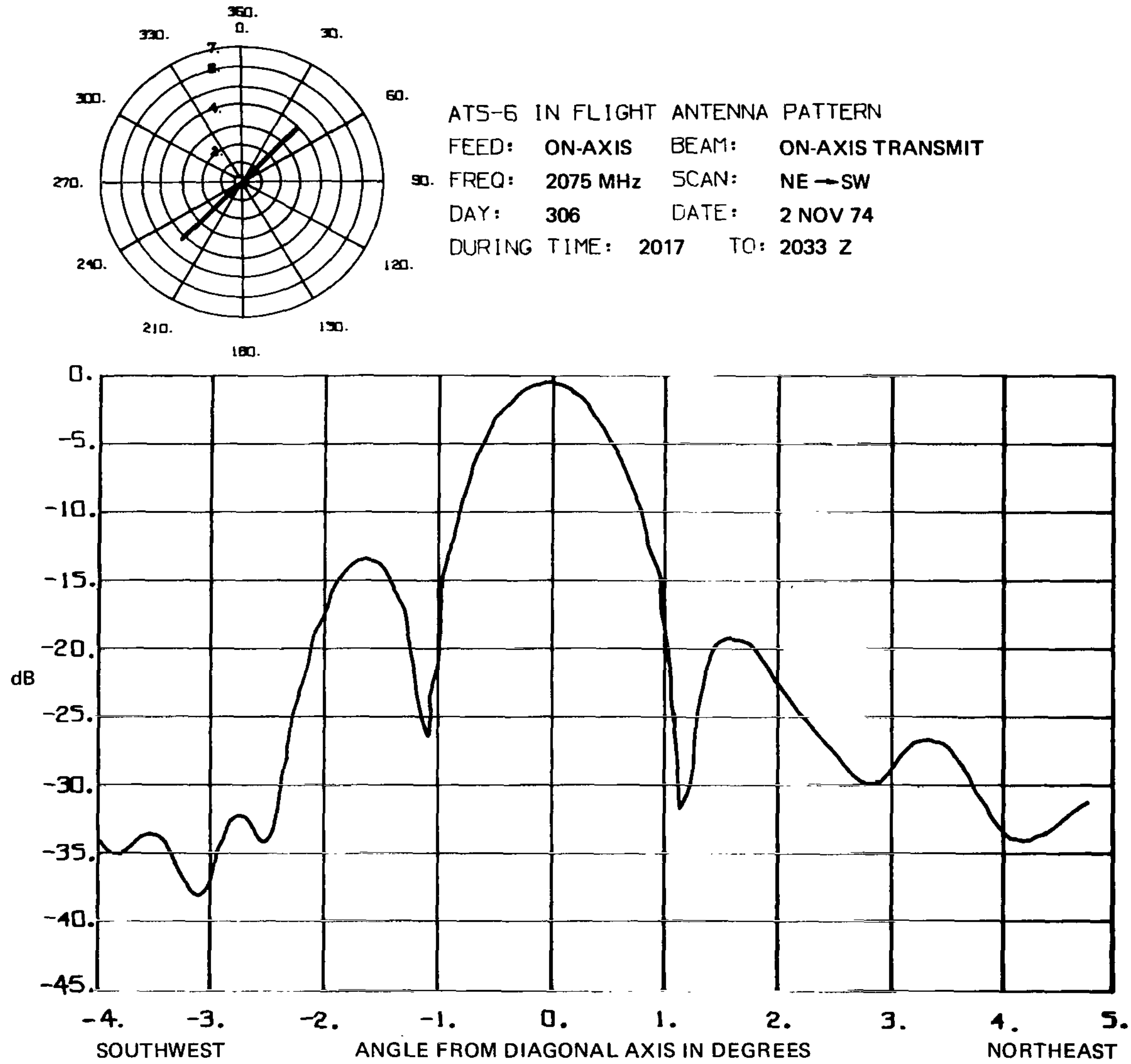

Figure 57. S-band on-axis beam SW – NE.

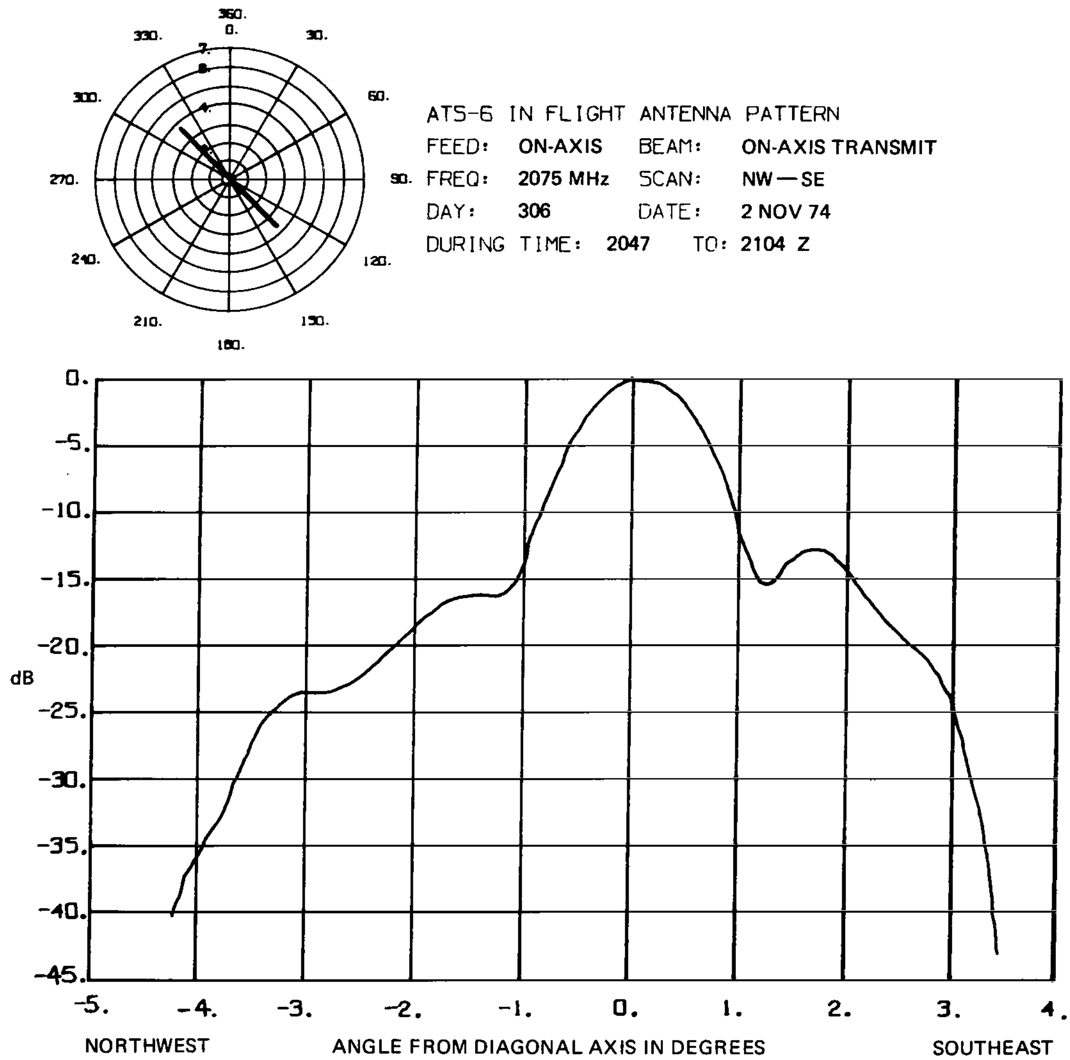

Figure 58. S-band on-axis beam NW – SE.

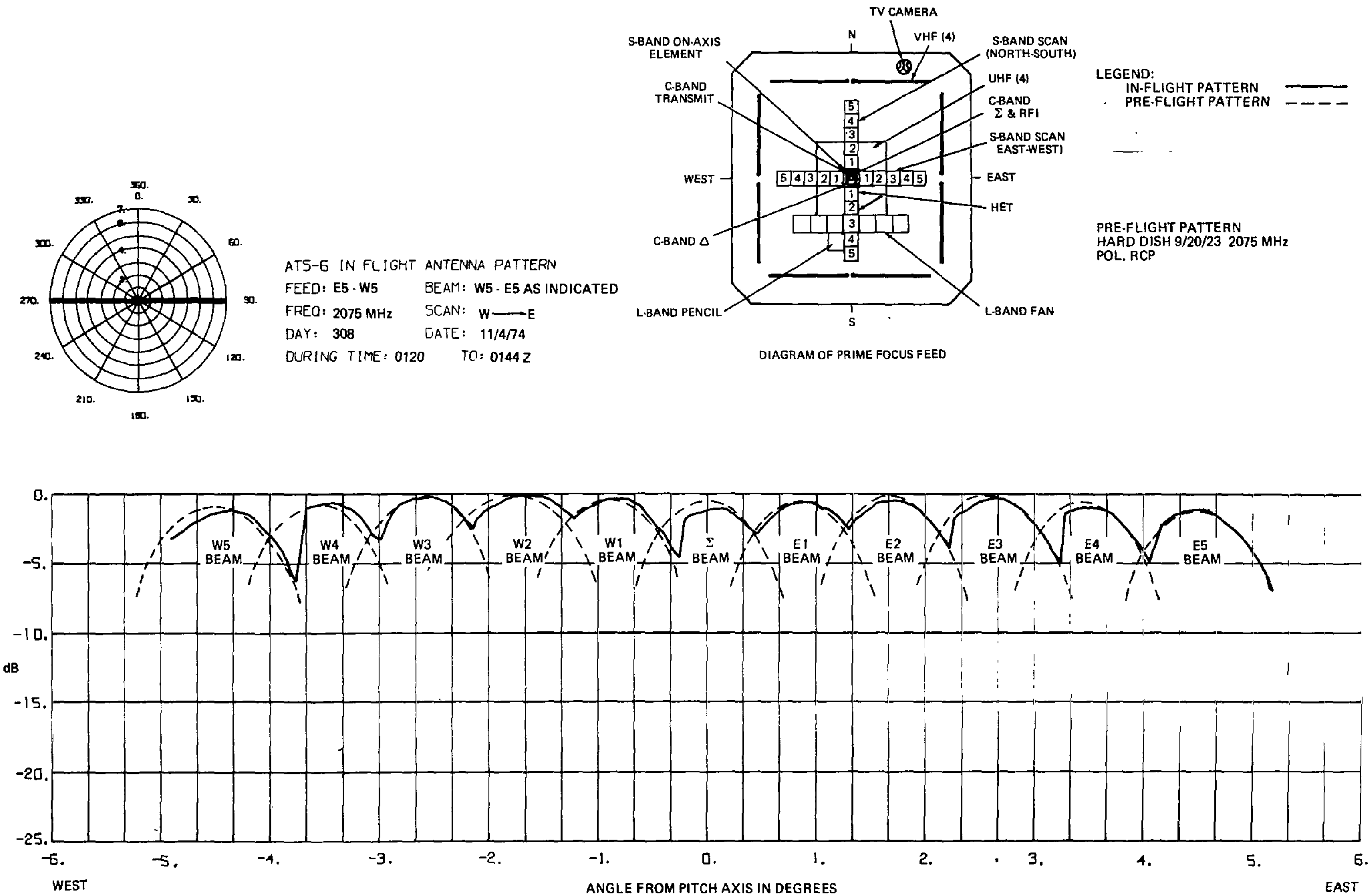

Figure 59. S-band cross-axis patterns E – W.

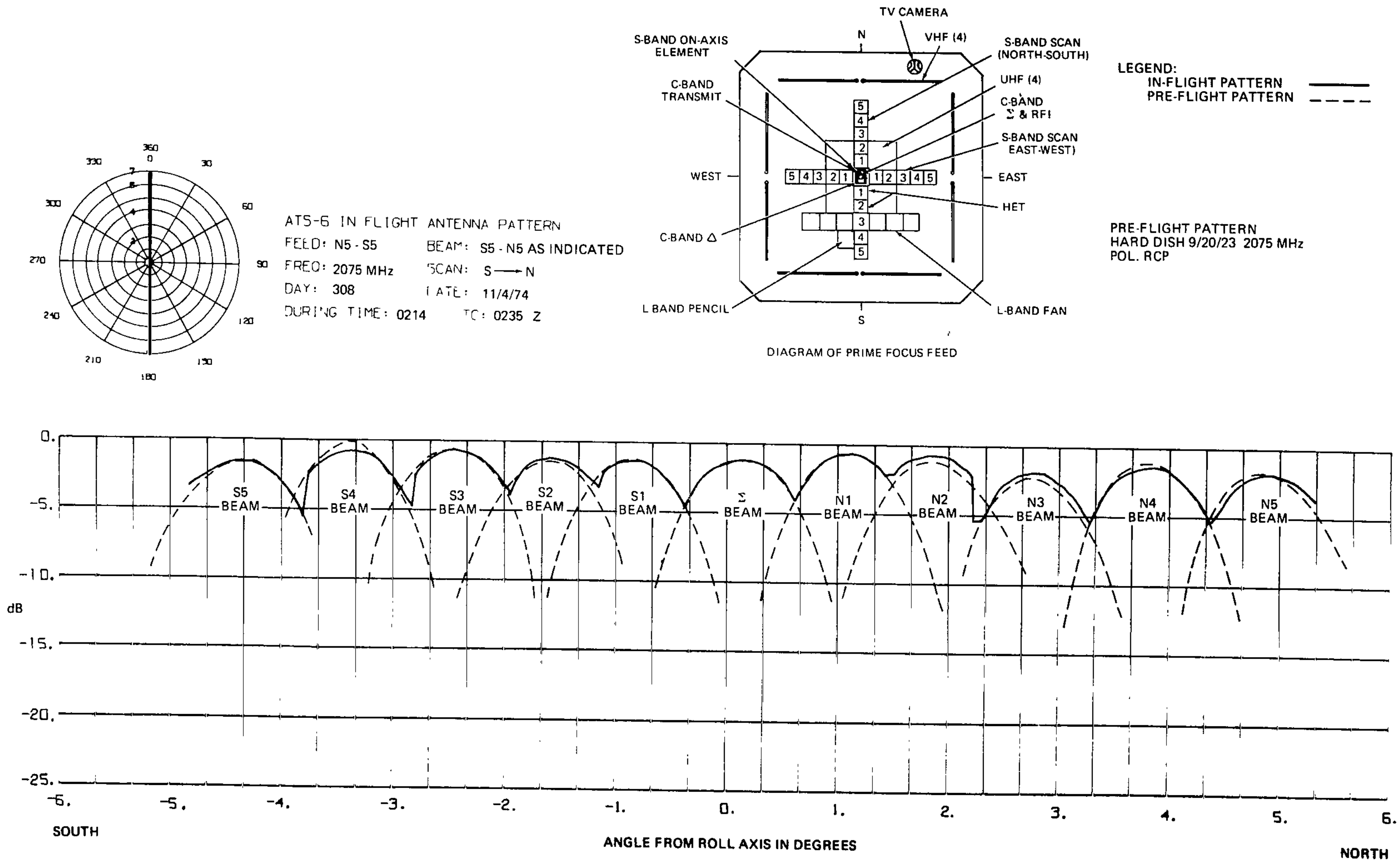

Figure 60. S-band cross-axis patterns N – S.

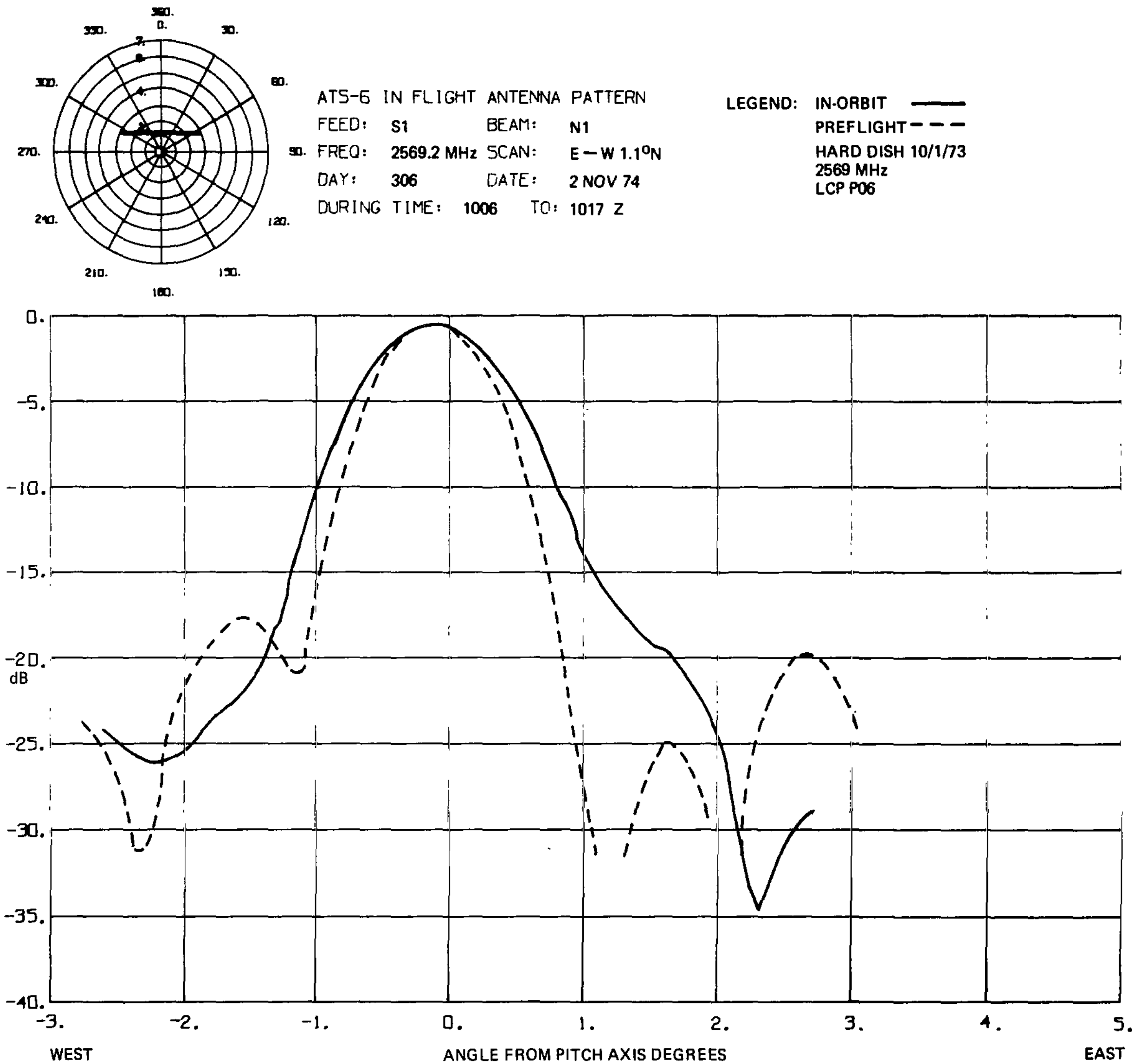

Figure 61. S-band beam N1 E – W 1.1° N (HET).

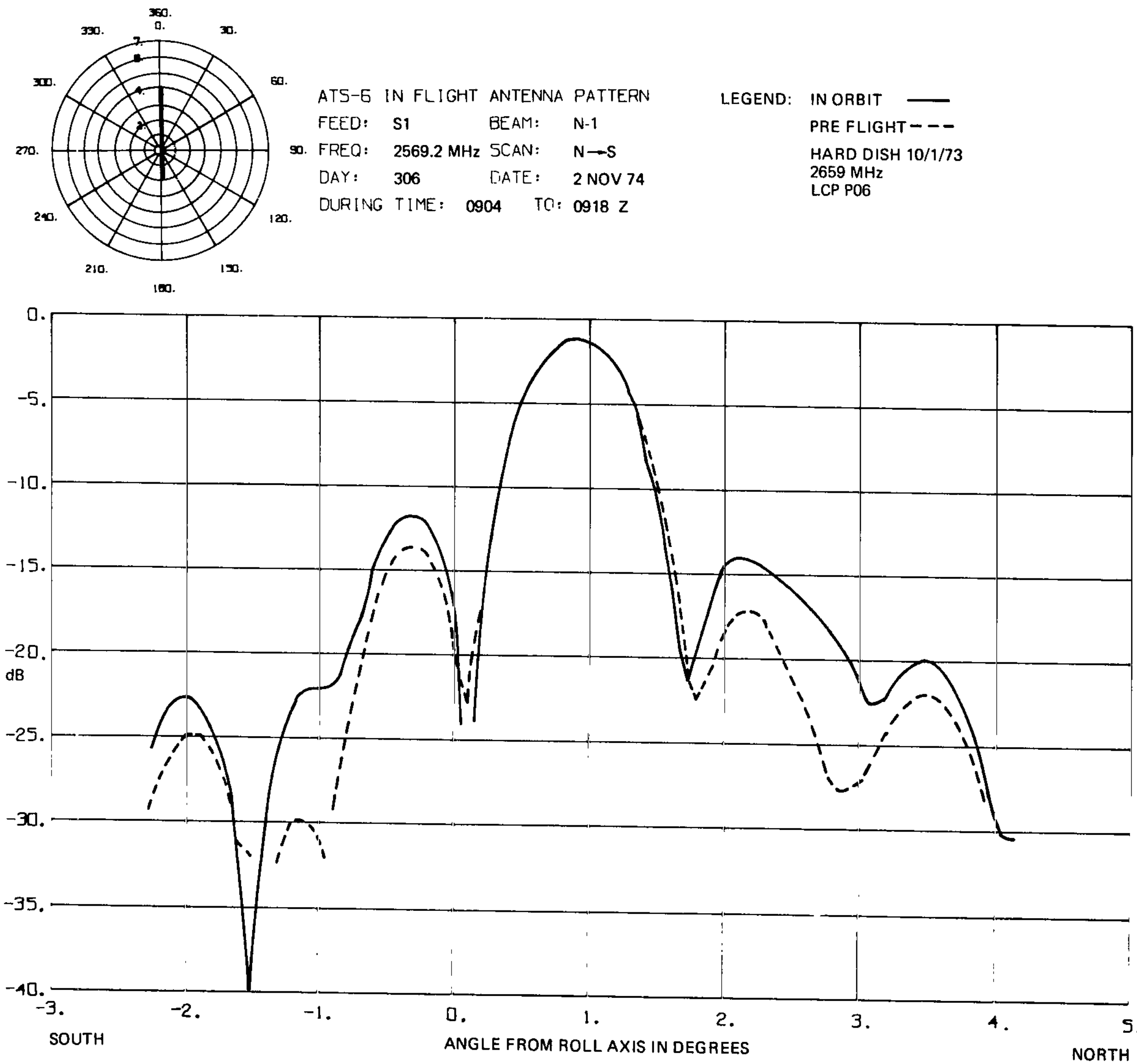

Figure 62. S-band beam N1 N – S (HET).

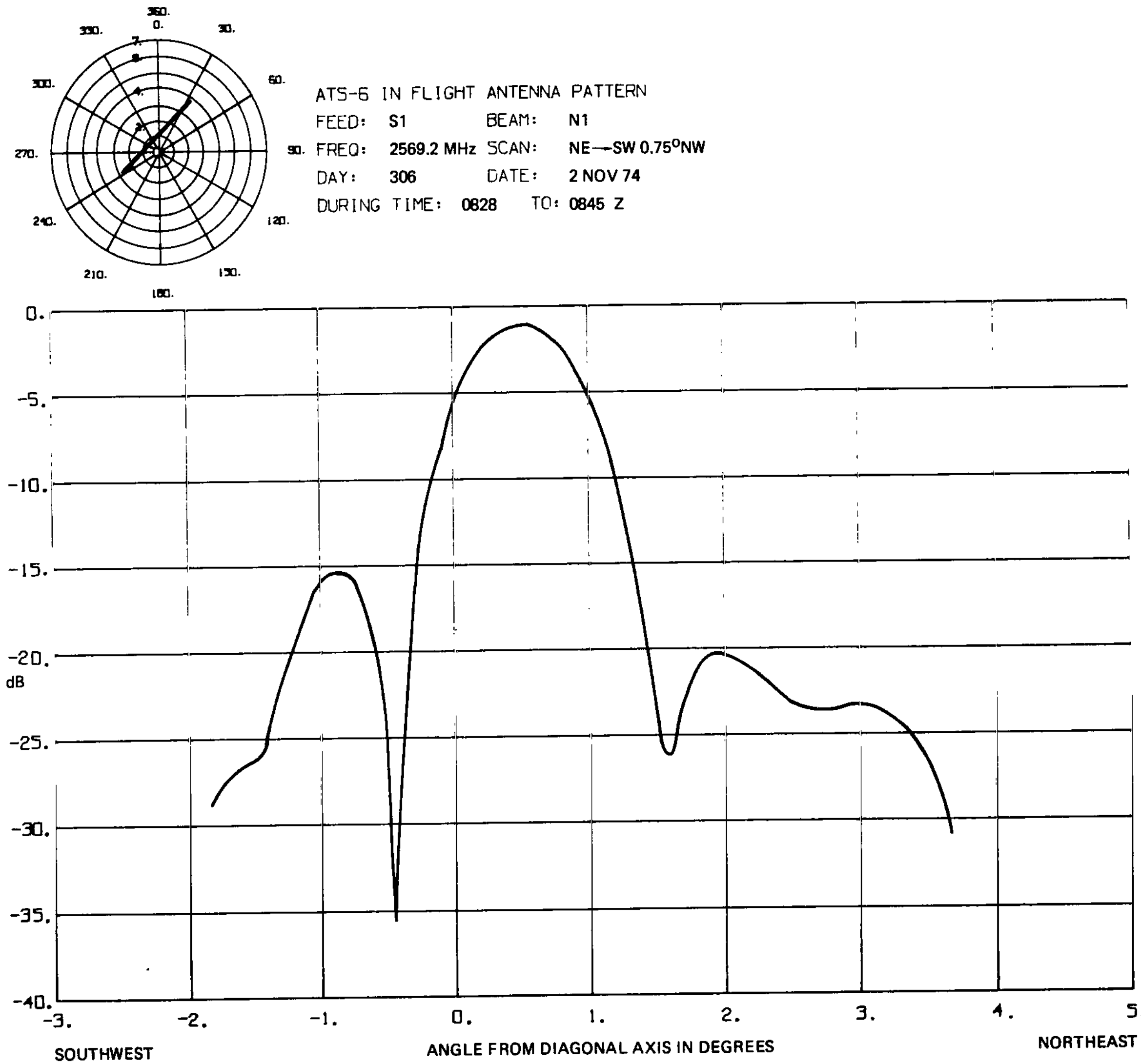

Figure 63. S-band beam N1 NE – SW 0.75° NW (HET).

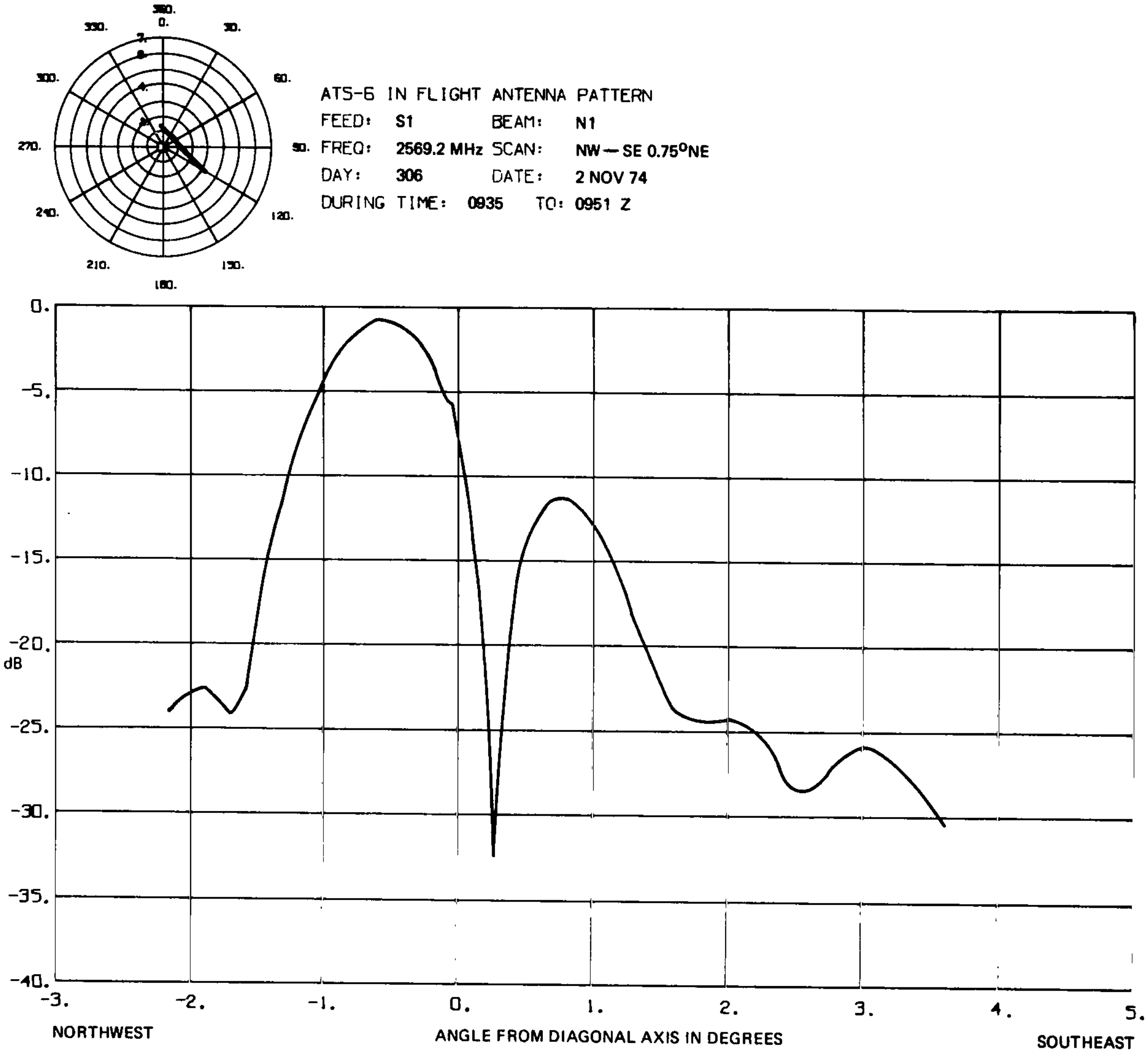

Figure 64. S-band beam N1 NW – SE 0.75° NE (HET).

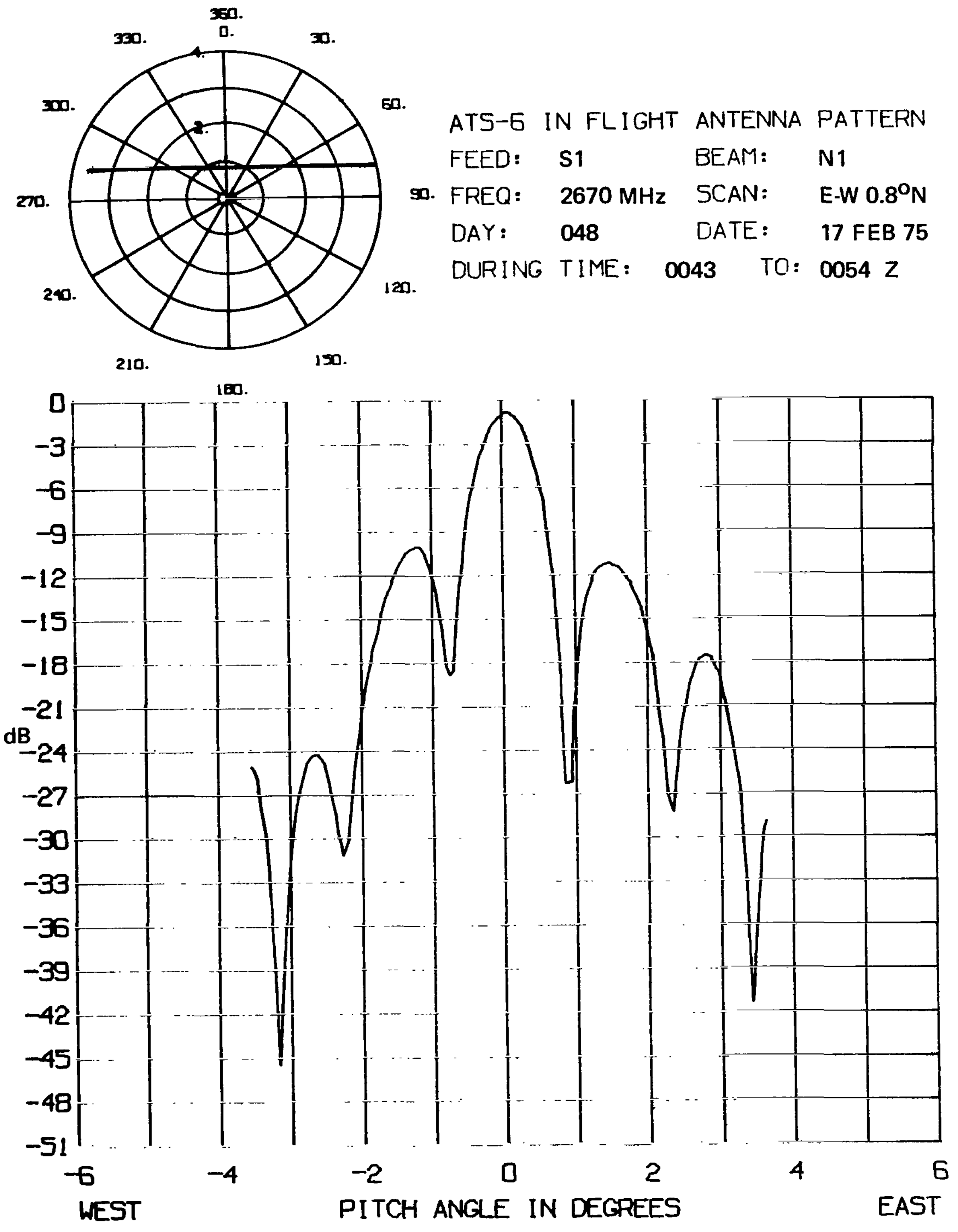

Figure 65. S-band beam N1 E – W 0.8° N (HET).

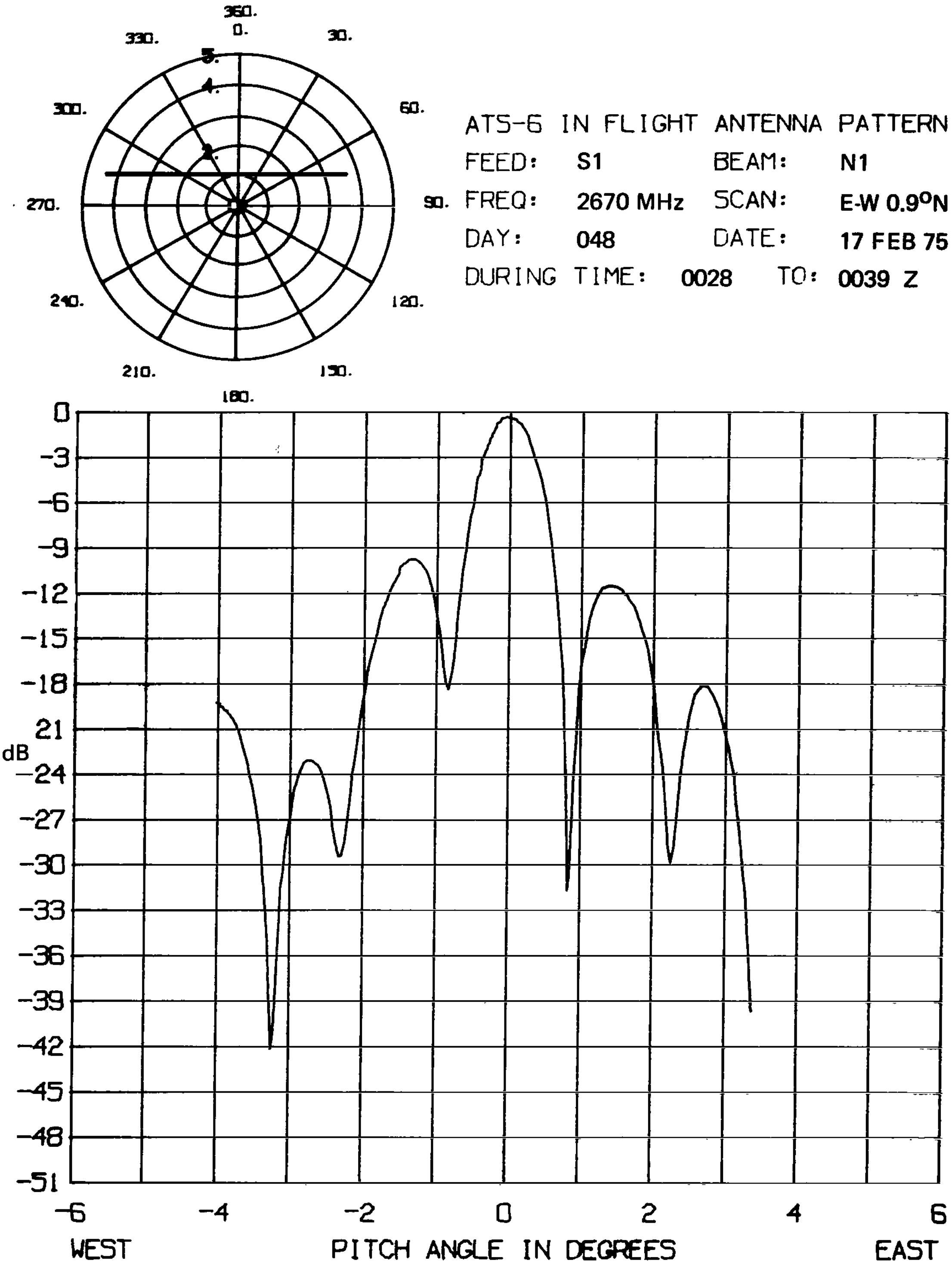

Figure 66. S-band beam N1 E – W 0.9° N (HET).

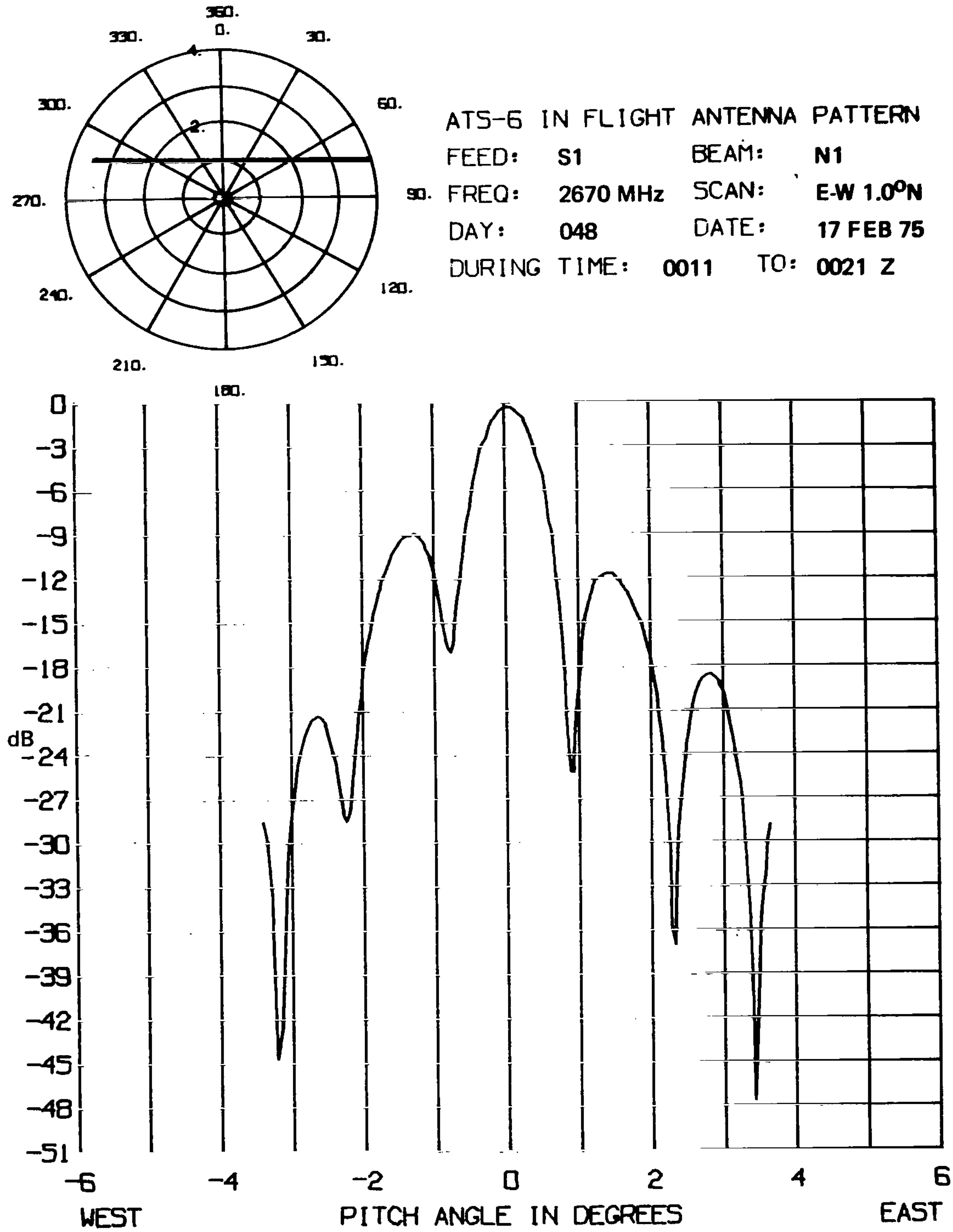

Figure 67. S-band beam N1 E – W 1.0° N (HET).

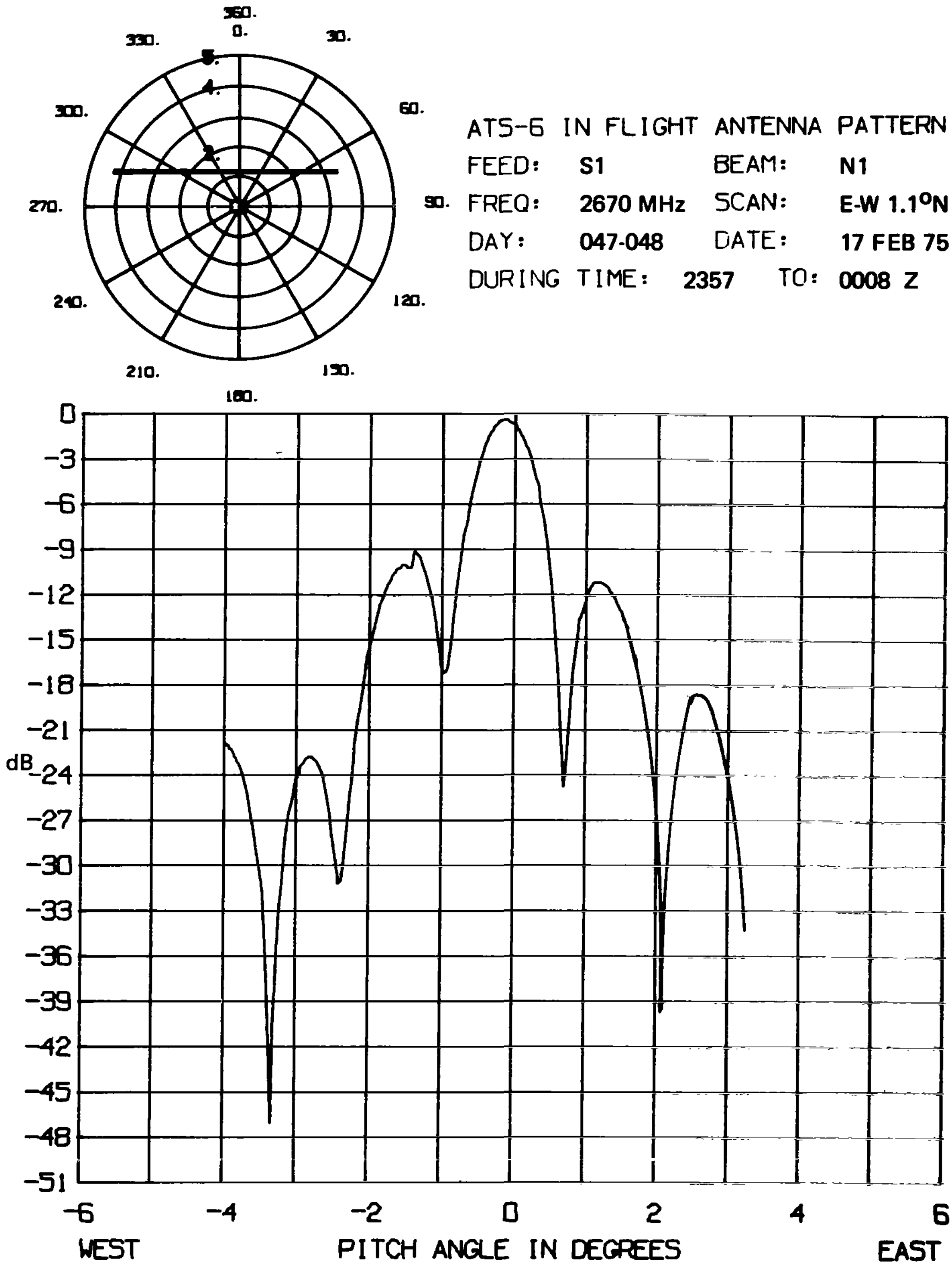

Figure 68. S-band beam N1 E – W 1.1° N (HET).

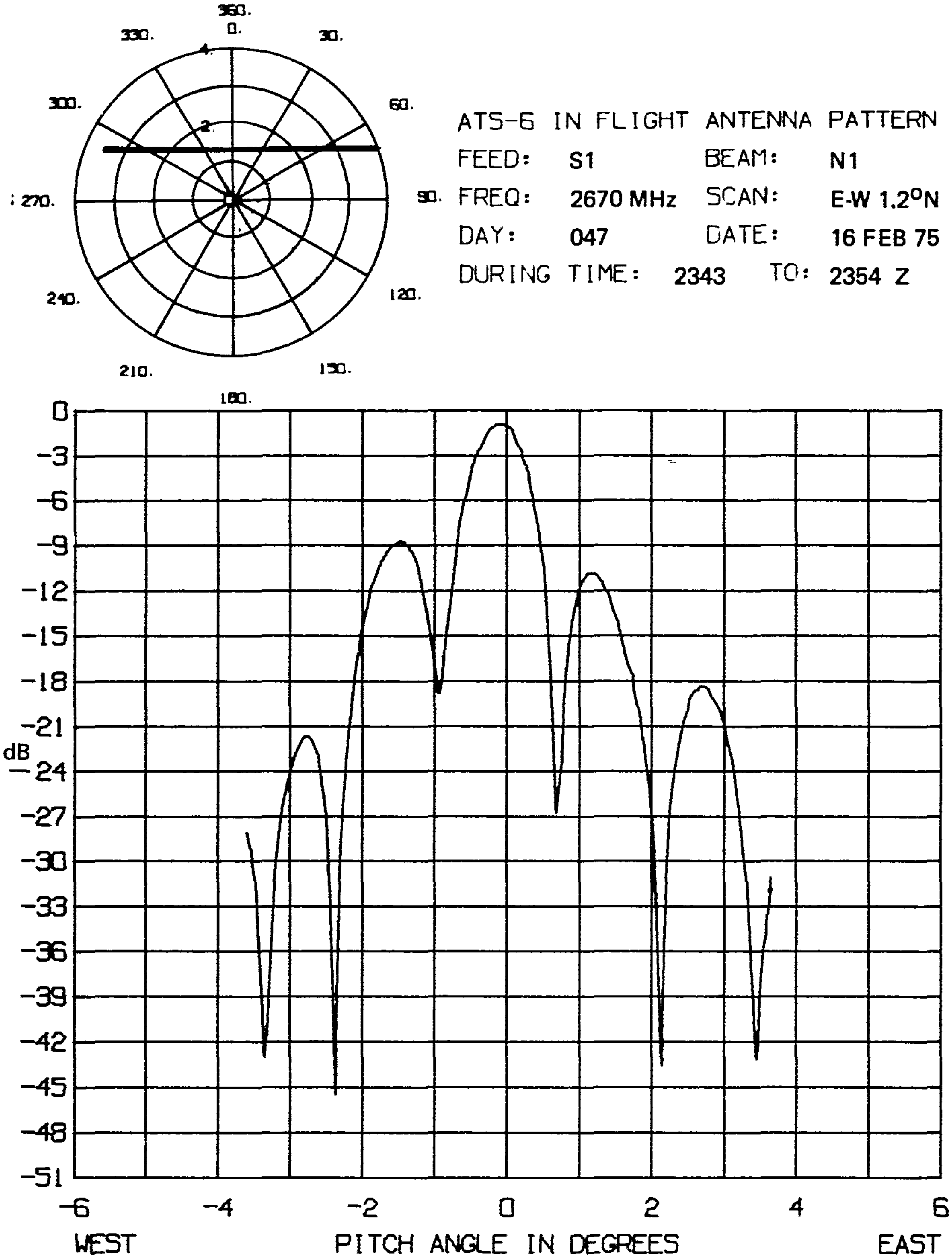

Figure 69. S-band beam N1 E – W 1.2° N (HET).

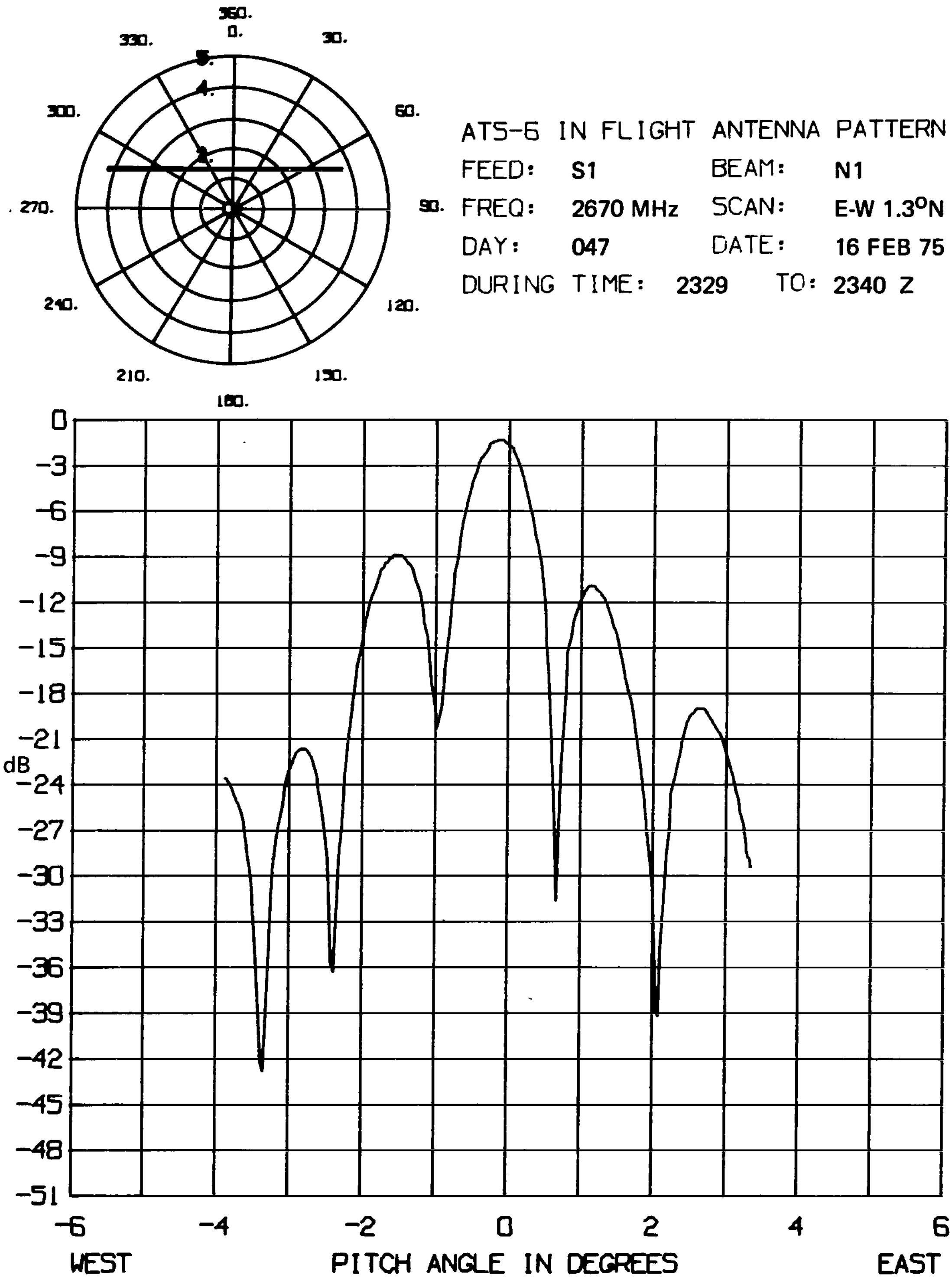

Figure 70. S-band beam N1 E – W 1.3° N (HET).

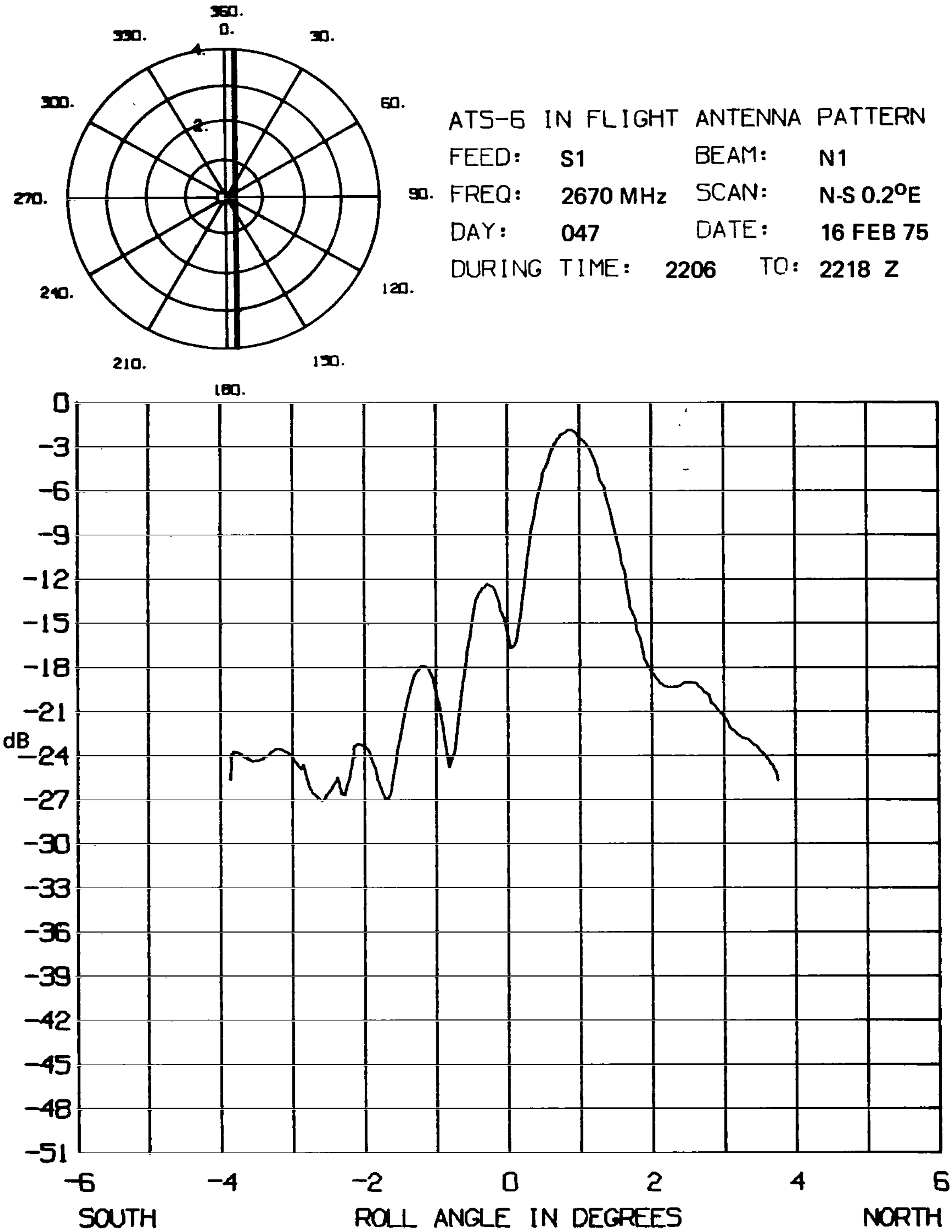

Figure 71. S-band beam N1 N – W 0.2° E (HET).

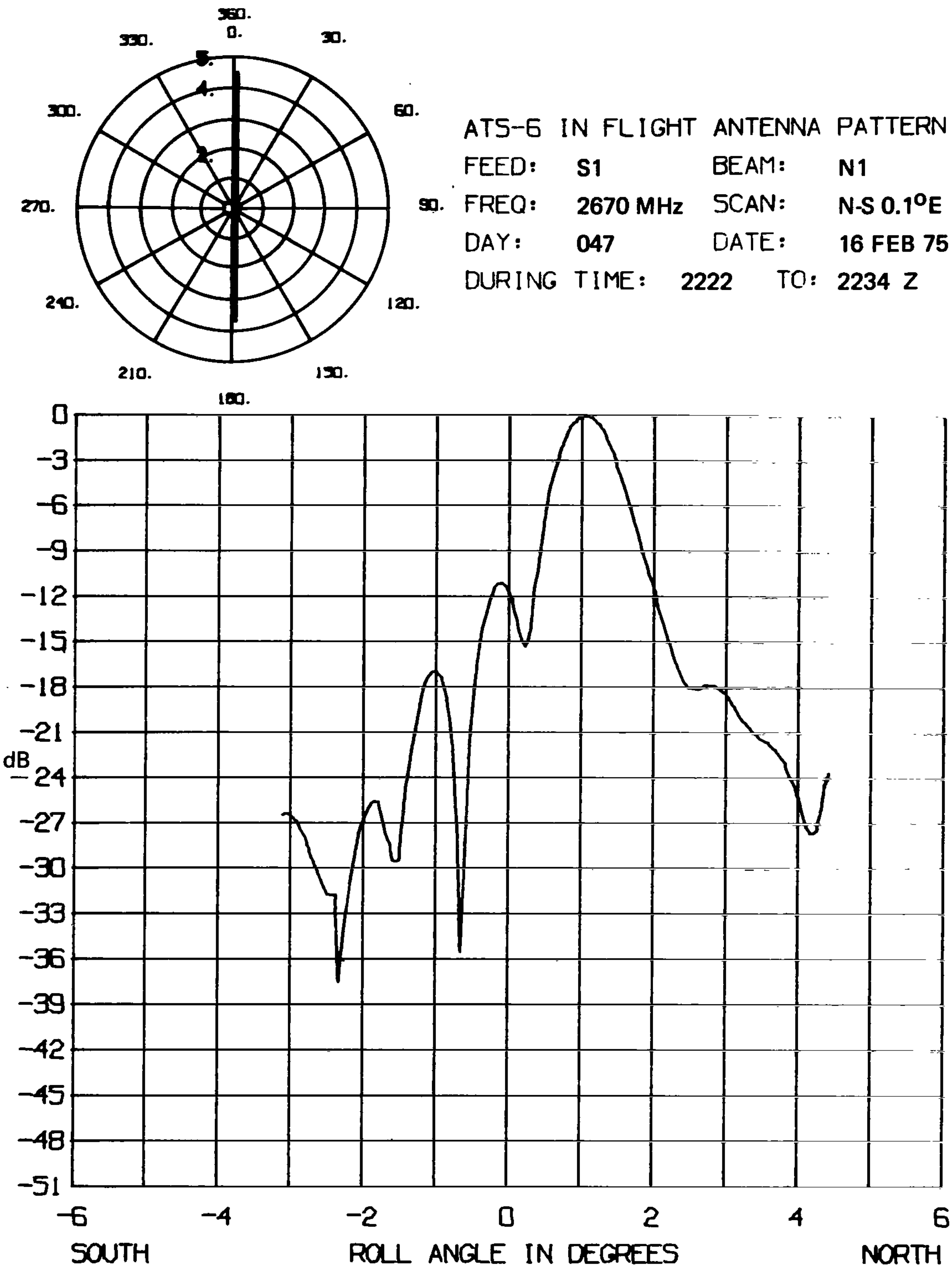

Figure 72. S-band beam N1 N – S 0.1° E (HET).

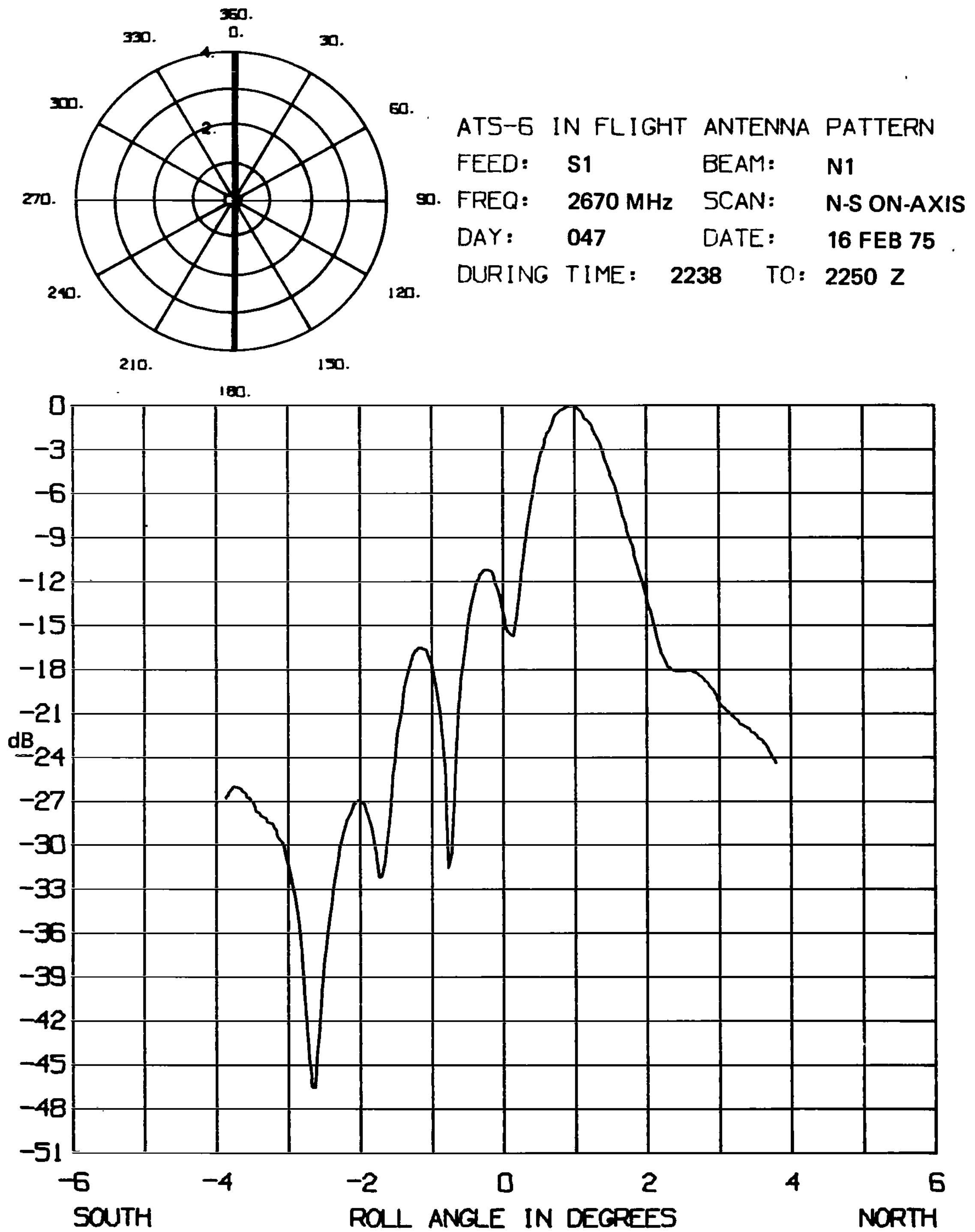

Figure 73. S-band beam N1 N – S on-axis (HET).

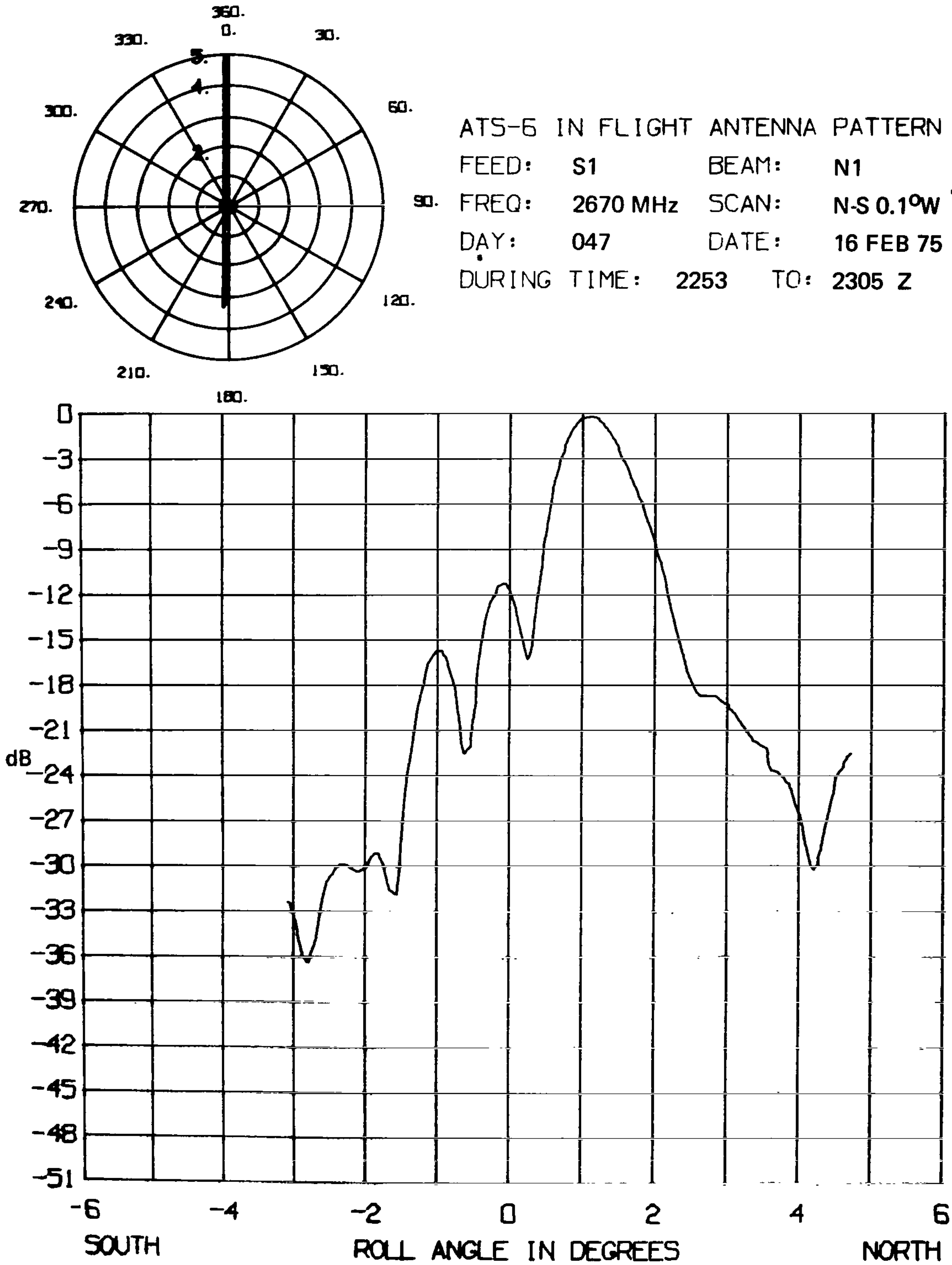

Figure 74. S-band beam N1 N – S 0.1° W (HET).

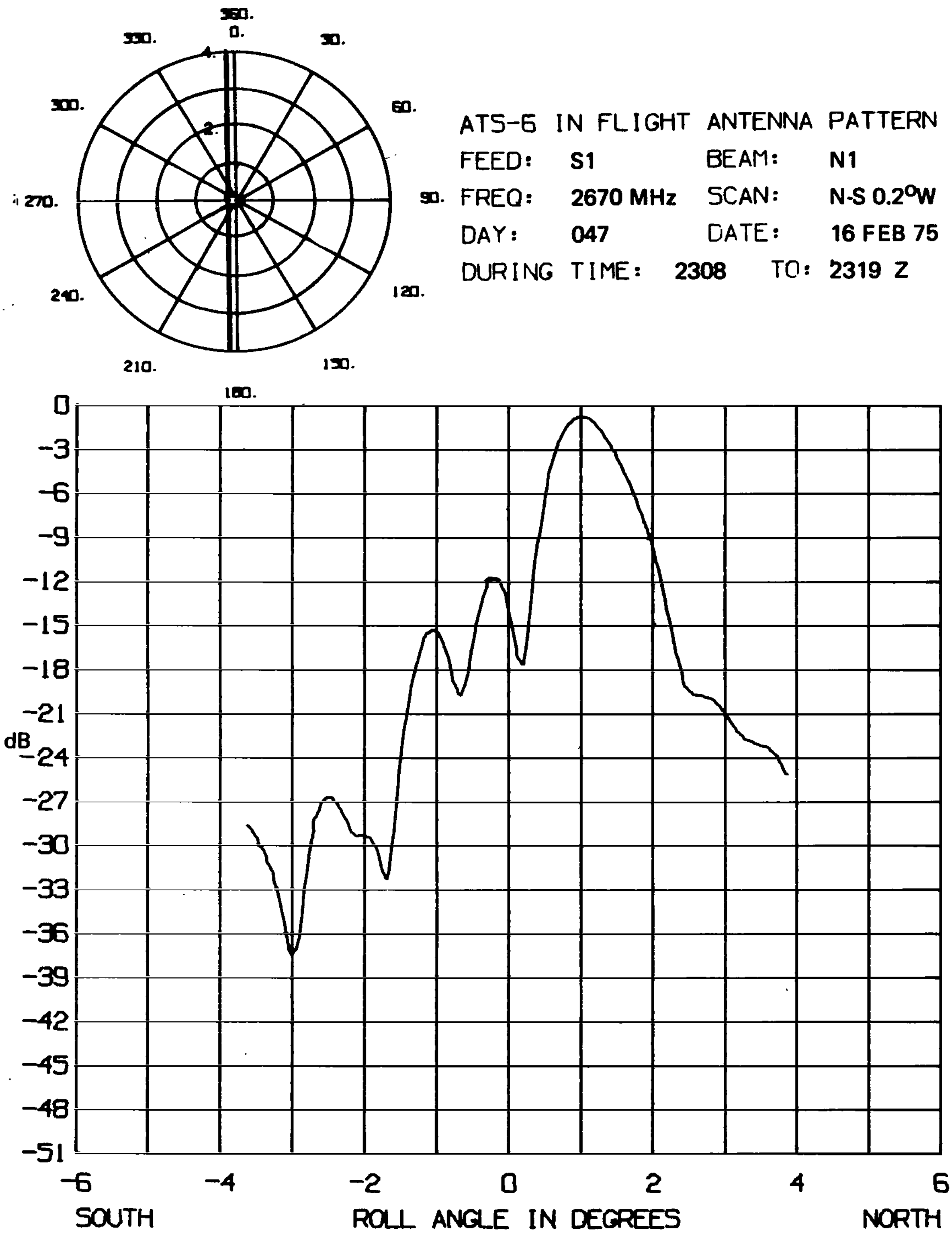

Figure 75. S-band beam N1 N – S 0.2° W (HET).

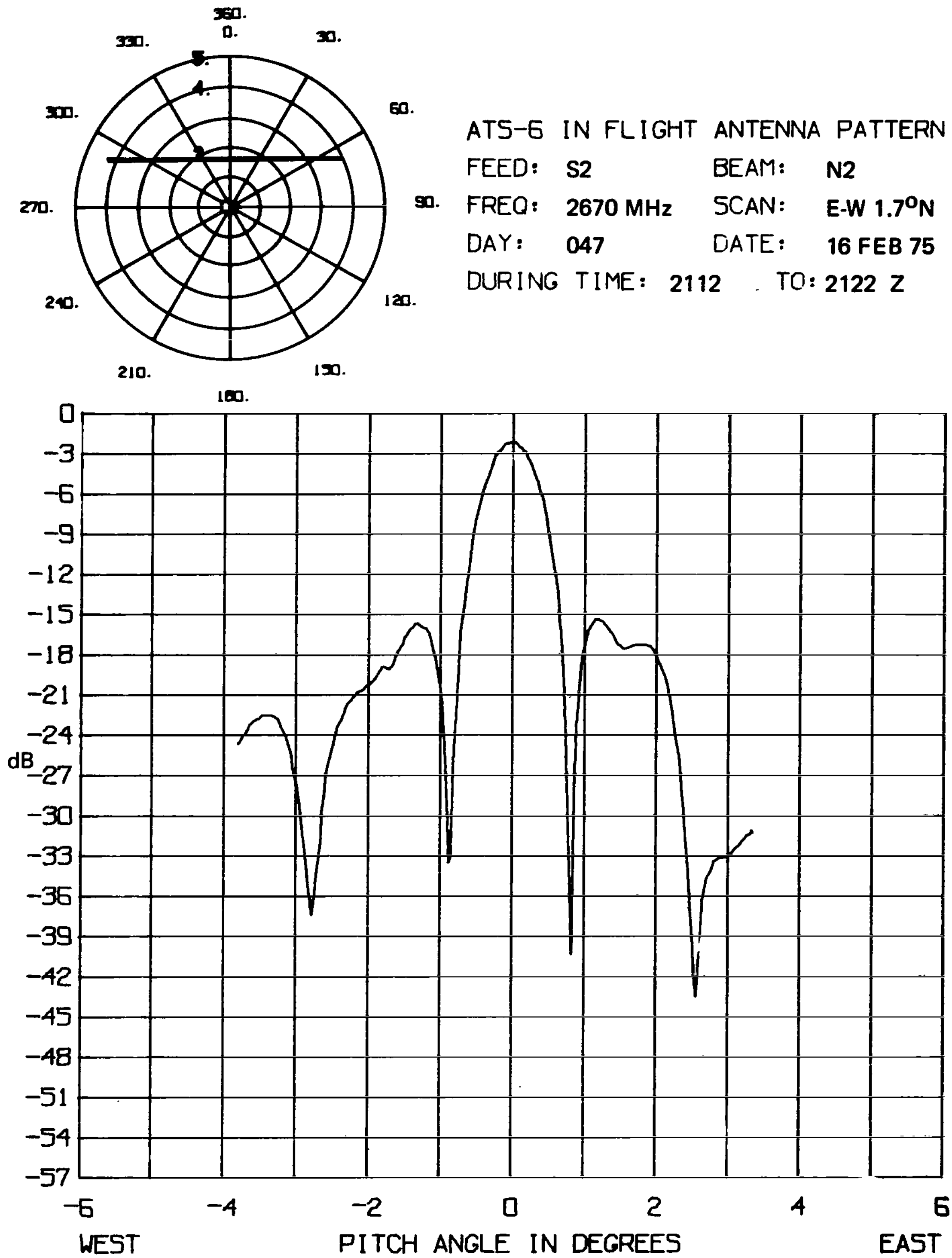

Figure 76. S-band beam N2 E – W 1.7°N (HET).

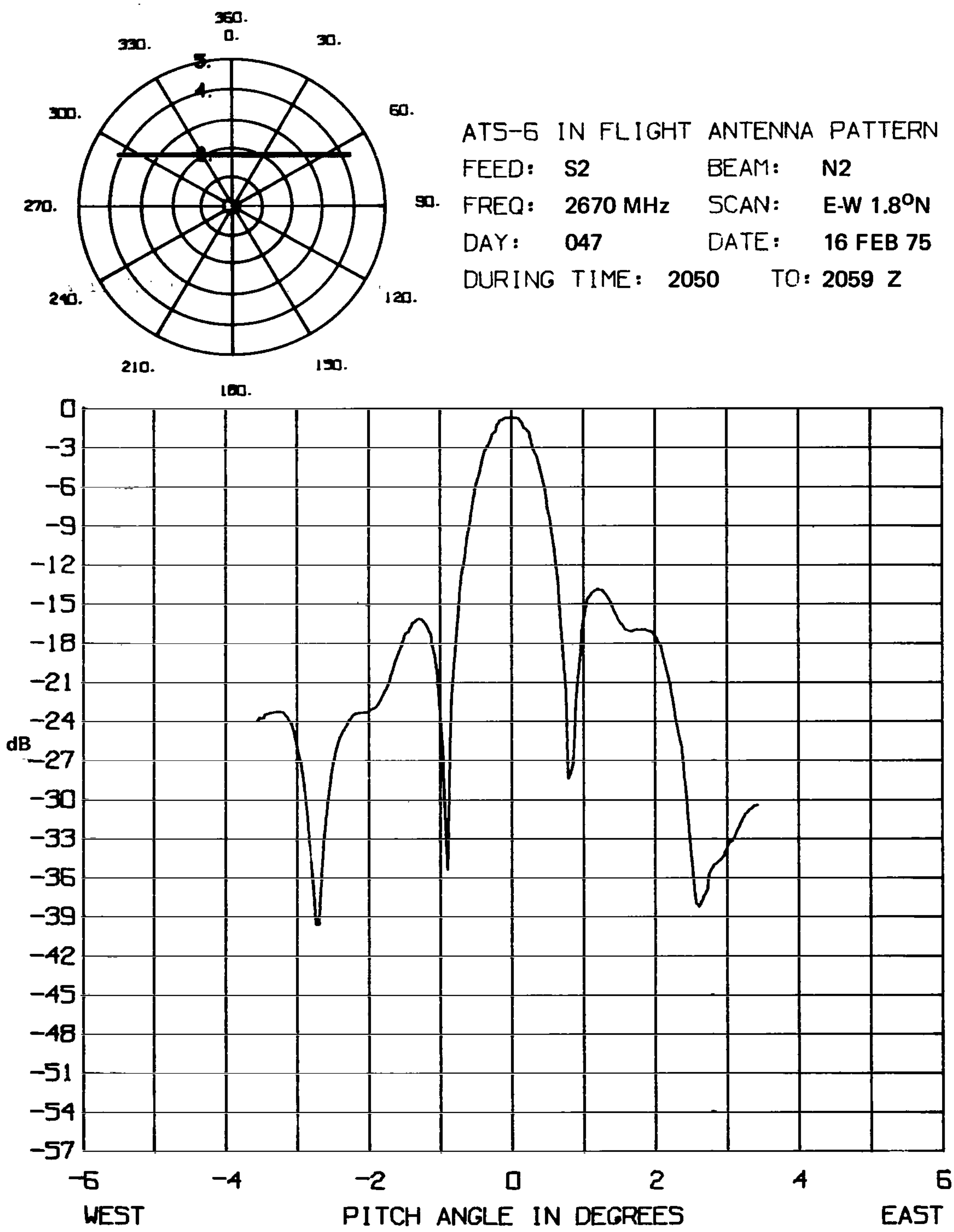

Figure 77. S-band beam N2 E – W 1.8° N (HET).

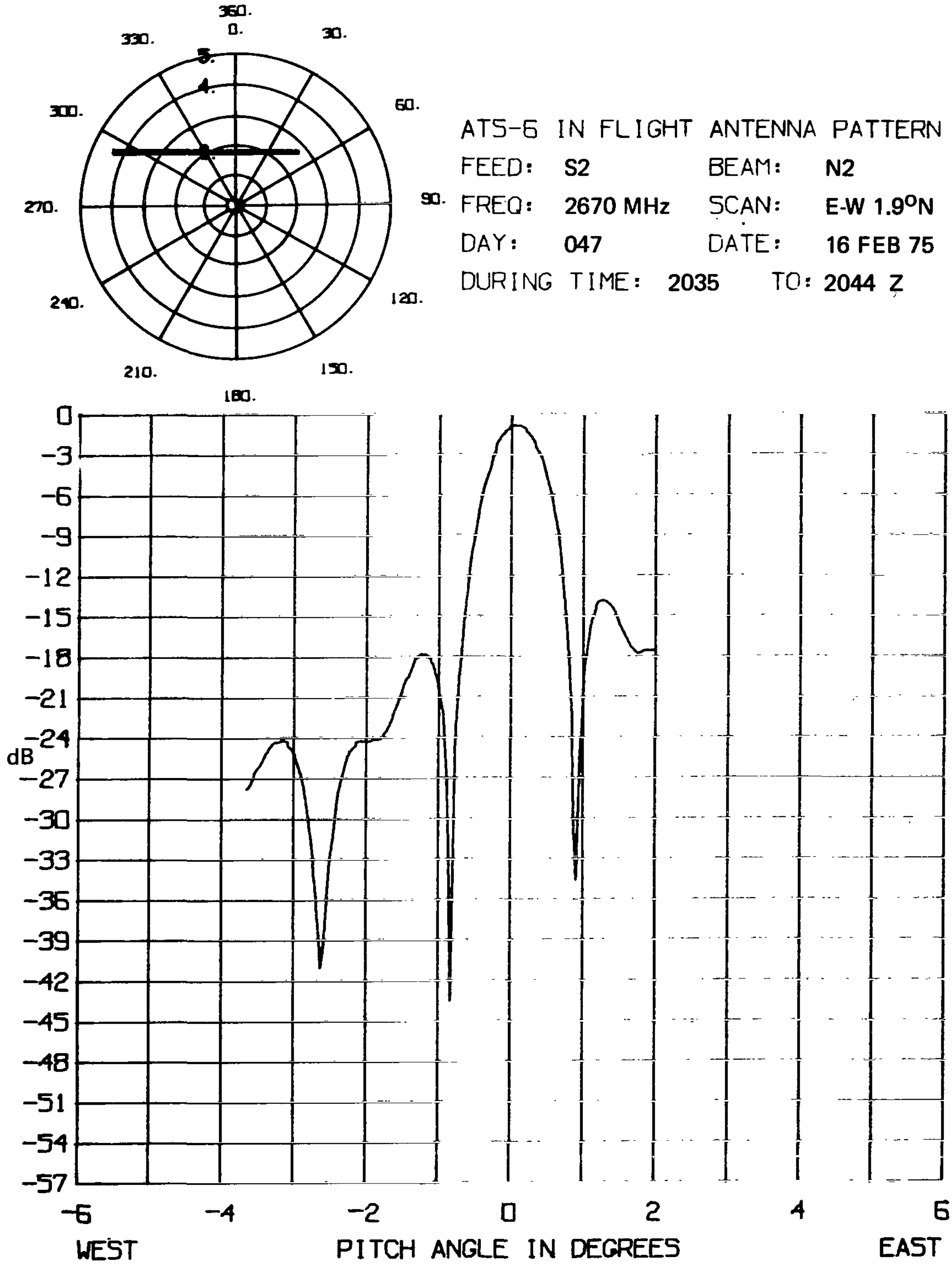

Figure 78. S-band beam N2 E – W 1.9° N (HET).

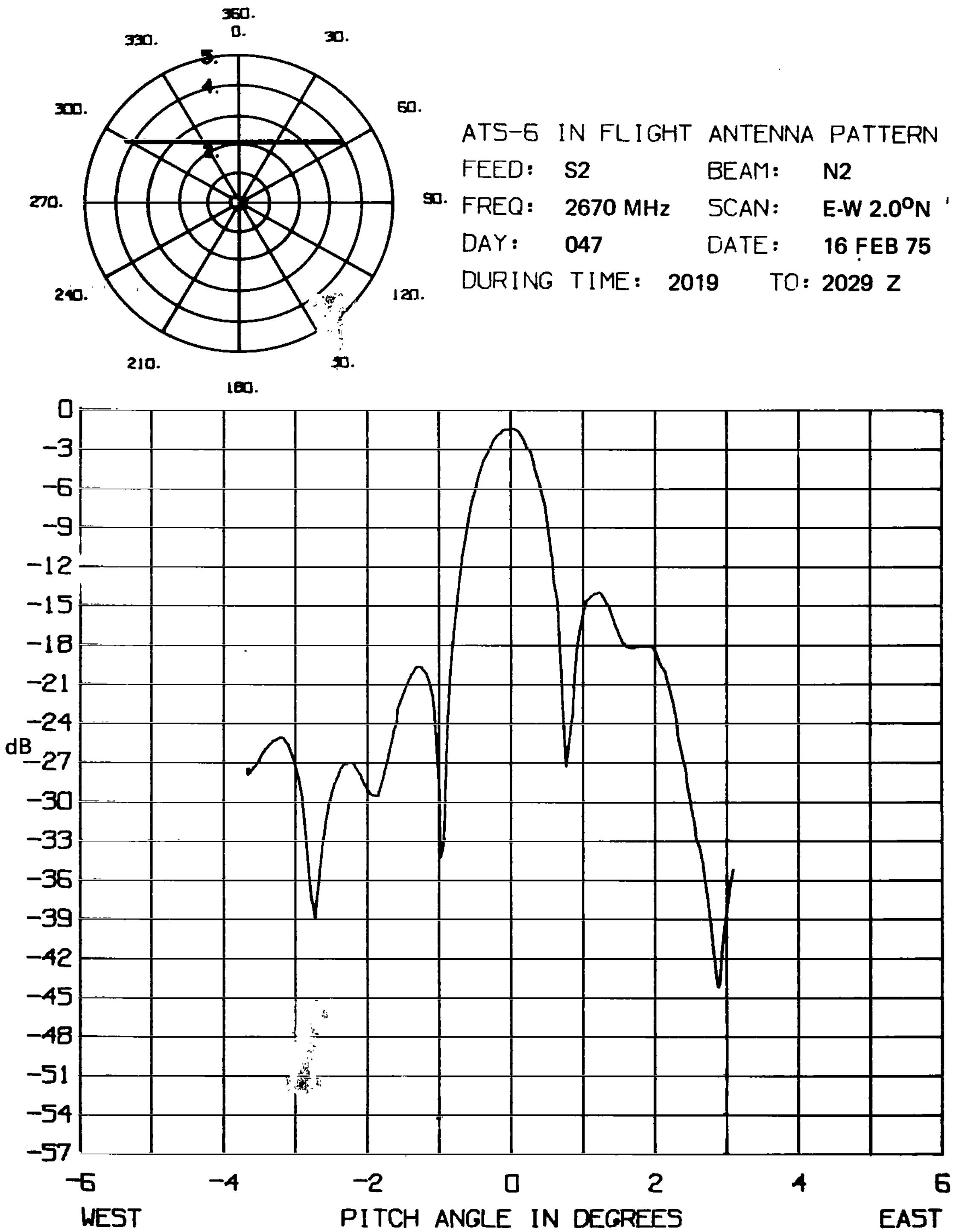

Figure 79. S-band beam N2 E – W 2° N (HET).

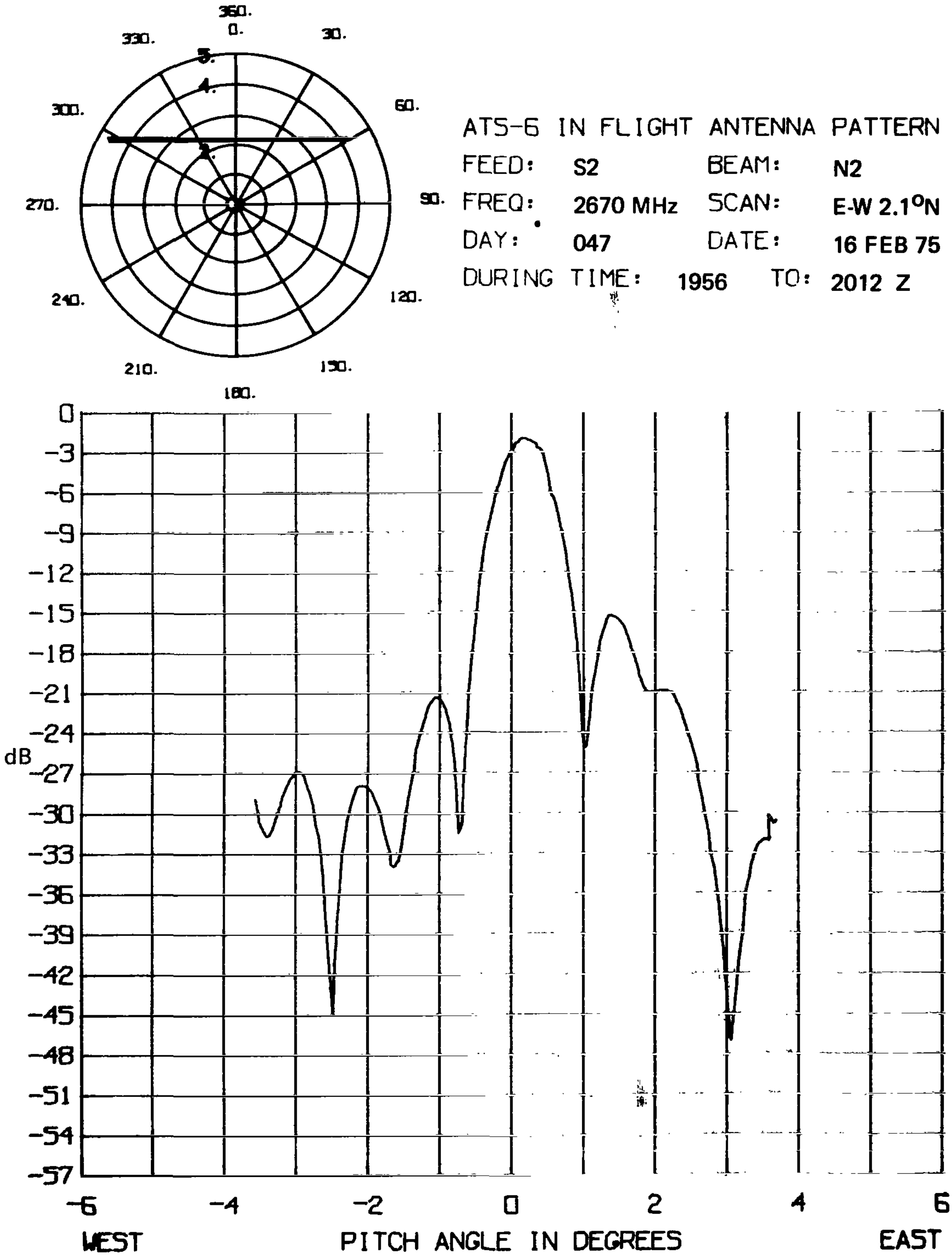

Figure 80. S-band beam N2 E – W 2.1° N (HET).

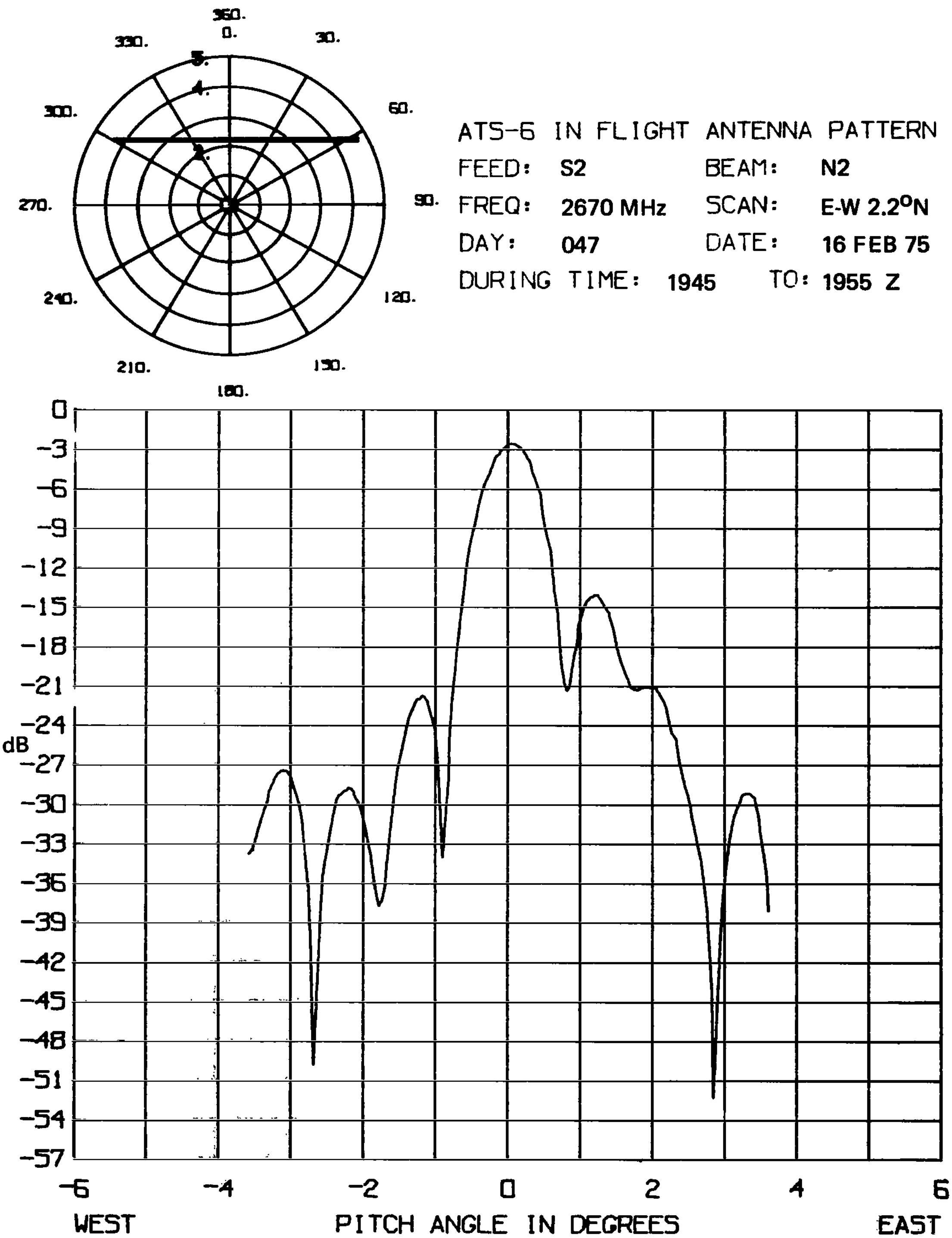

Figure 81. S-band beam N2 E – W 2.2° N (HET).

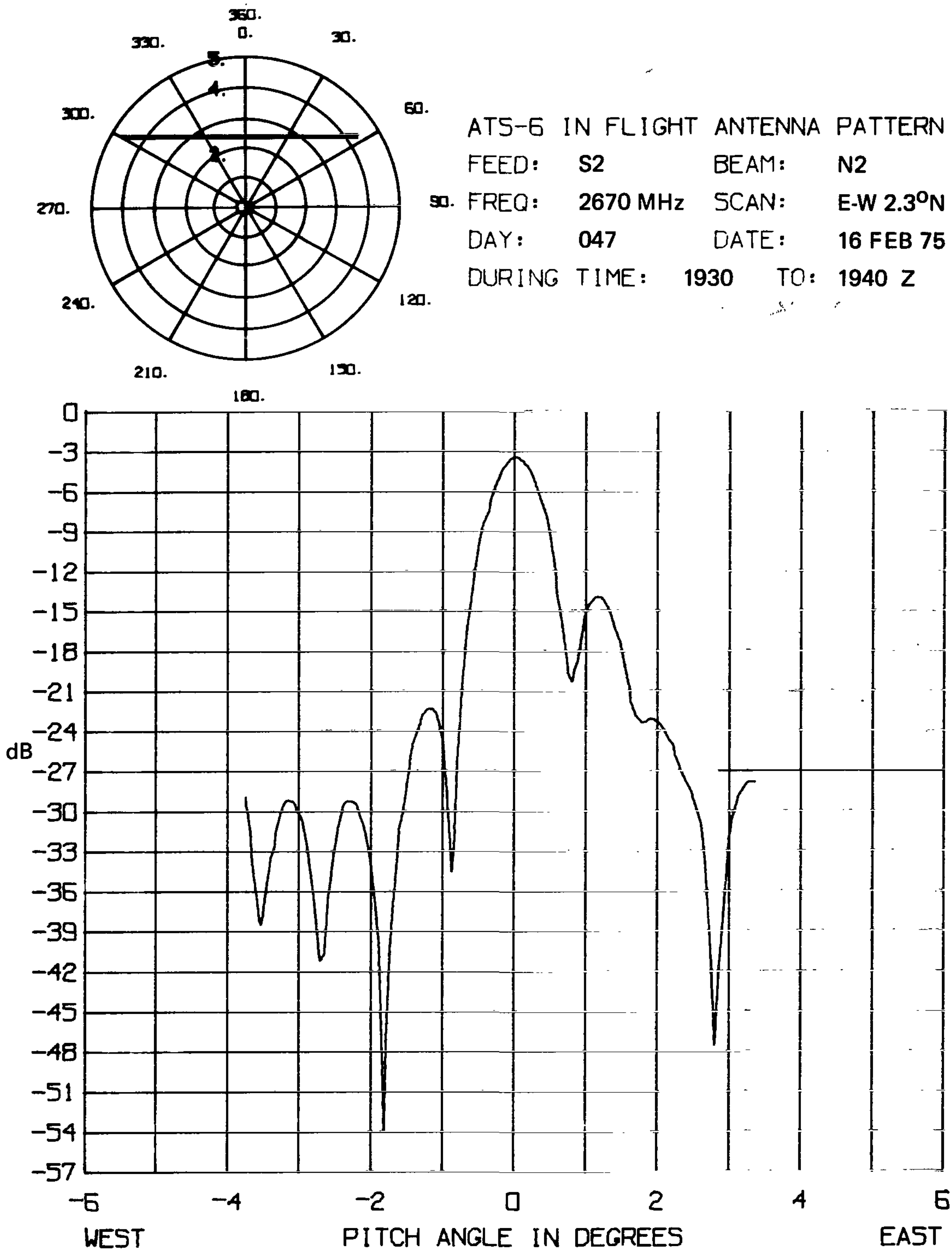

Figure 82. S-band beam N2 E – W 2.3° N (HET).

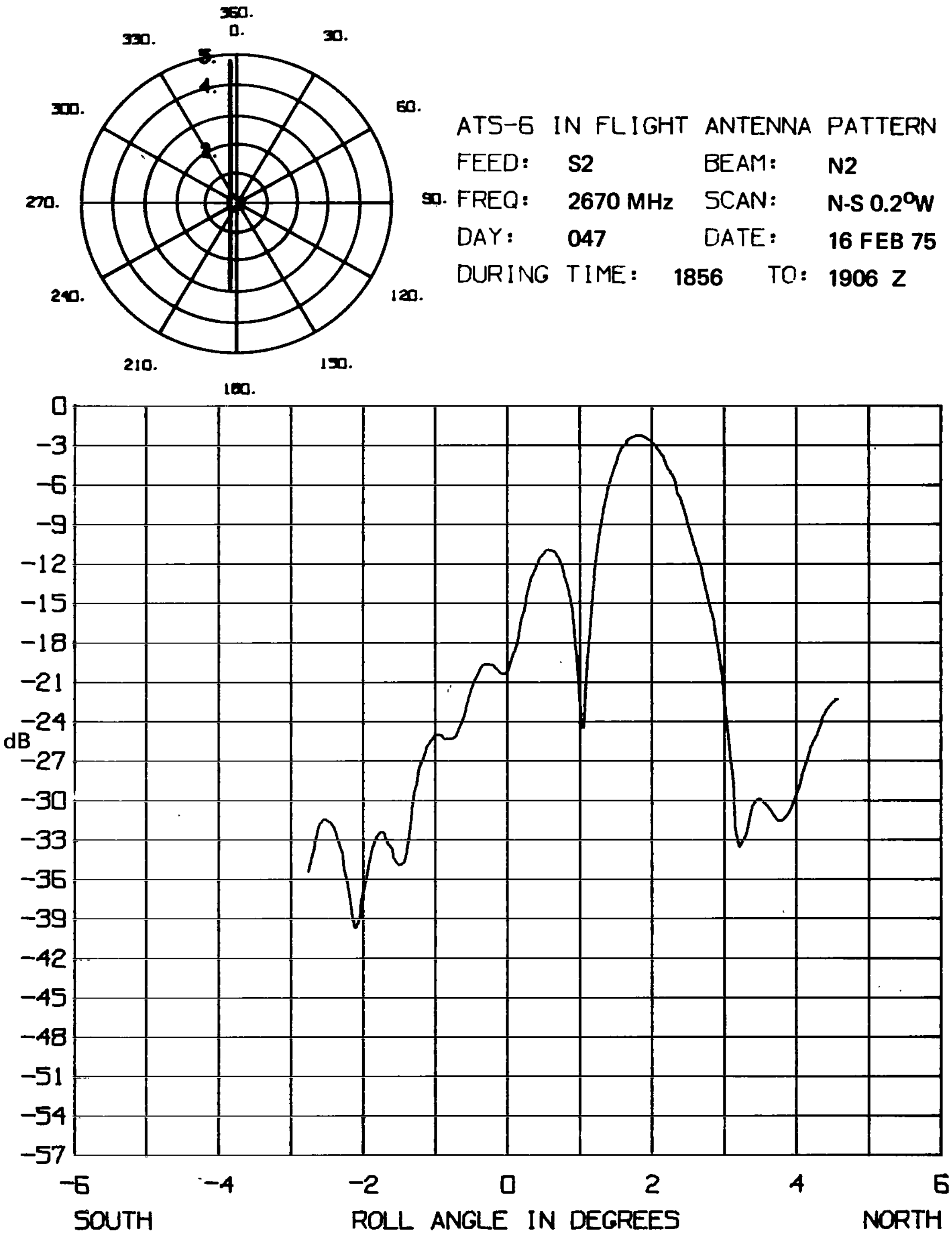

Figure 83. S-band Beam N2 N – S 0.2° W (HET).

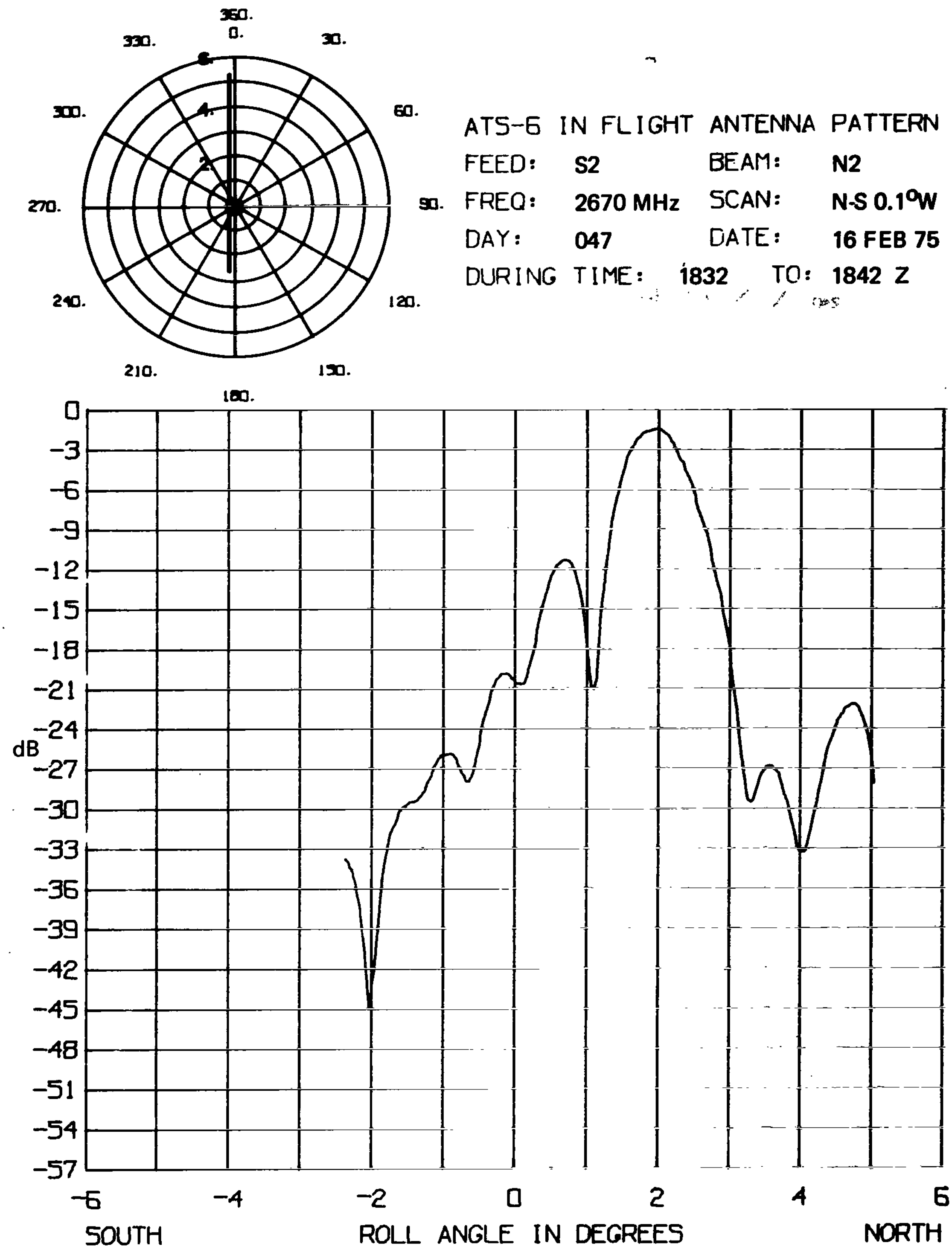

Figure 84. S-band beam N2 N – S 0.1° W (HET).

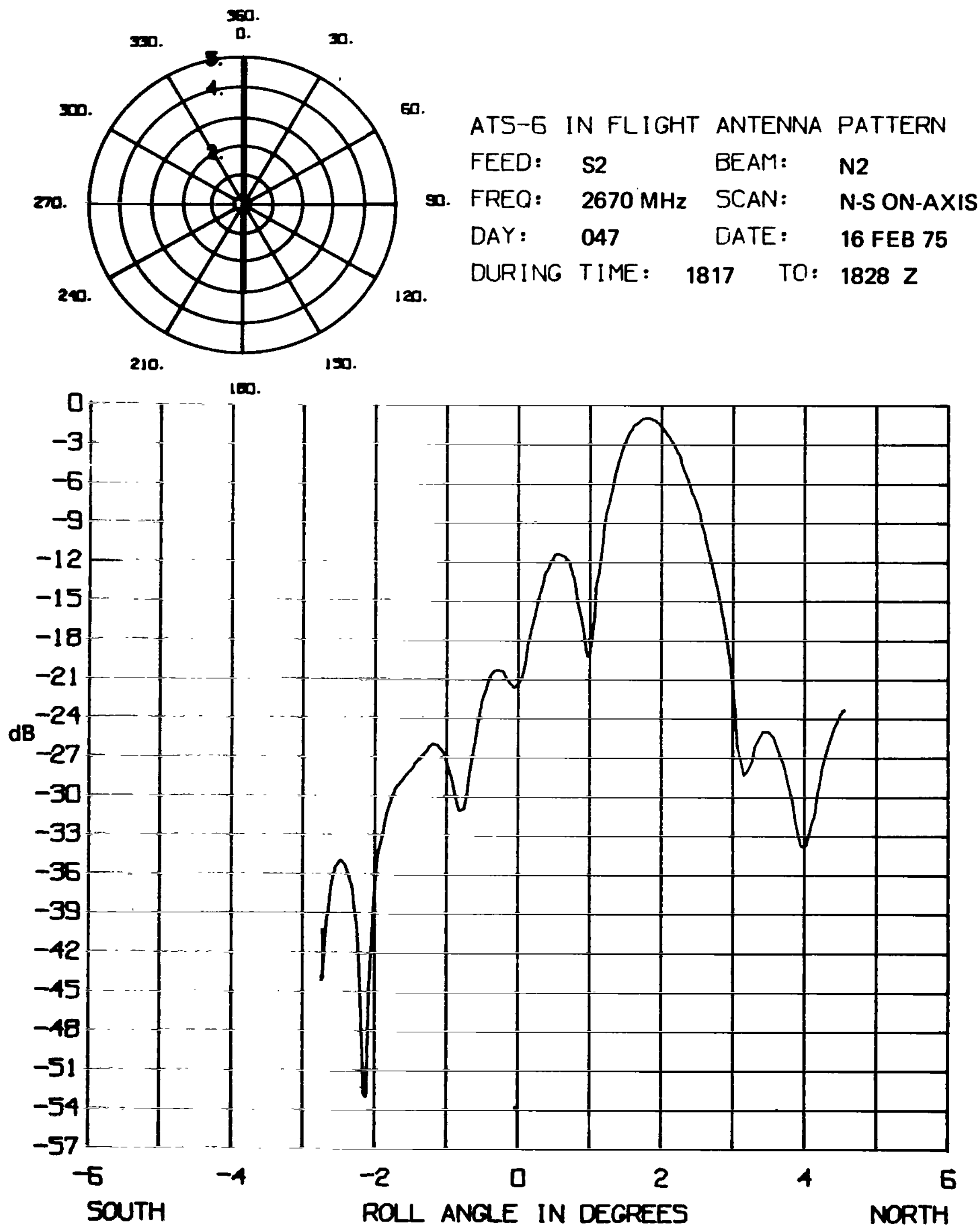

Figure 85. S-band beam N2 N – S on-axis (HET).

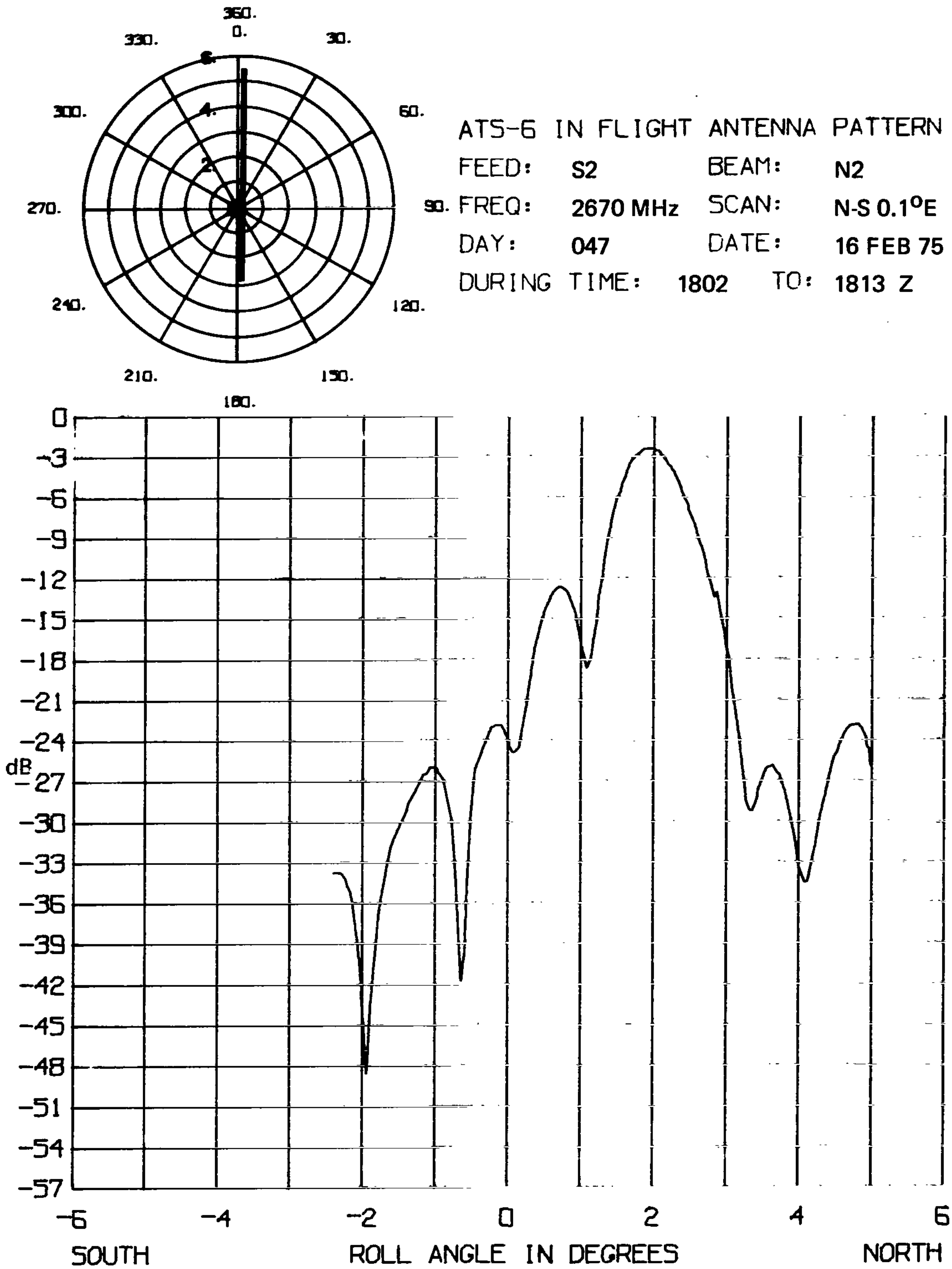

Figure 86. S-band beam N2 N – S 0.1° E (HET).

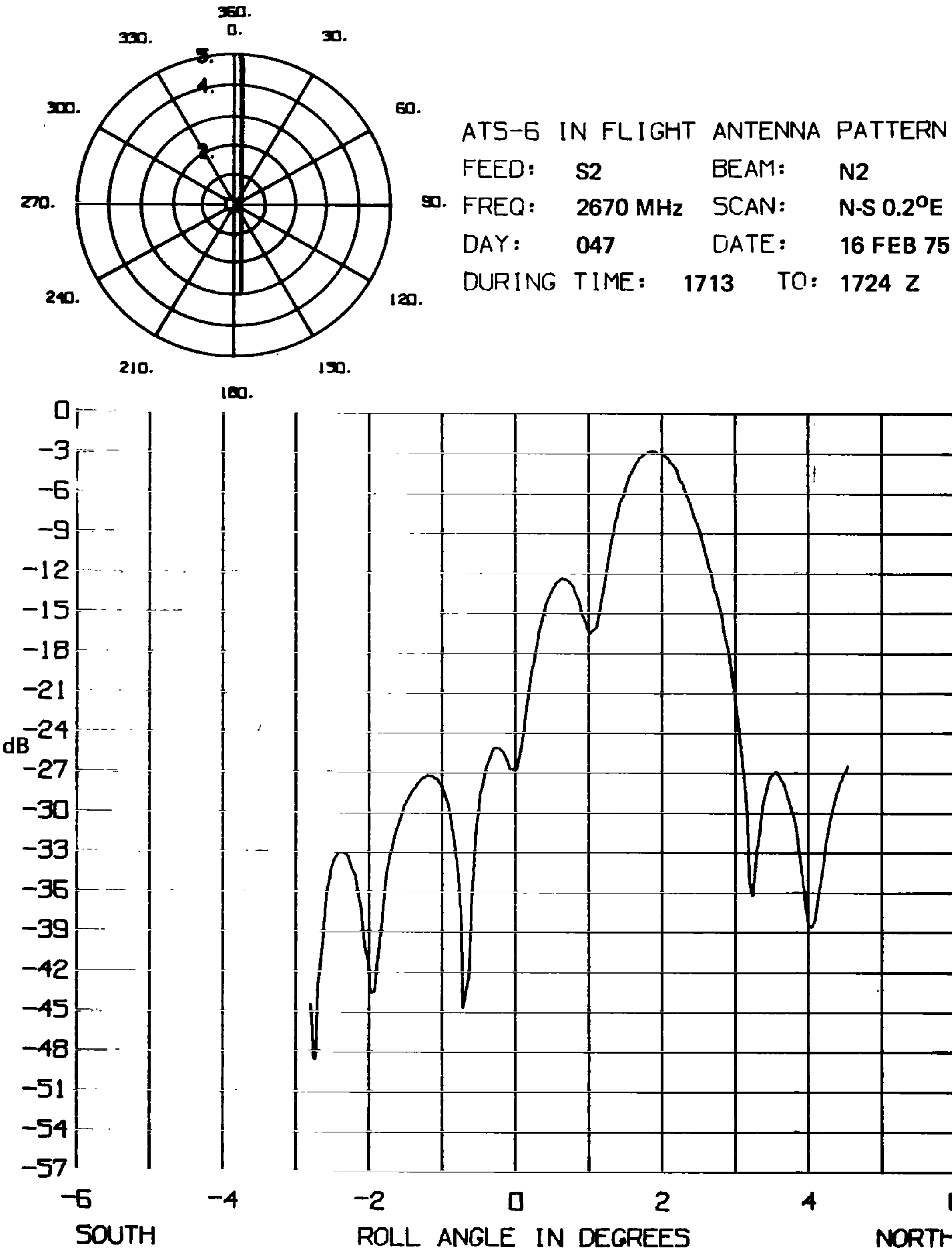

Figure 87. S-band beam N2 N – S 0.2° E (HET).

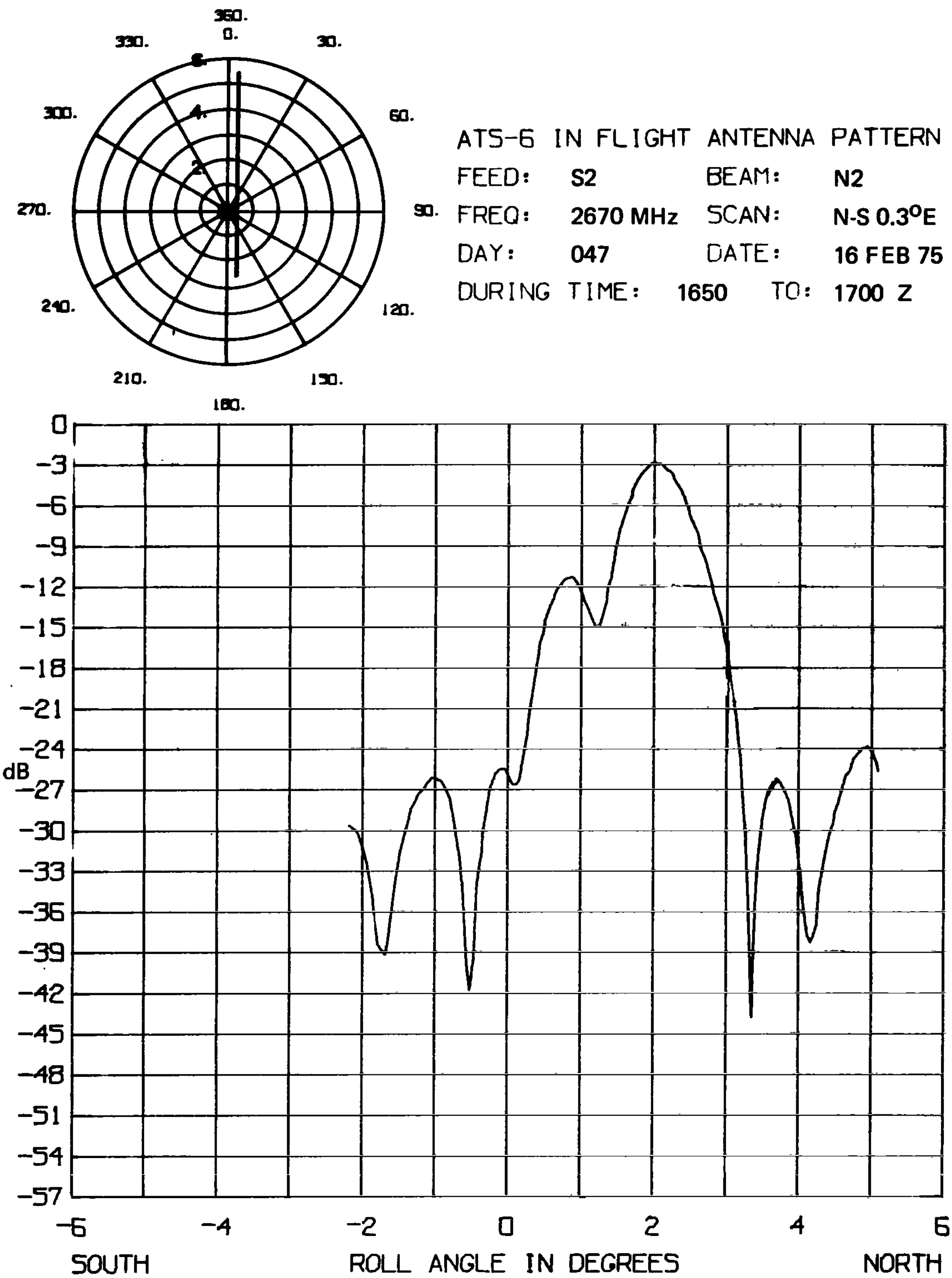

Figure 88. S-band beam N2 N – S 0.3° E (HET).

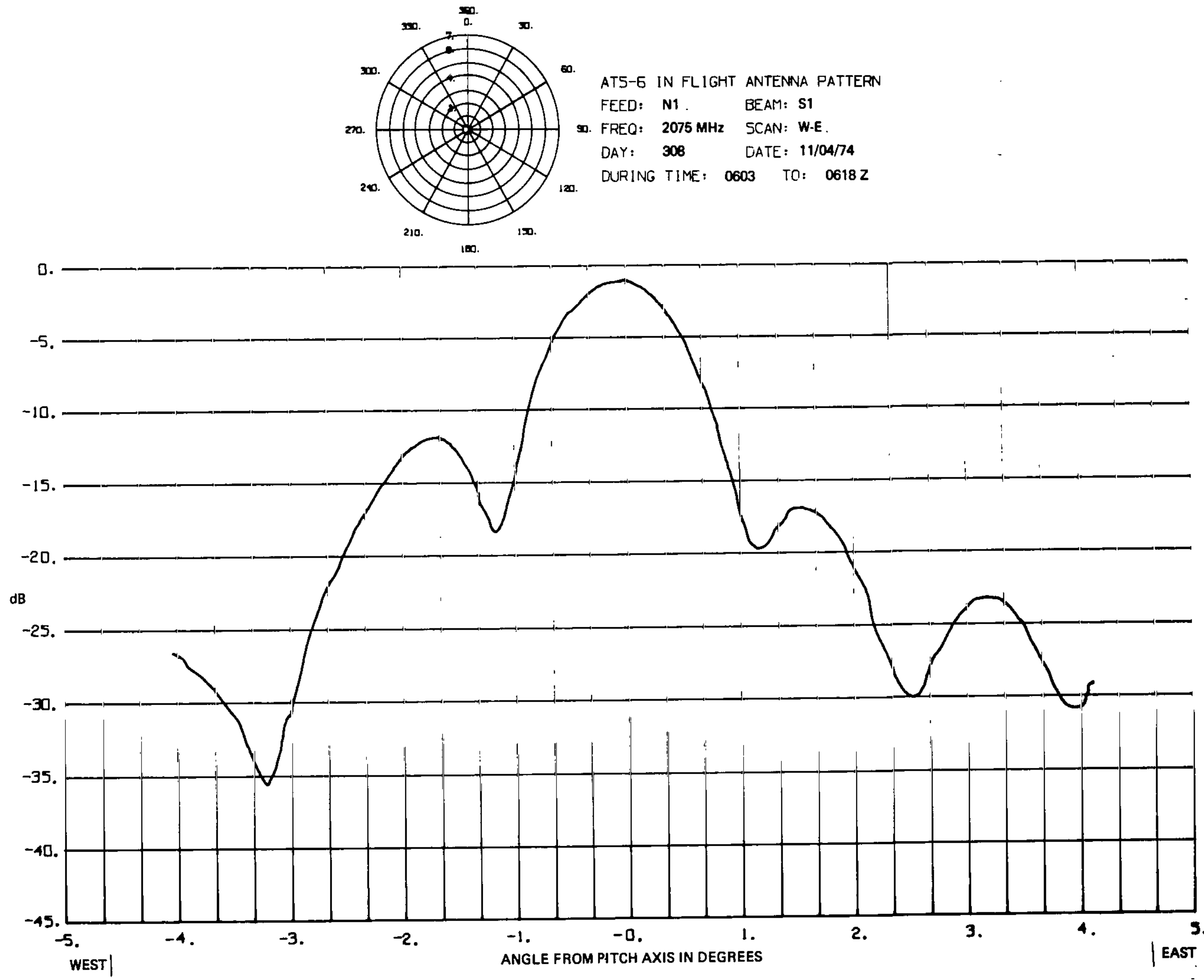

Figure 89. S-band beam S1 E – W.

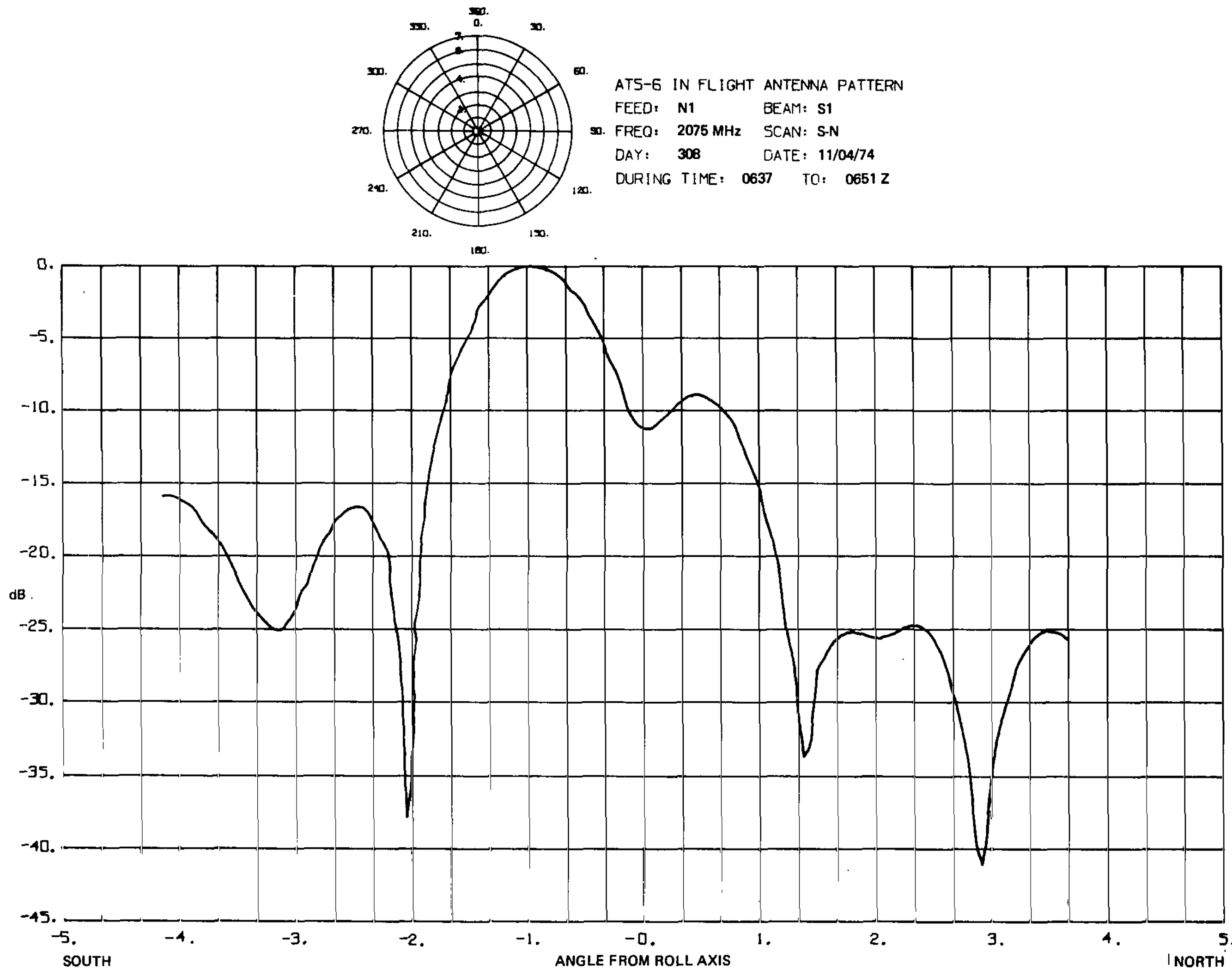

Figure 90. S-band beam S1 N – S.

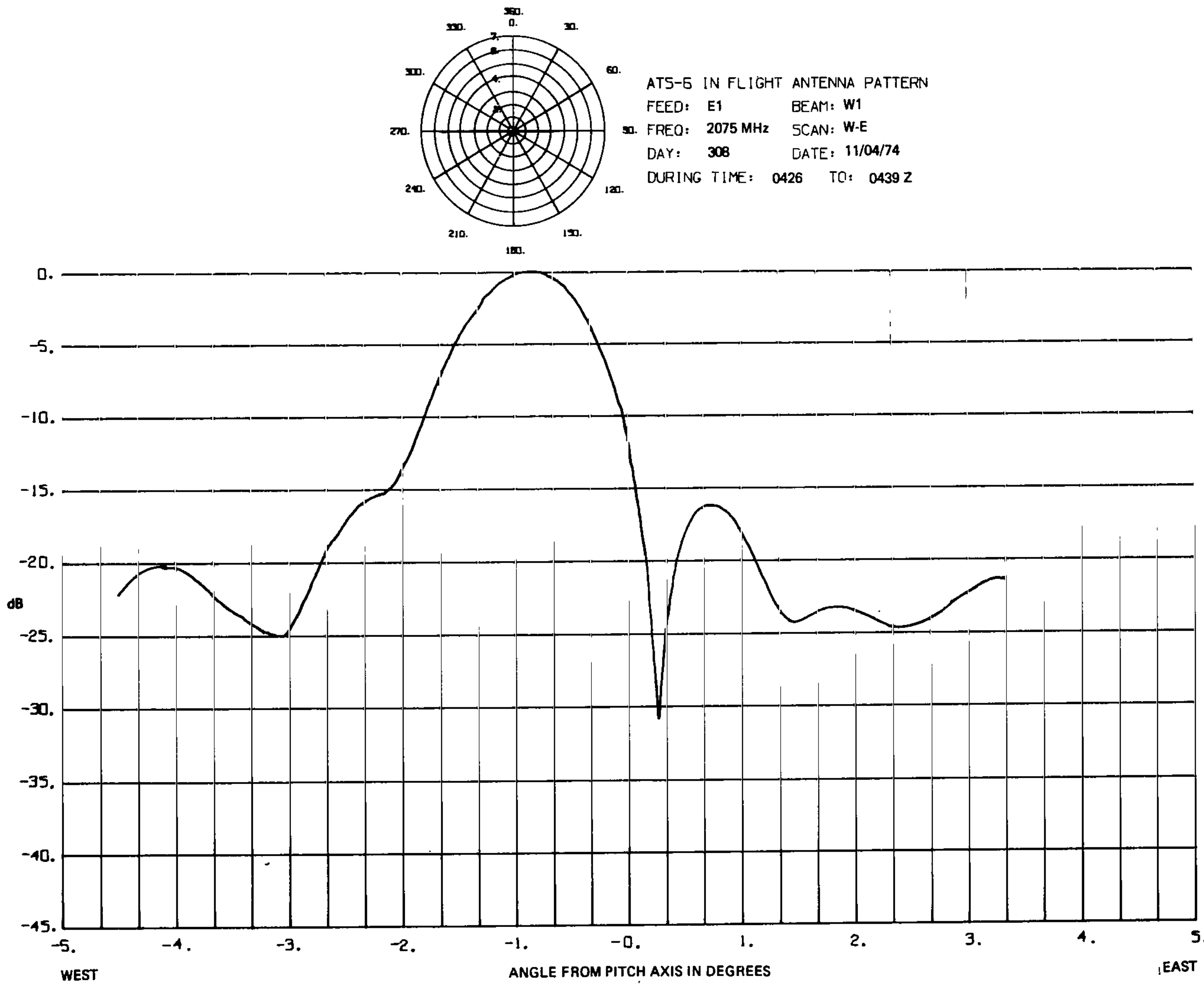

Figure 91. S-band beam W1 E – W.

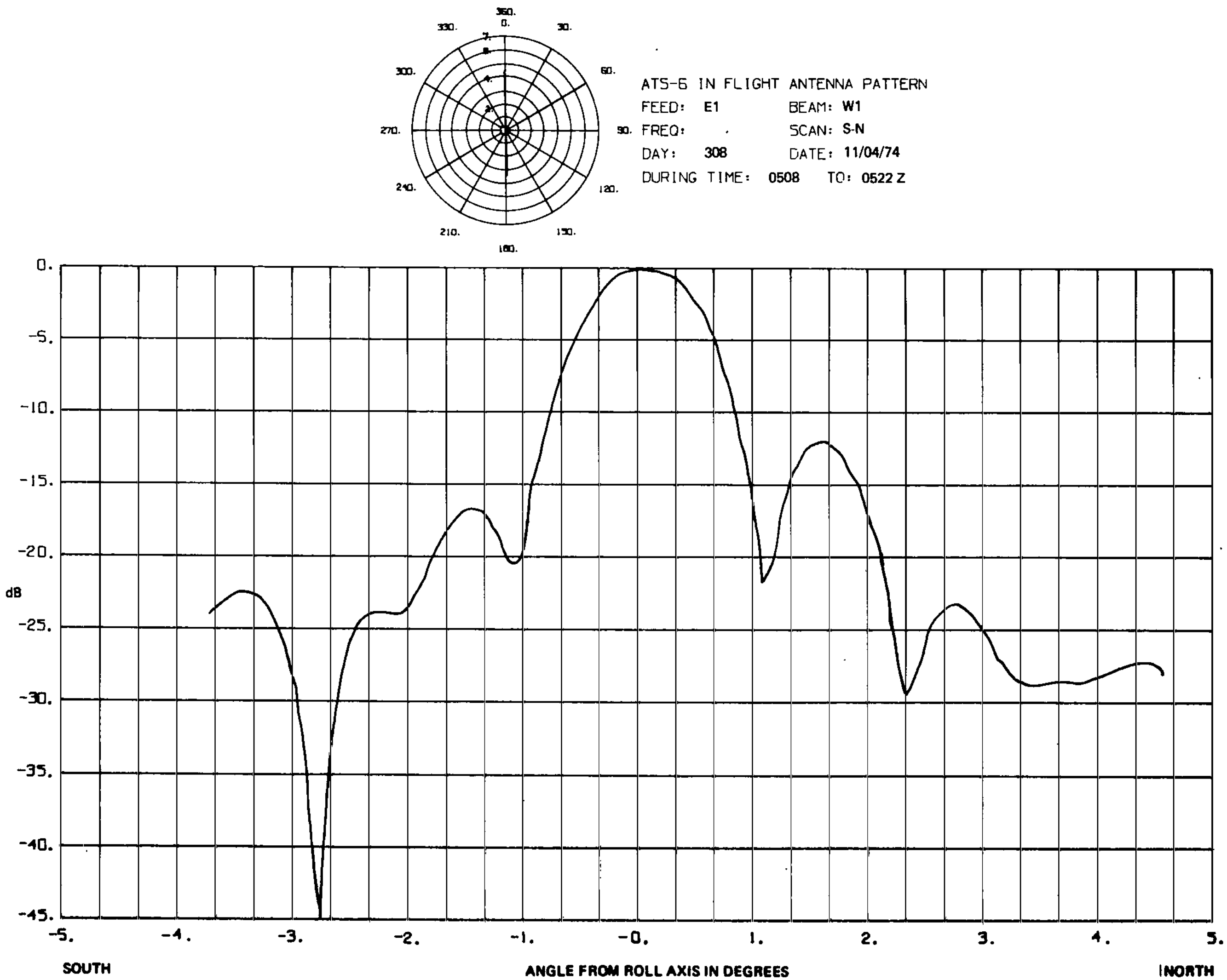

Figure 92. S-band beam W1 N – S.

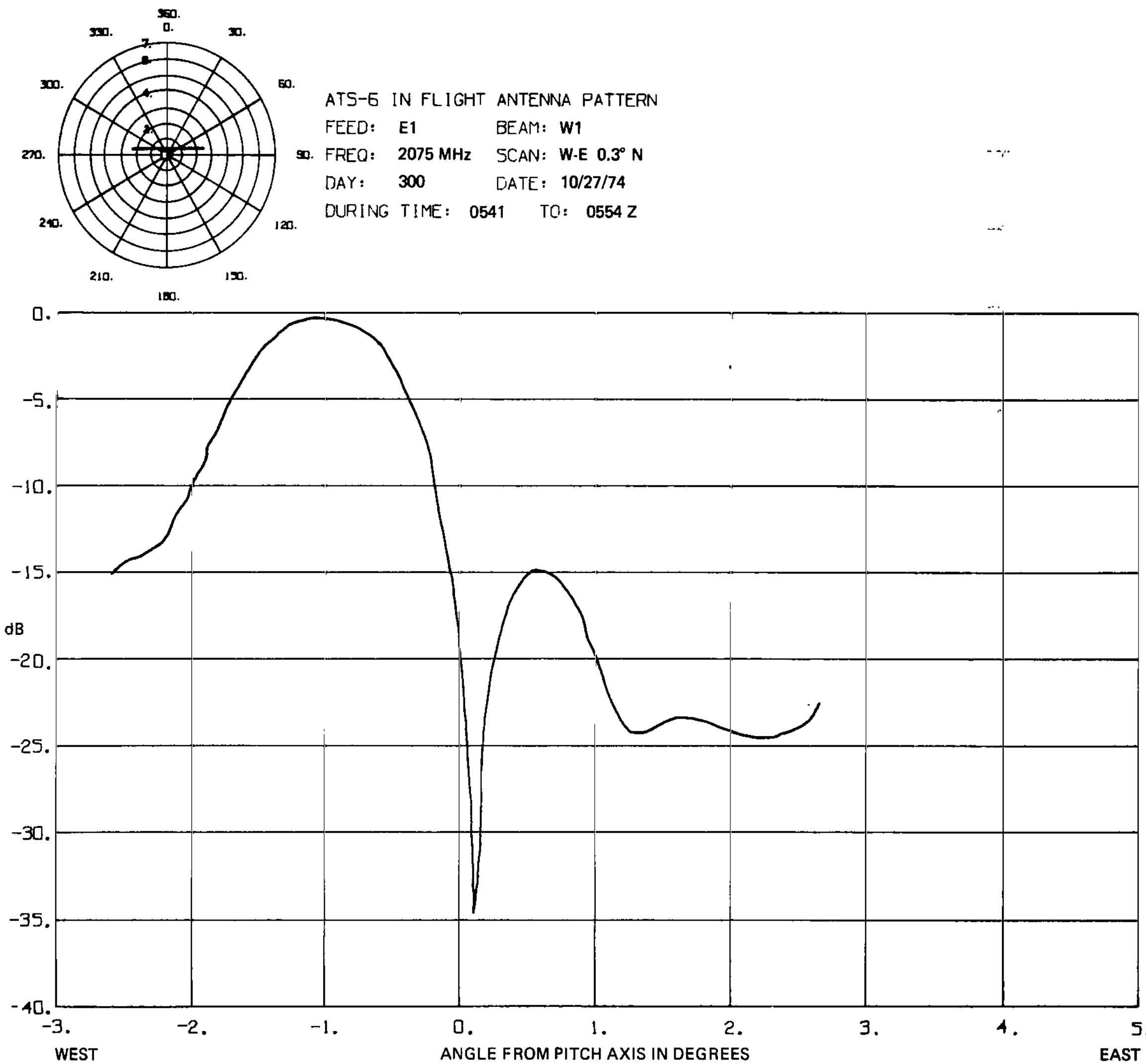

Figure 93. S-band beam W1 E – W 0.3°N.

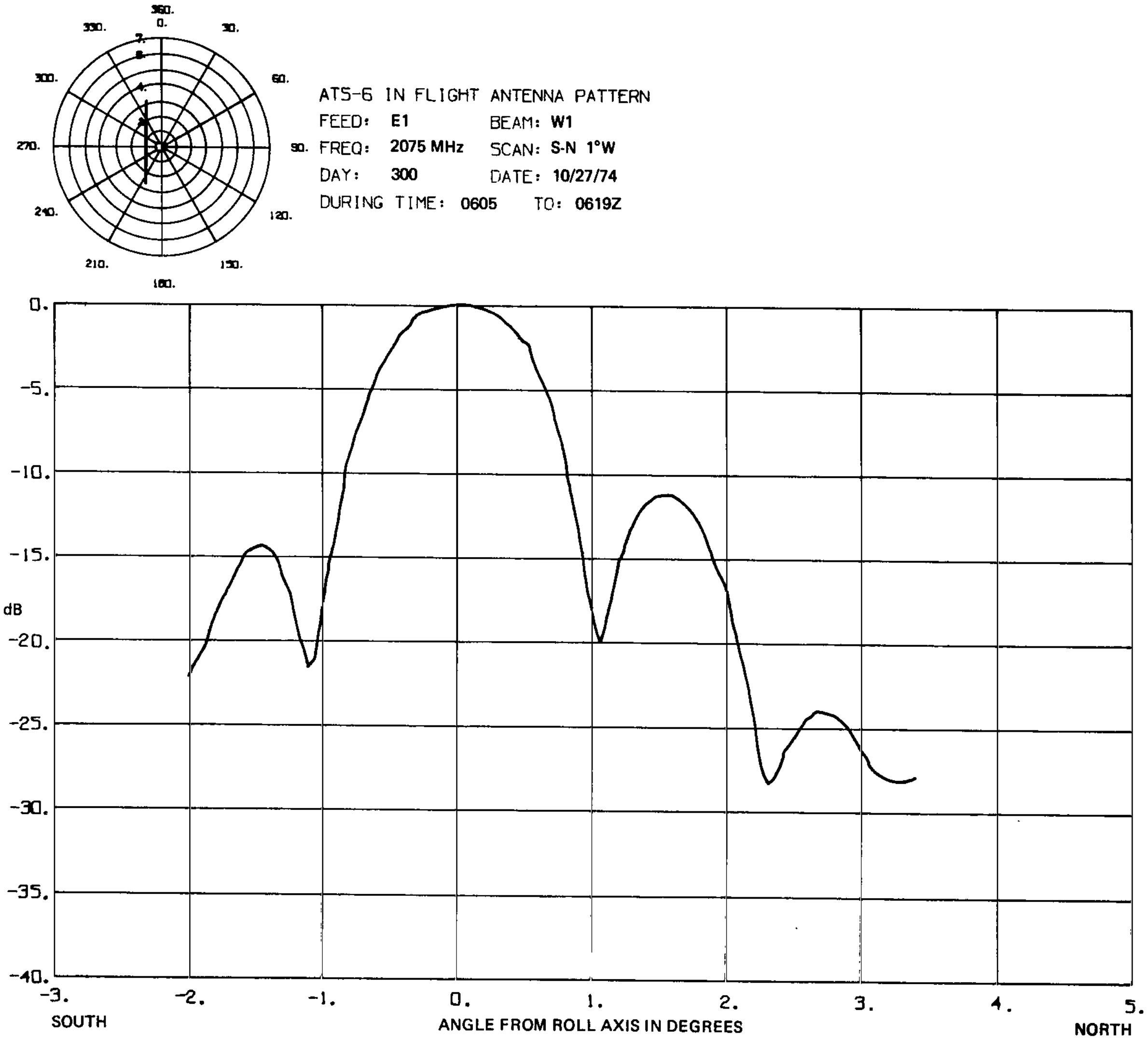

Figure 94. S-band beam W1 N – S 1° W.

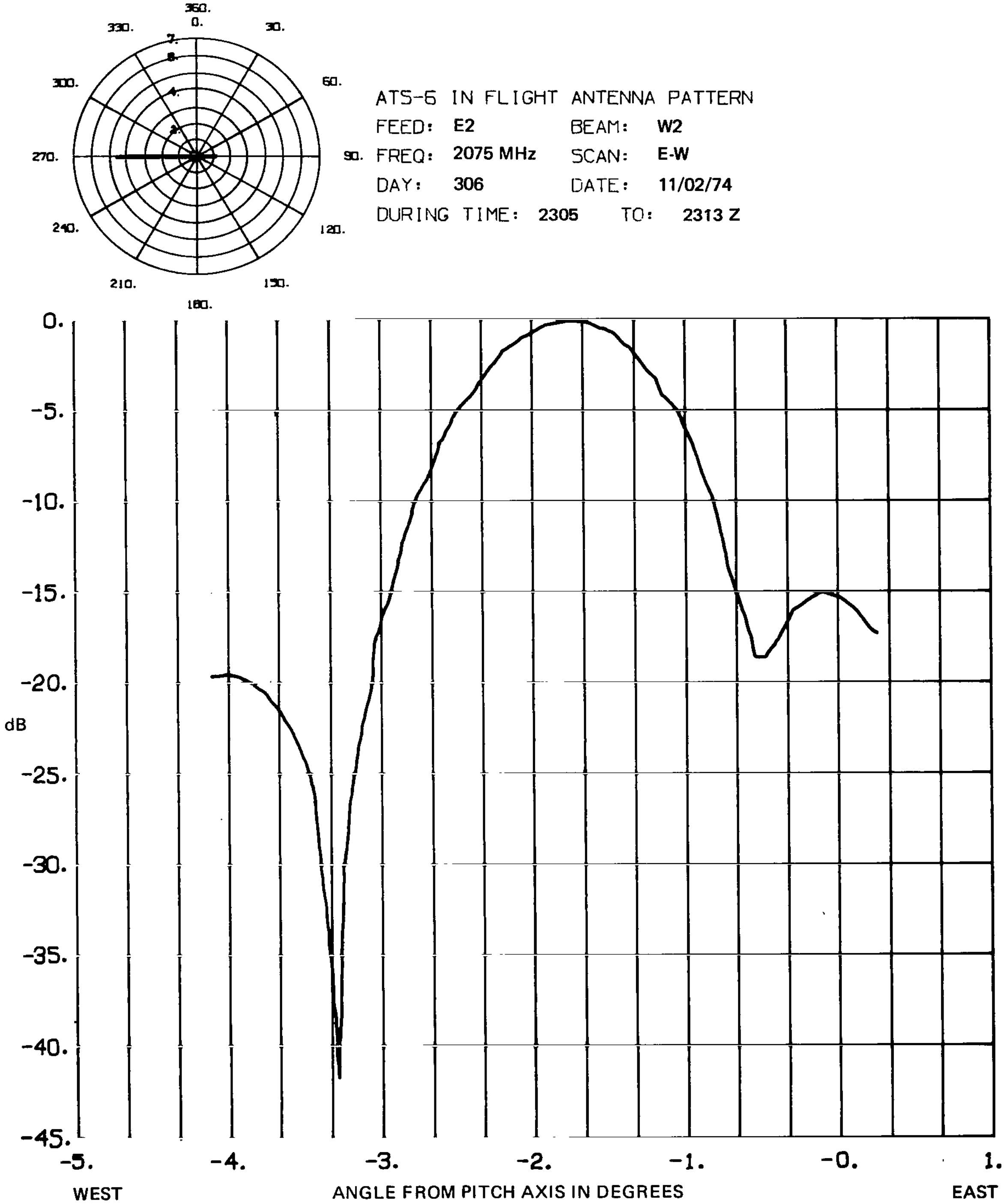

Figure 95. S-band beam W2 E – W.

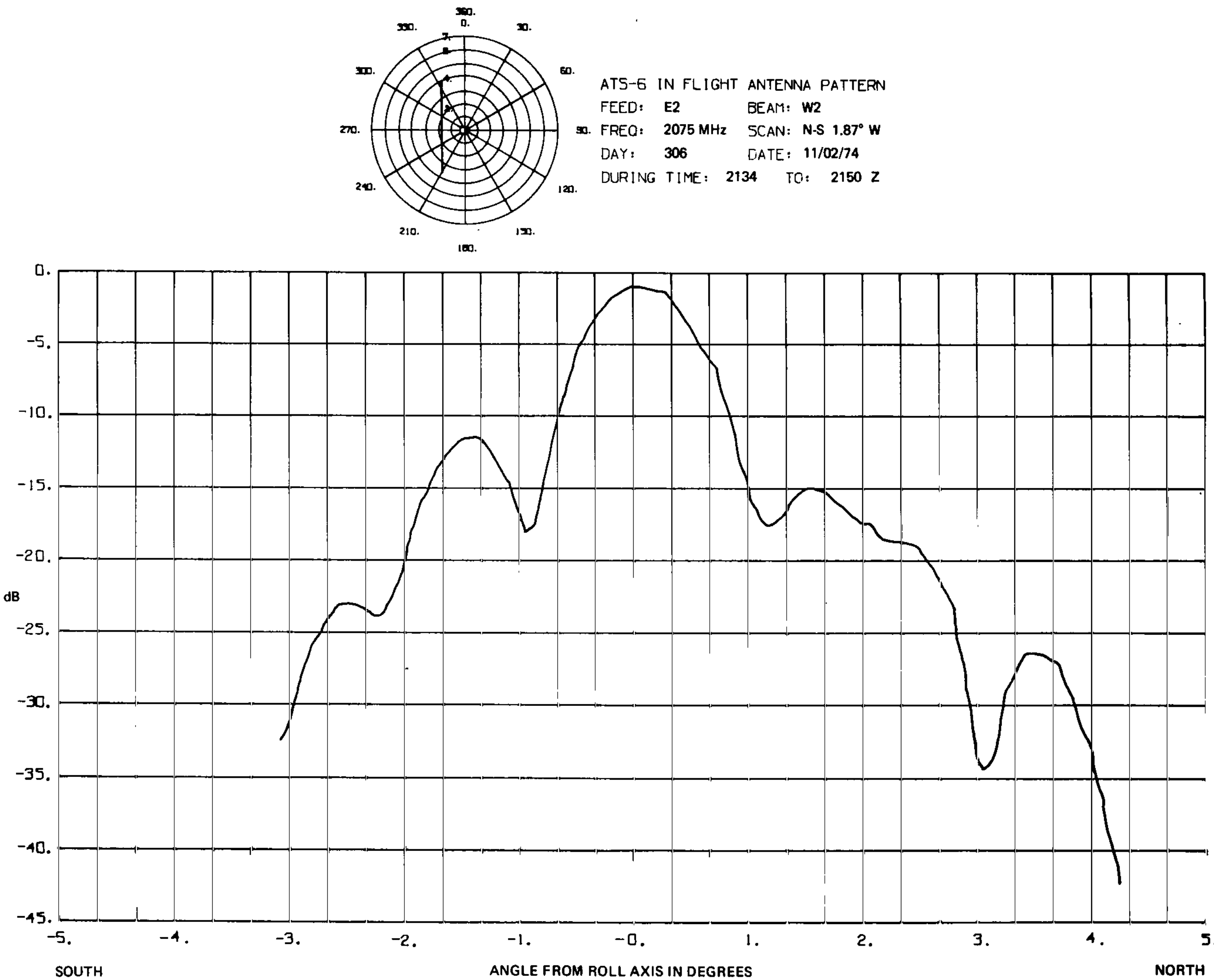

Figure 96. S-band beam W2 N – S 1.87° W.

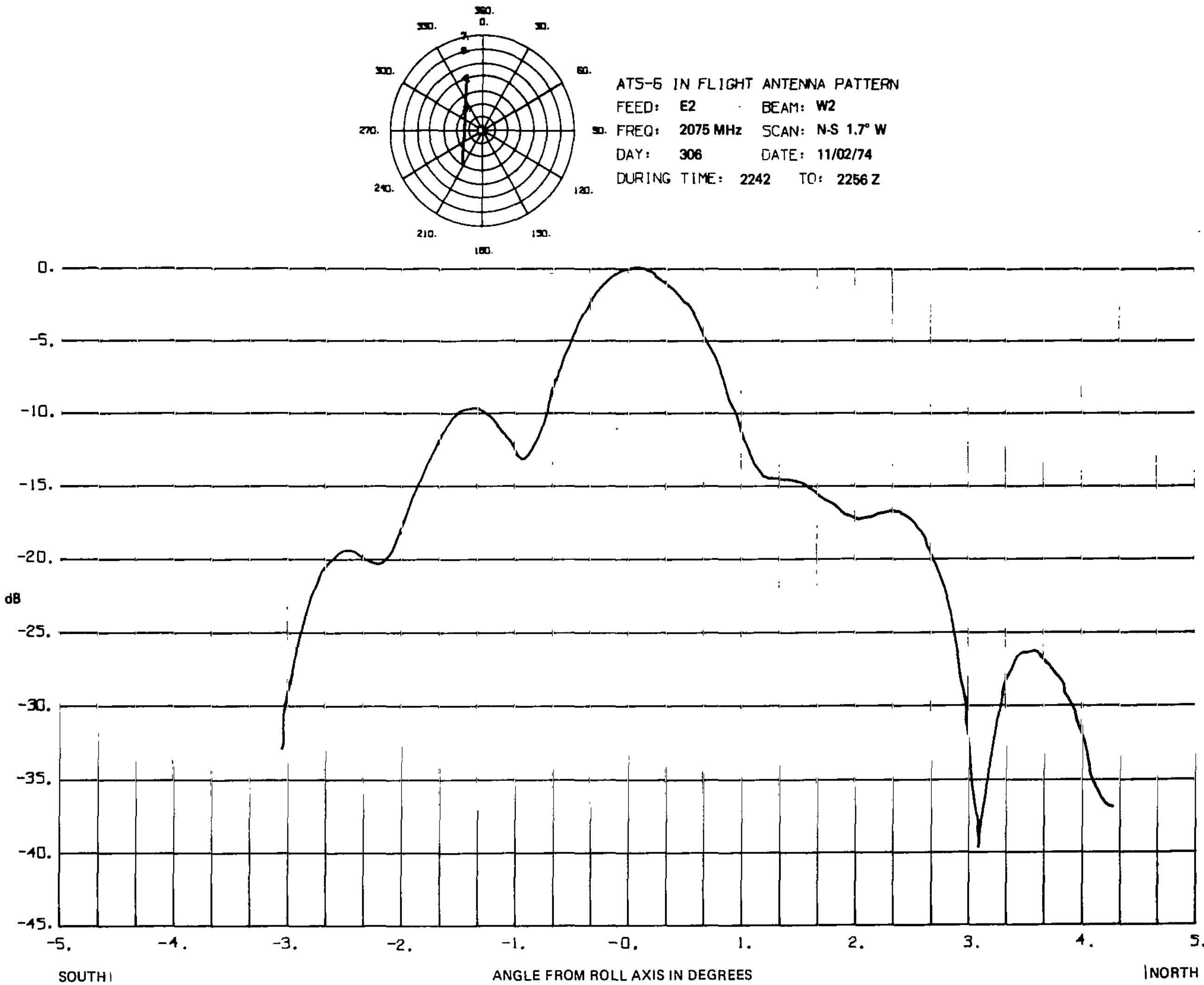

Figure 97. S-band beam W2 N – S 1.7° W.

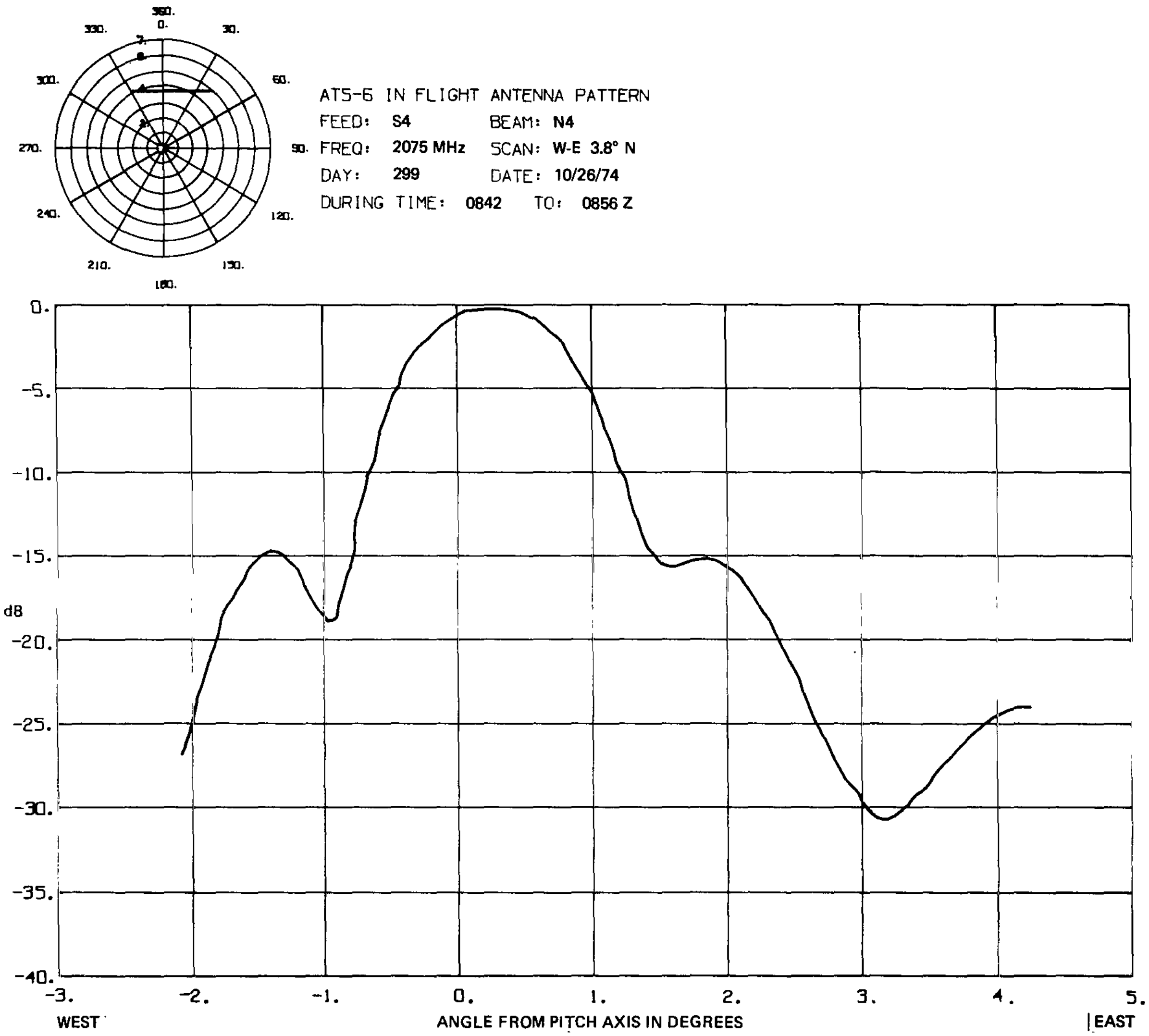

Figure 98. S-band beam N4 E – W 3.8° N.

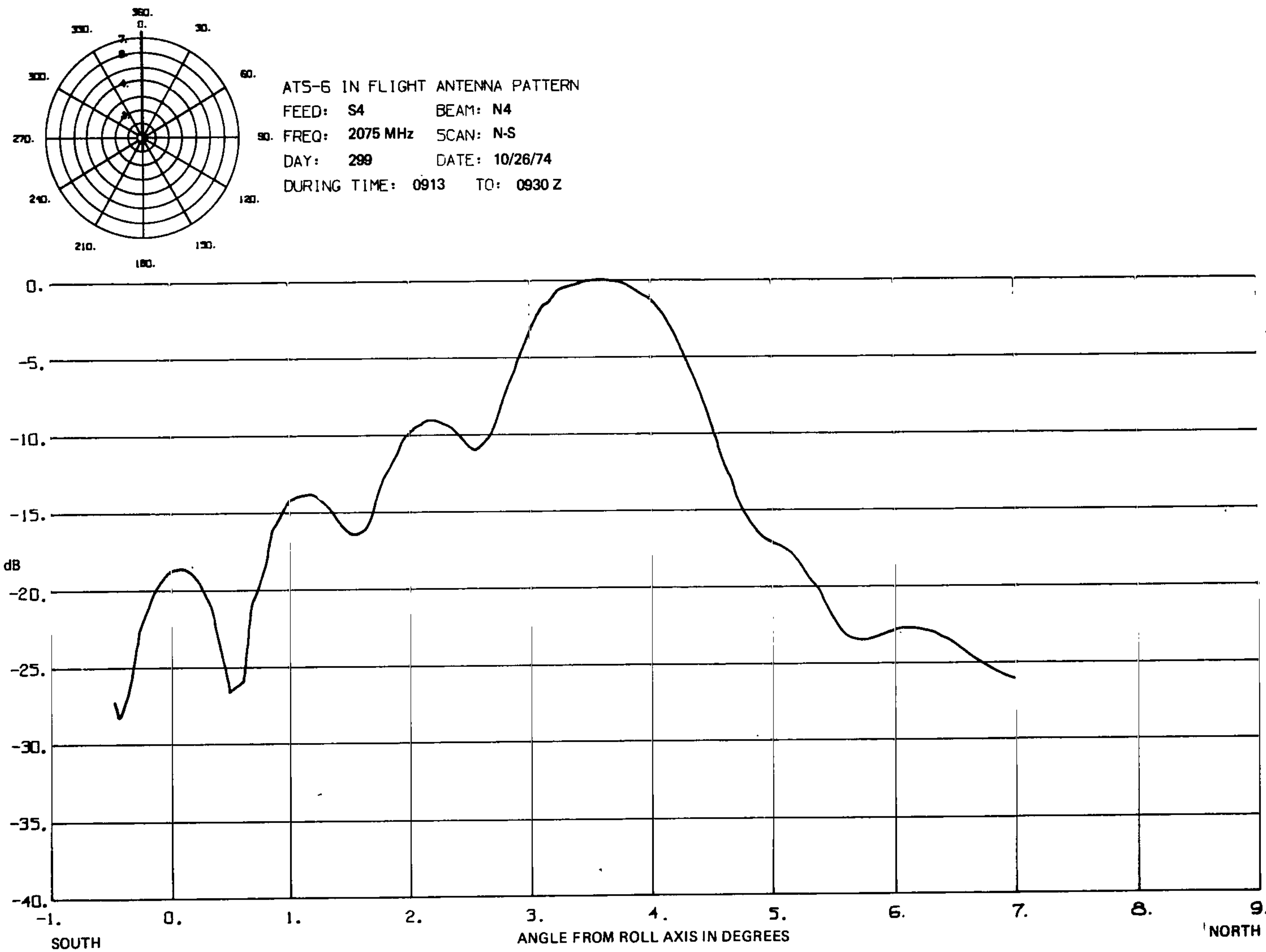

Figure 99. S-band beam N4 N – S.

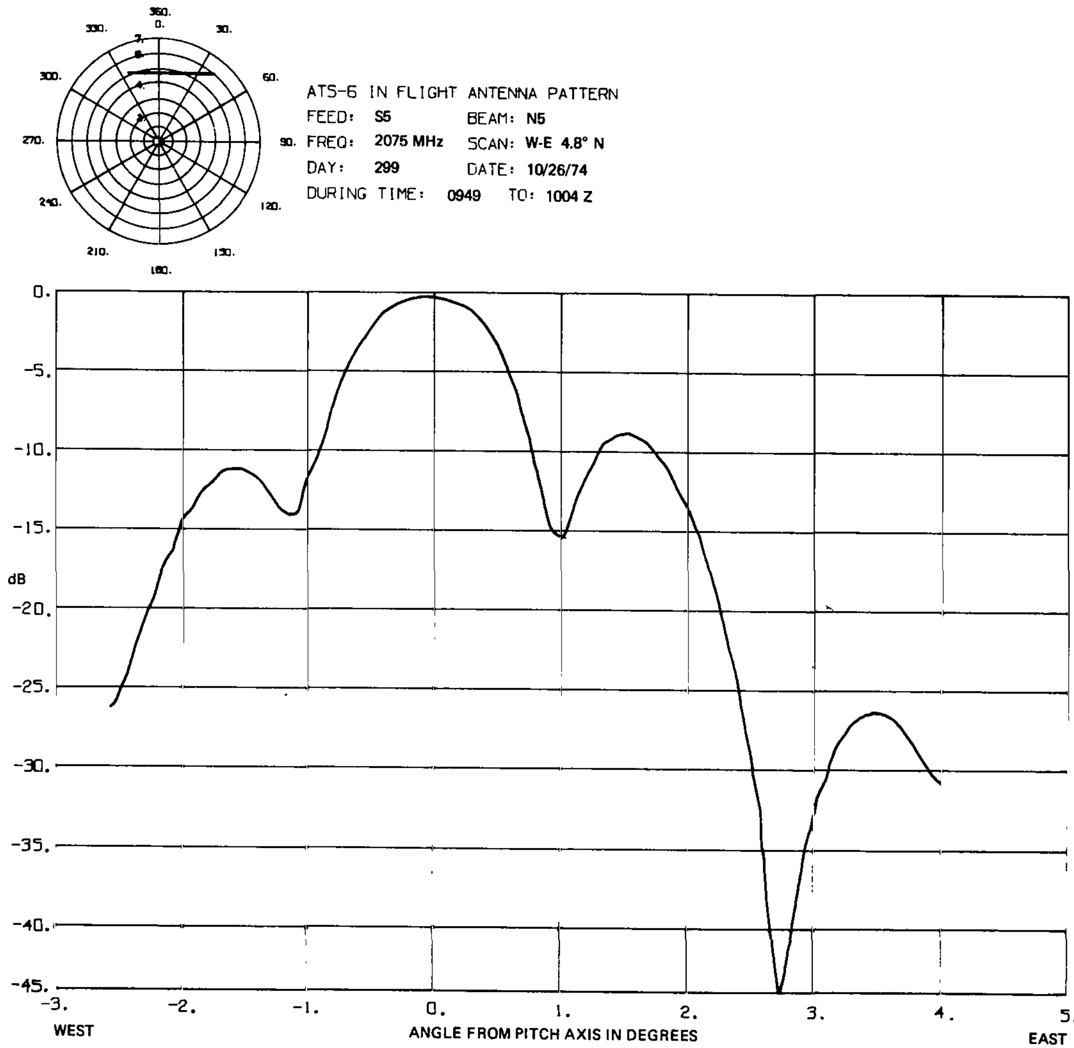

Figure 100. S-band beam N5 E – W 4.8° N.

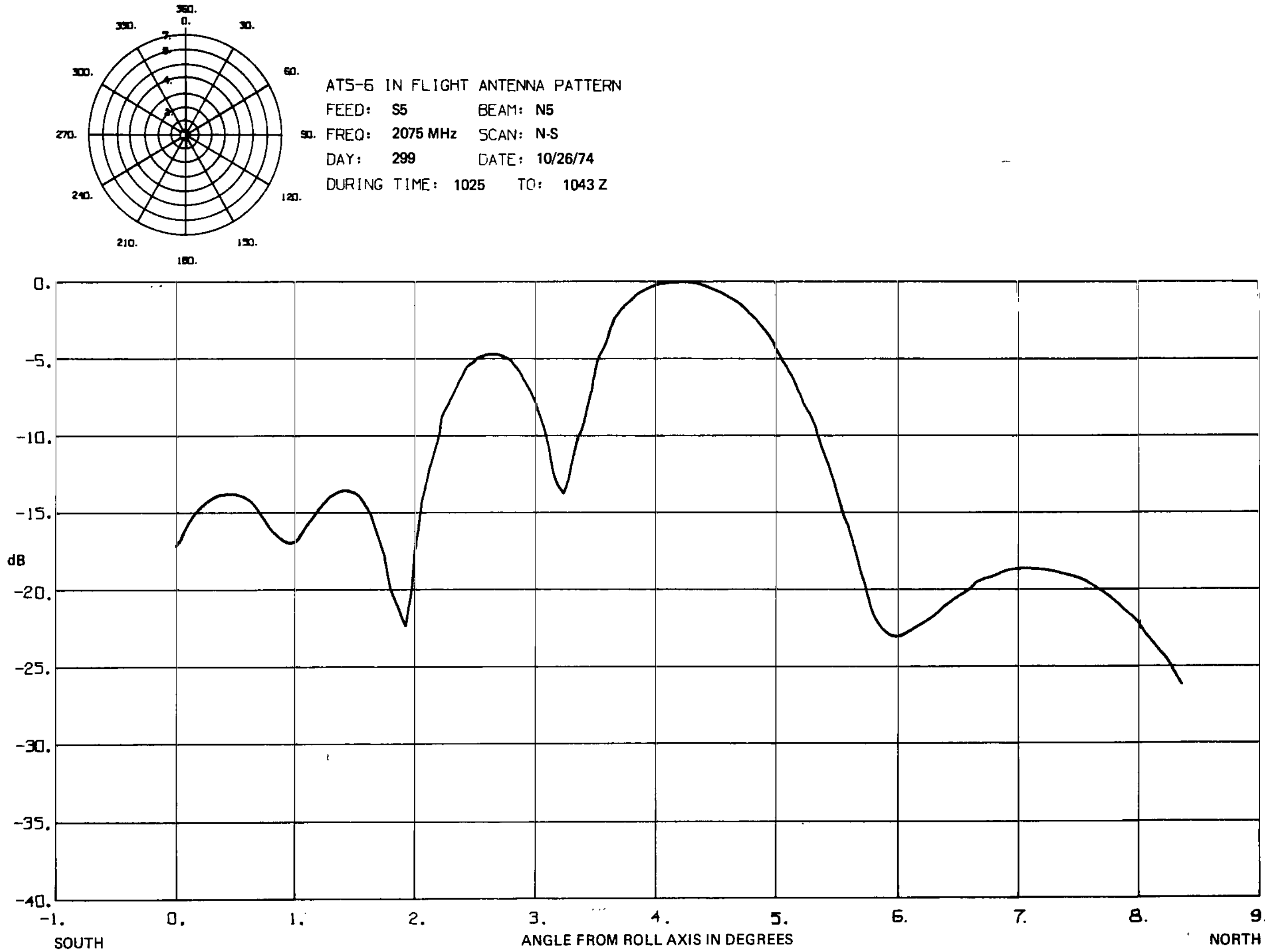

Figure 101. S-band beam N5 N – S.

C-BAND ON-AXIS PFF BEAM PATTERNS

These C-band beam patterns are of special interest because of its narrow beam width. The contour of the 9.1-meter soft dish parabola forming the C-band beam may possibly be studied by means of the antenna patterns. The patterns may be correlated to parameters like the the time of day and sun angle. Any shift in the peak of the beam, or shape of the pattern, may reveal the behavior of the 9.1-meter parabola while in orbit.

Figures 102 and 103 are patterns showing both preflight and postflight results. The differences may be explained, in part, by the preflight model (hard dish) being different from the flight model (soft dish) structure.

A series of patterns were made for cuts 0.1° apart in the E – W directions (Figures 104 through 112) as well as for the N – S directions (Figures 113 through 121). The angular scale has been amplified, and where possible, the actual plotted points are shown.

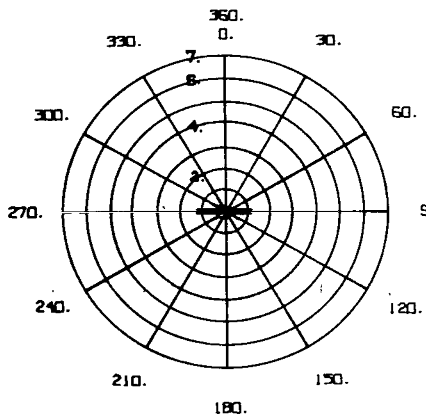

ATS-6 IN FLIGHT ANTENNA PATTERN

FEED: C-BAND PFF BEAM: RECV. ON-AXIS

FREQ: 5972 MHz SCAN: E-W

DAY: 19 DATE: 01/19/75

DURING TIME: 0148 TO: 0154 Z

PRE-FLIGHT PATTERN NO. 6

9/25/73

HARD DISH 5925 MHz

LEGEND: PRE-FLIGHT PATTERN

IN-FLIGHT PATTERN -O- -O- -O-

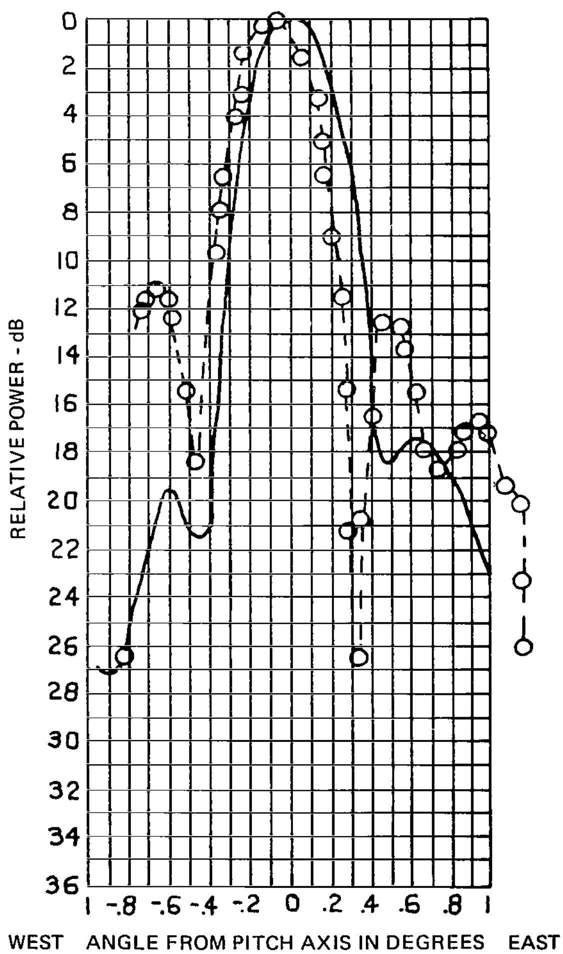

Figure 102. C-band beam E – W.

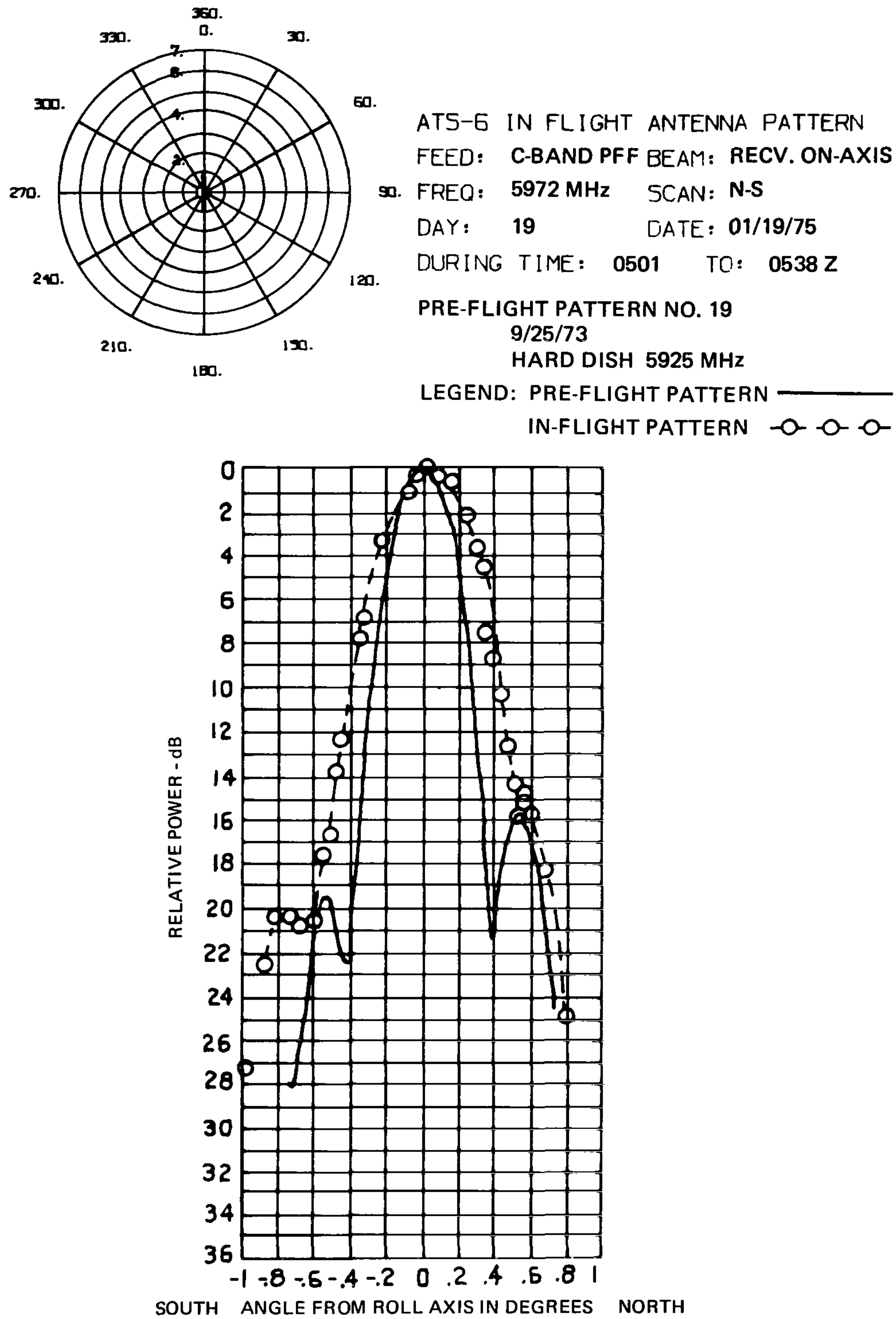

Figure 103. C-band beam N – S.

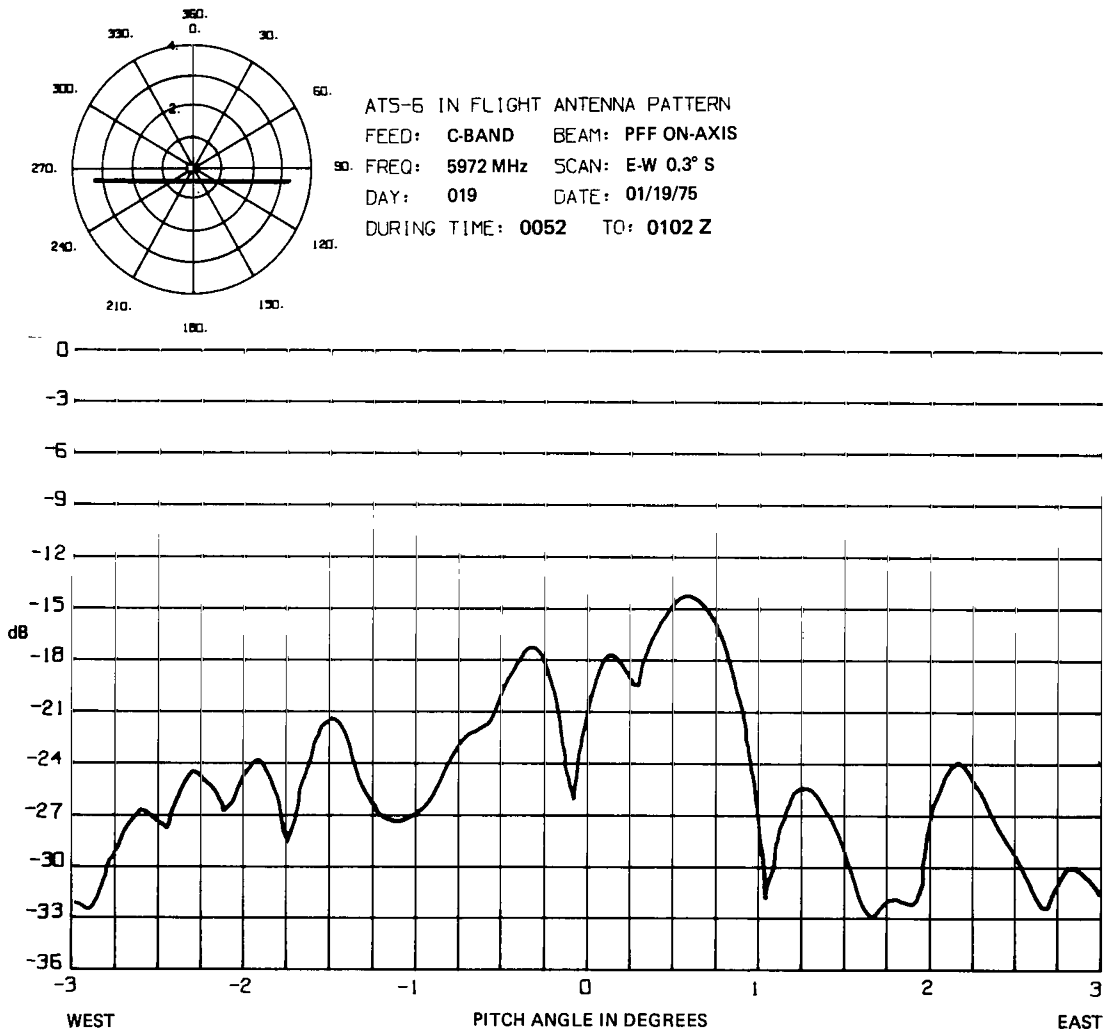

Figure 104. C-band beam PFF on-axis E – W 0.3° S.

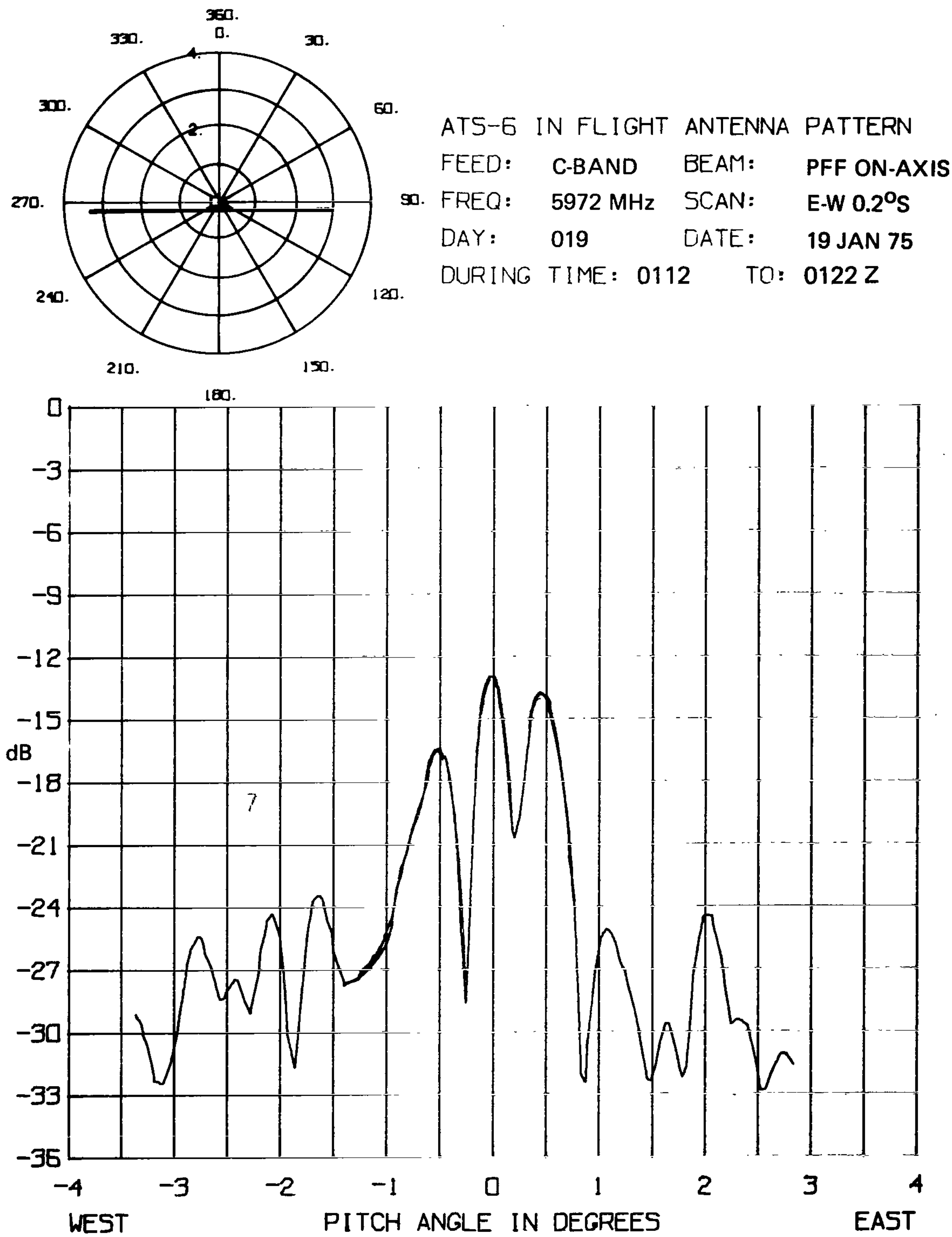

Figure 105. C-band beam PFF on-axis E – W 0.2° S.

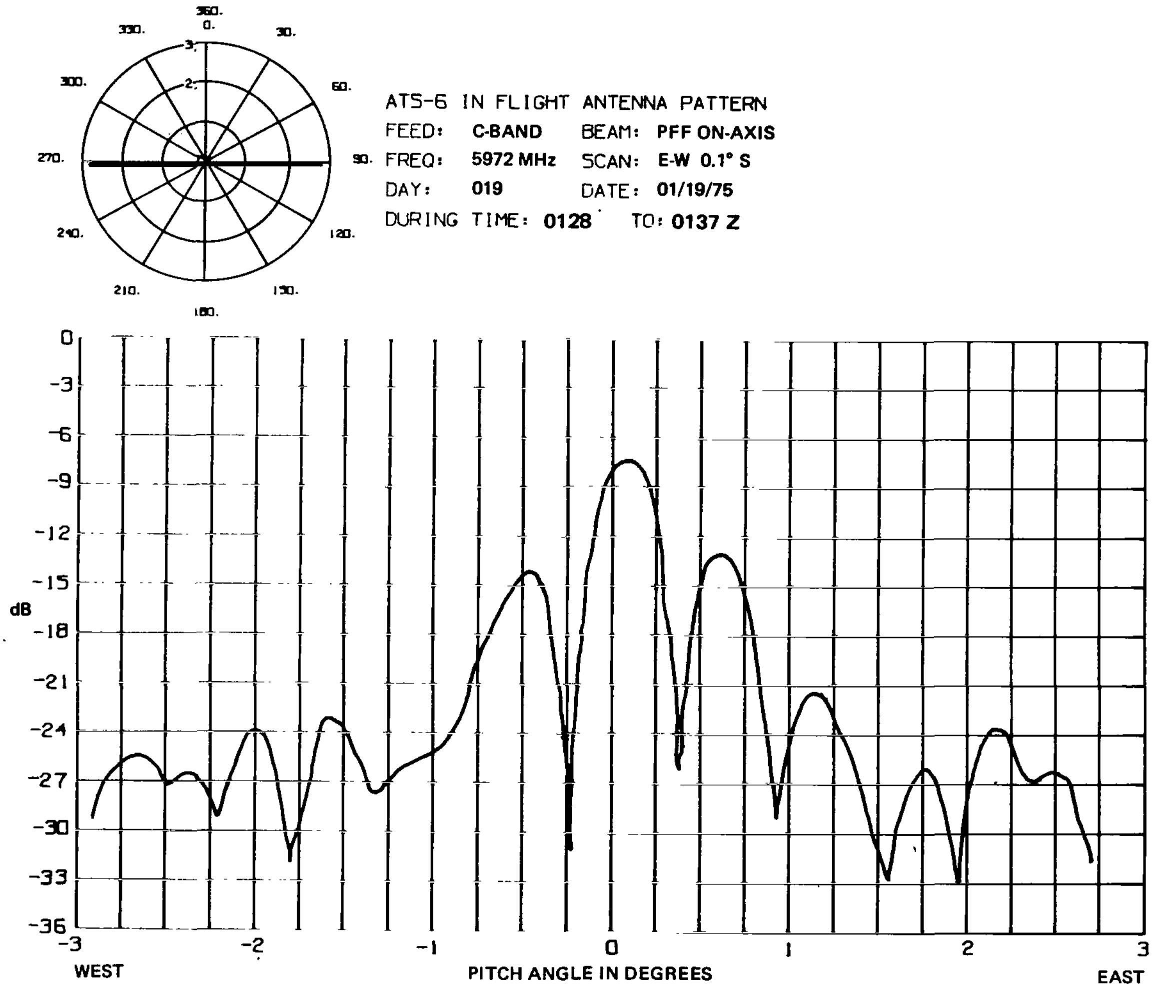

Figure 106. C-band beam PFF on-axis E – W 0.1° S.

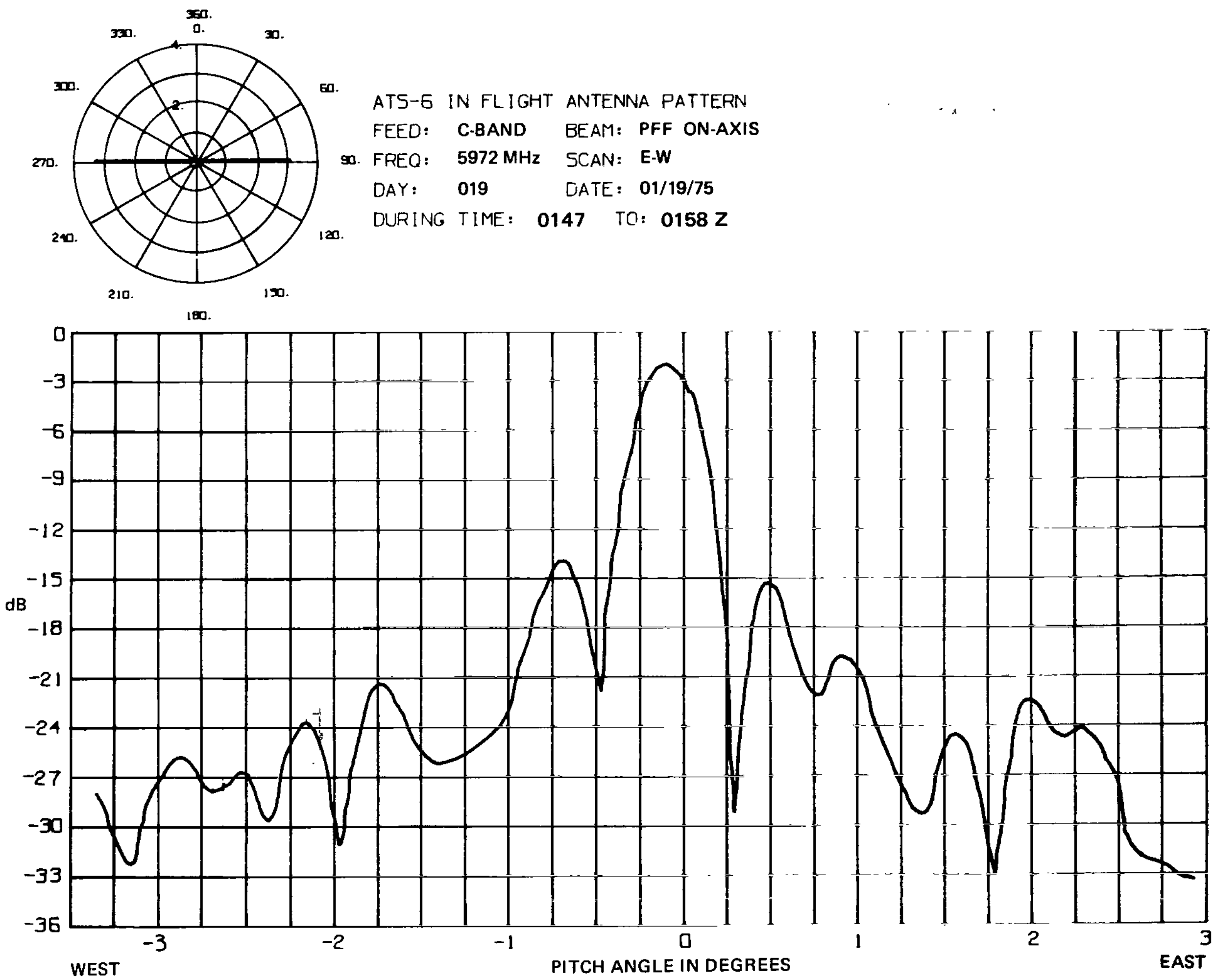

Figure 107. C-band beam PFF on-axis E – W.

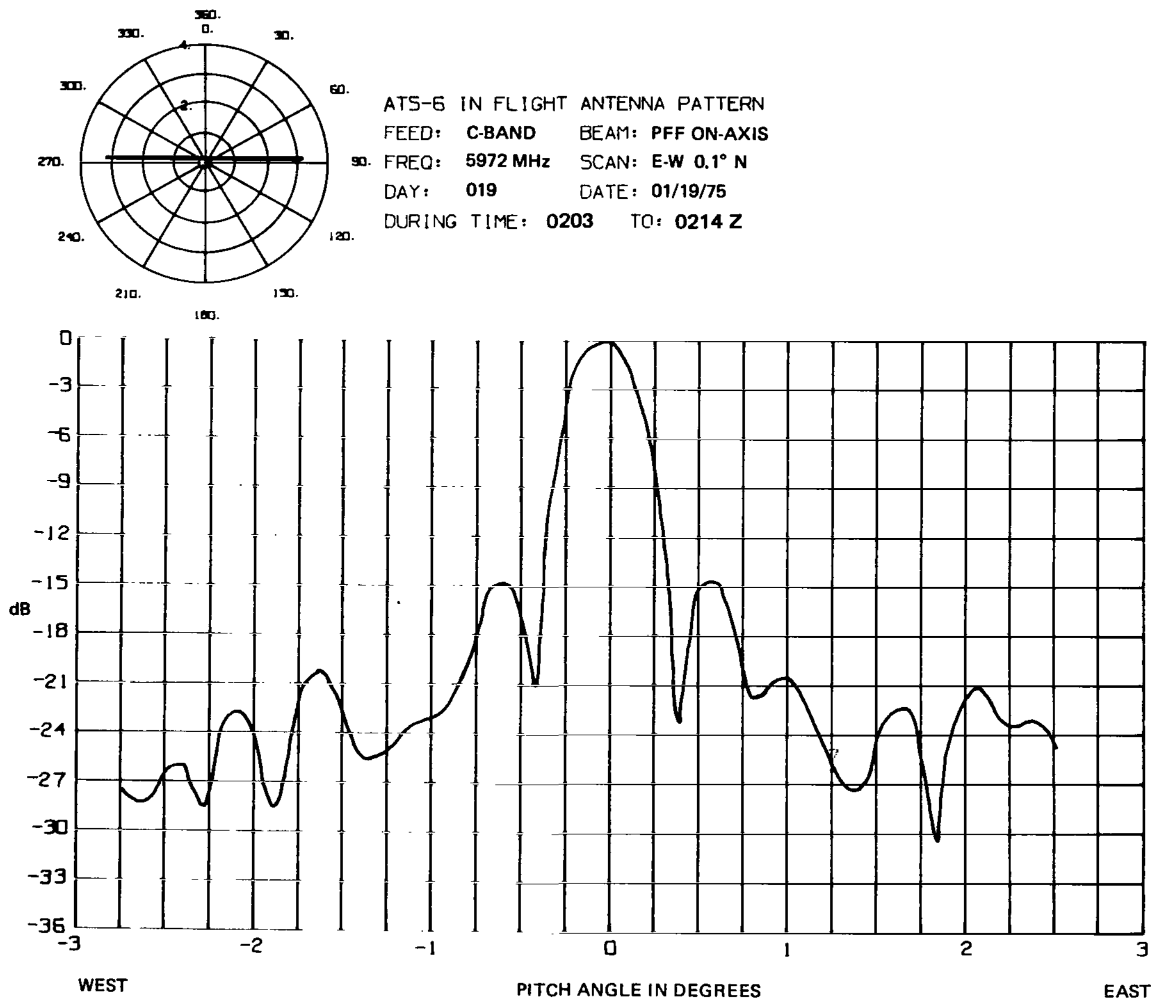

Figure 108. C-band beam PFF on-axis E – W 0.1° N.

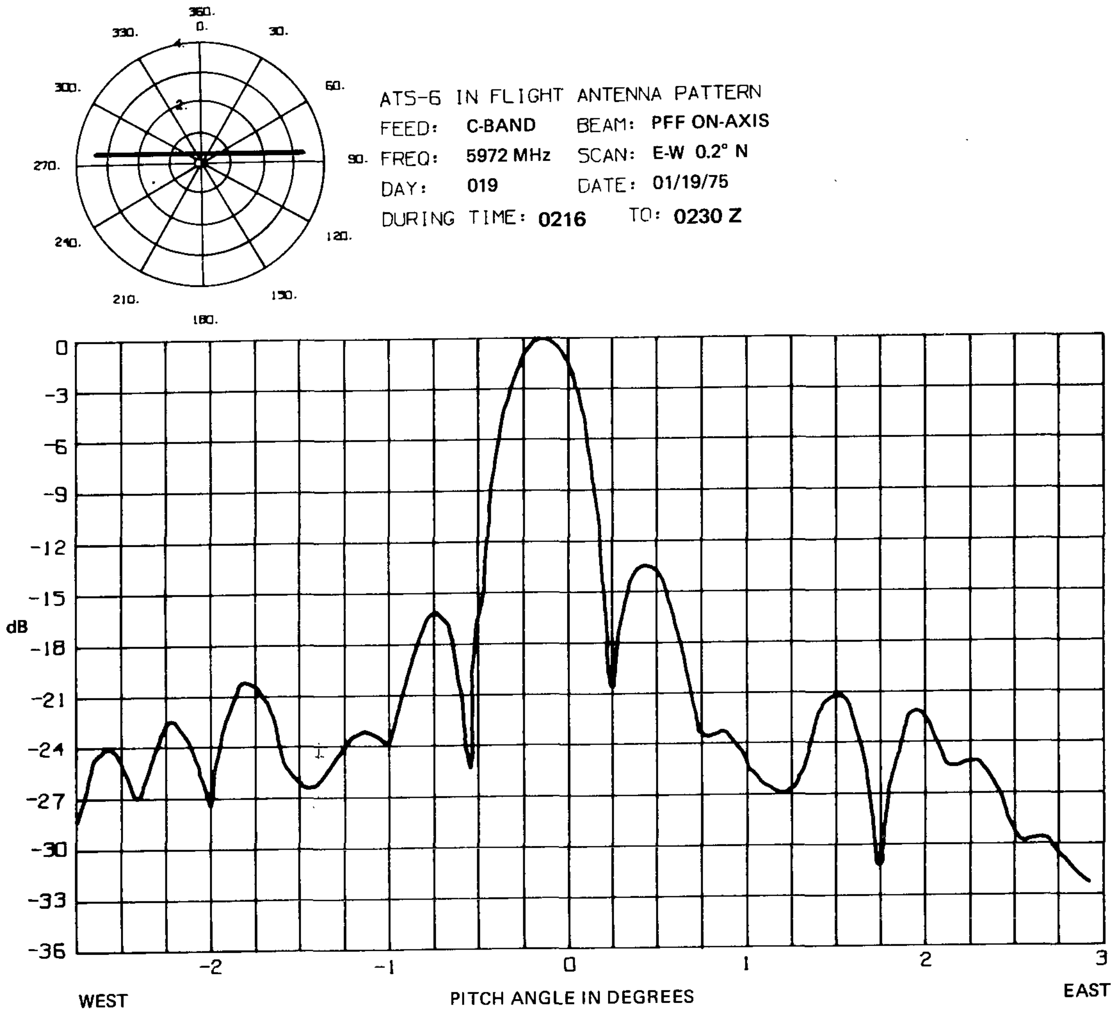

Figure 109. C-band beam PFF on-axis E – W 0.2° N.

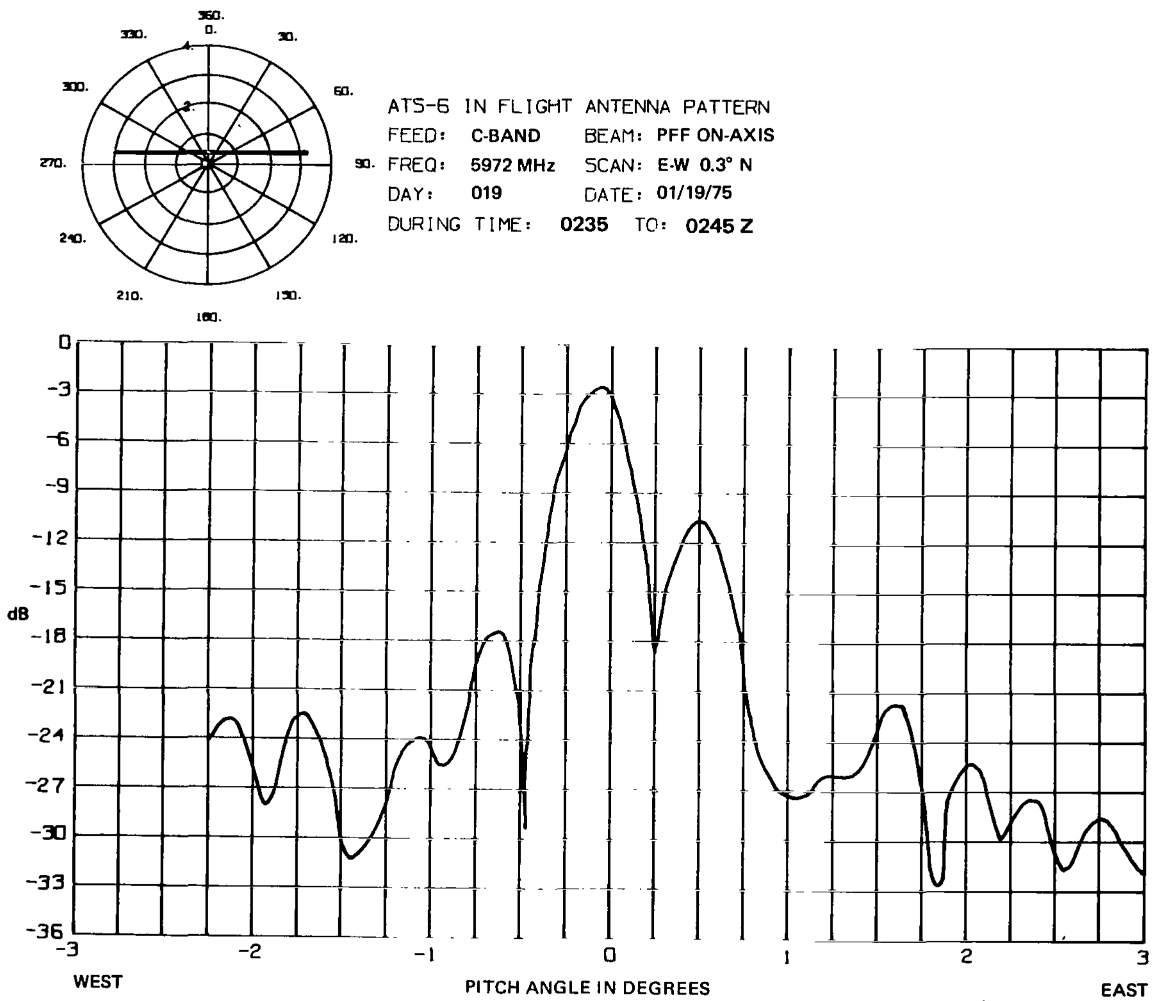

Figure 110. C-band beam PFF on-axis E – W 0.3° N.

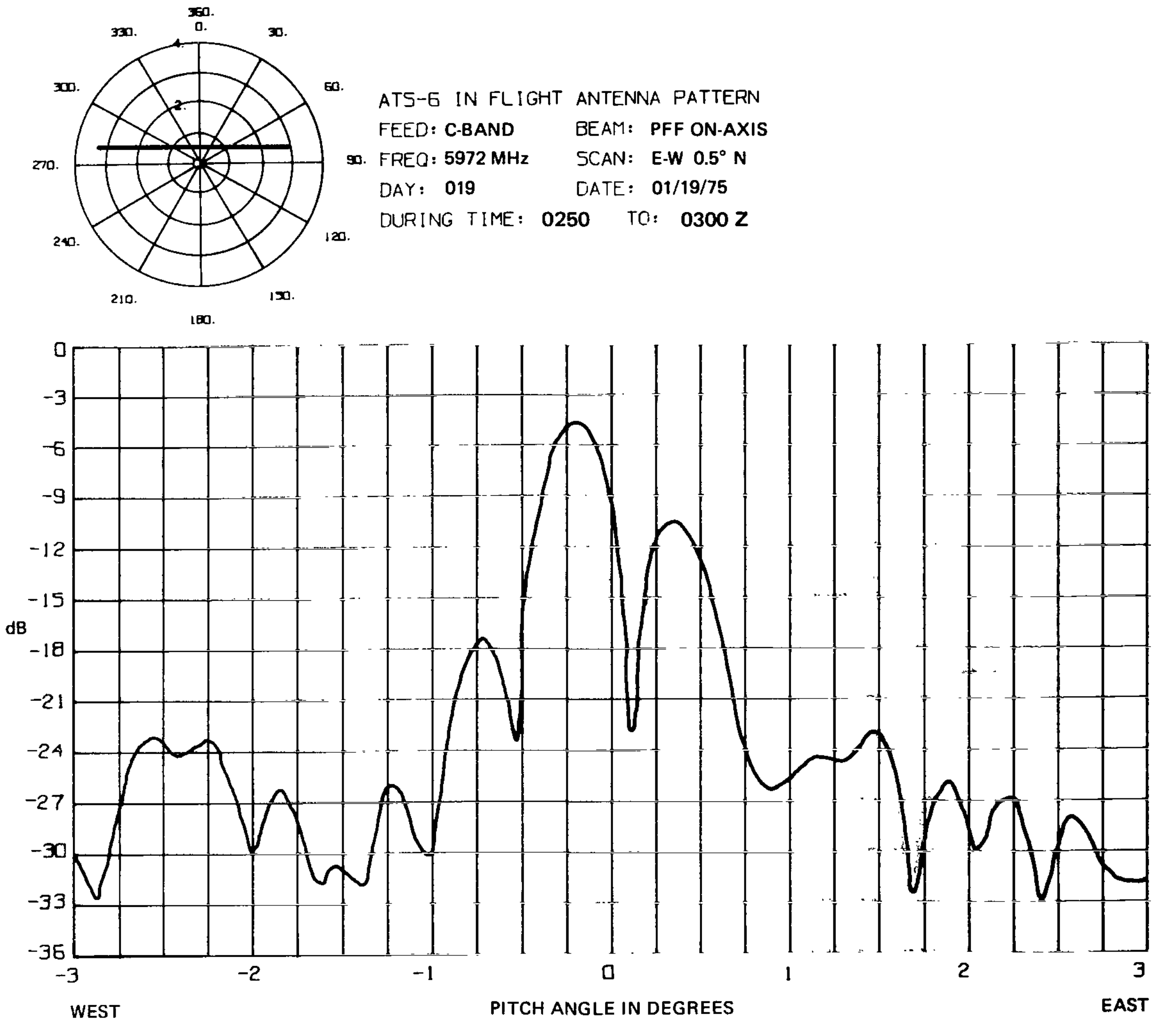

Figure 111. C-band beam PFF on-axis E – W 0.4° N.

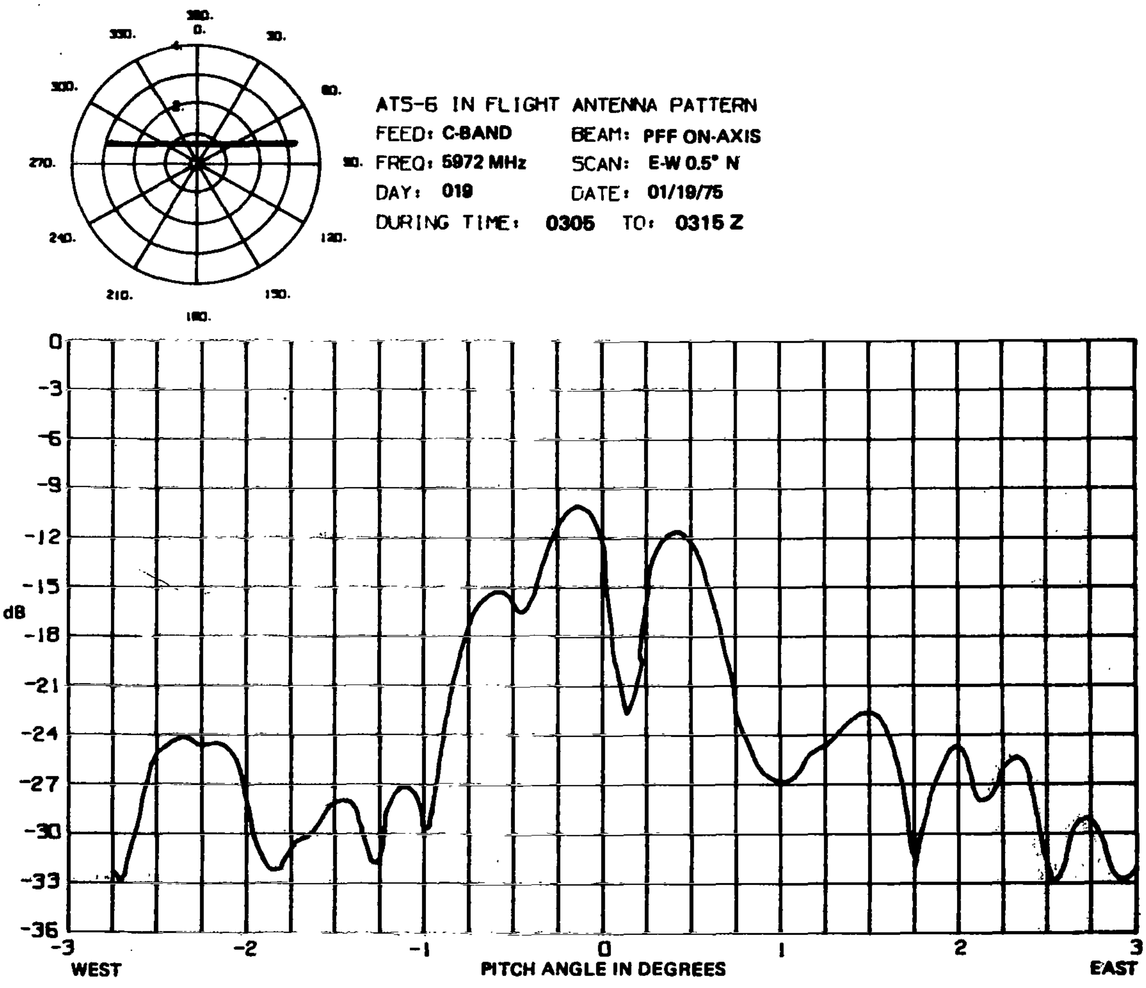

Figure 112. C-band beam PFF on-axis E – W 0.5° N.

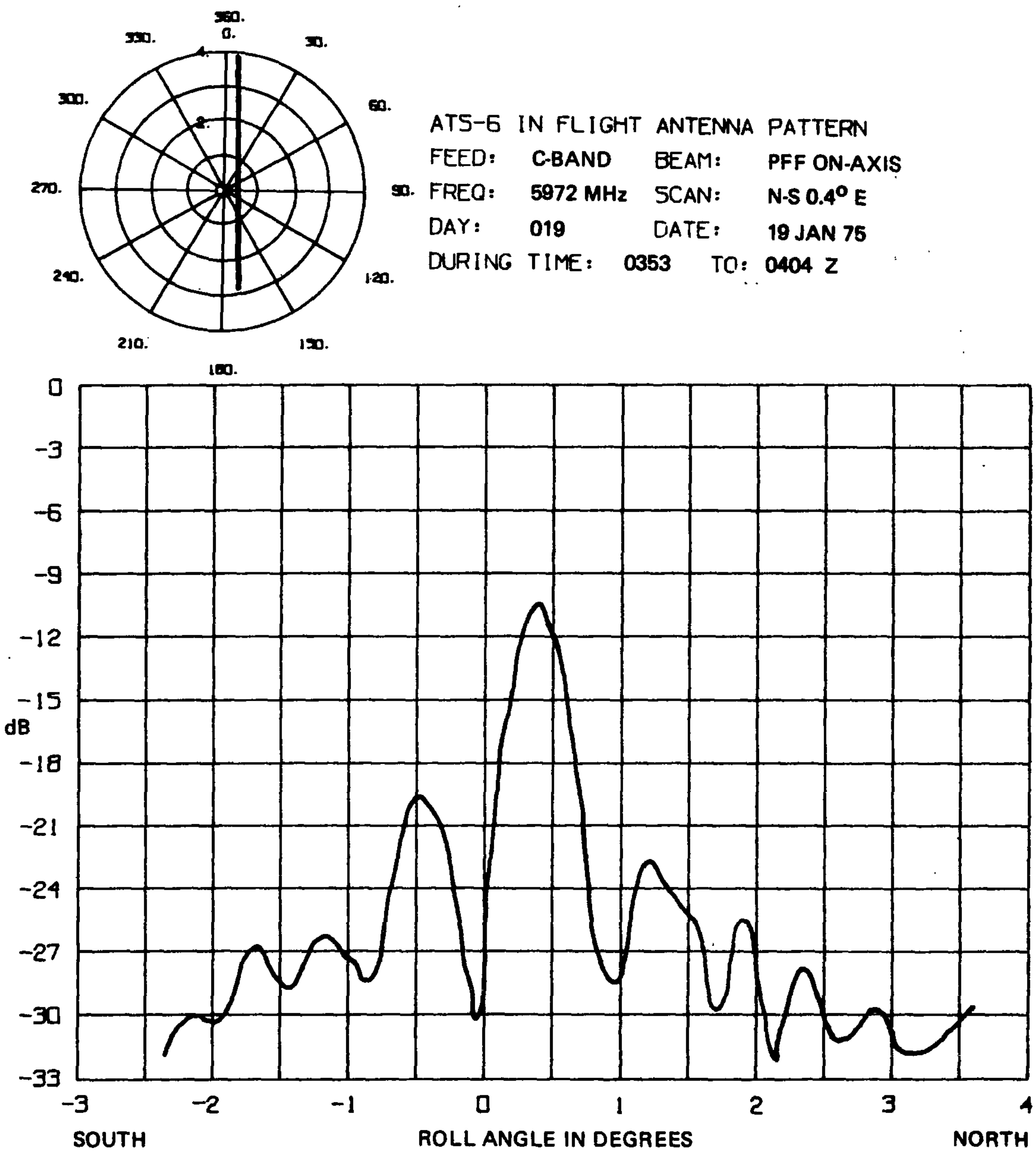

Figure 113. C-band beam PFF on-axis N – S 0.4° E.

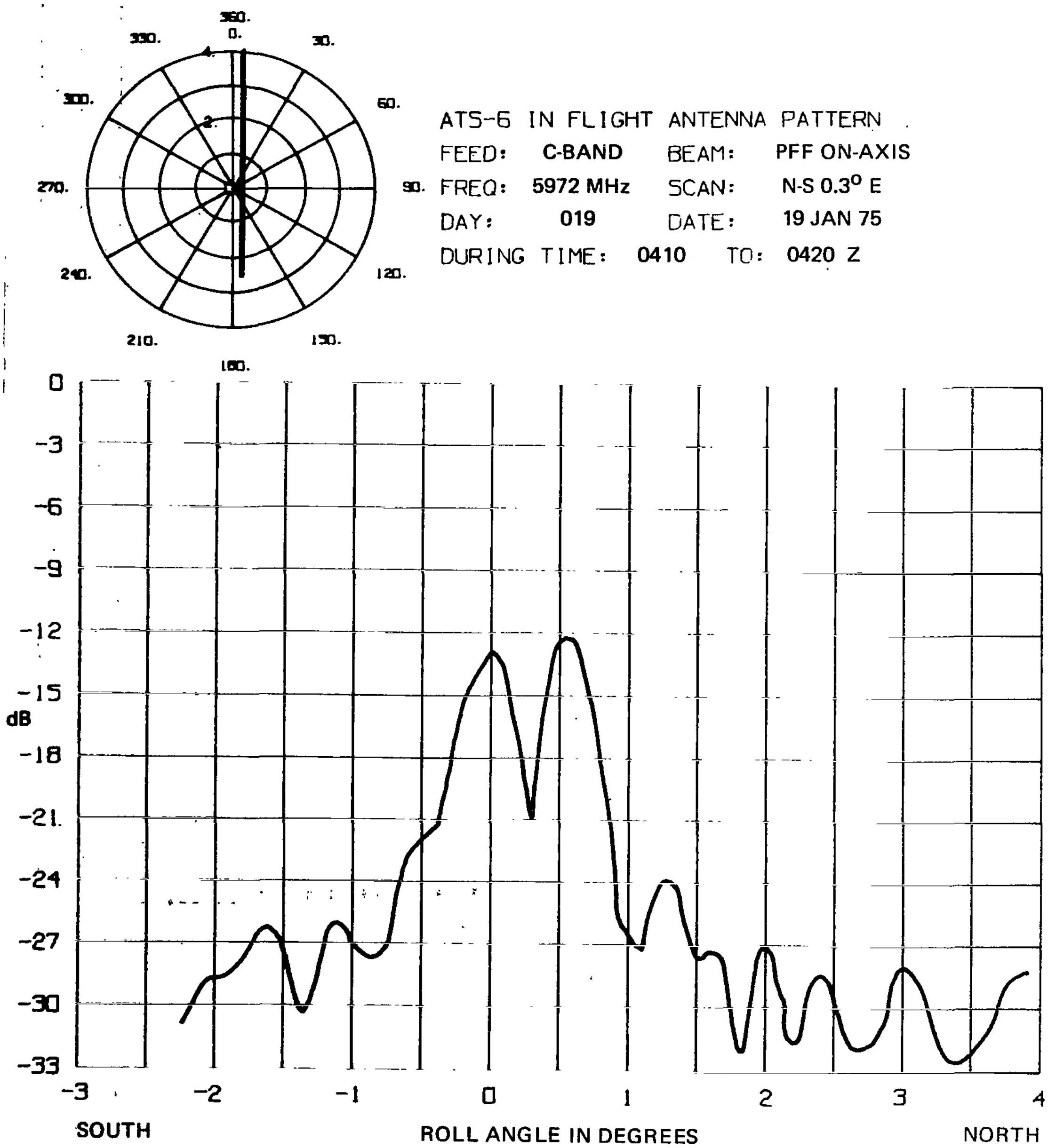

Figure 114. C-band beam PFF on-axis N – S 0.3° E.

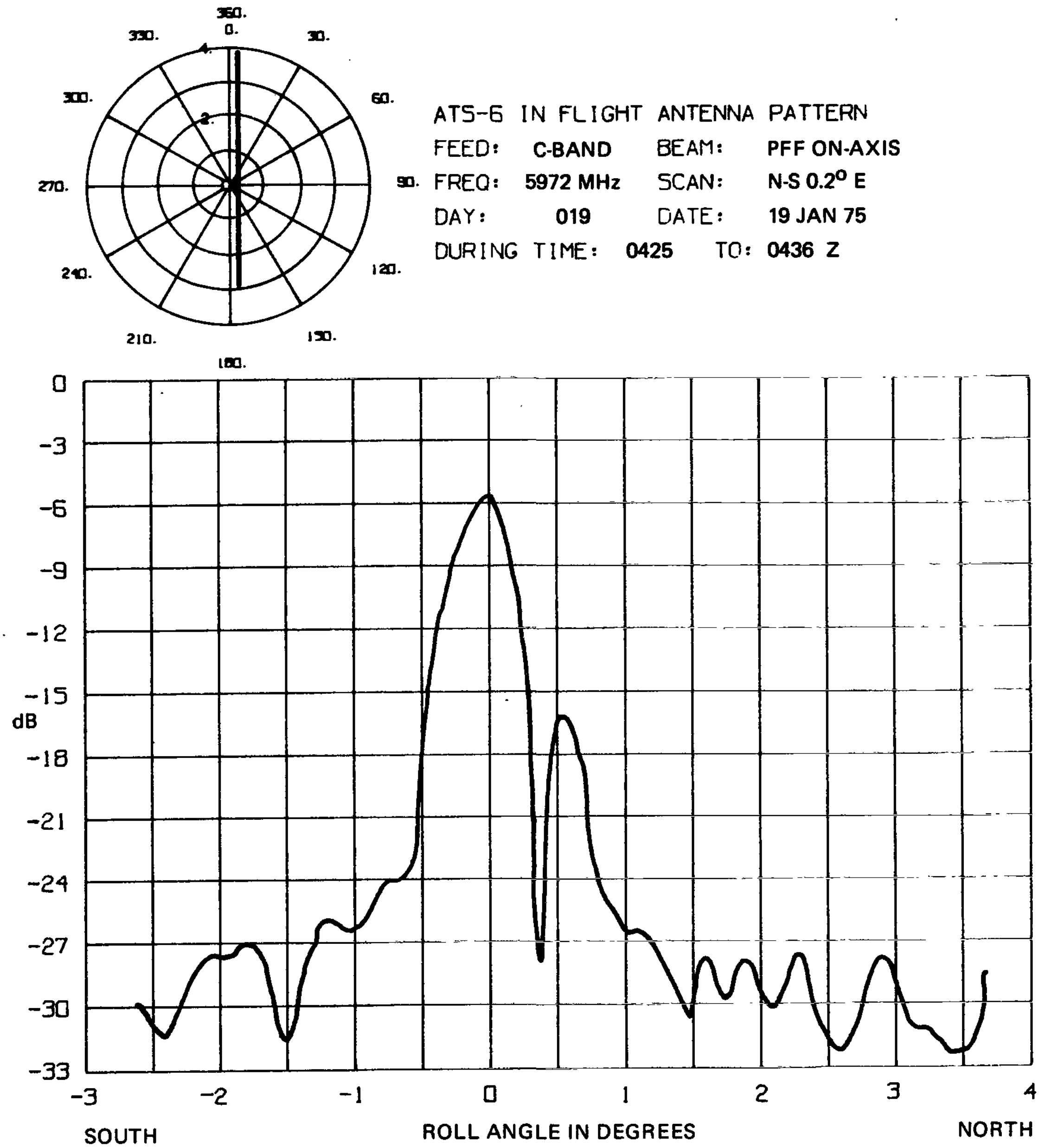

Figure 115. C-band beam PFF on-axis N – S 0.2° E.

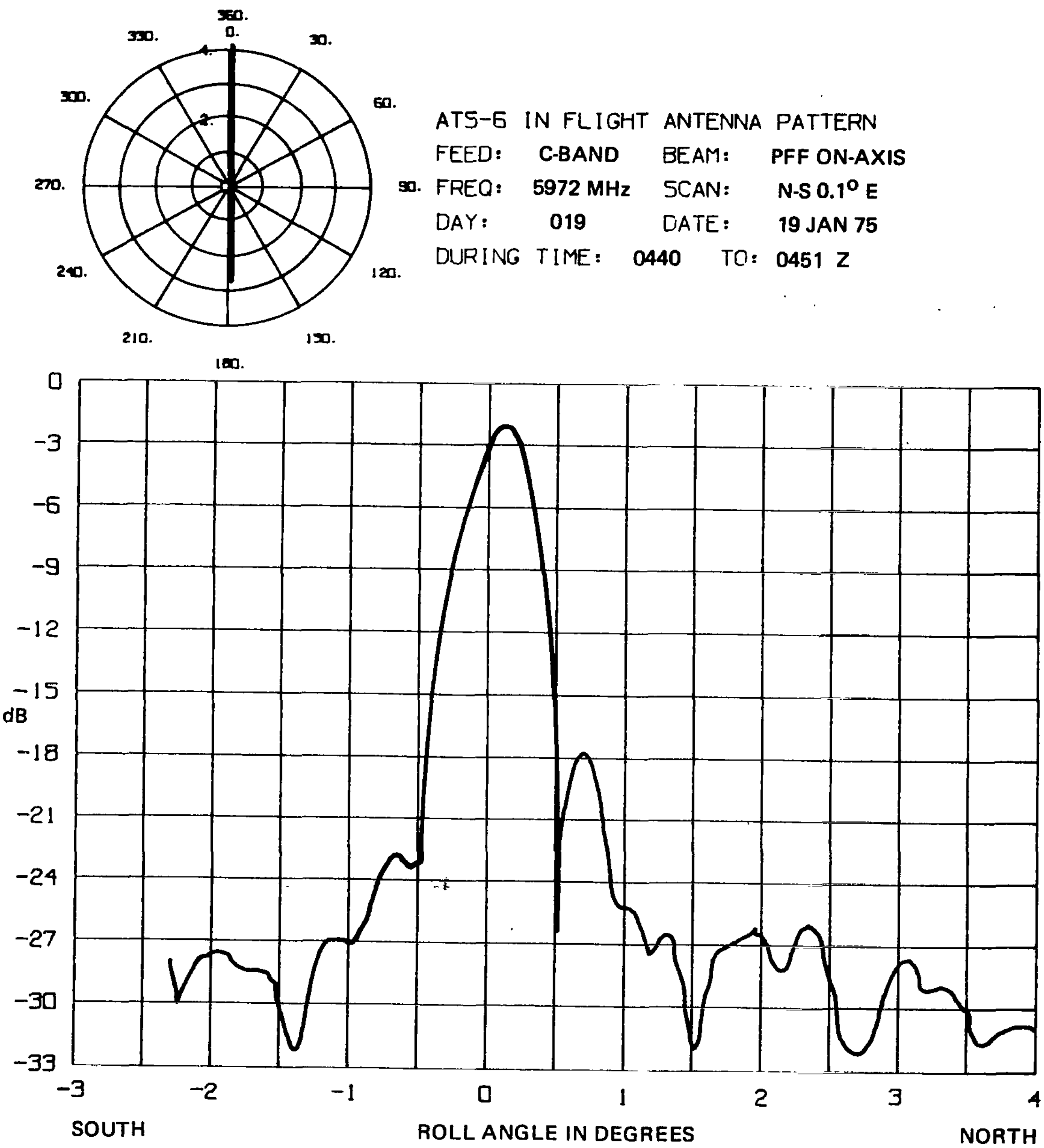

Figure 116. C-band beam PFF on-axis N – S 0.1° E.

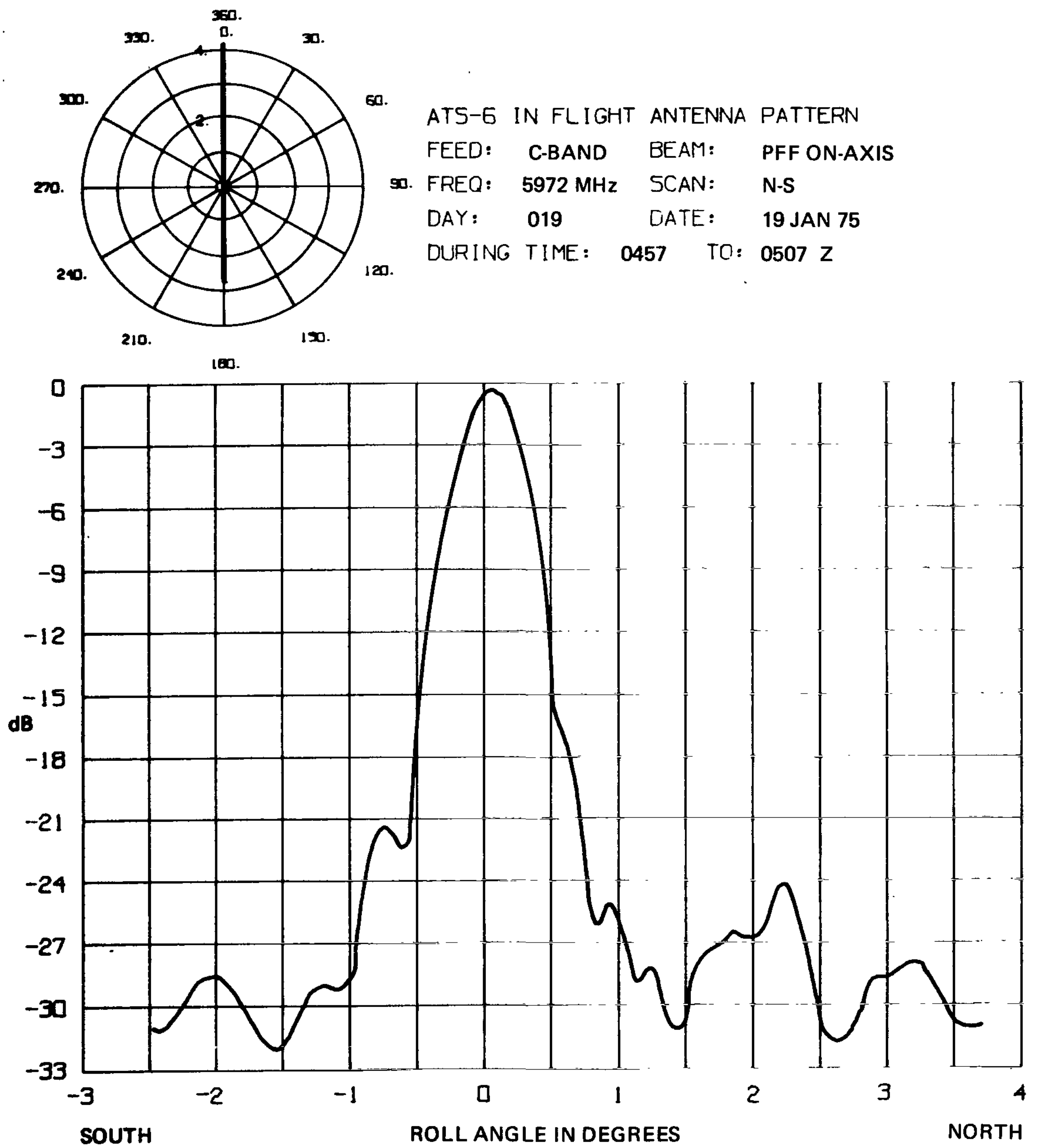

Figure 117. C-band beam PFF on-axis N – S.

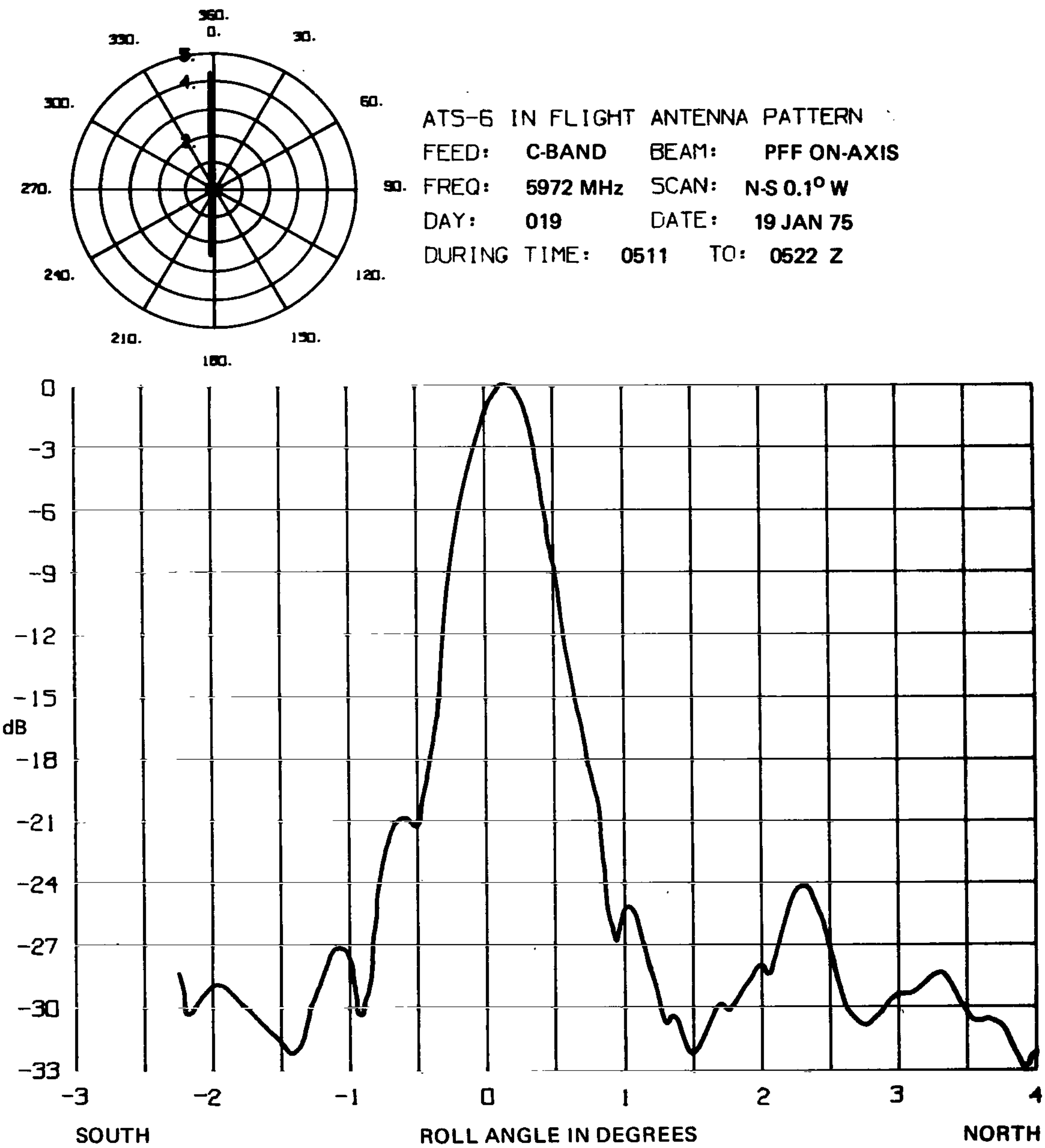

Figure 118. C-band beam PFF on-axis N – S 0.1° W.

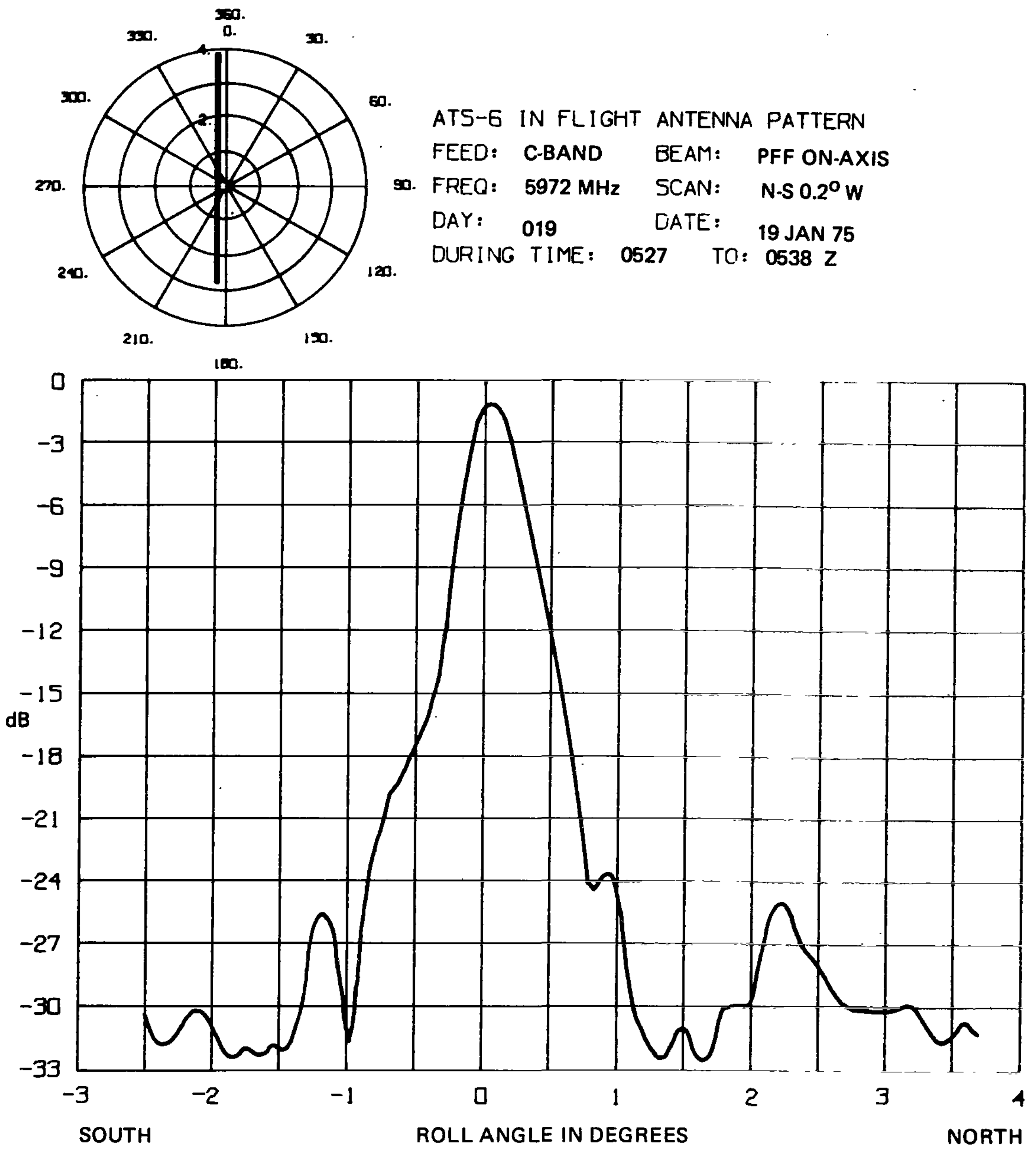

Figure 119. C-band beam PFF on-axis N – S 0.2° W.

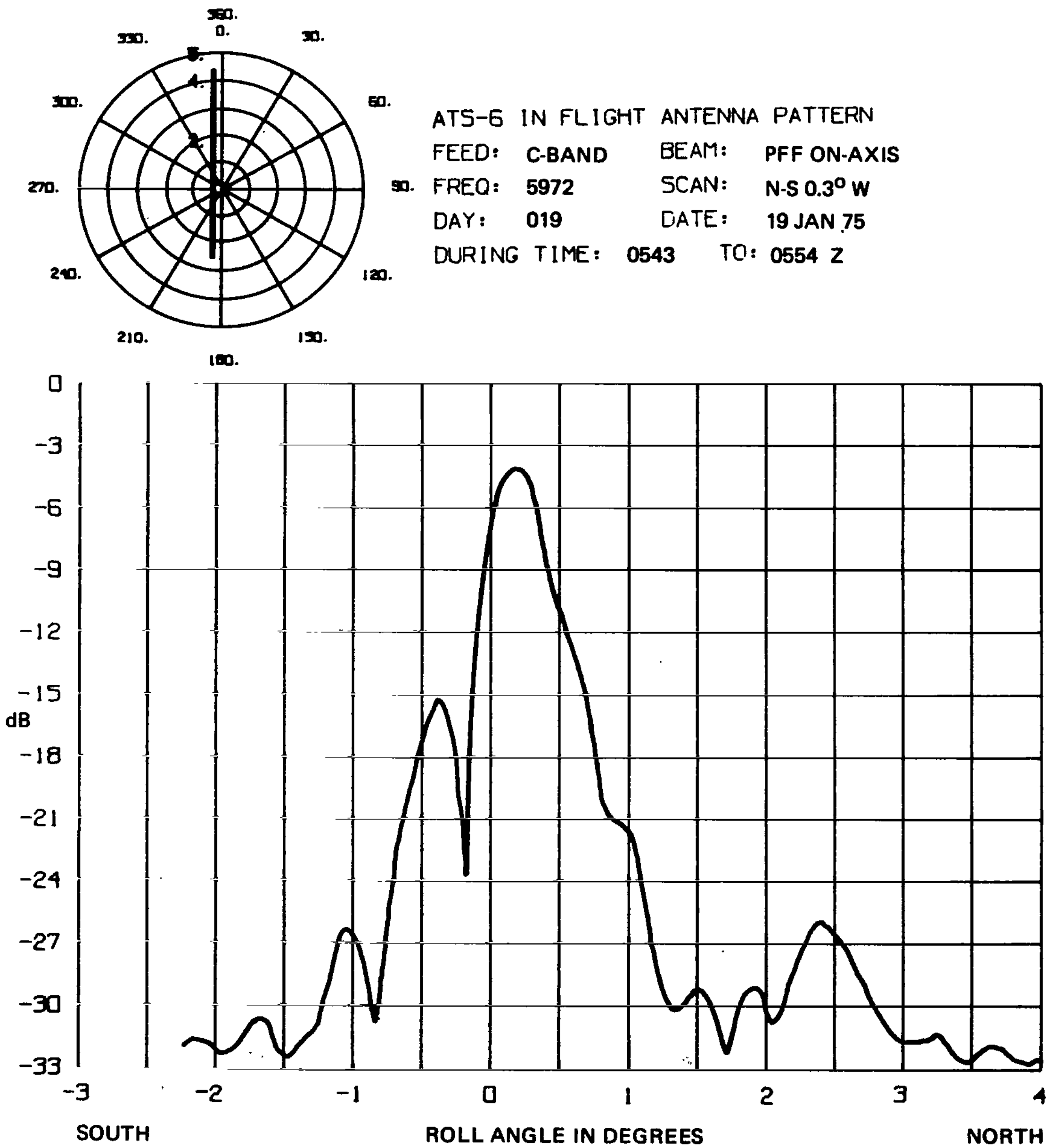

Figure 120. C-band beam PFF on-axis N – S 0.3° W.

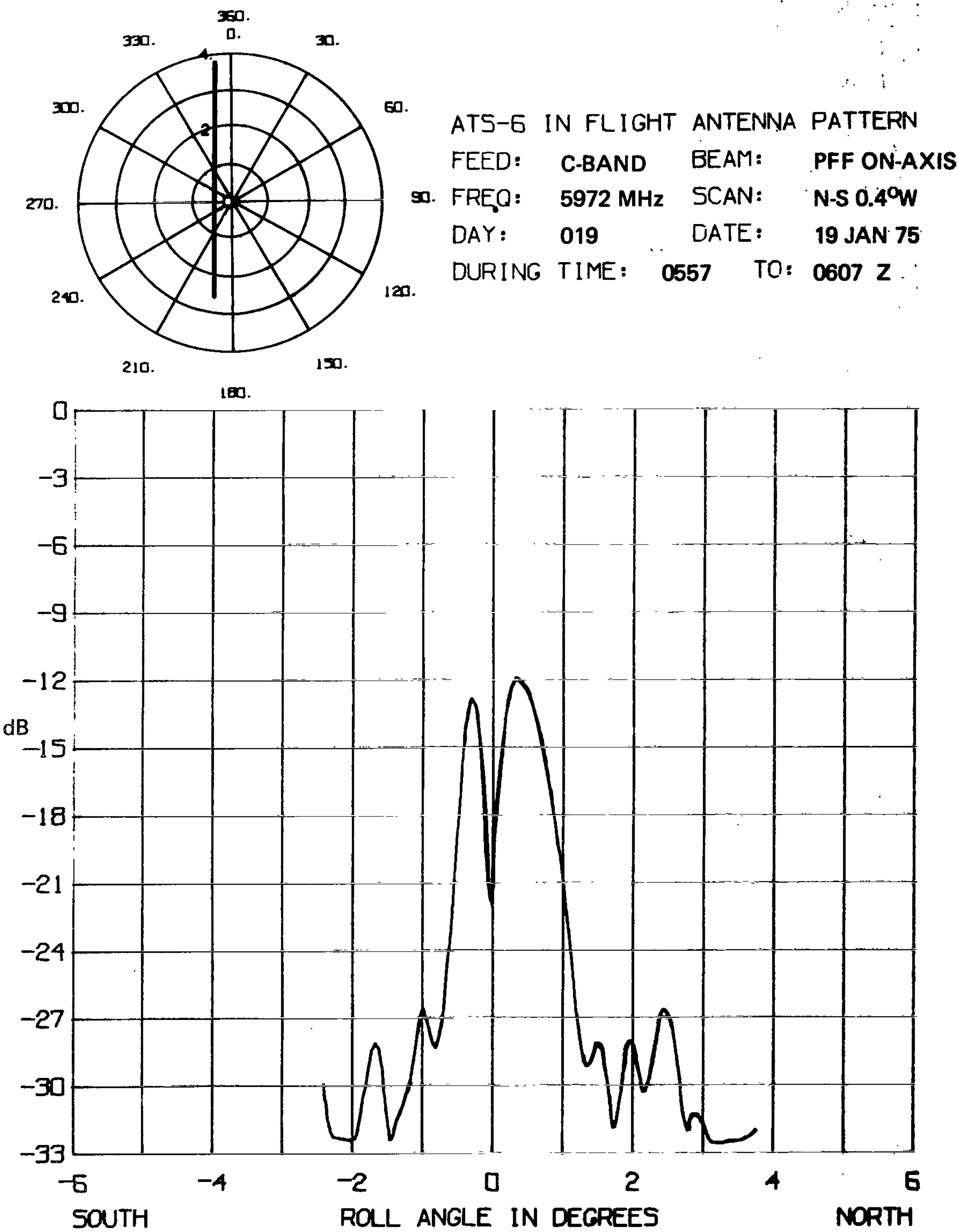

Figure 121. C-band beam PFF on-axis N – S 0.4° W.

CONCLUSION

The ATS-6 antenna pattern measurement was made possible because of the cooperation of many people and a great deal of management support. The patterns presented were those obtained by means of the 9.1-meter parabolic dish. Appendix A is an example of "footprints" for various antenna beams, whose field of view may be derived from the antenna patterns.

REFERENCES

1. *The ATS-F Data Book,* Rev. May 1974.

APPENDIX A

APPENDIX A

INTRODUCTION

The purpose of presenting the following figures is to provide an example of a useful application of measured antenna patterns. Antenna patterns provide the values of relative power levels of RF energy with respect to the angular distance from the antenna's boresight. ATS Antenna Footprints show how the transmitted beam from the ATS-6 9.1 meter parabolic antenna at synchronous altitude illuminates the earth. Footprints shown on maps represent the beamwidth or 3 dB contour (half-power points) unless otherwise noted.

Description of Figures

Fig. A-1, Footprints in Increments of 2° from ATS-6, shows how the conical angles emanating from ATS-6 at synchronous altitude, intercept the earth when it is pointing to its subsatellite point on the equator at 94° West Longitude.

Fig. A-2, VHF Beam 137.11 MHz to Ahmedabad from 35° East Longitude, India, contains contours in steps of 1 dB relative power. Corresponding beamwidths to the relative power contours are given. The limits of visibility or horizon from ATS-6 are shown.

The UHF beam is shown in Fig. A-3. It is centered on Ahmedabad, India from ATS-6 at 35° East Longitude. This beam is used for instructional TV.

The L-band Pencil Beam and Fan beam are shown in Figures A-4 and A-5, respectively. Fig. A-4 shows the L-band Pencil Beam centered on Halifax, Nova Scotia from 94° West Longitude. Fig. A-5 shows how the L-band Fan Beam illuminates the North Atlantic air traffic corridor. This specific antenna footprint was accomplished by pointing ATS-6 0.4° South of Rosman from 94° West Longitude.

The S-band beams used in the HET (Health Education TV) experiment are shown in Figures A-6 through A-8. The HET experiment also used the C-band beam shown in Figure A-9.

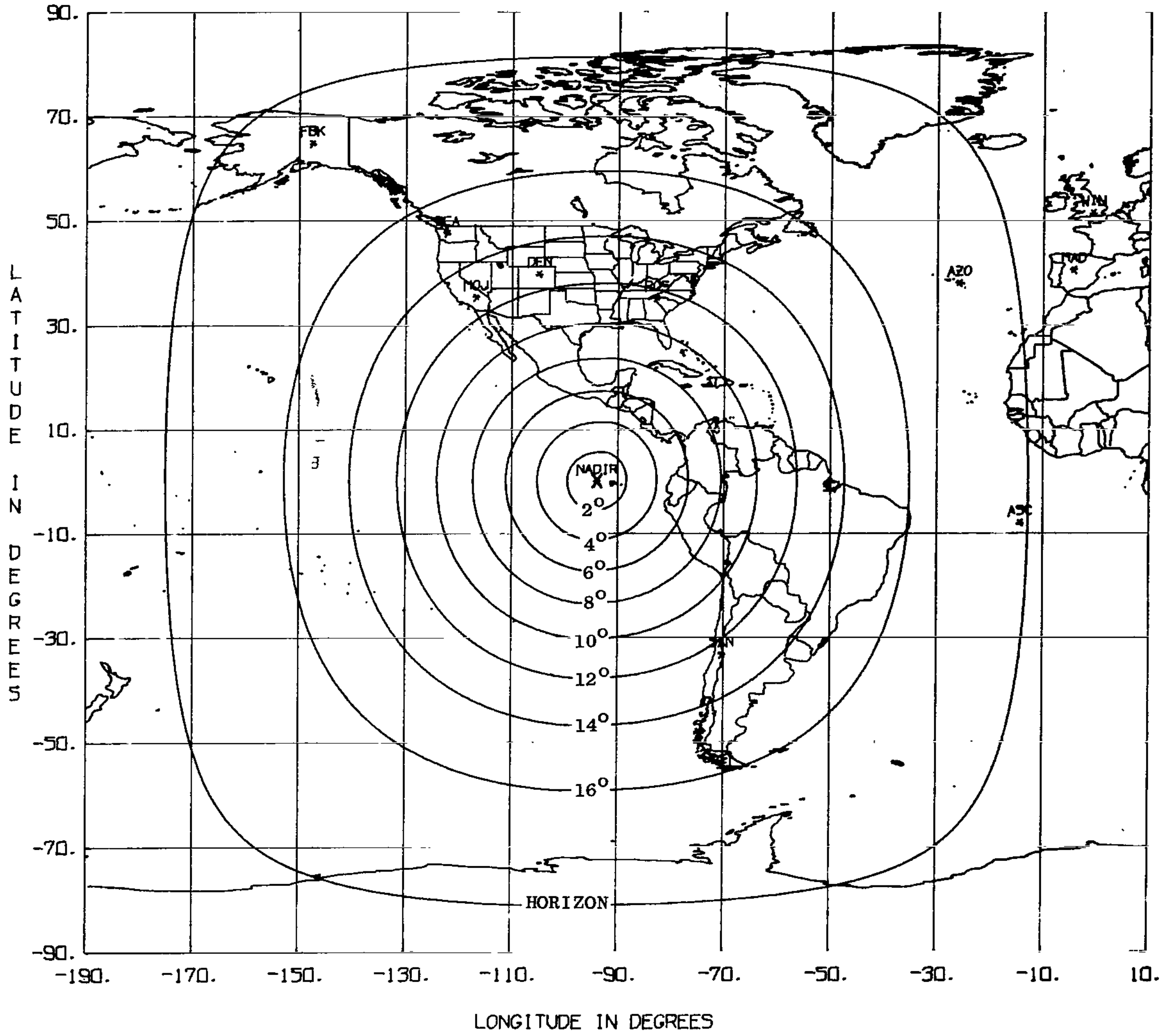

Figure A-1. Footprints in increments of 2° from ATS-6.

ATS ANTENNA FOOTPRINT

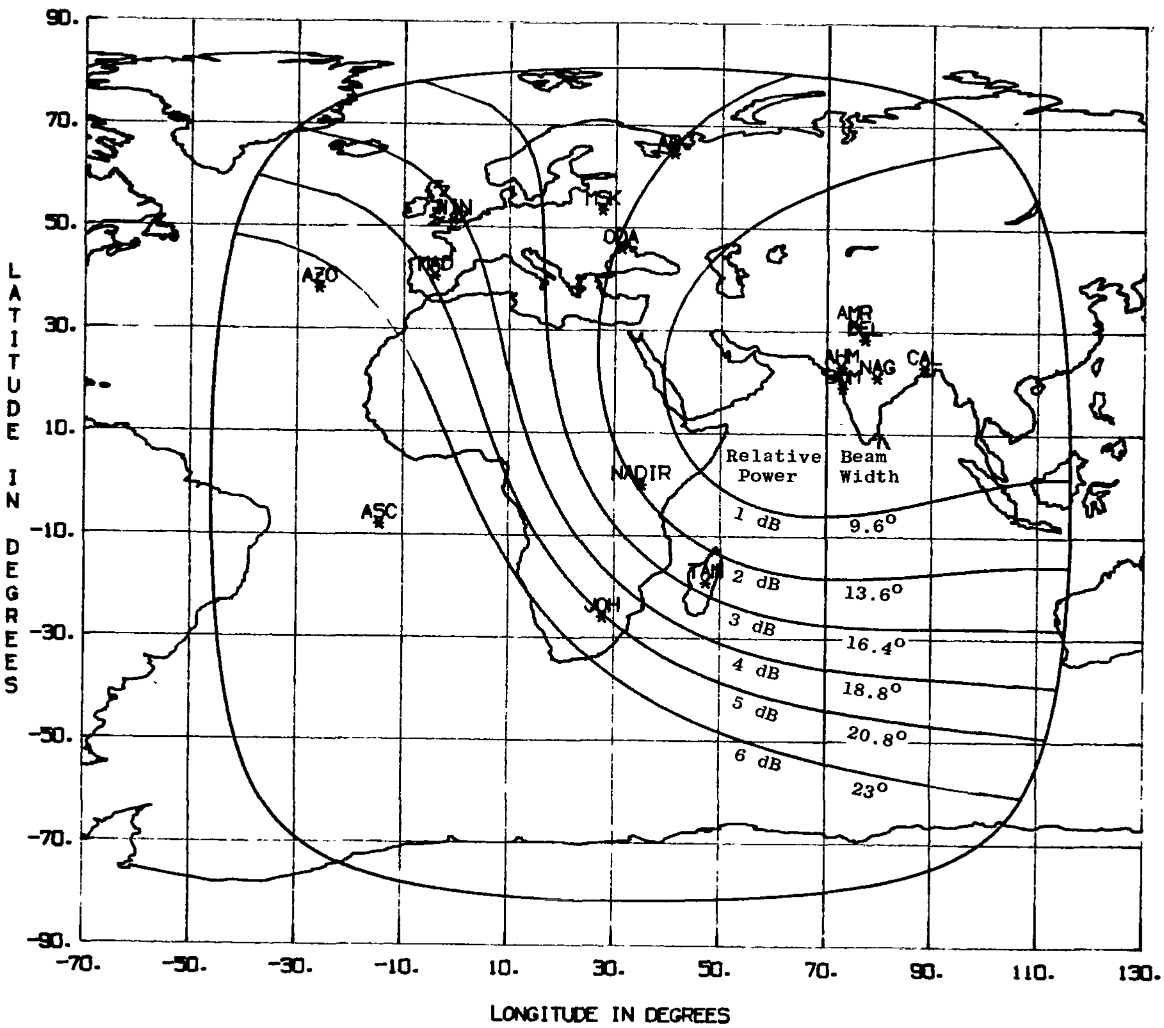

Figure A-2. VHF beam 137.11 MHz to Amedabad, India from 35° east longitude.

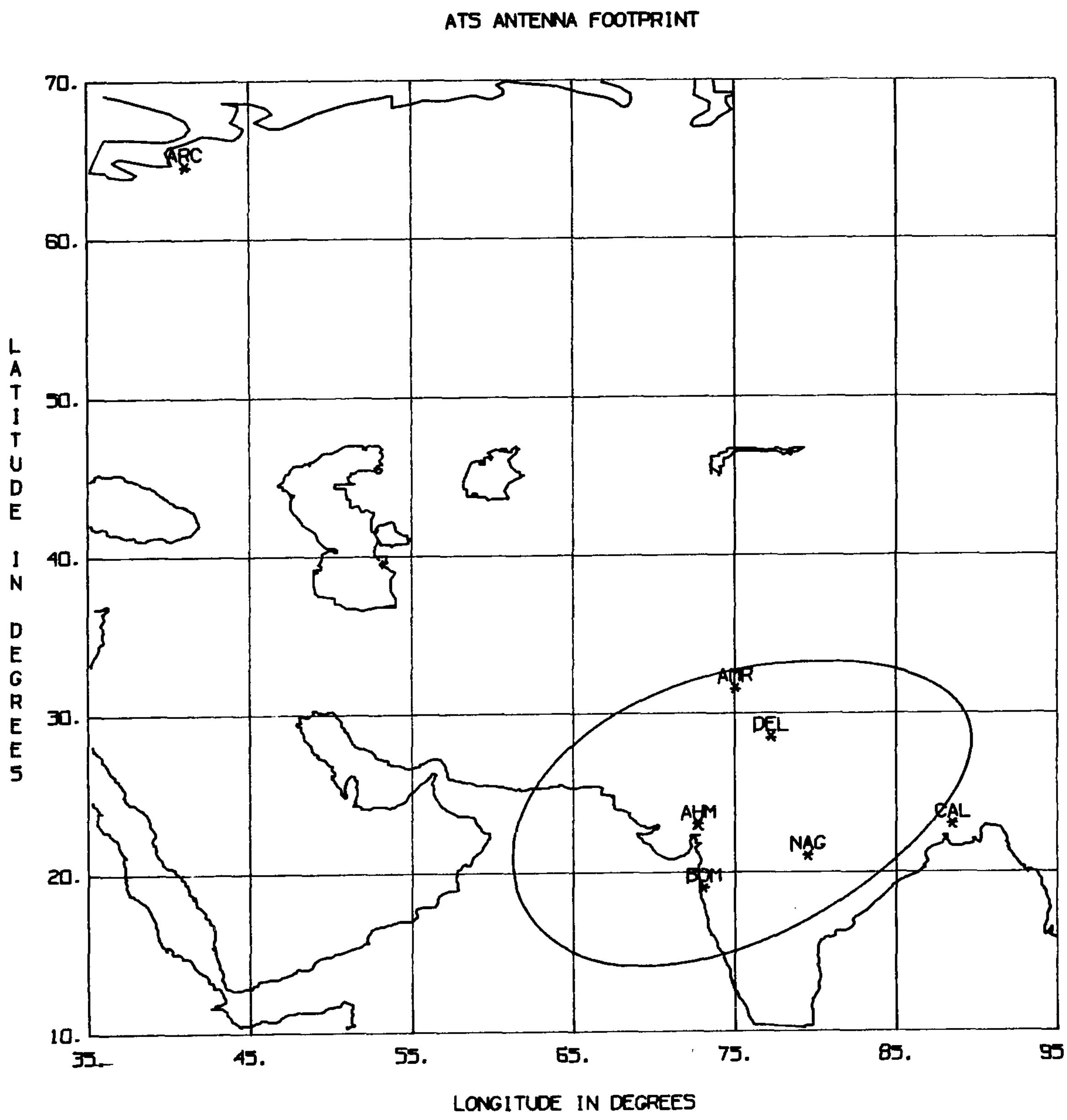

Figure A-3. UHF beam centered on Ahmedabad, India from 35° east longitude.

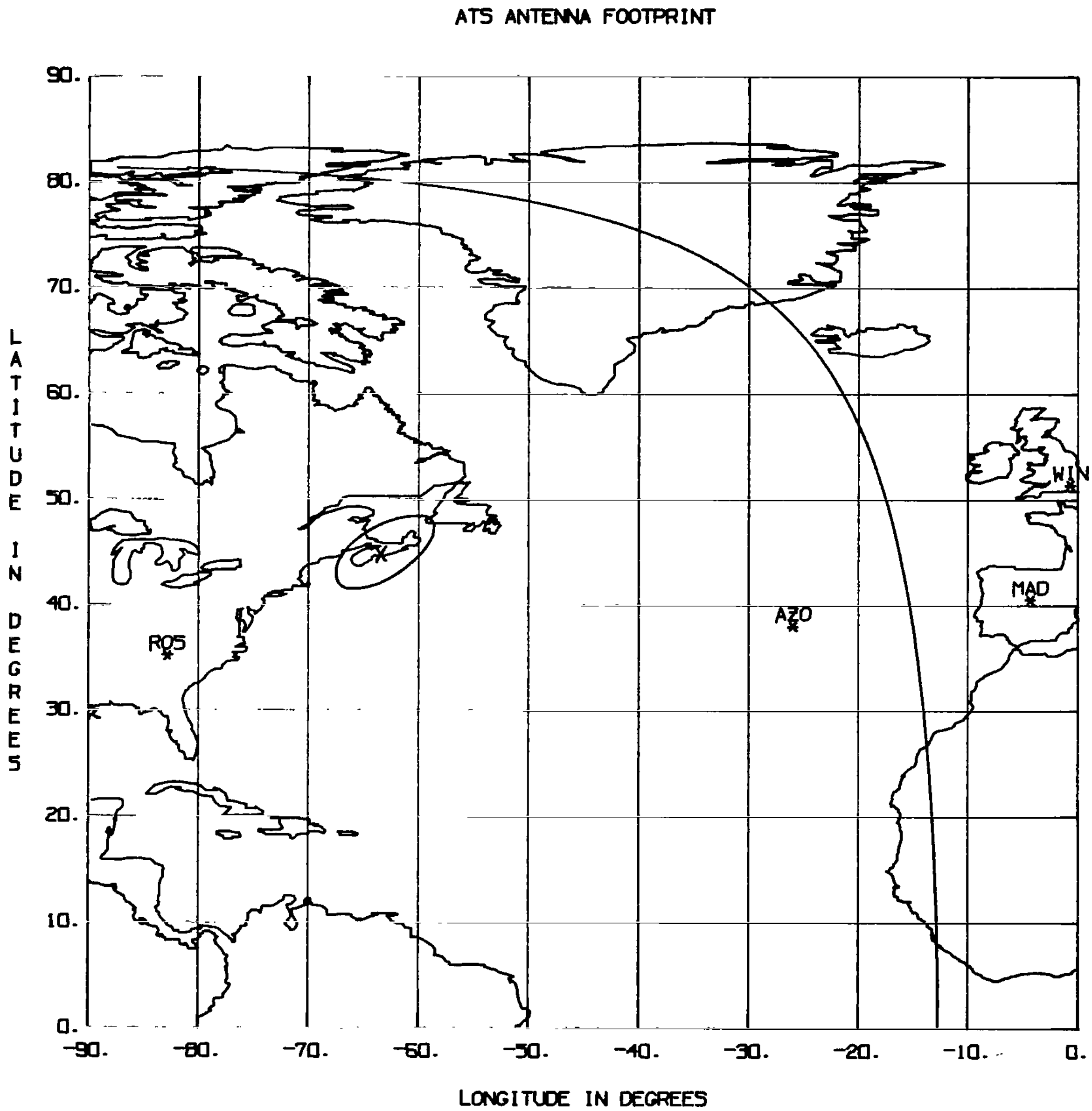

Figure A-4. L-band pencil beam centered on Halifax, Nova Scotia from 94° west longitude.

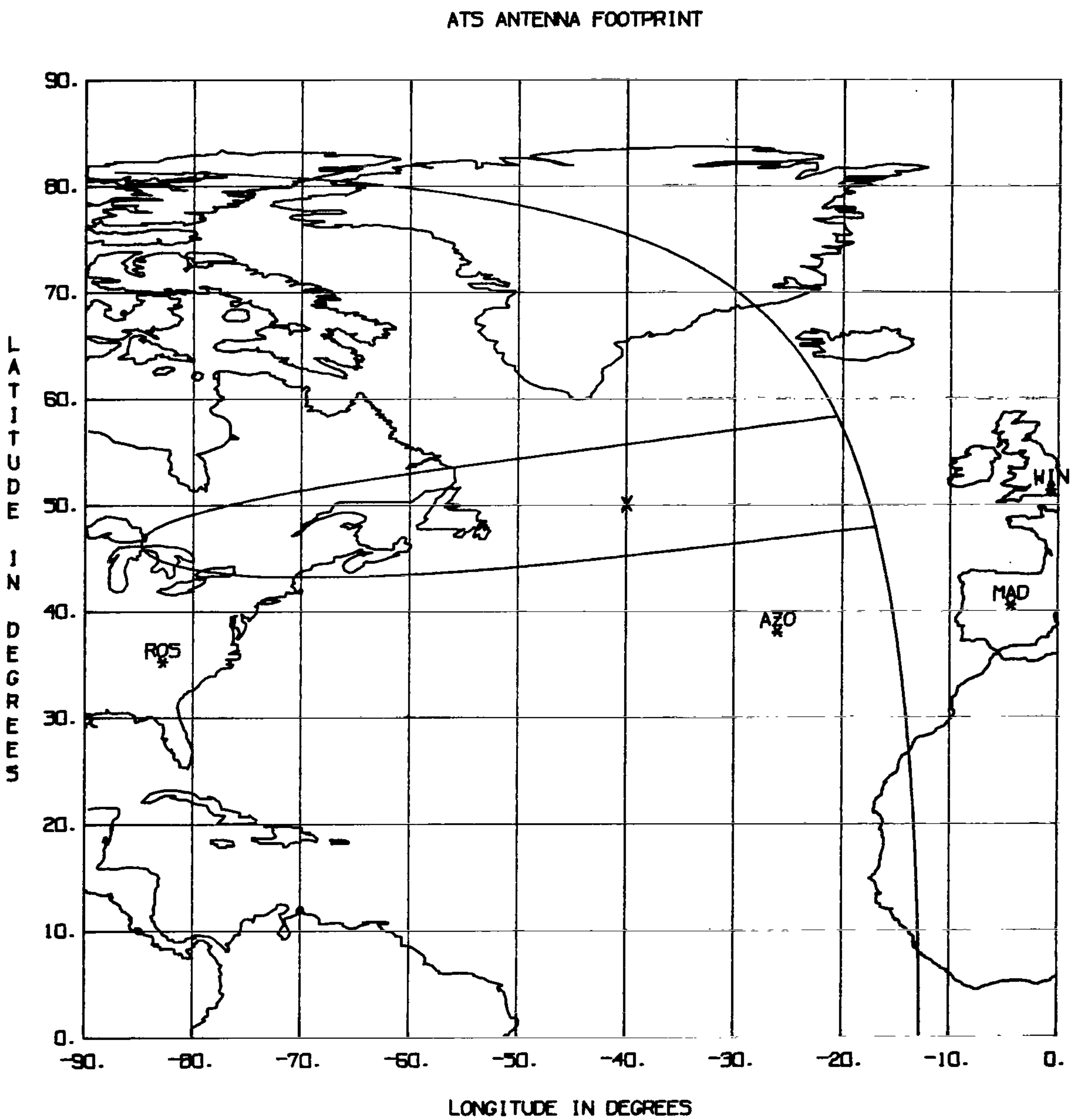

Figure A-5. L-band fan beam illuminating the North Atlantic air traffic corridor ATS-6 pointing 0.4° south of Rosman from 94° west longitude.

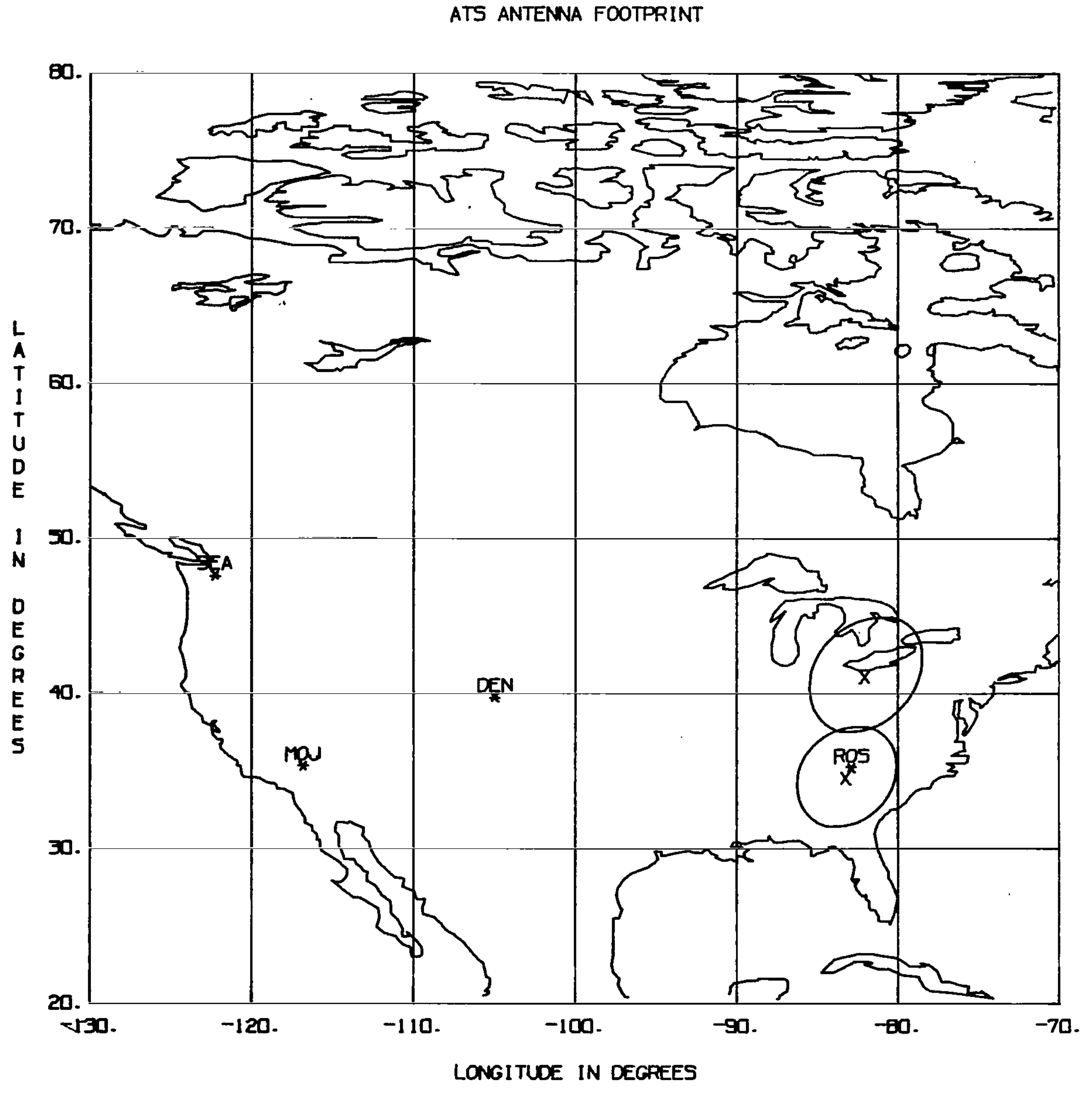

Figure A-6. S-band beams to HET Appalachian region council from 94° west longitude.

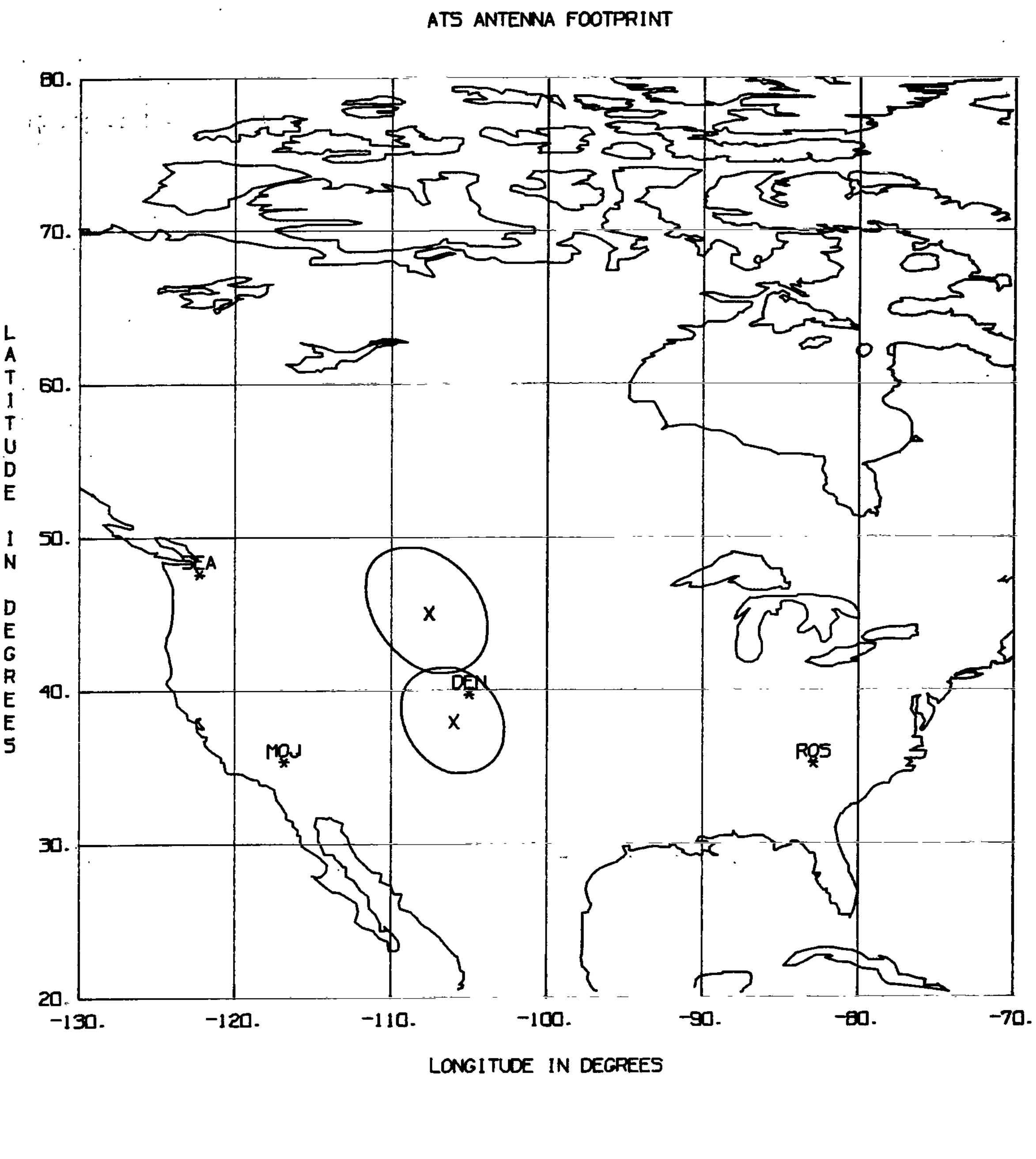

Figure A-7. S-band beams to HET Rocky Mountains east region from 94° west longitude.

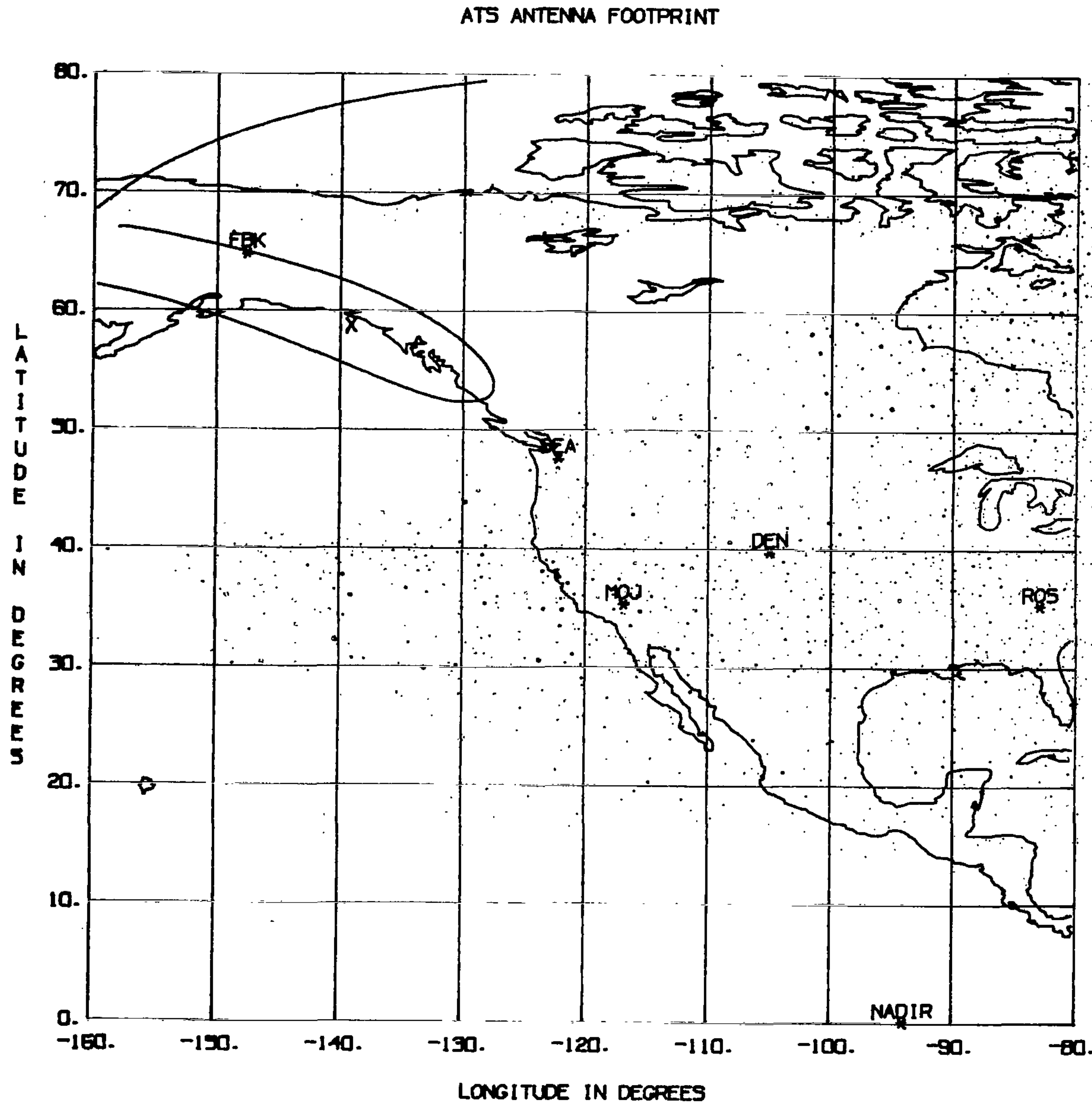

Figure A-8. S-band beam to HET Alaska from 94° west longitude.

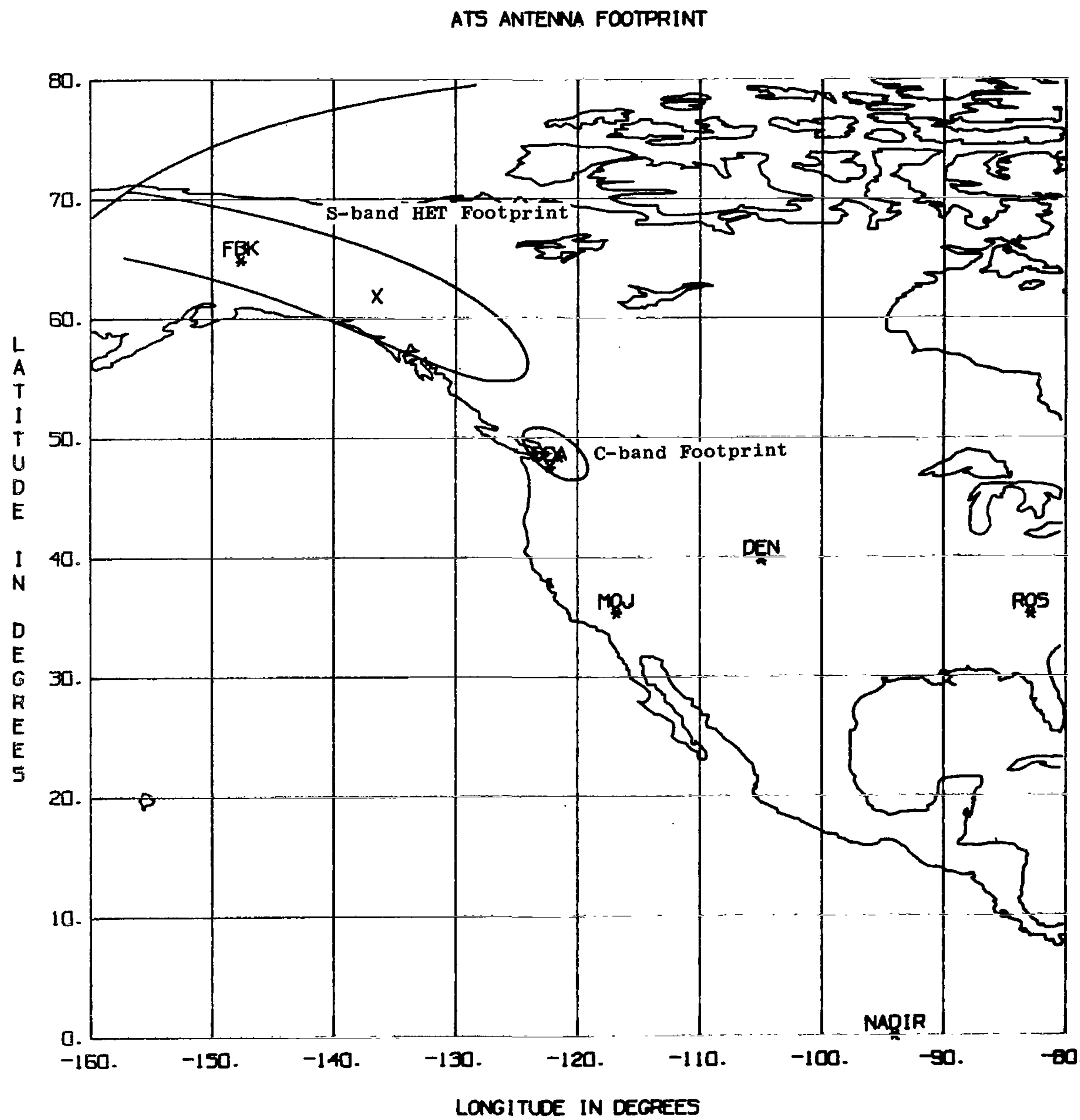

Figure A-9. C-band PFF Beam to Seattle & Omak and HET beam to Alaska from 94° west longitude.

*U.S. GOVERNMENT PRINTING OFFICE: 1976 - 635-275/56

NATIONAL AERONAUTICS AND SPACE ADMINISTRATION
WASHINGTON, D.C. 20546

OFFICIAL BUSINESS
PENALTY FOR PRIVATE USE $300

SPECIAL FOURTH-CLASS RATE
BOOK

POSTAGE AND FEES PAID
NATIONAL AERONAUTICS AND
SPACE ADMINISTRATION
451

U.S.MAIL

142 001 C1 U D 751212 S00903DS
DEPT OF THE AIR FORCE
AF WEAPONS LABORATORY
ATTN: TECHNICAL LIBRARY (SUL)
KIRTLAND AFB NM 87117

POSTMASTER: If Undeliverable (Section 158 Postal Manual) Do Not Return

"The aeronautical and space activities of the United States shall be conducted so as to contribute . . . to the expansion of human knowledge of phenomena in the atmosphere and space. The Administration shall provide for the widest practicable and appropriate dissemination of information concerning its activities and the results thereof."

—NATIONAL AERONAUTICS AND SPACE ACT OF 1958

NASA SCIENTIFIC AND TECHNICAL PUBLICATIONS

TECHNICAL REPORTS: Scientific and technical information considered important, complete, and a lasting contribution to existing knowledge.

TECHNICAL NOTES: Information less broad in scope but nevertheless of importance as a contribution to existing knowledge.

TECHNICAL MEMORANDUMS: Information receiving limited distribution because of preliminary data, security classification, or other reasons. Also includes conference proceedings with either limited or unlimited distribution.

CONTRACTOR REPORTS: Scientific and technical information generated under a NASA contract or grant and considered an important contribution to existing knowledge.

TECHNICAL TRANSLATIONS: Information published in a foreign language considered to merit NASA distribution in English.

SPECIAL PUBLICATIONS: Information derived from or of value to NASA activities. Publications include final reports of major projects, monographs, data compilations, handbooks, sourcebooks, and special bibliographies.

TECHNOLOGY UTILIZATION PUBLICATIONS: Information on technology used by NASA that may be of particular interest in commercial and other non-aerospace applications. Publications include Tech Briefs, Technology Utilization Reports and Technology Surveys.

Details on the availability of these publications may be obtained from:

SCIENTIFIC AND TECHNICAL INFORMATION OFFICE

NATIONAL AERONAUTICS AND SPACE ADMINISTRATION

Washington, D.C. 20546